



EVALUATING THE VIABILITY OF OBTAINING DNA PROFILES FROM DNA ENCAPSULATED WITHIN THE LAYERS OF COUNTERFEIT BANKNOTES

Ross Tsz Kit Kwok

BSc., MSc., MSc.

A thesis submitted in partial fulfilment of the requirement of Staffordshire University
for the degree of Doctor of Philosophy

April 2023

Abstract

The use of digital printing has made the linking of counterfeit banknotes from the same organised crime groups difficult for law enforcement agencies and Central Banks. A more reliable and objective means of attributing counterfeits to a common source is therefore required. An area of potential forensic evidence could be from the acquisition of trace DNA encapsulated between the layers in a multilayer counterfeit or from the adhesive used for adhesive external features such as foil patches or foil strips. By establishing a novel method for the removal and extraction of DNA, the possibility of profiling encapsulated DNA from counterfeit euro banknotes could be evaluated.

Preliminary research established that DNA could be removed from the adhesive side of dot matrix holograms using Chelex resin and phenol chloroform extraction. However, the percentage yield of DNA successfully extracted was low, with most results being below 20%. To increase the release of DNA from the adhesive layer of the dot matrix holograms, xylene, a 1,2-indandione working solution and ethanol were shown to be successful at separating the adhesive layers of two-layer counterfeits and on the adhesive used on dot matrix holograms present on some counterfeit banknotes. Xylene was applied in the swabbing of dot matrix holograms in a simulated procedural study involving the extraction of DNA through three extraction processes. Samples were then quantified and DNA profiled to establish the condition of present touch DNA. Both Chelex resin and phenol chloroform gave partial DNA profiles in the majority of samples, counter to what the qPCR data suggested in prior analysis.

A modified Chelex resin extraction with ethanol-based swabbing was applied to seized counterfeit banknotes to show the potential of the methodology established. However, no profiles were successfully acquired from either the dot matrix holograms or the imitation metallic threads analysed. To account for a potential loss of DNA, direct PCR was carried out on segments of imitation metallic thread taken from 24 counterfeit banknotes. Two of the samples gave partial DNA profiles that had alleles that could be used for RMP analysis and one profile where the allelic peaks were challenging to interpret. Although no link between the DNA profiles could be established using profile comparisons, the results do highlight the potential of acquiring DNA profiles from DNA encapsulated in the layers of counterfeit banknotes.

This research shows the capability of acquiring DNA from counterfeit banknotes for forensic investigations, which with further research could be part of a standard procedure for counterfeit banknote processing to gain intel on organised crime groups.

Funding Declaration

The research detailed in this thesis has been funded by the European Central Bank.

Acknowledgments

I would like to thank the European Central Bank who funded this project.

Special thanks should be extended to David Kenny, MSc. (Principal Counterfeiting Expert) who has provided me with a significant amount of knowledge and support in his role as supervisor. My thanks also to Dr Jean-Michel Grimal (Head of Currency Development Division) and Paloma Varela, MSc. (Head of the Anti-Counterfeiting Section) whose interest in and support for new tools in the fight against counterfeiting, made this project possible.

I would also like to thank Sabine van Doremalen (MSc.), counterfeit expert at the De Nederlandsche Bank and Ed Quinlan (BBS), counterfeit expert at the Central bank of Ireland, who kindly provided the counterfeit samples that were used in the laboratory work described herein.

A huge thank you should also go to all of the Staffordshire University technical team who have helped with countless aspects of the research and made working in the laboratory so much fun. Special mentions should go to Mishele Barrigas, Robin Parsons and Dr Rob Manning for their invaluable guidance and knowledge.

Thank you to the volunteers who kindly donated their time and fingermarks to my research, helping to establish the work in this thesis.

I would like to thank my supervisors Dr Sarah Fieldhouse and Professor Graham Williams for their guidance and support throughout my studies. Also, thank you to Professor Andy Platt for all his feedback and guidance with the many drafts of the final thesis. In addition, I would like to thank Staffordshire University for giving me this opportunity.

Thank you to my Ph.D. research family in s419 who have helped make some of the most memorable experiences I will ever have. In alphabetical order they are: Mia Abbott, Peter Bird, Dr Angela Bonner, Dr Mark Broadhead, Dr Megan Needham, Amy Osborne, Robin Parsons, Dr Keith Silika, Elli Toulson and Dr Laura Wilkinson.

To my family and friends, thank you for your support throughout the research, especially Dr Deon Roos for his help with my statistics struggles and Aimée Stuart for editing my 5-line sentence horrors.

Last but not least, a massive thank you should go to my mum who has always supported me in following my love of science which has got me to where I am today.

Table of Contents

Chapter 1 Literature Review	1
1.1 Introduction to Currency and Counterfeiting	1
1.1.1 The Extent of Counterfeiting Banknotes and Legal Protections of Currency	1
1.1.2 The Anti-Counterfeiting Features of Banknotes	4
1.1.3 The Manufacturing of Counterfeit Banknotes	12
1.2 The Nature of DNA and Banknotes	14
1.3 Sources of DNA and Recovery Processes	19
1.4 Visualisation of Trace DNA	21
1.5 DNA Extraction	22
1.6 DNA Quantification and Allelic Typing	26
1.6.1 Quantifying DNA	26
1.6.2 DNA Profiling	30
1.7 Interpreting Trace DNA Evidence	32
1.8 DNA Databases	34
1.9 The Reliability of Evidence Using the Balance of Probabilities	35
1.10 Effect Sizes	37
1.11 Conclusion	38
1.12 Aims and Objectives	41
1.12.1 Aim	41
1.12.2 Objectives	41
Chapter 2 Evaluation of DNA in Composite Counterfeit Banknotes	42
2.1 Introduction	42
2.2 Methodologies	43
2.2.1 Preliminary Examination of Deposited DNA on Dot Matrix Holograms	43
2.2.2 Xylene, 1,2-Indandione and Hexane Adhesive Separation	46
2.2.3 Ethanol Adhesive Separation	47

2.2.4 Evaluation of DNA Sampling in Counterfeit Banknotes.....	48
2.3 Results.....	51
2.3.1 Preliminary Examination of Deposited DNA on Dot Matrix Holograms	51
2.3.2 Xylene, 1,2-Indandione and Hexane Adhesive Separation	53
2.3.3 Ethanol Adhesive Separation.....	55
2.3.4 Evaluation of DNA Sampling in Counterfeit Banknotes.....	56
2.4 Discussions.....	58
2.4.1 Preliminary Examination of Deposited DNA on Dot Matrix Holograms	58
2.4.2 Xylene, 1,2 Indandione Separation and Hexane Adhesive Separation	60
2.4.3 Ethanol Adhesive Separation.....	62
2.4.4 Evaluation of DNA Sampling in Counterfeit Banknotes.....	63
2.5 Conclusions.....	65
Chapter 3 Simulated Procedural Study to Evaluate the Presence of DNA in Composite Counterfeit Banknotes	67
3.1 Introduction	67
3.2 Methodology.....	67
3.2.1 Sample Preparation and Extraction.....	67
3.2.2 DNA Quantification	69
3.2.3 DNA Profiling	70
3.3 Results.....	70
3.3.1 DNA Quantification	70
3.3.2 DNA Profiling	74
3.4 Discussion.....	86
3.4.1 DNA Quantification	86
3.4.2 DNA Profiles.....	88
3.5 Conclusion.....	95
Chapter 4 Genetic Evaluation of Counterfeit Banknotes	96

4.1 Introduction	96
4.2 Applied Procedural Study	97
4.2.1 Methodology	97
4.2.2 Results	101
4.2.3 Discussion	102
4.3 Direct PCR	104
4.3.1 Methodology	104
4.3.2 Results	107
4.3.3 Discussion	111
4.4 Diamond Dye Targeting of Fingermarks	114
4.4.1 Methodology	114
4.4.2 Results	115
4.4.3 Discussion	117
4.5 Conclusion	118
Chapter 5 Conclusions and Future Considerations	119
5.1 Conclusions	119
5.2 Future Considerations and Recommendations	120
Chapter 6 References	124

Table of Figures

Figure 1. The front of a genuine €10 banknote under UV light highlights the European Union stars and triple coloured security fibres. The paper itself does not fluoresce (European Central Bank, 2014).	5
Figure 2. The offset printing detail can be seen on the bridge depicted on the back of a genuine €10 banknote (European Central Bank, 2014).....	5
Figure 3. Stars featured on the front of a genuine €10 banknote, printed as part of the offset printed background (European Central Bank, 2014).....	6
Figure 4. The Europa portrait and value of the banknote can be seen when viewed in transmitted light. (European Central Bank, 2014).....	7

Figure 5. When viewed in transmitted light the security thread is visible with the denomination present in the thread in a genuine banknote (European Central Bank, 2014).	8
Figure 6. The holographic stripe on the front of a genuine Europa series €10 banknote (European Central Bank, 2014).	8
Figure 7. The numerical value on the bottom left of the Europa series of notes, in this image a €10 banknote, under visible light a “rolling bar effect” can be seen if the viewing angle is changed (European Central Bank, 2014).	9
Figure 8. A genuine €100 banknote from the first series under magnification, showing the numerical value of the note in incorporated into the design of the note in microprinting (Flegar and Radovanovic, 2013).	9
Figure 9. Under infrared light a genuine €5 banknote’s watermarks, serial number, metallic thread, holographic strip and parts of the artwork can be seen (Bruna et al. 2013).	10
Figure 10. The two images on the left-hand side are taken from a genuine €100 banknote, with transmitted light through the note (left) and with reflected light (centre). The image on the right is an example of a counterfeit with transmitted light through the note (Flegar and Radovanovic, 2013).	10
Figure 11. The average concentration of DNA acquired from the Chelex extraction technique and the phenol-chloroform extraction technique alongside the STR loci used to quantify the concentration. The legend indicates the concentration of DNA placed on the adhesive side of the hologram before swabbing.	51
Figure 12. The removed imitation security thread removed using xylene from a counterfeit banknote.	54
Figure 13. Two sides of the same counterfeit banknote that have been separated through the addition of indandione.	54
Figure 14. The paper surface of a counterfeit banknote where a counterfeit hologram has been removed using xylene, exposing the paper layer underneath.	55
Figure 15. The removed hologram from a counterfeit €50 banknote (left), with the removed hologram (right) using 100% ethanol. Counterfeit banknote provided by the Central Bank of Ireland.	55
Figure 16. The separated paper layers of a counterfeit €500 banknote, with the removed imitation metallic thread using 100% ethanol. Counterfeit banknote provided by De Nederlandsche Bank.	55
Figure 17. The average detected concentration of DNA using the male SRY marker (pg/μL) from primary (A) and secondary (B) swabs taken from the adhesive	

hologram residue left on counterfeit banknotes. Reaction volumes were all set to 25 μL	57
Figure 18. The average detected concentration of DNA using the male SRY marker (pg/ μL) from primary (A) and secondary (B) swabs taken from the adhesive hologram residue left on counterfeit banknotes. Reaction volumes were all set to 12.5 μL	57
Figure 19. The quantified concentration of DNA for the three extraction techniques using the RPPH1 marker as part of the Quantifiler™ Duo Quantification kit.	73
Figure 20. The quantified concentration of DNA for the three extraction techniques using the SRY marker as part of the Quantifiler™ Duo Quantification kit.	73
Figure 21. The alleles detected from the external sourced samples from the composite counterfeit banknotes according to the associated volunteer within each extraction group. This comprises of the alleles for volunteer C who handled the external aspects of the composite counterfeit banknote alongside the alleles shared with the other two volunteers that appeared in the DNA profile.	79
Figure 22. The alleles detected from the internal adhesive layer of the composite counterfeit banknotes according to the associated volunteer within each extraction group. This comprises of the alleles for volunteers A and B who placed their fingermarks on the adhesive side of the dot matrix holograms alongside the alleles shared with the male volunteer (C) that appeared in the DNA profile.	79
Figure 23. The average RFU for the detected DNA profiles on both the external and internal components of the composite counterfeit banknotes.	80
Figure 24. The average RFU for the detected DNA profiles according to the volunteers' profiles on the external surface of the composite counterfeit banknotes.	80
Figure 25. The average RFU for the detected DNA profiles according to the volunteers' profiles on the internal surface of the composite counterfeit banknotes.	81
Figure 26. The average heterozygote balance for the DNA profiles taken from the external and internal surfaces of the composite counterfeit banknotes.	81
Figure 27. The alleles detected that were not directly attributable to volunteer C from the external surface of the composite counterfeit banknotes.	82
Figure 28. The alleles detected that were not directly attributable to volunteers A or B accordingly from the internal adhesive of the composite counterfeit banknotes. .	82
Figure 29. The electropherogram of the partial DNA profile acquired from the 2015 counterfeit banknote removed from circulation in South Holland.	108

Figure 30. The electropherogram of the partial DNA profile acquired from the 2016 counterfeit banknote removed from circulation in North Holland.	109
Figure 31. The electropherogram of the partial DNA profile acquired from the 2016 counterfeit banknote removed from circulation in North Brabant.	110
Figure 32. Dot matrix hologram with a sebaceous fingerprint present with ridge detail visible with the addition of diamond dye 5.01.....	115
Figure 33. Dot matrix hologram with a sebaceous fingerprint present but not as visible with the addition of diamond dye 6.01	116
Figure 34. Dot matrix hologram strip 8.01	116

Table of Tables

Table 1. List of the €50 counterfeit banknotes examined and their respective County within the Republic of Ireland where they were taken out of circulation. Samples were provided by the Central Bank of Ireland. The indicative aspect refers to the categorization of the counterfeit banknote by the ECB according to the general area it was from (EU), the series of banknote it is a counterfeit of (A being the first series of euros), the denomination being counterfeited (50 euros), the process applied (P = traditional offset printing or C colour copying using equipment such as inkjet printers) and a final numerical value for the sequential order in which it was found.	44
Table 2 The €50 counterfeit banknotes provided by the Central Bank of Ireland with the dot matrix holograms present and which county they were received from. The indicative aspect refers to the categorization of the counterfeit banknote by the ECB according to the general area it was from (EU), the series of banknote it is a counterfeit of (A being the first series of euros), the denomination being counterfeited (50 euros), the process applied (P = traditional offset printing or C colour copying using equipment such as inkjet printers) and a final numerical value for the sequential order in which it was found.	48
Table 3. The detected DNA concentrations (pg/μL) of DNA from the Chelex extraction technique and the phenol-chloroform extraction technique alongside the STR loci used to quantify the concentration of DNA on the volunteer and counterfeit banknote counterfeit holograms.....	53
Table 4. Descriptive statistics of the DNA concentration (pg/μL) detected by the two markers, SRY and RPPH1 alongside the location of the samples.....	72

Table 5. Descriptive statistics of the number of alleles detected externally from the composite counterfeit banknotes after extraction. These consist of the number of total alleles detected followed by: The number of alleles that can be contributed to the primary individual who handled the composite counterfeit banknote, the alleles that were unique to that individual within the group, the number of alleles that could be contributed to the volunteer who introduced their DNA to the adhesive side of the dot matrix hologram, alleles that were unique to that volunteer and the number of alleles that were shared between the two volunteers.	77
Table 6. Descriptive statistics of the number of alleles detected internally from the composite counterfeit banknotes after extraction. These consist of the number of total alleles detected followed by: The number of alleles that can be contributed to the primary individual who placed their fingermark onto the adhesive side of the dot matrix hologram banknote, the alleles that were unique to that individual within the group, the number of alleles that could be contributed to the volunteer who introduced their DNA to external aspect of the composite counterfeit banknote, alleles that were unique to that volunteer and the number of alleles that were shared between the two volunteers.	78
Table 7. Descriptive statistics of the RFU values for the external and internal sourced samples alongside the RFU values for the volunteer specific alleles.	83
Table 8. Lists the €50 counterfeit banknotes provided by the Central Bank of Ireland with the dot matrix holograms present. The indicative aspect refers to the categorization of the counterfeit banknote by the ECB according to the general area it was from (EU), the series of banknote it is a counterfeit of (A being the first series of euros), the denomination being counterfeited (50 euros), the process applied (P = traditional offset printing or C colour copying using equipment such as inkjet printers) and a final numerical value for the sequential order in which it was found.	98
Table 9. Lists the €500 counterfeit banknotes provided by De Nederlandsche Bank alongside the county they were taken out of circulation from. The indicative aspect refers to the categorization of the counterfeit banknote by the ECB according to the general area it was from (EU), the series of banknote it is a counterfeit of (A being the first series of euros), the denomination being counterfeited (500 euros), the process applied (P = traditional offset printing or C colour copying using equipment such as inkjet printers) and a final numerical value for the sequential order in which it was found.	99
Table 10. Lists the €500 counterfeit banknotes sourced from the Netherlands provided by De Nederlandsche Bank and the respective counties they were found.	

The indicative aspect refers to the categorization of the counterfeit banknote by the ECB according to the general area it was from (EU), the series of banknote it is a counterfeit of (A being the first series of euros), the denomination being counterfeited (500 euros), the process applied (P = traditional offset printing or C colour copying using equipment such as inkjet printers) and a final numerical value for the sequential order in which it was found. 105

Table 11. The detected alleles for the two interpretable partial DNA profiles acquired from the imitation metallic threads of two counterfeit banknotes. The * icon indicates alleles that may be homozygous due to the RFU values..... 107

Notice to Reader

All images in the literature review have been sourced from either the European Central Bank or literature sources as to avoid any legal issues in the use of images of genuine banknotes.

Papers Published as Part of The Thesis

Kwok, R., Kenny, D. and Williams, G. (2019). Evaluating the viability of obtaining DNA profiles from DNA encapsulated between the layers of composite counterfeit banknotes. *Forensics Science International: Genetics Supplement Series*, [online] 7, pp. 438-440.

Abbreviations

CE	Capillary Electrophoresis
CODIS	Combined DNA Index System
Ct	Cycle Threshold
C _q	Quantitative Cycle
DI	Degradation Index
DNA	Deoxyribonucleic Acid
DOVID	Diffractive Optically Variable Image Device
ENFSI	European Network of Forensic Science Institutes
EU	European Union
IPC	Internal Positive Control
qPCR	Quantitative Polymerase Chain Reaction
NDNAD	National DNA Database
NGS	Next Generation Sequencing
NIDNAD	Northern Ireland DNA Database
OCG	Organised Crime Group
OVD	Optically Variable Device
OVMi	Optically Variable Magnetic Ink
PCR	Polymerase Chain Reaction

RFU	Relative Fluorescent Units
RMP	Random Match Probability
RT-PCR	Real-Time Polymerase Chain Reaction
SDNAD	Scottish DNA Database
STR	Short Tandem Repeat
STRidER	STRs for Identity ENFSI Reference Database
UV	Ultraviolet
WGA	Whole Genome Amplification

Chapter 1 Literature Review

1.1 Introduction to Currency and Counterfeiting

1.1.1 The Extent of Counterfeiting Banknotes and Legal Protections of Currency

Counterfeiting poses a very real threat to the integrity of banknotes and consequently to the degree of trust in banknotes as a secure method of payment. This applies to both public and retailers alike (de Heij, 2010a). Furthermore, counterfeiters may exploit the fact that not all retail sector employees are adequately trained with regard to banknote authentication and accordingly, may be targeted by criminals seeking to dispose of counterfeit currency (de Heij, 2010a). To combat this, the security printing industry and banknote issuing authorities invest considerable effort in the development and deployment of security features designed to keep ahead of emerging print technologies which are available to the general public, including criminals (de Heij, 2009 and 2010b). In all cases, the technical evolution of new security features must be accompanied by ongoing public awareness campaigns, so as to ensure that the authentication value of the new features is optimised (de Heij, 2009 and 2010b).

Manufacturing and circulating counterfeit currency is a major area of criminal activity. Investigating such crimes can be an arduous task given the sheer volume of counterfeits that are seized. The history of counterfeit currency goes as far back as the 4th Century BCE (Giovannelli et al. 2006). However, the earliest set of regulations dealing with counterfeiting stemmed from the Geneva Convention of 1929 at the International Convention for the Suppression of Counterfeiting Currency and Protocol (Geneva Convention, 1929). Every member state which signed the Convention document was bound by the International Treaty to prevent and prosecute those involved in the manufacturing and “uttering” of counterfeit currency (Geneva Convention, 1929). This was the first instance of an internationally motivated procedure to quash the production of counterfeit money. The agreement states that countries are not just responsible for maintaining the integrity of their own currency but are equally responsible for eliminating the production of all counterfeit currency.

Additional Regulations were implemented in Europe in the earlier 2000s to address the complications of the introduction of the euro as a universal currency. The 1998, 2000 and 2001 European Regulations and Decisions subsequent to the Geneva

Convention ensured a unified framework operating across Europe against counterfeiting (European Union, 1998, 2000 and 2001, Flegar and Radovanovic, 2013). All member states that adopted the euro currency are required to abide by these regulations. (European Union, 2001, European Union, 2014). The requirements include both rules on production of currency and also how notes and coins are taken out of circulation, including counterfeit notes (European Union, 2000 and 2001). The Directive also states what constitutes the illegal use of digital tools for counterfeiting as well as providing guidelines on the extent of sentencing for specific crimes. These include the lawful imprisonment of an individual for a maximum eight years for: manufacturing counterfeit currency, modifying legal currency or for the early introduction of legal unreleased currency into circulation all stated in Article 5, section 3 (European Union, 2014). A maximum sentence of five years is suggested for knowingly adding counterfeit currency into circulation or being involved in the movement of counterfeit currency, according to Article 5, section 4 of the Directive (2014). A recent example of the benefits the EU regulations and Geneva convention was provided in the detention of 8 suspects by Europol in 2016 (Europol, 2016a). These individuals were associated with a worldwide organised crime syndicate and were found to be in possession of €3 million worth of counterfeit notes. Notes manufactured by this group were identified as being in circulation in every EU country. This information provided weight for the prosecution case and highlights the effectiveness of having a European union wide network for investigations by Europol and the EU Central Office for Combating euro Counterfeiting (Europol, 2016a).

In the United Kingdom, sub sections 14 to 23 of part II of the Forgery and Counterfeiting Act (1981) provide that it is an offence for an individual to create a counterfeit banknote or coin with the intention to then attempt to pass it off as genuine, or simply to make the counterfeit without express permission from a lawful body, (that being the Treasury for the pound sterling). Furthermore, it is illegal to own currency that you believe to be counterfeit with the intent of passing it on as genuine. It is illegal to produce or own materials that the individual intends to use for the production of counterfeit currency or allow someone else to use such items for such a purpose. The Act goes further to state that any movement of counterfeit currency, written plan or agreement to make said counterfeits, is also illegal. Breaching any of these provisions can lead, on conviction, to a penalty of a minimum fine of £1000. In the past, cases have resulted in imprisonment for a period of 12 months for attempting to use counterfeit £20 notes (R. v Edirin-Etareri (Jamil)). More severe cases whereby an

individual was planning to make counterfeit notes resulted in 10 years imprisonment (R. v Hartley).

Counterfeit currency is often of such poor quality that it does not pose any true threat to a Country's economy given it can easily be identified and removed from circulation. That said Organised Crime Groups (OCGs) producing large quantities of high-quality counterfeit notes could result with a public loss of trust in banknotes. Normally, the only counterfeits that pose any true threat are the ones produced to a sophisticated level which closely emulate genuine banknotes (de Heij, 2010b). A significant percentage of euro counterfeits, emanate from criminal group activity operating around Naples, Italy (Donadio, 2012 and Scherer, 2016). In 2018, the euro system removed 301,000 counterfeit banknotes from circulation in the first half of that year (European Central Bank, 2018). A further 262,000 counterfeit banknotes were identified and removed in the latter half of the same year (European Central Bank, 2019). The €20 and €50 euro denomination notes were those most often counterfeited (European Central Bank, 2018 and 2019). Over 80% of counters withdrawn from circulation were lower denominations (European Central Bank, 2018 and 2019). These statistics rather than suggesting that the central banks' abilities to lower counterfeiting are lacking, highlight that the measures taken to detect and deter counterfeiting are working. The number of counterfeit notes must be assessed in context. In excess of 251,000 counterfeit euro banknotes were removed from circulation in the first half of 2019 (European Central Bank, 2019). Although this figure is not excessive, considering the twenty-two billion genuine banknotes in circulation at time of writing (European Central Bank, 2019), the damage is predominantly against the retail sector within the euro area. In addition to this, significant quantities of counterfeit banknotes are seized annually by police forces within and outside Europe, prior to these counterfeits entering circulation, i.e. without there being a financial victim. In the case of the pound sterling, the large majority of counterfeit banknotes are seized while in circulation, with 20,000 being seized before entering circulation and 175,000 counterfeit banknotes taken out of circulation in 2020 (Bank of England, 2022). It is reported in the United Kingdom that counterfeit pound notes totalled 103,000 notes in 2021, 72,000 less than in the previous year (Bank of England, 2022). In total the value of these notes was £2.7 million. The £20 note was evidenced as being the note most often counterfeited, there being approximately 74,000 counterfeit banknotes of this denomination. The figures disclose that the counterfeiting of the £20 note was so prolific it constituted just over 83% of the total number of all counterfeit sterling notes that year (Bank of England, 2019). This trend

of decreasing circulation counterfeit currency could be attributed to the reduced circulation of physical currency during the nationwide lockdown. However, the trend was also present in specific banknotes that new security characters had been introduced prior to the nationwide lockdown, such as the changing of paper to polymer for the £10 banknote (Bank of England, 2022).

1.1.2 The Anti-Counterfeiting Features of Banknotes

The quantity of counterfeit banknotes in circulation at any one time is small when compared to the number of genuine banknotes. However, the authorities in all countries continue to expend time and financial resource in ways to counter counterfeit currency. Many countries have implemented a variety of changes to manufacturing techniques in an effort to make it more difficult and expensive for criminals to emulate them (Sarkar et al. 2013). Inbuilt features introduced into genuine notes help both the public and banks distinguish a counterfeit from a genuine note. In the case of euro banknotes, there have been a series of two redesigns termed the first series, which began circulation in 2002 (European Central Bank, 2005) and the second series (or Europa series) that was introduced in 2013 (Marchand and Palazzeschi, 2014). This allowed for the introduction of newly developed security characteristics to be included as well as improve on the previous designs.

The key features introduced have to be such that they aid the general public in distinguishing a genuine note from one that is a counterfeit. Although not completely fail-safe, it has been established that 79% of counterfeits are distinguishable from genuine currency by the general public (van der Horst et al. 2016). Three levels of security exist which act as a barrier to counterfeiters producing an effective simulation of a genuine banknote.

1.1.2.1 Level 1 Security Features

Firstly, the level 1 security features comprise those aspects that can be examined by any individual without the need of specialist equipment (Berenguel et al. 2016). These incorporate characteristics that individuals with impaired eyesight can detect namely by feel or colour of the note (de Heij, 2009).

The initial feel of a euro banknote is crisp and is instantly recognisable by an individual (Berenguel et al. 2016). The exact process by which paper banknotes are manufactured before introducing the security characteristics is not widely available

due to the security risks. The notes' texture and sheen result from the initial manufacturing process of the paper using short cotton fibres (Flegar and Radovanovic, 2013, Mann et al. 2015). The type of paper used for banknotes does not fluoresce when placed under UV light, as can be seen in

Figure 1 where areas of blue can be seen (van Renesse, 1998). This distinguishes it from other commercially available paper which produces a light blue fluorescence when placed beneath UV light. This fluorescence is due to whitening agents used in the standard paper manufacturing process (van Renesse, 1998).



Figure 1. The front of a genuine €10 banknote under UV light highlights the European Union stars and triple coloured security fibres. The paper itself does not fluoresce (European Central Bank, 2014).

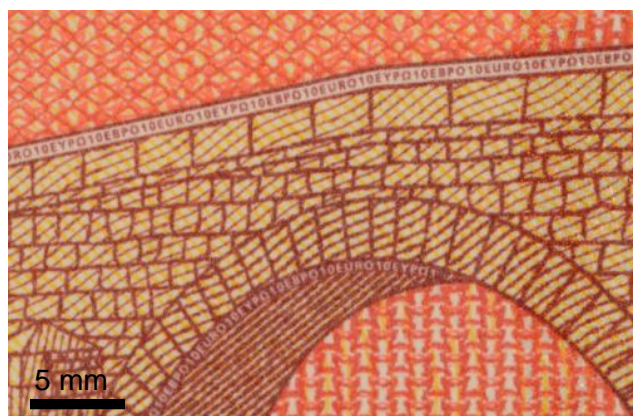


Figure 2. The offset printing detail can be seen on the bridge depicted on the back of a genuine €10 banknote (European Central Bank, 2014).

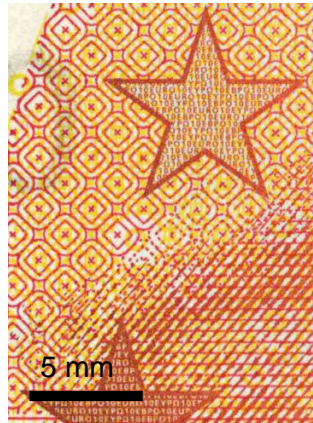


Figure 3. Stars featured on the front of a genuine €10 banknote, printed as part of the offset printed background (European Central Bank, 2014).

The tactile characteristics associated with banknotes are due to the intaglio printing process (Gillich et al. 2016, Hofman et al. 2014). Before the intaglio printing is applied to the note, offset printing applies the background imagery that forms the basis of the note's design, which can be seen in

Figure 2 (Soukup et al. 2009, Roy et al. 2010). This is achieved through several rolling printing cylinders that ensure an even spread of the ink is applied to the ink adhering print cylinder (Verikas et al. 2011). The use of multiple cylinders in tandem allows different coloured designs to build and align together on the paper after the application of each colour (Verikas et al. 2011, Soukup et al. 2009, Geusebroek et al. 2011). Similar to offset printing, the desired ink colour for the intaglio patterns is applied to a set of printing cylinders in a manner that produces a uniform thickness of ink before it is applied to printing plates (Hofmann et al. 2014). In this process a machine etched plate is used that allows the ink to make its way into the grooves of the printing plate through capillary action (Hofmann et al. 2014, Kyrychok et al. 2014, Funk et al. 2014). The excess ink is wiped away from the non-grooved area, avoiding unwanted patterning across the note or bleeding out of the ink (Hofmann et al. 2014, Kyrychok et al. 2014, Funk et al. 2014). The printing plates are then pressed against the paper substrate under several tonnes of force that helps the ink within the printing plates adhere to the substrate (Hofmann et al. 2014, Kyrychok et al. 2014). Intaglio printing is located on the edges of all the Europa euro notes both in the form of raised lines and incorporated in the printed designs themselves (seen in Figure 3). The orientation of such features helps visually impaired persons to assess the denomination of euro notes, given each denomination has a unique pattern (Felgar and Radovanovic,

2013, Funk et al. 2016, de Heij, 2009). Printing of this detail is only available to manufacturers responsible for the issuing of security documentation (Negru et al. 2017). Most paper notes incorporate an image embedded into the paper itself which is only seen when the note is placed in front of a light source. These features are more commonly known as watermarks (Figure 4). They are introduced into the paper at the wet end of the manufacturing process, using a process called cylinder moulding (Bicknell and Laporte, 2009, Chambers et al. 2015 and Flegar and Radovanovic, 2013). A watermark is essentially produced by varying the paper density in different parts of the image (Kumar, 2011, Chambers et al. 2015). Variations in the depth of the cylinder allows for the change in density of the paper when put under the pressure of the cylinder mould (Bicknell and Laporte, 2009). As well as the watermark, there is an embedded security thread in the notes, with the note's value visible on the thread, depicted in Figure 5 (Marabello et al. 2017, Flegar and Radovanovic, 2013 and Chambers et al. 2015). This can be seen by the naked eye (albeit faintly) but does not appear fully until light is transmitted through the note (European Central Bank, 2014). Security threads are often made of a polymer or metallic material, although in some documents it is polyester (Bicknell and Laporte, 2009, van Renesse, 1998). The possible addition of iron oxide pigment produces a thread of a dark black colouration, as in the first series of Euros (Marabelo et al. 2017). The exact materials used, and techniques implemented to produce banknotes are often withheld from public knowledge, to further protect the currency from counterfeiting.



Figure 4. The Europa portrait and value of the banknote can be seen when viewed in transmitted light. (European Central Bank, 2014).

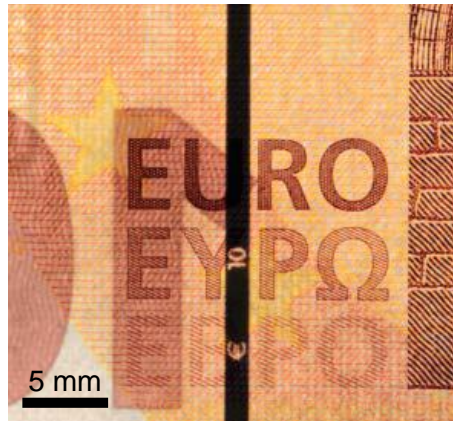


Figure 5. When viewed in transmitted light the security thread is visible with the denomination present in the thread in a genuine banknote (European Central Bank, 2014).



Figure 6. The holographic stripe on the front of a genuine Europa series €10 banknote (European Central Bank, 2014).

1.1.2.2 Level 2 Security Features

A key security feature is the Diffractive Optically Variable Image Device (DOVID) that appear as a partial foil strip or a foil stamp hologram that exhibit diffractive properties when tilted (Figure 6). The holographic effect is achieved using nanoscale diffractive grating (Staub and Tompkin, 2000, Tamulevičius et al. 2018). The specific orientation and shape of the nanoscale structures allows for the reflection of varied colours of light from different viewing perspectives (Staub and Tompkin, 2000). The engineering and design used in generating the holograms lead to an easy to recognise feature and thus a barrier to counterfeiting. Achieving an equivalent metallic structuring requires expensive and specialised equipment (Tamulevičius et al. 2007 and 2018). An example of this detailed feature can be seen in the foil viewing window with a

portrait of the Greek mythological figure, Europa (seen in Figure 6), that the new series is named after (Kinegram®, 2019). These are key features readily recognised by members of the public and used by them in authenticating notes (de Heij, 2010b). The Europa series of notes from 2013 incorporates several additional visual security features. In all the Europa notes, the numerical value of the note is depicted in the bottom left-hand corner (Figure 7) using what is generically referred to as the emerald (Papadimitriou, 2013). When the note is tilted, a “rolling bar effect” can be seen moving down the number (seen in figure 8) as it changes colour from green to gold (Papadimitriou, 2013, de Heij, 2010b). This feature was first introduced in the 10 Yuan banknote in China (Papadimitriou, 2013, de Heij, 2010b). The specific colour change is to aid recognition but also means notes with this feature are almost impossible to counterfeit without reproducing the exact manufacturing techniques employed by the banknote producer (Papadimitriou, 2013).



Figure 7. The numerical value on the bottom left of the Europa series of notes, in this image a €10 banknote, under visible light a “rolling bar effect” can be seen if the viewing angle is changed (European Central Bank, 2014).

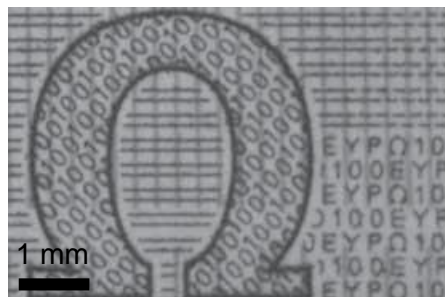


Figure 8. A genuine €100 banknote from the first series under magnification, showing the numerical value of the note is incorporated into the design of the note in microprinting (Flegar and Radovanovic, 2013).

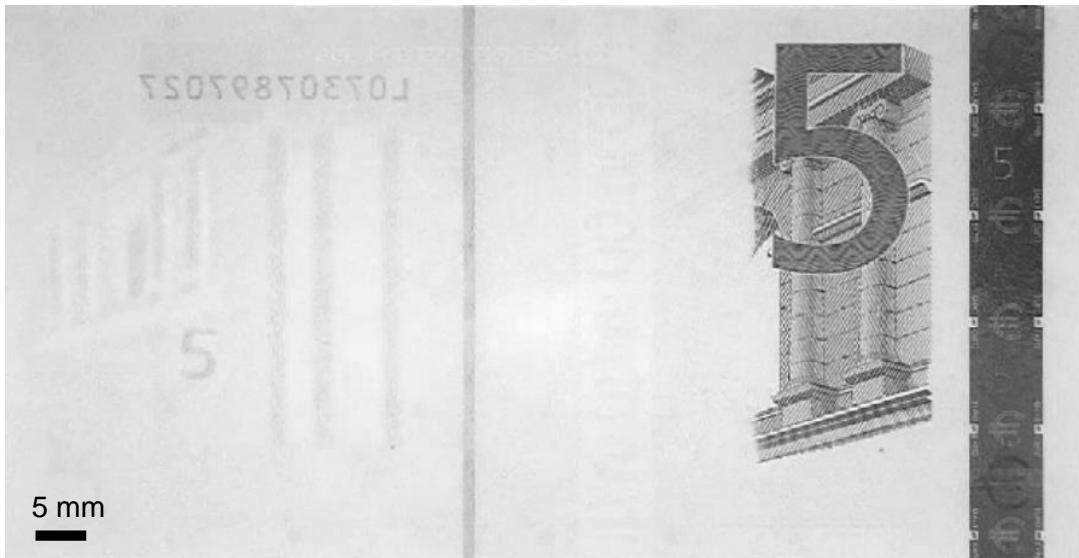


Figure 9. Under infrared light a genuine €5 banknote's watermarks, serial number, metallic thread, holographic strip and parts of the artwork can be seen (Bruna et al. 2013).

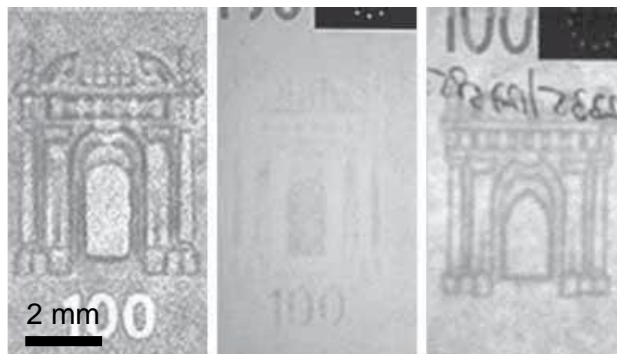


Figure 10. The two images on the left-hand side are taken from a genuine €100 banknote, with transmitted light through the note (left) and with reflected light (centre). The image on the right is an example of a counterfeit with transmitted light through the note (Flegar and Radovanovic, 2013).

Level 2 security features require specialised equipment to see them and as such are deployed in specialised machinery such as cash deposit or vending machines which verify notes (Brown 2004, Flegar and Radovanovic, 2013, Heinonen, 2015). An example of such a secondary level security feature is the metallic thread which runs through the note (Figure 5 and Figure 9). The machine can read the strip which incorporates a magnetic barcode which encodes the note's value (Heinonen, 2015, de Heij, 2010b). Although this feature is not used by the public, the thread itself is visible to the naked eye when held to a light. This of itself acts as a basic verifying feature (de Heij, 2010b). Some of the more basic hidden security features can be located using a magnifying glass or microscope. Microprinting is a level 2 feature

most obvious to the public as it can be faintly seen without the need of a microscope. Microprinting is incorporated into the larger printed objects on the note such as the number value or the art depicted on the note using the offset printing process (Heinonen, 2015, Flegar and Radovanovic, 2013). Some of the microprinting can be seen at 0.8 mm tall but the 0.2 mm printed lettering is impossible to see without using specialist magnifying equipment. (Flegar and Radovanovic, 2013). The minute sizing of the lettering and the detail achieved (seen in Figure 8) at this scale makes it currently difficult to replicate this feature without utilising the same mechanical process as in the genuine notes' manufacture (Flegar and Radovanovic 2013, van Renesse, 1998). However, in time the possibility of more sophisticated intaglio printing becoming available to the public is a genuine concern (Corzo et al. 2016).

The inclusion of specialist inks used in the printing process cause visual changes which become apparent under different light sources. Infrared light discloses specific changes allowing the DOVID strip to be visible or partial sections of the depicted artwork to appear. By way of example, the first series €5 banknote (Figure 9) when viewed under infrared light only has the foil strip and the number five alongside part of the background artwork visible (Bruna et al. 2013). The serial number on the opposite side of the note and the magnetic strip can be seen faintly (Bruna et al. 2013). Other features are distinguished when viewed under UV light.

Figure 1 shows some of the ink used for specific parts of the note's artwork becomes fluorescent when placed under various wavelengths of UV light such as a red-orange fluorescence (Berenguel et al. 2016, Bünzli, 2010 and 2017, Steudel et al. 2018, Suyver and Meijerink, 2002). This security property is not restricted highlighting properties within inks but can identify the fibres incorporated into the paper. In the first series of euro notes these fibres generated green, orange and blue fluorescence under UV light at a wavelength of 365 nm (Mutanen et al. 2003). The Europa series of notes include fibres in three colours: red, blue and yellow. Each fibre fluoresces under UV light of a wavelength of 365 nm (European Central Bank, 2014). These fibres are introduced into banknote paper in such a way that they are completely random in their distribution (van Renesse, 1998).

Lastly, the level 3 security properties are fully covert and confidential, known only to the Central Banks. This is to prevent the replication of these properties. These tend to be features incorporated at the point of the banknotes' paper manufacture before

the application or introduction of the primary and secondary security features (Berenguel et al. 2016).

1.1.3 The Manufacturing of Counterfeit Banknotes

The trend monitored following the release of new banknotes, is that there is an initial decrease followed swiftly by an increase in counterfeit note production, emulating the new security features (de Heij, 2010b). Such changes are to be expected as counterfeiters look to simulate or emulate the new characteristics to more successfully fool individuals not familiar with the newly introduced notes. Counterfeiters often 'attack' the security features by emulating them using cheap stationery or counterfeit composites acquired online such as digital images for printing or stick on holograms. The production of counterfeit notes can be linked to personal use by criminal groups, individual use, or the forward selling of the counterfeits themselves (Ciancaglini et al. 2013). Online acquired US dollar banknotes from the darkweb for example, can fetch for 25% to 50% of their face value (Ciancaglini et al. 2013). These counterfeit notes claim to simulate the microprint, security thread, watermarks and the different inks used in genuine notes (Moore and Rid, 2016). The easy access to counterfeit components and counterfeit notes themselves present a threat to public confidence in euro banknotes. Counterfeit euro banknotes do not need to be made to the same quality of those that the central banks of the Eurosystem, they simply have to convince a busy shop owner or blend into a handful of notes during a transaction (Prime and Solomon, 2010, Itrić and Modrić, 2017, Bicknell and Laporte, 2009). Counterfeiting is not likely to be reduced with the increase of ecommerce as the use of physical currency will still be needed for many years to come. This is evident as many countries rely heavily on physical currency such as Japan's Yen with 18.9 billion banknotes in circulation (Bank of Japan, 2022) or still use a mixture of digital and physical currency regularly such as the UK with 4.6 billion banknotes of Pounds Sterling in circulation (Bank of England, 2022).

A forensic examiner looking at a potentially fake document, must first identify what characteristics are dissimilar to those found on a genuine example (Bicknell et al. 2009). Commonly, the intaglio print effect of counterfeit notes is simulated to give the distinctive feel a handler can expect from a genuine note. Techniques to achieve this to the same quality are mostly beyond the scope of the general public, but counterfeiters can emboss the desired print onto an offset printed design to closely replicate intaglio printing (Pfeifer et al. 2016, Negru et al. 2017). The machinery to

simulate this effect at a low quality is available to buy, providing an avenue for counterfeiters to produce a more convincing product (Negru et al. 2017).

If the counterfeiter is looking to produce a more sophisticated counterfeit they can incorporate UV inks into the printing process (Andres et al. 2014). Whilst this simulates the features of a genuine note when placed under UV light, the inks often used can appear much brighter in terms of the intensities of the colours under UV light (de Heij, 2010b). UV light can also reveal the use of standard printing paper given standard paper often fluoresces white when placed under UV light. The security paper used in genuine notes does not demonstrate this property. The difference is due to wood-based cellulose used in most commercial or high-quality plain office paper, whereas cotton fibres are used in the production of paper banknotes (van Renesse, 1998, Marabello et al. 2017). It must be borne in mind that rag paper composed of a cotton cellulose mixture that can be bought in stationary retailers, may be a more convincing substitute (Prime and Solomon, 2010).

Among one of the most counterfeited security counterfeits are the notes' watermarks. These are purposely designed to make them hard to reproduce accurately. However, given this feature is used by shop keeps or consumers to validate notes, attempts are made to simulate the feature in various ways. The simplistic approach adopted is by using two layers of paper to produce the counterfeit banknote. This technique allows the counterfeiter to print the watermark onto one side of the paper before it is adhered to another layer giving the illusion of an internal watermark. From the literature it is not clear as to what adhesive is used to adhere the paper layers of a counterfeit banknote. However, this is likely to reduce the information available to the public.

The use of a double layered counterfeit note also allows for the inclusion of an embedded thread (Voinea et al. 2015). The skill and time needed for to manually position the thread in each note means the thread is sometimes drawn or printed (Marabello et al. 2017, Chambers et al. 2015). The same is true for the positioning of a watermark as well as the level of detail needed for this to appear genuine (Flegar and Radovanovic, 2013). A poorly drawn watermark example can be seen in Figure 11. A series of raids carried out in 2016 in Lithuania, resulted in the seizure of €3 million worth of unassembled counterfeit banknotes discovered in houses and vehicles. This seizure included unprinted paper that had the watermarks and security threads already incorporated. Machinery for offset and laser printing, UV and offset

inks, as well as €50 dot matrix holograms were confiscated. The counterfeiters had already succeeded in putting some low-quality notes into circulation. Even though they were relatively poor quality, they managed to circulate across the EU, eventually being detected in 15 of the 27 European member countries (Europol, 2016b). This case example emphasises the broad reach counterfeiting can have, including the potential difficulties in identifying the source when they are found across such a widespread geographical area.

Some counterfeiters may not include a watermark in their product and instead focus on the easy to spot OVDs in an effort to fool busy note handlers (de Heij et al. 2010b). OVDs are one of the most prevalent features in banknotes for the general public to identify (de Heij, 2010b). Due to the sensitive nature of OVD production the information on processes involved in the production of the genuine characteristic is not widely available. This is likely to reduce potential harm such information possesses. However, the production of lower quality holograms is accessible to the general public. These OVDs, previously had been imitated through cheaper metal foils that were heat stamped onto the paper (Negru et al. 2017, Hartl et al. 2013, Bicknell and Laporte, 2009). More recently there has been the use of dot matrix holograms that emulate the authentic OVDs (Boyle et al. 2002). These can be bought on the internet as sheets of several 'stickers' that can then be manually applied to fabricated note (Boyle, 2002, Lancaster, 2004). This allows for the application of the hologram securely to the paper surface in a similar manner to which a modern self-adhesive stamp is applied (Ruprecht et al. 2021). As of yet there is no research indicating the types of adhesives used by OCGs to produce these adhesive dot matrix holograms. Europol searches have commonly found adhesive holograms in Europe such as a series of searches in 2019 in Portugal that resulted in taking down of the second largest counterfeit currency group in Europe (Europol, 2019). With so many routes of attack for counterfeiters, and the constant upgrading of technology, the central banks of the world are always developing new hurdles for counterfeiters to overcome in an effort to stem the flow of counterfeit currencies.

1.2 The Nature of DNA and Banknotes

More reliable and objective means of attributing counterfeits to a common source is required. Ideally, this should individualise the human operator(s) in preference to the machine as counterfeiting operations frequently employ multiple printers at a single location producing the same counterfeit type, albeit with slightly different print

characteristics (Donadio et al. 2012, Pfeifer et al. 2016). New approaches are required to recognise links between confiscated counterfeit items and the criminal groups who produced same. One route worthy of examination is analysis of trace DNA (deoxy-ribose nucleic acid) evidence (Barash et al. 2010, Subhani et al. 2019). It is hypothesised that during the counterfeit manufacturing process, DNA from the manufacturer is transferred and trapped by adhesives used in the counterfeit production. The DNA fixed in the adhesive matrix may be protected from any external DNA contamination which results from the counterfeits circulation. The technique used to separate the adhesive will ultimately destroy the counterfeit, but it may generate an evidential connection to those involved in its manufacture.

Studies have investigated the persistence of DNA on the surface of banknotes but to date there are no studies to evidence if DNA can persist between the layers in banknotes, particularly within pockets in the adhesive matrix. Research by van den Berge et al. (2016), established that mixed profiles of between 2 to 6 people could be identified on the surface of notes. However, the research only examined what are assumed to be genuine banknotes and external DNA deposits. The researchers' findings do not necessarily suggest that DNA from a counterfeiter can persist on the surface of a counterfeited item once in circulation. The research could have been extended to include additional note denominations. Some notes, particularly those of lower value are used more extensively than others (European Central Bank, 2018 and 2019) and as such could have varied persistence of DNA. Genuine banknotes are unlikely to hold any encapsulated DNA pockets due to the stringent manufacturing processes used in their production. Although the researchers used 52 samples, the sources of the note samples were limited. The notes were removed from 13 individuals each providing an average of 4 notes. A more significant result could have been achieved using an increased sample size. Details as to the year of issue of the notes examined should have been supplied as this suggests how long they may have been in circulation. Notwithstanding these deficiencies, the results identify the risk of contamination by innocent bystanders who do no more than handle the notes whilst in circulation. The risk of contamination from innocent individuals of any DNA found within a counterfeit banknote when it is extracted is therefore a consideration.

Raymond et al. (2009) analysed the persistence of trace DNA over time when left in different environments. Their comparisons were between samples left within a lab setting and those taken from an outdoor environment. They found that the successful acquisition of a complete profile diminished rapidly, over a period of a few weeks

when the trace DNA was left on outdoor environment objects. In comparison, samples of trace DNA persisted in lab stored samples for nearly six weeks. The research was conducted in the context of trace DNA in burglary situations, but the findings highlight the difficulties which exist in recovering a profile from surfaces that are exposed to environmental variables (Raymond et al. 2009). Counterfeit notes are sometimes in circulation for some time and as such the possibility of introducing other DNA profiles linked to innocent bystanders is increased. DNA has been found to persist for several days on surfaces (Quinones and Daniel, 2012). The encapsulation of DNA in the adhesive matrix of counterfeit banknotes may provide a viable source of intact DNA, uncontaminated by those who have innocently handled the notes.

The introduction of banknote security features have provided counterfeiters with significant challenges in producing counterfeit notes which would be accepted as genuine by both the public and commercial institutions. That said, the key issue which remains a problem for authorities looking to stamp out counterfeiting is the fact that it is difficult to trace counterfeit notes to the point of origin once they have been released into general circulation. Examination of counterfeit notes handed into central banks which look similar to one another have, when examined in detail, been shown to demonstrate varying characteristics (Božičević et al. 2012). The variations which existed in counterfeited notes that may have been manufactured by the same group of individuals made them easier to link to any single source. This is due principally to the fact that counterfeiters do not pay as much attention to the uniformity of each batch of notes they produce as is demanded by the treasury (Hofman et al. 2014). Counterfeiters use machinery which can achieve only limited accuracy levels (Božičević et al. 2012).

Traditionally, when most counterfeits were offset printed (Pfeifer et al. 2016), technical analysis of the printed image and in particular print defects associated with the origination artwork was sufficient to determine if two or more counterfeits came from the same source (Gillich et al. 2016, Bicknell et al. 2009). The advent and increasing dominance of digital printing (in particular inkjet) means that this is no longer the case (Berenguel et al. 2016). This scenario is exacerbated by the number of makes and models on the market and the rapidly evolving nature of the technology, which in some cases has effectively neutralised the value of traditional security features, e.g. microtext and rainbow printing (Brown et al. 2017). Due to the accessibility of cheaper digital printing, OCGs have been found using the modern inkjet approaches and older printing process to increase production. An example of which happened in a case

across Italy and France where a crime syndicate was dismantled after successfully producing and distributing 45,000 €100 counterfeit banknotes causing €4.5 million worth of damage in that denomination alone (Europol, 2018). If not for a tip off to the French National Police, the operation would likely have continued to cause financial damage to the economy (Europol, 2018). Cases like this highlight the need for forensic techniques to help reduce the damage caused by OCGs and help provide further evidence for criminal proceedings. As with most OCGs, the production and use of counterfeit currency is used to facilitate other illegal activities such as drug dealing. One such case in 2022 had counterfeit 50-euro banknotes of a value of €25,000 seized from a series of properties that was primarily being used to help fund production and distribution of marijuana in Spain (Europol, 2022). It can be said that establishing the source of counterfeit currency may also lead to the dismantling of other OCG activities.

Given its evidential significance the holographic patches and strips on the counterfeit euro banknotes may be worthy of forensic analysis. These elements of a counterfeit banknote manual application most likely in a non-sterile environment. This distinguishes counterfeits from notes produced legitimately in sterile conditions. Given the adhesive nature of these dot matrix holograms, DNA may be transferred from the individual applying the hologram to the counterfeit during application. It may also be possible to source trace DNA profile from within the main body of a counterfeit note. The DNA fixed in the adhesive matrix may be protected from any external DNA contamination which results from the items' circulation. The technique used to separate the adhesive will ultimately destroy the counterfeit, but it may generate an evidential connection to those involved in its manufacture. Counterfeiters regularly use multiple layers of paper to replicate attributes such as the watermarks which exist in genuine notes (Voinea et al. 2015, Takolo et al. 2015B). By using two pieces of paper when creating a note, a counterfeiter can print a simulation of a watermark on one side of the paper and include an internal simulation of a metallic thread. The two layers are then glued together providing a note with potentially deceptive security features (Voinea et al. 2015). Utilising this technique provides a simulated watermark and metallic thread which appear when the document is viewed in transmitted light, much like a genuine banknote. These double layered counterfeits may provide a valuable source of a suspect's DNA profile (Voinea et al. 2015). During the manufacturing of double layered counterfeits, some of the counterfeiter's DNA may get trapped within the adhesive layer during production. The difficulty is in successfully extracting a potential suspect's DNA profile from the adhesive matrix

without compromising its integrity to allow the evidence to be used by the prosecution in a court case.

There is the potential of removing any external DNA that could contaminate the downward DNA analysis through the use of pre-swabbing of the surface (Ruprecht et al. 2021, Haas et al. 2021). Haas et al. (2021) used double distilled water to wash the external surface of postcards sent during the First World War. This ensured that there was no contamination present in their samples which were highly sensitive due to the age of the saliva deposits being 100 years old. Although in Ruprecht et al. (2021) state that there is unlikely to be a risk of contamination after the stamp has been placed firmly on the paper substrate they still state remove of any external contamination is still advised in case work. However, research by Ng et al. (2007) did not take this approach when investigating direct DNA extraction of envelope flaps. Instead, they opted to introduce cuttings of the flaps directly into the DNA extraction process before moving onto the downstream processing of the DNA sample for profiling. From their findings it was not reported that there were any contamination issues with either the mock samples or case work samples that were processed in this way. It could be inferred therefore, that the removal of any external biological material may be less of a concern when dealing with methodologies that are targeting the internal aspects of adhesive samples through such processes as swabbing. In all the above examples the substrates have been paper porous based surfaces with an adhesive. As of 2022, there has been no research directly comparing the persistence of DNA on paper-based and polymer-based banknotes. Champion et al. (2021) did investigate the use of Diamond™ nucleic acid dye on both types of banknote substrate. The researchers found that there was a difference in the amount of cellular material between polymer and paper but this could easily be down to the difficulties of the visualising steps used (which had to be adjusted for the paper banknotes). It would be expected that the amount of DNA would vary as there has been shown that the type of material trace DNA is deposited on can affect its transfer (Attketbi and Goodwin 2019, Daly et al. 2012, Hefetz et al. 2019).

Due to the low expected concentration of DNA present on trace DNA, it would be expected that gaining an STR profile would prove difficult when considering DNA samples sourced from adhesive (Ng et al. 2007). In the case of Ruprecht et al. (2021) the expected amount of DNA for stamps was not the case when looking at the number of STR loci detected, with a majority of samples being above the EDNA upload threshold, some of which had 16 loci present. Hypothetically, given the manual

contact of counterfeiters when they construct the counterfeit note their fingerprints may be deposited between the layers in a similar manner to other surfaces investigated in forensic cases such as stamps (van Oorschot et al. 1997, Haines et al. 2013, Ruprecht et al. 2021). The adhesive nature of the glues used in the notes' construction may capture the fingerprints but distort them to the extent that they cannot be used for a match search. Any fingerprints whether they are damaged or intact may still contain genetic material worthy of examination and cross matching as was shown by Haines et al. (2013). They used SYBR Green I effectively to demonstrate the presence of DNA in fingerprints. Further research has shown that recovering the DNA present in fingerprints is beneficial to forensic cases. The DNA can be recovered from the application of a variety of fingerprint lifting techniques (Templeton and Linacre, 2014, Lowe et al. 2003). Recent research by Subhani et al. (2019) has expanded the research demonstrating that DNA profiles can be successfully acquired utilising most standard fingerprint lifting techniques. Furthermore, they identified that there was no statistically significant variation in the success of acquiring DNA profiles regardless of the different fingerprint lifting techniques used. The evidential potential of extracting DNA profiles from fingerprints has promoted the development of specialised DNA kits which optimize the extraction process (Kopka et al. 2011). Previous research has demonstrated successful extraction of DNA profiles from fingerprints (Subhani et al. 2019) or even latent contact points is possible (Balogh et al. 2003). The same may be possible and techniques may be developed to extract profiles from encapsulated DNA in counterfeit banknotes.

1.3 Sources of DNA and Recovery Processes

The resulting DNA profile established from a counterfeit banknote could be a robust means of linking an individual to a case, or at least identifying a common source for counterfeit items (Butler, 2006). The process of extracting and profiling any sample can be automated to save time, but the initial recovery of the suspected DNA source must be carried out by a specialist forensic examiner (Phillips et al. 2012, Guo et al. 2017). DNA extraction from bodily fluid and hair samples has become a widely used forensic process. However, the value of trace DNA is often overlooked. Gill and Budowle define trace DNA or low template DNA, as being a DNA sample of 100 picograms (Gill et al. 2001) to 200 picograms (Budowle et al. 2009A). The source of these levels of trace DNA is not currently fully understood. Recent research has identified that the likely source of trace DNA in fingerprints is a mixture of corneocytes

(Burrill et al. 2021a) and cell free DNA contained in sweat (Burrill et al. 2021b). Corneocytes are epidermal skin cells that have cellularly differentiated to lose their cell nucleus and replaced parts of the cell wall with keratin, termed cornification (Bragulla and Homberger, 2009). Although corneocytes may have lost their nucleus, they still contain degraded fragments of DNA that can be profiled to a varying degree of success (Burrill et al. 2021a).

The general consensus of forensic geneticists is that these samples are at such a low concentration of DNA, that they are susceptible to being missed in analysis. The loss of such evidence can be a result of higher concentration DNA profiles overpowering the weaker trace signals (van Oorschot, 2010). Contaminants from the evidence (Bright and Petricevic, 2004) or the material composition of the evidence can affect the persistence of trace DNA over time (Meakin et al. 2017, Goray et al. 2012, Raymond et al. 2009). In an effort to compensate for this, examiners have increasingly used tapelifts (Barash et al. 2010). By first lifting a partial sample from the area of interest, the risk of contamination or damaging the material evidence is reduced (Barash et al. 2010). The resulting tapelift can then be used for the DNA extraction process, either by swabbing the adhesive side of the tape (May and Thomson, 2009) or by direct extraction from the tapelift (Forsberg et al. 2016, Joel et al. 2015). Some studies have looked to remove the adhesive from tape types using either swabbing or a serrated approach using a solvent such as hexane (Steadman et al. 2015). The researchers' findings indicated that although scrapping the adhesive away from the tape was successful in removing a large portion of the adhesive, this was not dissolved in the applied extraction methodology and resulted in variable results in terms of quantifiable DNA. The encapsulation of any present DNA in the adhesive likely inhibited the ability to effectively extract any present DNA. This would suggest that the swabbing of an adhesive surface is one of the most optimum DNA recovery methods, especially when including a solvent for the active recovery of any DNA present. Swabbing technique can also vary the outcomes of the recovery of DNA evidence. Previous research has highlighted the variable results depending on the implementation of single swabbing and double swabbing. Double swabbing consists of the initial swabbing of a piece of evidence followed by a secondary swab to recover any remaining potential evidence (Hedman et al. 2020). Often the primary swab is soaked in a swabbing agent such as water or triton-x (Thomson and Foran, 2012) but the second swab can either be dry or also soaked, depending on the evidence being evaluated (Hedman et al. 2020). Acetone has also been used the swabbing of electrical tape used for improvised explosive devices which led to an

increase of 70% in DNA recovery (Feine et al. 2017). Although in these cases the sample preparation has led to an improved success rate in acquiring a STR (short tandem repeat) profile, other techniques may cause downstream negative effects on the DNA analysis. As shown by Peterson and Kaplan (2011), it is possible that techniques to recover DNA may in fact be causing binding issues for the DNA extraction step leading to a loss of yield. However, this has not been shown in Chelex resin (Tobe et al. 2007) and phenol chloroform (Poon et al. 2009) extractions that do not rely on the binding of DNA molecules to facilitate extraction. The techniques implemented in tapelift DNA analysis could be extrapolated to affect the extraction of DNA from the adhesives which exist in counterfeit banknotes. Extracting DNA from an adhesive matrix could have further implications in forensic cases involving adhesive substances and trace DNA.

1.4 Visualisation of Trace DNA

A growing field in forensic trace DNA work has examined the use of a non-toxic DNA dye that was originally used for gel electrophoresis (Haines et al. 2015). Known as Diamond™ nucleic acid dye, it is proving a useful tool as it is able to permeate the cell membrane and bind to DNA leading to a fluorescent effect. It does this through its minor groove binding chemistry that actively binds to the DNA backbone (Haines et al. 2015). This has led to several researchers applying it to trace DNA on surfaces such as on fingerprints before swabbing (Kanokwongnuwut et al. 2018a) or lip prints (Kanokwongnuwut et al. 2019a). In highlighting the DNA present on a surface, a forensic examiner is able to swab areas where DNA has been shown to be present. However, although the dye has shown promise while using fingerprints on glass slides and in DNA solutions, it has not yet been successful in visualising DNA on the adhesive of counterfeit holograms. A set of two alternative approaches have been hypothesised to further establish the use of the dye on counterfeit banknote layers. Firstly, it has been shown that the fluorescence from the dye binding to DNA can be visualised on swabs (Kanokwongnuwut et al. 2018a and 2018b). Instead of adding the dye to the hologram directly, it could instead be placed on a swab that has been used to swab an adhesive layer with xylene, freeing the DNA from the adhesive. Research also suggests that the dye could be used to highlight areas of evidential value of evidence tapes (Cook et al. 2021). The researchers found that the use of Diamond™ nucleic acid dye was successful to a varying degree in the visualisation of deposited DNA depending on the tape types. This would suggest that the successful visualisation of DNA Diamond™ nucleic acid dye can vary according to

different substrate types and adhesives indicating more research is needed in other areas such as counterfeit banknote components. Other fingerprint enhancement techniques have been used to target swab areas of interest without specifically targeting the presence of DNA. 1,2-indandione fingerprint enhancement is one such reagent commonly used in the application of highlighting ridge detail in porous based fingerprint evidence (Nicolasora et al. 2018). Instead of highlighting genetic material, the reagent reacts with present amino acids that allows for the fluorescence of ridge detail within a fingerprint (Assis et al. 2022). However, fingerprint enhancement reagents such as 1,2-indanedione have been shown to be detrimental to downstream DNA sampling (Lee et al. 2019). The use of diamond dye could therefore provide a potential methodology to target swab areas of evidential value within the adhesive layers of counterfeit banknotes without inhibiting the downstream DNA analysis.

1.5 DNA Extraction

To obtain a DNA profile from a sample, it must first be extracted from the source. This source may be one of many forms: hair, skin cells or as previously mentioned, from fingerprints. Dealing with such minute pieces of evidence requires the expert understanding of a forensic examiner to both locate and identify same. It can be worth all of the time and effort to locate such evidence given the impact having such evidence holds for a legal case. The importance rests in what they contain at a molecular level, DNA. This barcode of information, which is unique to every individual, comprises four bases, adenine, guanine, thymine and cytosine (Cowell et al. 2015). The varying order of the bases provides a unique variation in each person's genetic code. Forensic examiners have in their armoury a wide repertoire of extraction methods to apply to whatever type of DNA evidence is available.

Polymerase chain reaction or PCR is a crucial reaction step in DNA profiling that involves replicating specific sections of the genetic code, creating a more concentrated sample of that replicated locus (Alaeddini, 2012). It has been demonstrated that PCR works without the need for extracting DNA from swabs. Notwithstanding this, for most forensic examiners, samples need to be extracted (Templeton et al. 2015). The reason for this tends to be to ensure removal of PCR inhibitors that can prevent the successful acquisition of a profile or profiles from any sample. This is particularly true in cases where testing trace DNA (Hu et al. 2014, Barbisin and Shewale, 2010, Samsuwan et al. 2018). Examples of PCR inhibitors are found in common source forensic DNA samples such as haemoglobin in blood

(Caputo et al. 2016) and indigo dye in jeans (Pîrlea et al. 2016). The main extraction technique used by forensic examiners involves using silica-based or solid phase spin columns such as the QIAamp kit from Qiagen. Extraction using this technique has been used to extract DNA of a quality sufficient to facilitate the production of DNA profiles from 55-year-old skeletal remains (Lee et al. 2010). The silica membrane in the spin columns allows for the selective filtration of any potential inhibitors in the sample by shifting the pH (Chancon-Cortes and Griffiths, 2014 and Boom et al. 1990). The change in pH forces any genetic material to temporarily bind with the silica membrane, leaving any inhibitors or contaminants to be centrifuged through the filter (Chancon-Cortes and Griffiths, 2014 and Boom et al. 1990). The genetic material in the column can then be spun out into an Eppendorf by altering the pH further through solutions (Chancon-Cortes and Griffiths, 2014 and Boom et al. 1990). Silica spin columns present a reliable and automatable approach to DNA extraction (Phillips et al. 2012). However, when extracting degraded DNA, short-fragmented DNA below 120 base pairs can be lost during the membrane washes (Carter and Milton, 1993). This poses a problem as degraded DNA containing STR loci that are shorter than this threshold could be lost through the matrix membrane (Alonso et al. 2018). A further potential problem is that large sequences may be broken apart by the silica matrix (Schiebelhut et al. 2017, Green and Sambrook, 2018). DNA also permanently binds to the silica membrane, removing it from any further analysis (Shaw et al. 2009). Furthermore, samples may not be appropriate for the silica membrane to filter given their viscosity, or because there is large a quantity of debris present (Cartozzo et al. 2018). Magnetic bead extractions use the same chemistry except the silica particles are attached to magnetic beads that allow the manipulation of the sample and extracting media through the washing steps (Stoop et al. 2017). This may be alternatively used to the spin column as it allows for more viscous or detritus filled samples to be processed (Harrel et al. 2018). Magnetic bead extraction has also been shown to have a higher recovery rate of short fragments (Rohland et al. 2007). The ease of use without relatively harmful reagents when using silica-based extractions, make them commonly used in forensic casework (Nimbkar and Bhatt 2022). However, silica-based DNA extraction is one of the most expensive of all the extraction techniques available (Schiebehut et al. 2016). As an alternative, resin-based extractions can be carried out such as Chelex bead extraction. DNA samples are produced using this technique through the introduction of styrene divinylbenzene copolymer beads that have an affinity to metallic contaminants present in the source sample (Walsh et al. 1991). The benefit of this technique is that the overall cost of each extraction is greatly reduced. It is a simpler process than the multiple extraction

tube changes required for silica column extractions (Pîrlea et al. 2016 and Lounsbury et al. 2012). Chelex bead extraction has been shown to be more effective at removing inhibitors such as the clothing dye phthalocyanine (Pîrlea et al. 2016). They found that Chelex extraction was successful in removing phthalocyanines, common denim dyes that inhibit processes in a PCR. Due to the risk of diluting the sample, Chelex is not often applied to trace DNA samples (Singh et al. 2018). However, the use of filter columns or a DNA precipitation step mitigates this issue (Norén et al. 2013, Singh et al. 2018). Recent research has utilised these to successfully acquire profiles from trace levels of DNA (Norén et al. 2013). Chelex extraction could prove a useful extraction technique when dealing with adhesive substances as the beads primarily act to remove inhibitors without any interactions with potentially encapsulated DNA (Walsh et al. 1991). The addition of solvent such as xylene would be required to help dissolve the adhesives present (May and Thomson, 2009). This process could be coupled with the scraping off of adhesive matrix (Ng et al. 2007) who did not consider the use of a solvent to help dissolve inhibitory adhesive in the examination of DNA from envelope adhesive flaps. As an alternative the adhesive side could be swabbed using a xylene (or other solvent) loaded swab that could then be extracted (May and Thomson, 2009). This extraction technique would avoid DNA on the non-adhesive surface of the counterfeit banknote that has been handled by innocent bystanders, such as cash handlers or examiners of the central banks, who analysed the note (Quinones and Daniel 2012). Solvent swabbing could be a useful technique to avoid any cross contamination from other points on the counterfeit banknote when it comes to the extraction step.

One of the most reliable extraction techniques that forensic examiners can use is organic extraction or more specifically termed: phenol chloroform extraction (Cartozzo et al. 2018, Kus et al. 2016). The use of phenol chloroform allows for the separation of genetic material in the sample using the varied solubility of genetic material and contaminants such as proteins. The proteins and lipids are separated by centrifugation into the organic and interphase layers while the DNA lies in the upper aqueous portion (Green and Sambrook, 2017, Cartozzo et al. 2018). The upper aqueous layer can then be removed and mixed with ethanol or isopropanol to force the precipitation of the present DNA, allowing it to be centrifuged to form a pellet (Tan and Yiap 2009). The use of phenol chloroform is dangerous as phenol and chloroform are toxic and phenol is flammable but not very volatile (Campos and Gilbert 2019, Kus et al. 2016, Chacon-Cortes and Griffiths, 2014, Kramvis et al. 1996). When used safely and correctly it can produce higher yield DNA samples which are purer than

those sourced using other extraction techniques (Schiebelhut et al. 2017, Kus et al. 2016, Iyavoo et al. 2013). Fridez and Coquoz (1996) demonstrated that phenol chloroform extraction was the most successful technique when extracting DNA from saliva samples under postage stamps. Up to 100 ng of DNA was extracted from a single stamp. This equates to the quantity of saliva placed under the stamps (Fridez and Coquoz, 1996). It was also reported that the delay in the placement of saliva on the stamp and the extraction of DNA did not affect the yield gained in extraction. This is significant when extracting DNA from counterfeit banknote as the time delay between the time of production of the item, the circulation of the notes and their eventual confiscation may be months. The use of Chelex was not as successful at producing high yields of DNA. Only 20% of the anticipated DNA being extracted when compared with the technique using phenol chloroform (Fridez and Coquoz, 1996). Unlike the silica column and Chelex bead extractions, a degree of special training and long periods of handling time are necessary to successfully carry out organic extraction (Chacon-Cortes and Griffiths, 2014, Mi et al. 2013). However, the results from phenol chloroform extraction can provide a greater yield of DNA when dealing with degraded samples such as bone compared with magnetic bead kits as shown by Iyavoo et al. (2013). The researchers compared several silica-based extraction kits and phenol chloroform and found that all extractions were successful in acquiring DNA with phenol producing the greatest yield. However, in more recent research, it has been shown that an extraction step could be skipped, instead opting for a direct introduction of the sample into the DNA profiling step when considering human bone samples. This has also been shown for other sample types such as clothing fibres (Blackie et al. 2018), substrate punches (Cavanaugh and Bathrick, 2018) and swabs (Templeton et al. 2013 and 2016). Blackie et al. (2018) and Templeton et al. (2016) demonstrate that using their methodology it was possible to obtain touch DNA profiles directly from the sample source. Their research investigated fingermarks (Templeton et al. 2016) placed on plastic slides and clothing fibres (Blackie et al. 2018). Both were shown to be successful sample sources. Templeton and Linacre (2014) were then able to utilise this technique in investigations involving drug shipments. They successfully produced a near complete DNA profile from a sample of tape taken from drugs packaging.

1.6 DNA Quantification and Allelic Typing

1.6.1 Quantifying DNA

For DNA extraction, it is important that both the concentration and quality of the DNA are high. To best assess the quantity and quality of the DNA sample, devices such as a nanodrop are used to spectrally measure the concentration of DNA, normally in nanograms per microlitre, and quality through applying Beer-Lambert's law (Green and Sambrook, 2018). The Beer-Lambert law value is expressed by the 260/280 ratio that gives the spectral ratio of DNA that has an absorbance of 260 nm to amino acids present with an absorption of 280 nm (Green and Lambert, 2018), effectively giving a value to the quality of the sample. However, with the levels of DNA expected from trace DNA samples, readings from a nanodrop may not be possible due to the technologies' lack of sensitivity to lower concentrations (Rohland and Hofreiter, 2007). The nanodrop also lacks the necessary sensitivity for other contaminants, as the method of measuring the ratios of the DNA and protein present will not quantify the non-protein-based contaminants that could affect later analysis (Green and Sambrook, 2018). Samples may also be made up of several different organisms' DNA given the presence of bacteria. This means any readings may in fact be as a result of nonhuman DNA extracted from a sample, due to spectrophotometry not being species specific (Rohland and Hofreiter, 2007).

Further conventional methods have been developed to evaluate the concentration of DNA from forensic evidence. One such technique is the use of quantitative PCR (qPCR) or real-time PCR (RT-PCR). First established using ethidium bromide, the protocol allows for the active monitoring of DNA concentration during the PCR process (Higushi et al. 1993). The ability to quantify the amount of DNA present in sample, allows an examiner to establish how much of an evidential sample needs to be added to the DNA profiling step (Vraneš et al. 2017). Modern uses of the process use DNA dyes that are not carcinogenic such as SYBR Green, a nonspecific dye or more specific locus probes like Taqman[®] probes (Alonso and Garcia, 2007, Bowyer et al. 2007). During a standard PCR protocol, a DNA sample of 2 ng/μL is added to a reaction mixture. The mixture includes solutions of magnesium chloride, the primers for the pre-designated site of interest, free unbound base nucleotides and a polymerase enzyme, normally a lab derivative of the enzyme taq polymerase (Hedman et al. 2009). The reaction itself involves a set of temperature changes carried out by a specialised heat block, termed a thermocycler, that cycles through pre-programmed steps (Giesse et al. 2009). The end-product is a sequence

corresponding to the template targeted by the primers that has been exponentially replicated. To monitor the reaction as it undergoes the cooling and heating stages, a dye or probe system can be utilised to give real time analysis of the reaction. The added dye loosely binds to the DNA in the case of SYBR green or is incorporated into the DNA replicate which leads to a fluorescence effect from an attached fluorophore when using probes (Valasek and Repa, 2005). As more DNA is replicated, the intensity of fluorescence increases (Valasek and Repa, 2005). A specialised thermocycler is used that incorporates both an emitter and detector (Valasek and Repa, 2005). By measuring the resultant fluorescence as the reaction takes place, the cycle at which it reaches a threshold is monitored. This is termed the cycle threshold (ct) (Alonso and Garcia, 2007) or quantitative cycle (C_q) (Ruijter et al. 2021) value. This value is monitored in the evidential samples of interest and in a set of DNA standards. These DNA standards are diluted down in a set of factors that leads to a variation of the ct value during the qPCR that can then be plotted logarithmically to produce a standard curve (Ruijter et al. 2021). By comparing the ct value of the DNA standards to the evidential samples of unknown DNA concentration, the concentration of the evidential samples can be calculated (Dhanasekaran et al. 2010). When using data from the standard curve, the R^2 value must be monitored ensuring all the data points are close to a linear regression with value close to 1 (Cropper et al. 2022).

DNA quantification techniques used in forensic applications have varying mechanisms to generate fluorescence (Valasek and Repa, 2005). SYBR green is one of the most widely used dye in qPCR assays given its general affinity for double stranded DNA (Dragan et al. 2012). SYBR Green binds to double stranded DNA specifically through the ionic interaction between its positive nitrogen binding site and the negative DNA phosphate group (Dragan et al. 2012). Its accuracy means it is often selected for various forensic examinations to assess DNA concentrations (Nicklas and Buel, 2003, Shewale et al. 2007). SYBR green is not autosomal DNA specific however, meaning any byproducts of the PCR, such as primer dimers that form a double strand structure, will be quantified alongside the desired sample sequence (Bowyer et al. 2007, Kumar et al. 2016). To overcome this, DNA specific probes can be used that anneal specifically on the desired DNA locus of interest (Thomas et al. 2013 and LaSalle et al. 2011). Therefore, any fluorescence will represent only the quantity of the desired DNA locus. Such probes include scorpion locus probes (Whitcombe et al. 1999 and Thomas et al. 2013) or TaqMan[®] assay probes (LaSalle et al. 2011). Scorpion probes consists of a fluorophore-quencher pair

that forms a hairpin loop at the end of the primer (Thelwell et al. 2000). When the extension stage occurs in the PCR, the action of the endonuclease enzyme, causes the hairpin molecular structure to change that allows the fluorescence of the fluorophore (Thelwell et al. 2000). Whereas Taqman has a fluorophore and quencher combined mechanism termed a donor-receptor FRET (fluorescence resonance energy transfer) pair (Belke et al. 2005, Nagyl et al. 2017, Thelwell et al. 2000). During the process of primer annealing and extension, the extension from the fluorescent probe causes the detachment of the fluorophore from the quencher, leading to the fluorescence of the fluorophore (Holland et al. 1991, Valasek and Repa, 2005).

The main benefit of using a probe system compared with a SYBR Green based qPCR is that multiple genomic regions can be identified and quantified to increase the successful detection of DNA, termed multiplexing (Correa et al. 2020). There are several kits that have been developed and validated for forensic DNA quantification purposes such as the Quantifiler™ Human DNA Quantification range of kits produced by Applied Biosystem™ (Thermo Fisher Scientific, 2020) and the PowerQuant systems from Promega (Promega, 2020). These kits often target at least one non-variable human autosomal region with some including a sex determining locus located on the Y chromosome such as the Quantifiler™ Duo DNA Quantification kit (Barbisin et al. 2009 and 2011). Alongside the sex determining locus (labelled with the dye FAM) and autosomal locus (labelled with the dye VIC) the Quantifiler™ Duo contains an internal positive control (IPC). The IPC is a section of artificial template in the form of a plasmid included in all the reactions and acts to monitor if the PCR has occurred and if there is any inhibition present (Barbisin et al. 2011). Inclusion of the IPC is achieved through the NED dye marker to allow it to be multiplexed alongside the quantifying markers. This kit has been used for several investigative areas due to it having both a general autosomal marker and a Y chromosome-based marker (Barbisin et al. 2011) making it useful for mixture interpretation in assault cases (Sethi et al. 2013) or degraded DNA such as in trace DNA evidence (Barbisin et al. 2011, Zoppis et al. 2014, Sessa et al. 2019).

The Quantifiler Trio™ DNA Quantification kit expands on the Quantifiler™ Duo DNA Quantification kit by including three human specific target primer sets (Griffin et al. 2022). This allows a degradation index (DI) to be established for samples that may prove difficult to STR profile due to degradation of the sample or present PCR inhibitors (Lin et al. 2018). The Quantifiler Trio™ kit establishes a degradation index through the use of two amplicons with one small amplicon (80 bp) and a larger

amplicon (214 bp) (Lin et al. 2018). By taking the ratio of the signal of the shorter amplicon compared to the larger amplicon a DI can be established (Vernarecci et al. 2015). Although quantification data may indicate there is sufficient DNA present to produce a DNA profile, the DI indicates the condition of the DNA present which will also affect the resulting DNA profile (Vernarecci et al. 2015). Vernarecci et al. (2015) established that any values greater than 4 are considered to indicate degradation with likely a partial or no DNA profile being present when analysed further using the Globalfiler® PCR amplification kit. If the DI is less than 4 this would indicate no or a minor level of degradation meaning a full or partial DNA profile may still be obtainable even at concentration between 33.3 pg/μL and 3 pg/μL.

Although SYBR Green assays use a different mechanism to detect DNA, they have been shown to be just as sensitive to DNA as probe-based assays (Tajadini et al. 2014). However, due to the risk of false positives with SYBR Green and the need to efficiently select evidential samples, Taqman is more commonly used (Bowyer et al. 2007). The use of pre-developed Taqman assays also removes the costs of developing and validating primer sets to be used in the SYBR Green qPCR assays if the primary information needed is the concentration of genomic DNA (Vraneš et al. 2017). For both DNA quantification mechanisms, the costs can be further reduced but maintain the accuracy of the kits by reducing the reaction volume. This allows for the same quantification result in terms of the fluorescence measured during the PCR cycles but reduces the price of reagents significantly (Adler et al. 2011, Cho et al. 2017, Frégeau and Laurin, 2015, Subhani et al. 2019). This has also been shown to be possible with some STR profiling kits (Lui et al. 2014).

Factors that influence the successful acquisition of a DNA profile in later lab analysis include the presence of PCR inhibitors or other contaminants. Their presence can slow down or prevent the replication reaction occurring. PCR inhibitors are chemical compounds that prevent the PCR from occurring at optimised functionality. The main way in which inhibitors cause this effect is through the interaction with the polymerase enzyme that carries out the reaction (Alaeddini et al. 2012). In these instances, the inhibitor may denature or breakdown the enzyme itself reducing its efficiency within the reaction (Alaeddini et al. 2012, Green and Sambrook et al. 2019). They may also actively compete with other components of the reaction such as the magnesium, reducing the efficiency of the reaction such as with calcium (Opel et al. 2010). Some inhibitors also bind to the DNA template preventing enzyme activity from accruing on those strands (Opel et al. 2010). Alternatively, inhibitors may prevent the detection of

the fluorescence emitted from fluorophores during qPCR when assessing the quantity of DNA present (Sidstedt et al. 2015).

1.6.2 DNA Profiling

After the samples have been quantified using a qPCR kit (LaSalle et al. 2011), the appropriate concentration of the sample can be added to an STR profiling PCR mixture (Durney, et al. 2015, Ham et al. 2016). Each STR is formed of a DNA code that repeats a specific number of times, with each locus only appearing at a specific frequency within each human population (Sun et al. 2003, Roewer, 2013, Butler, 2007), except in case of monozygotic twins (Li et al. 2013). Each locus is given a numerical value for the number of repeats in the sequence, termed the allele, when creating a DNA profile (van der Gaag and de Knijff, 2015). STRs provide forensic geneticists with a form of molecular barcode that can be linked to each individual (Edwards, 1991, Gill, 1997). These unique molecular barcodes are used by forensic geneticists when attempting to identify potential suspects involved in a crime (Bornman et al. 2012). To assess the STR allelic profile of a given sample, the profile must be acquired through the use of capillary electrophoresis (CE).

To first prepare a set of samples for CE, a PCR must be conducted to allow for the analysis of the specific STR loci of interest (Phillips et al. 2014). In order to establish a forensic DNA profile for a sample, a mixture of fluorescently labelled primers are used that replicate specific STRs during a PCR, these are incorporated into the strand copy as a fluorescent label (Alonso et al. 2018, Butler et al. 2004, Hill et al. 2009). The resulting PCR product samples are then prepared for CE by the addition of a loading dye mixture consisting of LIZ internal size standard and HiDi™ formamide. The HiDi™ acts to separate the DNA strands into single stands to allow for the detection step of CE (Butler et al. 2004). The LIZ internal sizing standard aids the downstream software analysis in establishing the peak heights of all the detected STRs through comparison of the predetermined peaks in the standard to the unknown peak (Butler et al. 2004 and Applied Biosystems, 2022). As the samples are passed through a set of polyacrylamide filled capillaries the fragments separate according to molecular weight as they travel (Dash and Das 2017, Durney, et al. 2015). This is achieved by applying a current through the system that attracts the negative charged DNA fragments through the capillary towards the detector, much like in gel electrophoresis (Butler et al. 2004). The detector at the end monitors the fluorescent

labels according to their specific wavelengths as they pass at specific time intervals (Butler et al. 2004).

Each of the STRs selected vary in length sufficiently meaning that each can be assigned a different fluorescent colour for its primers. This allows for multiplexing where several loci can be analysed in one sample, reducing the time and the amount of sample required in each experiment (Kimpton et al. 1993 and Bano et al. 2015). Various kits include numerous STR loci, alongside different dyes depending on the country or lab (Green et al. 2013). In the UK one of the main kits is the AmpFLSTR NGM Select PCR amplification kit, which uses 4 dyes (Shackleton et al. 2019). The dyes are coloured blue using the dye FAM, green using VIC, yellow with NED and red with the dye PET (Green et al. 2013). FAM corresponds to the STR loci D10S1248, vWA, D16S539 and D2S1338 (Applied Biosystems, 2015). VIC is designated to the Amelogenin locus, D8S1179, D21S11 and D18S51. NED labels D22S1045, D19S433, TH01 and FGR loci. Lastly, PET is linked with the loci D2S441, D3S1358, D1S1656, D12S391 and SE33.

Although there are only a limited number of dyes available, the different STR loci can be evaluated separately due to the variation of their molecular mass (Kimpton et al. 1993, Jiang et al. 2012). Each STR locus varies in base length sufficiently so that no two STR loci with the same dye colour have the same molecular weight. As they migrate through the acrylamide during CE, STR loci that share the same dye label will arrive separately at the detector, allowing them to be measured independently (Lazaruk et al. 1998, Durney et al. 2015). The detector provides the data in the form of peaks where the dye signal has been measured (Fujii et al. 2018, Gill et al. 2000A). Each peak, measured in relative fluorescence units (RFU), corresponds to a measured allele within each STR locus that is compared to an allelic ladder that has run alongside the process (Lazaruk et al. 1998, Budowle et al. 2009B, Karkar et al. 2018). The allelic ladder is composed of all the possible STR alleles. When analysing the output, the allelic ladder provides a framework for the by which the peak present in the profile can be assigned an allelic designation (Budowle et al. 2009B, Gill et al. 2000B). A forensic geneticist must first interpret the peak output from capillary electrophoresis before uploading the evidence profile to a national DNA database. In the case of trace DNA, this can be particularly challenging as the peaks present will not be pronounced or may have become subject to allelic drop out or drop in (Petricevic et al. 2010, Westen et al. 2009). Allele drop-outs, whereby the allelic signal is lost, is largely due to the low level of genetic material in trace DNA, making the

resulting profile incomplete (Petricevic et al. 2010, Westen et al. 2009). The loss of alleles makes profile matching more difficult and reduces the reliability of such evidence if used in court (Balding and Buckleton, 2009, Dørum and Bouzga, 2015). Researchers have compensated for the loss of alleles through altering the sample injection process (Westen et al. 2009). However, this process may in some cases lead to allele drop ins. This means that alleles that are not truly present in the sample are produced, thus reducing the reliability of the evidential analysis (Gill et al. 2000B, Petricevic et al. 2010). Each allele of a STR locus appears at a specific rate in every population (Buckleton et al. 2016, Moretti et al. 2016). By measuring the rate of appearance for each allele within each population, a match probability can be derived. This is reported as the chance that a random individual taken from the population would be a match to an evidence profile (Thompson et al. 2018).

Current research is looking to replace allelic peak DNA profiles by directly sequencing the genome, using next generation sequencing, to provide the nucleotide base information (Sobiah et al. 2018, Bornman et al. 2012, Wang et al. 2017). Bornman et al. (2012) have demonstrated that next generation sequencing could effectively sequence STR loci used in the American DNA profile database, CODIS. Furthermore, Sobiah et al. (2018) shows that single nucleotide polymorphisms, where there are single nucleotide base differences in sections of DNA, could replace STR profiling using next generation sequencing (Sobiah et al. 2018 and Alonso et al. 2017) The cost of lab machinery necessary for the sequencing is a major consideration. At \$100,000 on average for each sequencer and necessary reagents, it may be some time before it becomes as affordable as STR kits and capillary electrophoresis (Sobiah et al. 2018).

1.7 Interpreting Trace DNA Evidence

Gill and Budowle define trace DNA or low template DNA, as being a DNA sample at a quantity of 100 picograms (Gill et al. 2001) to 200 picograms (Budowle et al. 2009B). The general consensus of forensic geneticists is that these samples are at such a low concentration of DNA, that they are susceptible to being missed in analysis or susceptible to profiling artefacts that make an STR profile difficult to interpret. Due to more sensitive detection techniques, samples with these low DNA concentrations are becoming more useful in forensic cases (Menchhoff et al. 2020).

Although modern techniques become more effective at acquiring DNA profiles from a few cells, this may pose problems in interpretation. As far back as 1997 it has been possible to take a few human cells and successfully detect the STR profile of the source (Findley et al. 1997). This sensitivity has only been improved in the following decades leading to quantification and profiling kits that can detect DNA that has been secondarily transferred. Where a person has touched a second person, who has then gone to transfer both individual's DNA to an object via contact (Farmen et al. 2008, Samie et al. 2019).

The loss of such evidence can be a result of higher intensity DNA profiles concealing the weaker trace signals (van Oorschot, 2010). In the case of STR artefacts these can appear for several different reasons. For instance, in the case of degraded DNA, longer STR loci can appear to have a weaker signal or peak height termed an RFU value compared to the shorter loci, creating a sloping affect in the overall profile (Bright et al. 2013, Balding and Buckleton 2009). In particularly low template DNA samples, larger sized alleles may be lost in the analysis, termed allele drop-out (Gill et al. 2000B, Van Nieuwerburgh et al. 2009). This is where the DNA has become too degraded in sections to be amplified. In other cases, profiles may have peaks that have "stuttered" which suggests the amplifying polymerase enzyme has slipped behind or ahead of its target locus, causing it to appear shorter or longer than the actual length of the amplicon (Gill et al. 1997, 2000B). Other artefacts can appear in both degraded and intact samples such as pull up alleles (Gill et al. 2000B, Fujii et al. 2018). This is where one allele in a specific dye channel is found in the other dye channels due to a pull up effect (Fujii et al. 2018). Therefore, a forensic scientist must correctly identify these and account for them, especially when interpreting trace DNA samples that may be found in counterfeit banknotes. Low concentrations of template DNA can be susceptible to contaminants from the evidence (Bright and Petricevic, 2004) or the material composition of the evidence can affect the persistence of trace DNA over time (Meakin et al. 2017, Goray et al. 2012, Raymond et al. 2009). In an effort to compensate for this, examiners have increasingly used tapelifts (Barash et al. 2010) or alternative swab types such as nylon FLOQ swabs (Comte et al. 2019). The methodologies used for these types of evidence techniques could be extrapolated to acquire DNA from the adhesive layers of counterfeit banknotes.

1.8 DNA Databases

When using DNA profiling, forensic examiners can compare the acquired profile to a local database of convicted criminals when there are no potential suspects (Amankwaa and McCartney, 2019). In the UK the primary database is the National DNA Database or NDNAD that is maintained so as to be compliant with laws in England and Wales (Maguire et al. 2013, Amankwaa and McCartney, 2019). Scotland and Ireland both have their own databases that contribute to the NDNAD, the Scottish DNA Database (SDNAD) and Northern Ireland DNA Database (NIDNAD) (Amankwaa and McCartney, 2018). In Europe, it is suggested that each member state adopts a system containing at least 12 STR loci to create the best-established database (European Union, 2009). Alongside this, member states who agreed to the Prüm Decision are eligible to search and share their own data with other members of the EU (Toom, 2018), effectively creating a continent-wide searchable database. In the United States their database termed CODIS has a total of 922,673 forensic profiles with over 13 million offender profiles (FBI, 2019). Different countries apply different numbers of STR loci in these forensic profile databases. Most, if not all, include at least one sex determining loci such as the Amelogenin locus on the X chromosome (Kayser, 2017). Currently Europe's guidelines state to include 12 STR loci in member's states DNA profiles (Council Res. 2009). However, some choose to go beyond this such as Germany (Hohoff et al. 2013), England and Wales at 17 STR loci in forensic profiling and 24 for Scotland (Butler et al. 2017). American forensic examiners expanded their datasets from 13 to 20 STR loci for their CODIS database (Hares, 2015). The greater number of STR loci effectively increases the statistical significance of a matching profile (Santos et al. 2013). By comparing the profiles taken from an incriminating item or deceased individual to a country's respective criminal DNA database, the probability of a match can be assessed (Dørum and Bouzga, 2015, Thompson et al. 2018).

Due to the variability of DNA profiles taken from a crime, there are guidelines as to how many loci a profile contains before it can be searched and stored on a database. The standard number of loci required in a search is 6 for many countries such as in the US (FBI, 2022) and members of the European Union (ENSFI, 2017) with the UK opting for 8 loci with a lower threshold if a non-routine search is carried out (Home Office, 2020). This threshold ensures that the evidential value of a match within a database is substantial enough for a forensic examiner to use in a case compared to a profile where only a few alleles would provide a less powerful probability value

(Pope and Puch-Solis, 2021). Hicks et al. (2010) found there is value in considering profiles with less than 6 loci depending on the available size of DNA database. However, this needed further study as their data was based on simulated data.

Due to the nature of circulating notes often ending up in multiple jurisdictions, large interlinking DNA databases would help to assess any potential suspect's profiles, especially in places like Europe and America with far reaching currencies (Goldberg, 2010). In the cases of particularly deceptive counterfeits, these can be circulated to several different countries (Europol, 2018). However, the Prüm Decision allows for the searching of other EU databases, thus allowing for an effective profile search in neighbouring countries where the items may have been produced (Toom, 2018).

1.9 The Reliability of Evidence Using the Balance of Probabilities

The probability of a DNA profile match between an evidential DNA sample taken from a counterfeit banknote and a DNA profile from a database forms the basis of how the evidence is evaluated in court (Gill et al. 2015). In order to present DNA evidence in court, a statistical approach must be taken to further emphasise the weight of finding a piece of DNA evidence. The random match probability is a probability value given that a DNA profile picked at random from a population could match a known DNA profile by chance (Ng et al. 2018). This is calculated by assessing the frequency of identified alleles in a sample with the frequency of the alleles in allelic frequency population database. This is different to the STR databases used by law enforcement. Instead of containing information on individual DNA profiles, the data collected is of the frequency of the alleles in each STR locus within a geographical population that is analysed according using the DNA profiling kits of the specific jurisdiction (Bodner et al. 2016). One such data base set up by ENFSI (European Network of Forensic Science Institutes) is STRidER (STRs for Identity ENFSI Reference Database) (Bodner et al. 2016). The database is open source with all datasets checked for accuracy to maintain it as a centralised reliable database (Bodner et al. 2016). The random match probability is then presented as 1 over the total allele frequency of each of the alleles found in the evidence profile. Care should be taken when applied RMPs by applying appropriate sub population corrections to the Theta value in the Balding – Nichols correction (Ng et al. 2018, Balding and Nichols et al. 1994). The correction seeks to compensate for the uncertainties of dealing with populations that may have subpopulation variation in their allelic frequencies (Balding and Nichols et

al. 1994). Within a subpopulation, the frequency of a given allele may be conserved due to common ancestry. Although this allele may be conserved within that subpopulation, in the wider population it may not be. Therefore, the RMP calculation may be skewed against the accused if they are from the subpopulation and the wider population frequency of that allele is being considered (Ng et al. 2018, Balding and Nichols et al. 1994). The applied Theta value for a population can have significant changes to the RMP outcome, especially when dealing with STR population data that may not truly represent the subpopulations present (Ng et al. 2018). Coupled with this is the likelihood ratio which establishes the ratio of probabilities of an observation (i.e. a piece of evidence) given the two competing hypothesis that represent the prosecution's hypothesis and the defence's hypothesis. This establishes the weight of the evidence being presented. In forensic genetics, the prosecution's hypothesis, often described as H_p (Stern et al. 2017) would be the probability that a DNA profile found at a crime scene and the reference profile of a suspect are from the same individual. The defence's hypothesis is the probability that the DNA profile from a suspect matches the crime scene profile by chance and the two are unrelated to one another, described as H_d (Gill et al. 2015, Stern et al. 2017, Ng et al. 2018). Allowing for the comparisons of the strength of the evidence through a likelihood ratio together with RMPs allows for the strength of the evidence to be evaluated in context of the Prosecution's and Defence's hypotheses (Martire, 2018).

These two statistical evaluations of DNA evidence are both used in court evidence, but problems can arise in some cases between the two when they have been inappropriately considered for non-mathematically based evidence types. In *R. v T* (2010), a likelihood ratio was established for the matching of a trainer to a footprint found at the scene of a rape. However, the forensic examiner converted a descriptive verbal statement as a numerical value, making the ratio subjective by using a footprint scale made up of seven values. This led to an appeal of the conviction to not guilty, as the weight of the evidence was over-stated through the use of a subjective value in the likelihood ratio (*R. v T*, 2010).

This is evident of the Prosecutor's fallacy whereby the evidence of probabilities inappropriately favours the prosecution (Martire, 2018). Also known as the transposed conditional, this happens when the probability of a match occurring is reported when the evidential and reference sample do not in fact match (Thompson et al. 2003). In the case of the Defence's fallacy, the evidence would need to be a probability value that incorrectly suggests a random match had occurred. In both

fallacies, this can happen if the probability value is incorrectly reported as including (Prosecutor's fallacy) or excluding (Defence's fallacy) the defendant from the list of suspects due to errors in the interpreting of the DNA profile prior to calculating the RMP or sampling errors (Thompson et al. 2003). The reporting of evidence incorrectly in terms of probability can therefore risk the evidence being considered under the Prosecution's or Defence's Fallacies depending on the resulting probability and how it is presented (Martire, 2018).

A growing area in forensic statistics is the use of Bayesian Theorem to expand on the use of likelihood ratios. Bayesian Theorem acts to predict the chances of having received a matching piece of evidence according to the two competing hypotheses. It does this by considering both the posterior odds (considered in likelihood ratios) and prior odds of having acquired a piece of evidence under a specific proposition (Kruse, 2012). In Bayesian theorem, the prior odds are the probability values of the evidence occurring according to the Prosecutor's and Defence's hypothesis. Thus, these pre-determined values act as the probability of an event occurring at a source level (Stern et al. 2017). An example of this is presented by Breathnach and Moore (2013). In the research, they looked to assess saliva and DNA evidence in oral intercourse cases together to establish a likelihood of whether the action had or had not occurred. To establish the prior odds, they established in a mock case the potential of gaining a positive result for saliva alongside obtaining a DNA profile which could link to a potential suspect. However, there were a number of factors not controlled in the study, the practical example of the use of a Bayesian framework is still evident in case work. Although the approaches of Bayesian frameworks are not routinely applied in everyday forensic casework, there is the potential for this extension of likelihood ratios to be applied to various evidence types in court especially DNA evidence (Gill et al. 2022).

1.10 Effect Sizes

When using statistical analysis, the p-value of a statistical test is often reported with > 0.05 , making the data not significantly different or < 0.05 indicating the data is significantly different, meaning the null hypothesis can be rejected considering the data (Benjamin and Berger, 2019). However, alongside this, the effect sizes of the dataset should be reported (Sullivan and Feinn, 2012). The resulting value of an effect size highlights the weight of which the data represents the statistical outcome. This ensures that the overall weight of the data is taken into account when

considering the statistical outcome of a comparative test. This is done by comparing the variation of the values within the groups of data analysed to ascertain the strength of the interaction of the variables (Sullivan and Feinn, 2012). A small effect size may indicate the variance in the data explains a small amount of a non-significant outcome and therefore more data is needed. Whereas a large effect size for a statistically significant outcome would indicate the variance in the data explains the relationship found within the data. Different statistical tests warrant various forms of effect size that consider the data depending on how the data is being statistically compared (Cohen, 1988). In this thesis the use of effect sizes will highlight the strength of the data such as the use of eta- squared (η^2) which is used alongside the ANOVA and Kruskal-Wallis tests. In the case of η^2 , a small effect size is considered below $\eta^2 = 0.01$, medium at $\eta^2 = 0.06$ and large at $\eta^2 = 0.14$ (Cohen, 1988). When using the Mann Whitney U test, a Pearson r correlation effect size was calculated with a small effect size considered below $r = 0.1$, medium at $r = 0.3$ and large at $r = 0.5$ (Cohen, 1988).

1.11 Conclusion

Notwithstanding the rise of digital money and electronic banking and commerce, the need for the ability to exchange hard currency remains. There will be a place for paper and polymer money for years to come particularly when one considers the part it plays in the economies of developing countries. Given this there is a need to increase the armoury available to investigate and successfully prosecute those criminals involved in producing counterfeit currency. The increasing prevalence of easy access to the worldwide internet has created an increased threat from counterfeiters, providing them with a larger network to exchange materials, methods and the end product counterfeit banknotes. Whilst large quantities of counterfeit items, including simulated banknotes are seized, many manage to enter circulation. If public trust in the World's currencies is to be maintained, new techniques to aid authorities in identifying and prosecuting incriminating individuals involved in counterfeiting must be developed.

The research detailed in this thesis will explore the use of commonly used techniques in DNA recovery and extraction to establish if these can be used to acquire DNA from adhesive layers of counterfeit banknotes. Previous research identifies that there are techniques that have been applied to other similar evidence types (Feine et al. 2017 and Ruprecht et al. 2021) that could be adapted and applied to assess the viability of encapsulated DNA in counterfeit banknotes. Preparation and extraction techniques

should be established to assess which is best in freeing DNA from the adhesive matrix or if the step in the process could be skipped completely through direct PCR (Blackie et al. 2018).

Counterfeit banknotes are not a major threat to most countries' economies due to them making up a small proportion of the overall money in circulation. However, they do pose issues for individuals and businesses that place their trust in the currency in question. This is where the influx of deceptive counterfeit banknotes can have a greater negative economic effect on members of the public. In the past, identifying the minute differences between counterfeits produced using offset printing was enough to link counterfeits from a common source (Pfeifer et al, 2016, National Research Council, 2006). However, with the advent of digital printing, counterfeit banknotes are printed without imperfections that can be used to link them together (Božičević et al. 2012, National Research Council 2006). Coupled with the ease of printing, characteristics such as security holograms or OVDs are available to counterfeiters through mass produced adhesive holograms that can make a counterfeit banknote difficult to spot at first glance (de Heij et al. 2010b, Cockburn et al. 2005).

Many studies have investigated the persistence of DNA on the surface of banknotes. To date there is only one study looking at the presence of DNA between the adhesive layers in counterfeit banknotes (Kwok et al. 2019). Van den Berge et al. (2016), established that mixed profiles of between 2 to 6 people could be identified on the surface of banknotes. However, the research only examined what are assumed to be genuine banknotes and external DNA deposits. The researchers' findings do not necessarily suggest that DNA from a counterfeiter can persist on the surface of a counterfeit item once in circulation. However, it did highlight the possibility of profiling trace DNA from banknotes.

Due to the difficulties in verifying the accountability of a counterfeiter's DNA profile being present on the surface of a counterfeit banknote, an alternative approach is needed. As stated by Voinea et al. (2015), some counterfeiters use two layers of paper that are then glued together while incorporating an internal imitation security thread and watermark. By utilising this technique, the watermark and metallic thread are visible when the document is inspected in transmitted light, much like a genuine banknote. These elements of the counterfeit banknote are applied manually most likely in a non-sterile environment. This distinguishes counterfeits from notes

produced legitimately in sterile conditions. This may mean that during the manufacturing process, some of the counterfeiter's DNA will get trapped within the adhesive layer (van Oorschot et al. 1997, Haines et al. 2013). The same may also be true for counterfeiters who have used adhesive holograms to simulate holograms used on genuine banknotes (de Heij, 2010b). These layered counterfeits may provide a valuable source of a suspect's DNA profile much like in cases where DNA is extracted from tape layers. The difficulty lies in successfully extracting a potential suspect's DNA profile from the adhesive matrix without compromising its integrity to allow the evidence to be used in a court case. Research by May and Thompson (2009) and Templeton and Linacre (2014) proved there were methods for extracting high quality DNA samples from evidence involving tape layers.

1.12 Aims and Objectives

1.12.1 Aim

The aim of the research detailed in this thesis was to establish if DNA can be extracted from the layers of a counterfeit banknote and if so, could a STR profile be acquired from it.

1.12.2 Objectives

In order to investigate this aim, the main objectives were:

- 1) investigate the use of manual and solvent approaches in the separation of counterfeit banknote adhesive layers.
- 2) Establish the appropriate extraction process through the testing of various extraction methods alongside a solvent incorporated into the swabbing and lysis step.
- 3) Have volunteers make composite counterfeits that were then given to a secondary volunteer for handling thereby simulating the circulation of a counterfeit banknote.
- 4) Apply the technique to counterfeit banknotes provided by the Central bank of Ireland and De Nederlandsche Bank to establish if DNA profiles could be extracted using the established methodology.

Chapter 2 Evaluation of DNA in Composite Counterfeit Banknotes

2.1 Introduction

The primary set of objectives for this chapter were 1) investigate the use of manual and solvent approaches in the separation of counterfeit banknote adhesive layers. and 2) establish the appropriate extraction process through the testing of various extraction methods alongside a solvent incorporated into the swabbing and lysis step. The research detailed in Sections 2.2.1, 2.3.1 and 2.4.1 look to address objective 2 by examining the use of Chelex resin and phenol chloroform extraction in a preliminary methodology of extracting DNA from the adhesive side of the dot matrix holograms. However, at this stage of the research, the types of solvents had not been fully investigated or researched. As research has shown the use of water on adhesive crime scene tapes, water was used instead to reduce the number of variables that were considered, instead focussing on the extractions (Phetpeng et al. 2015) using a set of known quantities of DNA for the “counterfeiter”. Sections 2.2.4, 2.3.4 and 2.4.4 follow on from this by using a widely used quantification kit, the Quantifiler™ Duo DNA quantification kit (Thermo Fisher Scientific, 2020), to apply a similar method on counterfeit banknotes as a mock protocol to greater understand the method by which objective 4 could be addressed. Alongside this the Quantifiler™ Duo DNA quantification kit was tested at full volume and half volume to establish if there was any benefit or detriment to using less of the reagents. Halving the reaction volume has been shown to achieve the same levels of sensitivity compared to the full volumes (Cho et al. 2017), making the process cost effective.

For objective 1, investigate the use of manual and solvent approaches in the separation of counterfeit banknote adhesive layers, various solvents and methods were being considered. As will be mentioned for the preliminary research sections in this chapter on the various DNA extraction approaches, the methods used were focussing on the use of manual techniques in separating the adhesive layers of counterfeit banknotes. However, in the process of using these techniques in sections 2.2.4, 2.3.4 and 2.4.4, the need for the application of a solvent was evident. The methodologies detailed in sections 2.2.2 and 2.2.3 looked to address the first objective through the use of solvents such as xylene, ethanol and 1,2-indandione. Xylene was initially used as there was evidence present in the literature that indicated it may be useful in its application on the adhesive layers of counterfeit

banknotes. 1,2-Indandione was also tested as there was some research indicated it could be used as a dual recovery method (Alketbi and Saif 2022) for fingerprint and DNA evidence. Research had shown this was possible with stamps (Ruprecht et al. 2021), it was therefore hypothesised that this would be possible with the internal adhesive sides of counterfeit banknotes. Later literature lead to the use of ethanol being investigated for its separation of adhesive layers detailed in sections 2.2.3, 2.3.3 and 2.4.3 (Ruprecht et al. 2021). This was being considered over xylene as ethanol is more commonly used with DNA samples and would likely be less of a detriment to the samples while processing (Lei et al. 2022).

2.2 Methodologies

Ethics Declaration

All experimental designs and involvement of volunteers were approved under Proportional Ethical Approval provided by the Staffordshire University ethics Committee, with written consent given from all volunteers for their involvement in the research herein detailed.

2.2.1 Preliminary Examination of Deposited DNA on Dot Matrix Holograms

2.2.1.1 Sample Preparation

A set of 5 serial dilutions at a factor of 1 to 5 from a 590 pg/ μ L pre-quantified extracted DNA stock were prepared to simulate the concentrations at which trace DNA is likely to be deposited. Each dilution was carried out in triplicate for each DNA acquisition technique. Of each dilution, 2 μ L was placed onto the adhesive side of a hologram before being placed onto banknote paper. The holograms themselves were dot matrix holograms with an adhesive present on one side. In total, 45 control samples were produced with known DNA content, 15 for each DNA acquisition process. A set of 9 adhesive holograms that had been manually placed onto a paper substrate by a volunteer were also prepared. Both the dot holograms and the paper substrate were provided by the European Central Bank. The paper substrate sheets were examples of the paper type used to produce euros and the holograms were purchased online (the exact source of which was not given due security reasons). The un-assembled banknote components were sterilised using UV light for a period of 15 minutes (Templeton and Linacre 2015) and wiped with 100% ethanol (Siriboonpiputtana et al. 2018) before applying the prepared DNA samples or being handled by the volunteer.

Alongside these substitute counterfeit banknotes, seized counterfeit banknotes were included in the initial analysis (Table 1).

Table 1. List of the €50 counterfeit banknotes examined and their respective County within the Republic of Ireland where they were taken out of circulation. Samples were provided by the Central Bank of Ireland. The indicative aspect refers to the categorization of the counterfeit banknote by the ECB according to the general area it was from (EU), the series of banknote it is a counterfeit of (A being the first series of euros), the denomination being counterfeited (50 euros), the process applied (P = traditional offset printing or C colour copying using equipment such as inkjet printers) and a final numerical value for the sequential order in which it was found.

Serial Number	Date Taken Out of Circulation	Date Received	Indicative	County
Y43811679599	07/03/2018	13/03/2018	EUA0050C00114a	Leitrim
Y83811672257	05/02/2018	22/03/2018		Kilkenny
Y43811679599	02/11/2018	06/11/2018		Kerry
Y13811670500	05/03/2018	26/03/2018		Tipperary
Y13811670500	22/03/2018	27/03/2018		Louth
Y43811679599	27/07/2018	16/08/2018		Westmeath

2.2.1.2 Sample Processing and DNA Extraction

After leaving the hologram to adhere to the paper substrate over a 7-day period (Tan et al. 2020), the holograms were manually lifted off the note paper using a scalpel and tweezers. The adhesive side and the surface area to which the hologram was adhered to were then swabbed using sterile cotton swabs (Deltalab, 2016) with DNA free water. In areas where the adhesive had bound to the paper substrate, a sterile scalpel was used to free the adhesive. The same separation and swabbing process was carried out on the seized counterfeit banknotes. All separation tools were either already sterile or sterilised through exposure to UV light for 15 minutes (Templeton and Linacre 2014) and wiped with 100% ethanol (Siriboonpiputtana et al. 2018).

The sample swabs were then extracted using either a Chelex resin extraction (Section 2.2.1.2.1) according to the protocol provided by the manufacturer (Biorad Laboratories, 2000a and 2019) or a 25:24:1 phenol chloroform isoamyl (Sigma Aldrich, 2019) extraction as per the protocol described by Green and Sambrook (2017) (Section 2.2.1.2.2). A third group was prepared for direct qPCR samples, these were cut into 6 equal segments and directly introduced into each PCR well using a sterile scalpel blade (Templeton et al. 2015 and 2016, Liu et al. 2014a and 2014b).

2.2.1.2.1 Chelex Resin Extraction

Each swab head was snapped into an Eppendorf before adding 1000 μL of DNA free water and 2 μL of proteinase K into each of the samples. The tubes were then vortexed briefly and then incubated in a shaker (1000 rpm) for 30 minutes at 56°C. These were then spun in a microcentrifuge for 3 mins at 13,000 rpm. The swab was then removed and 175 μL of a 5% chelex working solution was added using a 1000ul pipette. The Chelex solution was on a magnetic stirrer for the duration of the time of pipetting to ensure adequate suspension of the resin. The samples were then incubated at 56°C for 30 minutes. Afterwards they were vortexed at high speed for 5 to 10 seconds and incubated at 100°C for 8 minutes using a screw-down rack. The final step had the samples vortexed again at high speed for 5-10 seconds and spun in a microcentrifuge for 2-3 mins at 13,000 rpm before pipetting aliquots of the extract into microcentrifuge tubes (ensuring not to uptake any of the resin).

2.2.1.2.2 Phenol Chloroform Extraction

Swabs were snapped into Eppendorf tubes and 600 μL of DNA free water and 2 μL of proteinase K was added before incubating at 56°C in shaker for 30 minutes at 1000 rpm. Afterwards the swabs were removed with a sterile toothpick. For the isolation step an equal volume of phenol: chloroform isoamyl (600 μL). The tube samples were then gently inverted until an emulsion formed before centrifuging at 12000 rpm for 1 minute. The top aqueous phase was then removed using a 1000 μL pipette and then a 200 μL pipette to a fresh Eppendorf, ensuring the aqueous layer was not disturbed when getting the last of the top layer. Any remaining interphase and organic phase were discarded appropriately. This washing step was repeated 3 times until no protein was visible at the interphase of the organic and aqueous phases. An equal volume of chloroform (600 μL) was added before repeating the wash step.

For the ethanol precipitation, sodium acetate 3M (20 μL) was added to each sample before adding 1200 μL of ice-cold ethanol. The sample was then vortexed briefly and left on ice to allow the DNA to precipitate (30 minutes). These were then centrifuged at 12,000 rpm for 10 minutes at -20°C. The supernatant was then removed using a pipette, ensuring not to disturb any pelleted genetic material on the bottom of the Eppendorf. The tubes were then halfway filled with 70% ethanol and recentrifuged at 12000 rpm for 2 minutes at 4°C in a microcentrifuge. The supernatant was then removed again and discarded. Any remaining ethanol was evaporated off by leaving the open tube at room temperature until the last traces of fluid evaporated. DNA free water (30 μL) was then added to resuspend any DNA present.

2.2.1.3 Quantitative PCR

The samples were then quantified using 2 sets of primers for the STR loci TH01 (Vanderheyden et al. 2007) and SE33 (Hill et al. 2011) in a SYBR Green master mix (Bio Rad, UK) as per the manufacturer's instructions (Bio-Rad Laboratories, 2000b) in a 20 μ L reaction. The samples were analysed using a StepOnePlus™ Real-Time PCR System (ThermoFisher Scientific, 2022a). Data was exported to Microsoft Excel (Microsoft Corporation, 2022) and statistical analysis was carried out using SPSS (IBM Corp., 2022). The two sets of primers were tested using annealing temperatures from 60 to 66°C in a standard PCR thermal cycler with analysis of the PCR products via gel electrophoresis to establish that the primers successfully produced PCR products for both loci. However, the SYBR Green Supermix has a standard annealing temperature set as of 60°C with the components of the Supermix compensating for any variability of annealing temperatures (Bio-Rad Laboratories, 2000b). Both primer sets were kept at a concentration of 1 μ M with the SYBR Green master mix throughout the analysis.

2.2.2 Xylene, 1,2-Indandione and Hexane Adhesive Separation

2.2.2.1 Application of Xylene

A counterfeit banknote consisting of a double paper layer with imitation metallic thread was totally immersed in xylene for one minute. A scalpel blade was then used to pry apart the paper layers around the ends of the embedded thread, where there was likely a weaker adhesive bond between the paper, as an access point. First the blade was pierced into where the imitation metallic thread was present, ensuring that the blade only passed between the layers and not through either the paper or the thread. The blade could then be moved through the layers, ensuring that the side of the blade that was prying through the layers was the blunt end. Using the sharp side led to the tearing of the paper layer in all instances this was tried. This was repeated on three other counterfeit banknotes but instead 100 μ L of xylene was added at a time to an access window that was made using a scalpel blade to form an access flap to the embedded thread. For the dot matrix hologram removal, a similar approach to the double paper layered banknotes was applied. Instead of using a scalpel blade however, a set of tweezers was used to lift the hologram off the paper substrate. Xylene was placed on the opposing side of the hologram and allowed to permeate through the paper layers behind the hologram. This was attempted on two counterfeit holograms present on counterfeit banknotes.

2.2.2.2 Application of 1,2- Indandione

Another solvent-based reagent 1,2-indandione was also investigated. Prior to the addition of a 1,2-indandione working solution the counterfeit banknote was split into four sections and the 1,2-indandione working solution was poured onto each section, ensuring enough of the solution was added to cover the segments. The segments were then left in an oven at 80°C for 5 minutes. The working solution consisted of 0.25g of 1,2-indandione, 45mL of ethyl acetate, 45mL of methanol, 10mL of acetic acid, 1 mL of zinc chloride stock solution (0.1g of zinc chloride, 4mL of ethyl acetate and 1mL of acetic acid), 1L of HFE 7100 (Defence Science and Technology Laboratory, 2019).

2.2.2.3 Application of Hexane

In a similar manner to Section 2.2.2.1, hexane was added to the adhesive layer of a counterfeit banknote consisting of a double paper layer with imitation metallic thread and a dot matrix hologram on its surface. For the paper layer separation, 100 µL of hexane was added repeatedly to allow for the permeation of the solvent through the paper before attempting to separate the paper layers by running a scalpel blade across the edges of the applied area. This was also applied in the same manner to the opposing side of the present dot matrix hologram, allowing the solvent to permeate to the other side of the paper where the hologram was attached. A set of tweezers were then used to attempt to remove the dot matrix hologram.

2.2.3 Ethanol Adhesive Separation

To remove the dot matrix holograms, 200 µL of 100% ethanol was added to the reverse side of counterfeit banknotes using a pipette, allowing for the ethanol to permeate through to the dot matrix hologram side. This volume was used as it allowed for the permeation of the ethanol to the opposing side of the paper layers, without over saturating it. A sterile scalpel was then used to lift a corner of the dot matrix hologram to allow for its removal using sterilised tweezers. This was applied to three samples of counterfeit €50 banknotes with the dot holograms present. A similar process was used to separate the adhesive paper layers of the counterfeit banknote. Ethanol was deposited using a pipette at 1000 µL, ensuring the edges around the banknote were saturated. If more ethanol was needed, a further 1000 µL was added. A sterilised scalpel was used to slide between the top of the region where the imitation metallic thread was exposed. Care was taken to ensure the tip of the blade was manoeuvred between one side of the paper layer and the imitation metallic thread to

avoid tearing through the paper layer. With the application of further ethanol, the scalpel blade was able to be manoeuvred around the edges of the counterfeit banknote, ensuring the non-serrated edge of the blade was used to help pry apart the two paper layers. To completely expose the imitation metallic thread, sterilised tweezers used to the pull apart the two layers, taking care to use the tweezers in such a way to avoid cross contaminating the external surface of the banknote with the internal. This was carried out on two counterfeit €500 banknotes that had been pre-selected with imitation metallic threads present, indicating they were composed of two layers of paper.

2.2.4 Evaluation of DNA Sampling in Counterfeit Banknotes

2.2.4.1 Sampling

To demonstrate the analysis of counterfeit banknotes for DNA in practice, six counterfeit banknotes were selected (Table 2) to have their hologram carrier foils removed. These were removed from circulation in The Republic of Ireland by Law enforcement and provided by the Central Bank of Ireland. The plastic carrier foil was manually removed using sterilised tweezers before the adhesive layer was swabbed twice (Hedman et al. 2020) with cotton swabs (Deltalab, 2016) soaked in 60 µL of xylene (May and Thomson 2009). Four sets of swab samples were prepared for each extraction, consisting of two swabs from each sample.

Table 2 The €50 counterfeit banknotes provided by the Central Bank of Ireland with the dot matrix holograms present and which county they were received from. The indicative aspect refers to the categorization of the counterfeit banknote by the ECB according to the general area it was from (EU), the series of banknote it is a counterfeit of (A being the first series of euros), the denomination being counterfeited (50 euros), the process applied (P = traditional offset printing or C colour copying using equipment such as inkjet printers) and a final numerical value for the sequential order in which it was found.

Serial Number	Date Taken Out of Circulation	Date Received	Indicative	County
Y83811672257	22/01/2018	05/02/2018	EUA0050C00114a	Monaghan
Y83811672257	11/01/2018	22/01/2018		Dublin
Y43811672505	11/01/2018	22/01/2018		Dublin
Y43811679599	–	–		Dublin
Y43811672500	03/01/2018	22/01/2018		Galway
Y43811672505	06/01/2018	22/01/2018		Kildare

2.2.4.2 DNA Extraction

Each swab was individually placed in investigator lyse and spin baskets (Qiagen, 2020) to be centrifuged alongside 2 μL of proteinase K and 300 μL of DNA free water (Bruijins et al. 2019, Horjan et al. 2016, Qiagen, 2020). In the case of the Fire Monkey kit this was altered to accommodate the initial digestion step (Section 2.2.4.2.1). The lysis spin baskets allowed for the removal of any material in liquid suspension on or within the swab (Bruijins et al. 2019). Each sample was then extracted using silica spin columns from Revolugen Fire Monkey Kit (Revolugen, 2020) or a magnetic bead extraction kit from Genesig (Genesig, 2020) according to the manufacturer's instructions or Chelex extraction (Biorad Laboratories, 2000a) according to the protocol provided by the manufacturer.

2.2.4.2.1 Fire Monkey Kit

To each sample 300 μL of LSDNA reagent and 20 μL of proteinase k was added before vortexing the samples. These were incubated for 20 minutes at 56°C. Each sample had 350 μL of reagent BS and was vortexed briefly. This was followed by adding 400 μL of 75% isopropanol and vortexed briefly, ensuring the solution was then clear. A 1000 μL pipette was then used to transfer 600 μL of the sample to a spin column. This was then centrifuged at 8000 rpm for 1 minute and the flow-through discarded. Any remaining sample was then added to the spin column and the wash step was repeated. To the spin column 500 μL of WS reagent was added and then centrifuged at 8000 rpm for 1 minute. The flow through was then discarded. Each sample then had 500 μL of 90% ethanol to the spin column and centrifuged at 14000 rpm for 3 minutes before discarding the flow through. The samples were then centrifuged again at 14000 rpm for 1 minute and any flow though was discarded. The column was then placed into a pre-warmed tube at 80°C and 100 μL of elusion buffer was added (also at 80°C) to the spin column and incubated at 80°C for 1 minute. For 2 minutes the column was centrifuged at 4000 rpm to remove the eluted sample from the column.

2.2.4.2.2 Magnetic Bead Extraction

To each sample, 20 μL of tube 1 and 200 μL of tube 2 was added alongside 10 μL of internal extraction control. These were then vortexed before leaving for 15 minutes. From tube 3, 500 μL was added to each sample tube before vortexing the sample briefly. They were then left to on the workbench for 5 minutes before placing on the magnetic rack and the liquid was removed. To each sample 500 μL from tube 4 was

added and then vortexed before leaving to stand for 30 seconds. They were then magnetised and the resulting supernatant removed. This was then repeated for reagent tubes 5 and 6. The final step had 200 µl of tube 7 added before vortexing and leaving the samples to stand for 30 seconds. These were then magnetised and the resulting liquid was removed to a new labelled Eppendorf to be analysed.

2.2.4.2.3 Chelex Resin Extraction

To each supernatant tube from the lysis spin basket step 175 µL of a 5% chelex working solution was added using a 1000ul pipette. The Chelex solution was on a magnetic stirrer for the duration of the time of pipetting to ensure adequate suspension of the resin. The samples were then incubated at 56°C for 30 minutes. Afterwards they were vortexed at high speed for 5 to 10 seconds and incubated at 100°C for 8 minutes using a screw-down rack. The final step had the samples vortexed again at high speed for 5-10 seconds and spun in a microcentrifuge for 2-3 mins at 13,000 rpm before pipetting aliquots of the extract into microcentrifuge tubes (ensuring not to uptake any of the resin).

2.2.4.3 DNA Quantification

The samples were then quantified using a Quantifiler™ Duo DNA quantification kit from Applied Biosystems™ (Thermo Fisher Scientific, 2020) at full volume at 25 µL total volume and half volume at 12.5 µL total volume according to the manufacturer's specifications and analysed using a StepOnePlus™ real-time PCR system (Thermo Fisher Scientific, 2022a). The Quantifiler Duo kit consists of a human DNA marker (RPPH1) detected, the male chromosomal marker (SRY) and an IPC. Data was exported to Microsoft Excel (Microsoft Corporation, 2022) and statistical analysis was carried out using SPSS (IBM Corp., 2022).

2.3 Results

2.3.1 Preliminary Examination of Deposited DNA on Dot Matrix Holograms

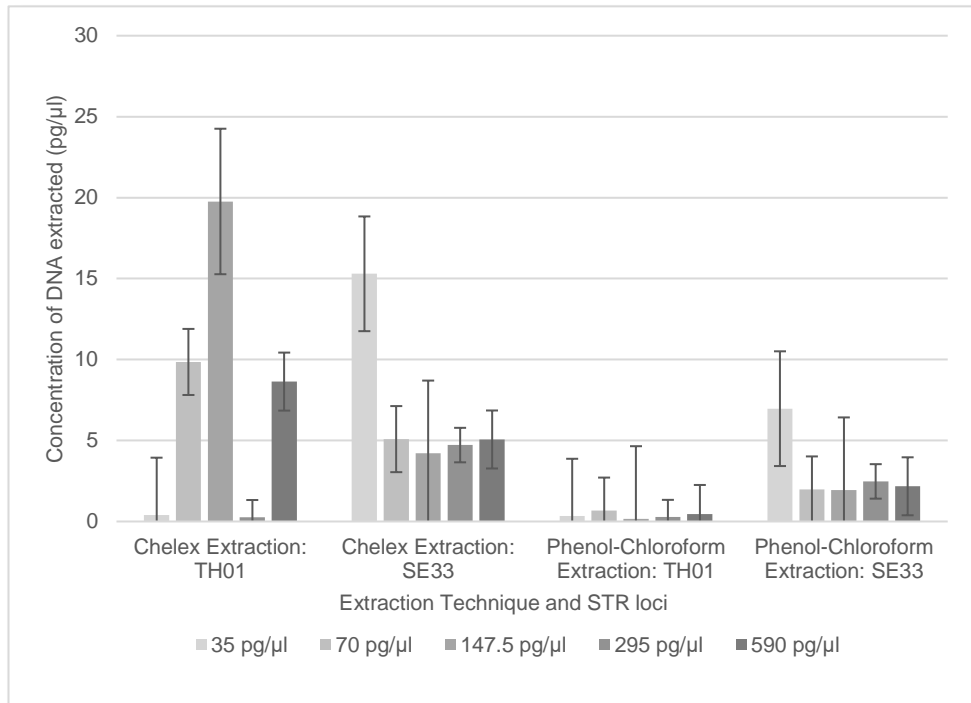


Figure 11. The average concentration of DNA acquired from the Chelex extraction technique and the phenol-chloroform extraction technique alongside the STR locus used to quantify the concentration. The legend indicates the concentration of DNA placed on the adhesive side of the hologram before swabbing. Error bars indicate the standard error of the data sets

The results for Chelex showed low levels of DNA detected, with the majority of samples only producing 10% or less of the originally placed DNA. The phenol chloroform extractions had the lowest detected concentrations of DNA, with levels appearing lower than 2% of the DNA placed on the holograms. In order to establish the distribution of the data, a normality test was carried out, to ensure that any assumptions made by further statistical analysis were appropriate to the data (Kaur and Kumar, 2015). The normality tests for both extraction groups gave p-values = 0.000 ($p < 0.05$), indicating the data was not normally distributed. As the data was not normally distributed, a nonparametric test was applied to the data as it did not meet the required parameters to carry out a more robust parametric test (Kaur and Kumar, 2015). A Kruskal-Wallis test was therefore carried out to establish the potential differences between the extraction method groups for each of the loci (Kruskal and Wallis, 1952). Both the comparison of the TH01 and SE33 loci between the Chelex

resin and phenol chloroform extractions were found to be not statistically significant ($p = 0.165$, $\eta^2 = 0.033$, $n = 30$ for TH01 and $p = 0.093$, $\eta^2 = 0.065$, $n = 30$ for SE33). Not included in Figure 11, are the detected DNA concentrations for the direct PCR carried out. The main reason for this is the data was not reliable due to the lack of established melt curves and many of the data points indicated no fluorescence was detected. In the case of the direct PCR approaches the melt curves did not represent the curve expected for the amplification of a DNA locus, instead it contained data points that indicated a large amount of fluorescent noise for the duration of the temperature variation. This data was therefore not included in Table 3. The detected levels of DNA for the volunteer and counterfeit banknote samples as shown in Table 3. As there was no way to ascertain how much DNA may have been placed on the hologram, the samples could not be compared to the potential deposited DNA (Table 3). All the volunteer and counterfeit banknotes gave readings of less than 100 pg/ μ L of DNA except for one of the volunteer samples that contained 122 pg/ μ L when measured using the TH01 STR locus after Chelex extraction.

Table 3. The detected DNA concentrations (pg/ μ L) of DNA from the Chelex extraction technique and the phenol-chloroform extraction technique alongside the STR locus used to quantify the concentration of DNA on the volunteer and counterfeit banknote counterfeit holograms.

Sample Type	Chelex extraction: TH01 (pg/ μ L)	Chelex extraction: SE33 (pg/ μ L)	Phenol chloroform extraction: TH01 (pg/ μ L)	Phenol chloroform extraction: SE33 (pg/ μ L)
Counterfeit banknote hologram	1.489	5.008	0.546	2.064
	0.520	6.732	0.060	2.519
	3.113	4.877	0.160	2.225
Volunteer prepared counterfeit hologram	3.986	4.915	0.782	2.914
	122.071	4.535	0.545	2.050
	4.465	4.372	6.212	2.030

2.3.2 Xylene, 1,2-Indandione and Hexane Adhesive Separation

On the addition of xylene, the layers easily separated, especially with the addition of more xylene between the layers as they detached, making it possible to completely separate the layers. As can be seen in Figure 12 it was possible to remove the imitation security thread within the paper layers without damaging the thread. This has been repeated a further 3 times with counterfeit banknotes with similar characteristics. Figure 13 shows the resulting effect of the addition of 1,2-indandione to a counterfeit banknote. The counterfeit banknote was a previously analysed item where the hologram was removed in Kwok et al. (2019), the remaining paper has then been cut into four segments.

As xylene was used for the separation of the paper layers of a counterfeit banknote, xylene was theorised to have the same effect on counterfeit holograms. Xylene was applied to the opposing side of a hologram present on a banknote and allowed to permeate through the paper layers to the side the hologram was present on. This proved successful in allowing for the weakening of the adhesive bonds underneath the hologram, enough so that the hologram could be lifted off using a pair of sterile tweezers (Figure 14). The similar process used for hexane was unsuccessful in separating either the adhesive layer of the paper aspects of the counterfeit banknotes and the removal of a dot matrix hologram from the paper substrate.

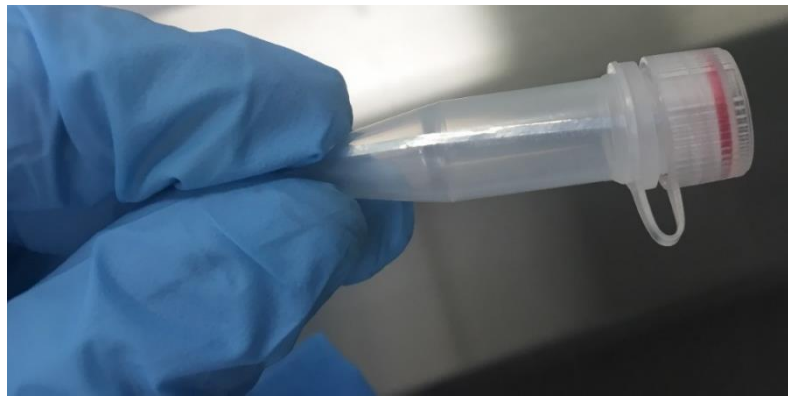


Figure 12. The removed imitation security thread removed using xylene from a counterfeit banknote.

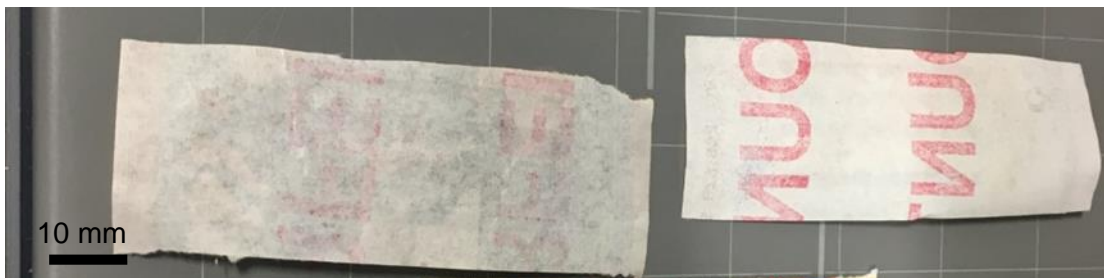


Figure 13. Two sides of the same counterfeit banknote that have been separated through the addition of 1,2-indandione.

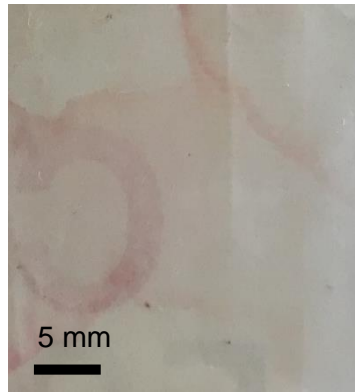


Figure 14. The paper surface of a counterfeit banknote where a counterfeit hologram has been removed using xylene, exposing the paper layer underneath.

2.3.3 Ethanol Adhesive Separation

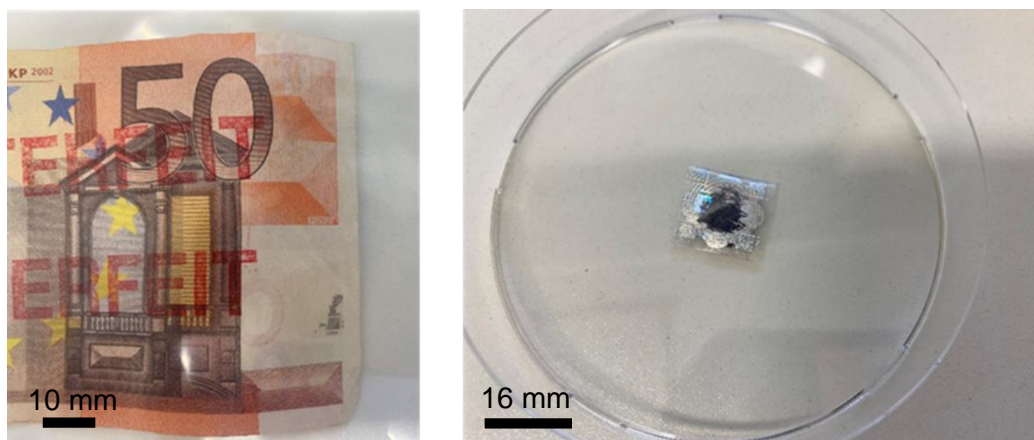


Figure 15. The removed hologram from a counterfeit €50 banknote (left), with the removed hologram (right) using 100% ethanol. Counterfeit banknote provided by the Central Bank of Ireland.

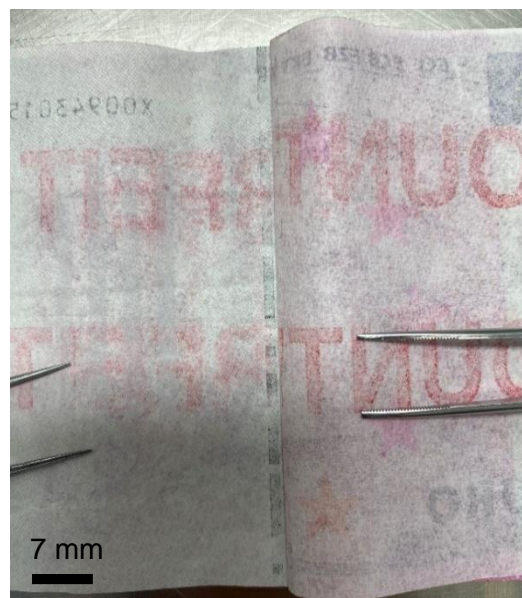


Figure 16. The separated paper layers of a counterfeit €50 banknote, with the removed imitation metallic thread using 100% ethanol. Counterfeit banknote provided by De Nederlandsche Bank.

From the use of ethanol, the dot matrix holograms were removed successfully from the surface of the paper substrate. The amount of time between depositing the ethanol and removing the dot matrix hologram was not monitored but the hologram had to be removed before the ethanol completely evaporated. Once the ethanol was no longer present, it was not possible to remove the hologram without damaging the sample. All three €50 samples had the dot matrix hologram successfully removed. In the case of the €500 counterfeit banknotes, the paper layers were successfully separated to expose the imitation metallic thread. One of the counterfeit banknotes proved more difficult to separate than the other sample. However, with the addition of more ethanol the layers were successfully separated.

2.3.4 Evaluation of DNA Sampling in Counterfeit Banknotes

The results show that more DNA was detected in samples while using a PCR reaction volume of 12.5 μL (Appendix 2-4). Although none of the samples had the human DNA marker (RPPH1) detected, the male chromosomal marker (SRY) was detected in many of the samples. The half volume reactions had the most successful set of results with only 7 of the reactions having no detected sample DNA (Figure 18). Whereas the 25 μL reactions (Appendix 5-7) had 23 reactions with unsuccessfully detected DNA readings for the SRY locus (Figure 17). The effectiveness of the different extraction techniques cannot be statistically compared due to the sample size. All standard curves were above a R-squared of 0.95, indicating the values detected for the standards could be reliably used to compare to the unknown samples. All samples had the internal positive control marker present suggesting the PCR did occur in all sample wells with ct values comparable to the negative controls indicating no inhibition was present (Barbisin et al. 2011). As the data was not normally distributed (p -value <0.05), a Mann-Whitney Test was conducted between the full 25 μL volume reaction mixture samples and the 12.5 μL to establish if there was a statistically significant difference in the medians between the two volumes. The results from the test gave a p -value of 0.114 ($p >0.05$, $n = 24$, $r = 0.331$) suggesting there was no significant difference in the results between using the full reaction volume and the half reaction.

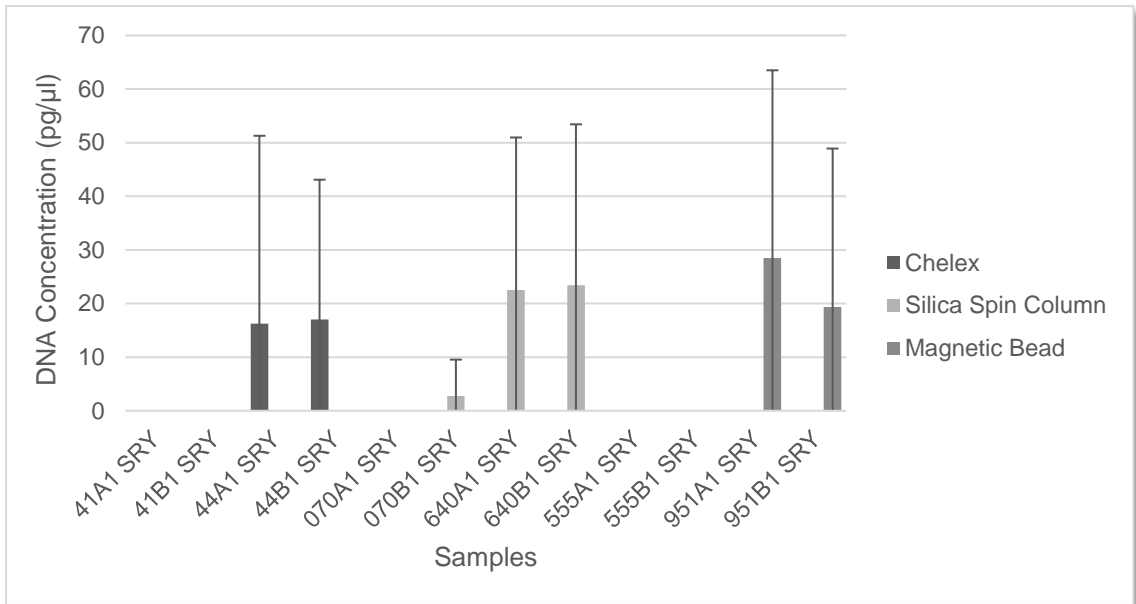


Figure 17. The average detected concentration of DNA using the male SRY marker (pg/μL) from primary (A1) and secondary (B1) swabs taken from the adhesive hologram residue left on counterfeit banknotes. Reaction volumes were all set to 25 μL. Error bars indicate the standard error of the data sets.

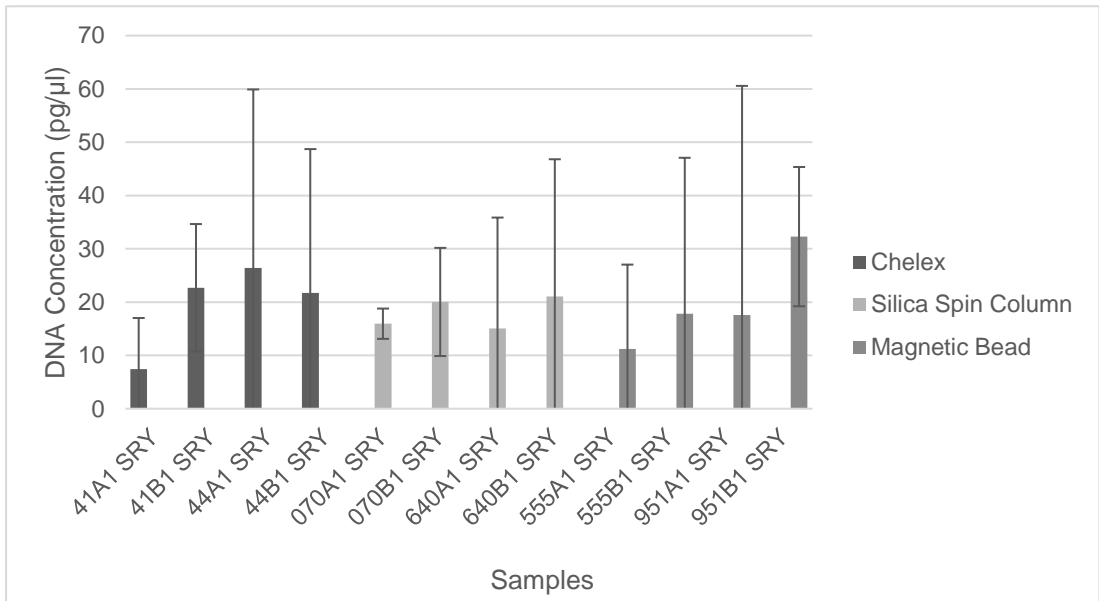


Figure 18. The average detected concentration of DNA using the male SRY marker (pg/μL) from primary (A1) and secondary (B1) swabs taken from the adhesive hologram residue left on counterfeit banknotes. Reaction volumes were all set to 12.5 μL. Error bars indicate the standard error of the data sets.

2.4 Discussions

2.4.1 Preliminary Examination of Deposited DNA on Dot Matrix Holograms

The Chelex based extraction technique was found to consistently achieve the highest yield in extracting detectable levels of DNA. The phenol-chloroform extractions did produce some detectable DNA, but most samples did not reach above 5 pg/ μ L of DNA, especially when using the TH01 based qPCR. A clear spike in the detected DNA is seen in the lower concentrations of DNA planted in the SE33 locus for both extractions. This is due to the percentage proportions being higher for lower concentrations rather than there being more DNA detected. The variable values of DNA acquired are likely due to the adhesive interaction with the deposited DNA, preventing it from being extracted efficiently (May and Thomson 2009). Water rather than a solvent was initially used in the study to first establish the extraction and overall sample preparation before moving onto solvent use detailed later in the thesis. Research has also shown that water as a moistening agent performs just as well as other swabbing reagents when dealing with adhesive on evidential tape (Phetpeng et al. 2015). Alternatively, the use of a solvent such as xylene was considered as it has been proven to be more effective than water or phenol chloroform in removing DNA from adhesive tape lifts. The TH01 and SE33 loci were both used to establish the condition of the samples. As the TH01 locus appears no longer than 200 base pairs and the SE33 locus appears longer at above 300 base pairs (Hills et al. 2010, Vanderheyden et al. 2007), the aim was to use these to quantify any degradation or damage to the DNA present in the form of a degradation index (Balding and Buckleton 2009, Bright et al. 2013). The data between the two different loci was expected to be different as larger loci degrade faster than shorter loci (Vernarecci et al. 2015) to compare the larger locus to the smaller locus to form a ratio to indicate how degraded a sample is (Lin et al. 2018, Vernarecci et al. 2015). However, as can be seen in Figure 11 the locus SE33 in most phenol chloroform samples indicated a higher concentration of DNA compared with the TH01 locus target. The same was true for the chelex extracted samples but only in two of the concentrations (35 pg/ μ L and 295 pg/ μ L). This was unexpected as the variability in the concentrations of the loci is expected to be skewed with the TH01 locus being the more prominent throughout the samples. The SE33 was expected to be much lower in concentration as the locus is larger than the TH01 locus, making it more susceptible to degradation (Vernarecci et al. 2015). A degradation index was not carried out for this reason. The disparity between the two loci could be down to inhibition within the PCR that could explain the

variability in the results (Steadman et al. 2015). In the methodology (Section 2.2.1) scalpel blades were used to help free the adhesive for swabbing. This may have contributed to the inhibition of the PCR as it has been shown to be less beneficial than using swabbing alone (Steadman et al. 2015). The use of a solvent to prevent any inhibition from present adhesive previously mentioned may have compensated for this.

To establish the significance of the results, a Kruskal-Wallis test was carried out on the separate extraction methods and the STR loci used. The comparison of Chelex extraction and phenol chloroform extraction for both loci gave p-values of >0.05 for both sets of STR loci at 0.165 for TH01 and 0.093 for SE33 from the Kruskal-Wallis test. This indicates there was no significant difference between the results. The effect size was found to be small for the TH01 ($\eta^2 = 0.033$, $\eta^2 > 0.01$, $n = 30$) locus indicating a small level of the variation in the data could be explained by the extraction processes (Cohen et al. 1988). The effect size for the SE33 locus was found to be medium TH01 ($\eta^2 = 0.065$, $\eta^2 > 0.06$, $n = 30$) indicating a moderate level of the variation in the data could be explained by the extraction processes. As phenol chloroform is a solvent it was expected that this would have been more effective freeing the DNA from any adhesive present in the sample. However, this was not the case as Chelex appeared to be more effective although not to a significant level. Adopting a different methodology in swabbing processes coupled with other types of extraction such as magnetic bead extraction and silica spin columns may improve the success of the sampling. The addition of a post extraction step where the DNA is concentrated down using devices such as Microcon[®] DNA Fast Flow Filters (MERCK, 2021) the chelex may improve the detectability of any DNA present as well as improve the results for DNA profiling (Norén et al. 2013). The use of xylene as a solvent directly on the DNA source while swabbing will also likely improve the results as was shown in similar research carried out by May and Thomson (2009). In the case of the direct PCR set of samples, the data was not sufficiently reliable to give an accurate reading for how much DNA was present or if the reaction was successful. This could be due to the adhesive interaction with the DNA and PCR mixture causing an inhibitory effect or the type of swab involved which has not been used before in this process. Alternative swab types have been used such as the microFLOQ swab produced by Copan for direct PCR approaches (Comte et al. 2019, Sherier et al. 2020), that could be researched further to establish a more successful method. This was attempted in a small number of the samples where the cotton swab used to swab the adhesive side of the dot matrix holograms was cut into segments before being introduced directly to the PCR well (Section 2.2.1). However, from the data there was a

concentration indicated from the qPCR but the melt curves indicated that there was no PCR product presence. Instead, the graphical representation of the melt curve consisted of fluorescent noise whereby the data points fluctuated drastically throughout the temperature change of the wells. The data could therefore not be verified by a distinct PCR product being present in the melt curve analysis.

2.4.2 Xylene, 1,2 Indandione Separation and Hexane Adhesive Separation

Previously, May and Thompson (2009) indicated the possibility of xylene being used to separate the adhesive layers of counterfeit banknotes. Although in their research they used solvents to swab the adhesive side of tape-lifts. It was hypothesised that a solvent could be used to separate the adhesive layers of a counterfeit banknote.

This was then attempted on other double layered counterfeit banknotes, but this was not as successful. Other attempts were made on four counterfeit banknotes using xylene to separate the paper layers but instead an access window to the imitation metallic thread was made. For three of the counterfeit banknotes this proved relatively straight forward, ensuring that the scalpel did not pierce straight through both layers of the paper. However, one of the notes proved more difficult to separate as the adhesive was not as readily dissolved by the xylene. This could be due to a couple of hypothetical factors, either: the type of adhesive used may have been different between each note or the concentration of the adhesive used varied between the counterfeit banknotes. It can be said that the use of xylene was successful in achieving the aim of separating the paper layers of counterfeit banknotes. Hexane, another solvent was also used (Testolin and Lain 2005 and Lappé and Kallmeyer 2011), but the adhesive bonding between the layers was not sufficiently weakened to remove the adhesive hologram or the adhesive paper layers.

In the research for Section 2.2.1 counterfeit holograms were separated manually using a pair of tweezers and scalpel blade. This may have allowed for any encapsulated DNA to remain trapped in the adhesive even when swabbed. In a similar process of adding xylene to the double paper layers of counterfeit banknotes, xylene was added to the paper layer underneath the dot matrix hologram on a counterfeit banknote (Figure 14). This proved successful in allowing for the weakening of the adhesive bonds underneath the hologram, enough so that the hologram could be lifted off using a pair of sterile tweezers. By applying xylene on

one side, the risk of introducing external DNA contamination is reduced while allowing for the effective removal of the hologram. The concern, however, is that some of the encapsulated DNA released by this process may be lost. A more reliable process was needed.

To combine the manual and xylene techniques to remove holograms from counterfeit banknotes, the carrier foil was first removed to leave the hologram and adhesive on the surface of the counterfeit banknote. The residual adhesive hologram could be then removed onto a cotton swab using xylene. This method allows for the swabbing of potentially encapsulated DNA without the risk of introducing external DNA or using excessive volumes of xylene that may remove any potentially encapsulated DNA. The resulting extracted and quantified results of the swabs can be found in Section 2.3.2. However, there was a concern that there may be DNA degradation due to the hazardous properties of xylene (Chen et al. 2008, Liu et al. 2010). Previous research by May and Thomson (2009) had considered the use of saliva quantities of DNA that would not reflect the concentrations of DNA expected from touch DNA samples. The researchers also compare their method of xylene solvent use with a standard procedure in their case work on mock crime scene tapes and found no detrimental effect on the recovery. However, this would not directly reflect the same quantities of DNA expected in single deposition samples compared to tape lifts taken from worn clothing due to the expected deposition variation between different surface types and duration of deposition (Ruan et al. 2017).

The use of 1,2-indandione proved successful in the separation of paper adhesive layers of the counterfeit banknote segments it was applied to. However, it was not clear what component of the working solution was causing the adhesive layers to separate. HFE 7100 and ethyl acetate were part of the working solution used which potentially could have allowed for the removal of the adhesive with them both being solvents (Nicolosora et al. 2018).

In the application of both xylene and 1,2-indandione a small number of samples were analysed. This would therefore not account for the possibility that other counterfeit banknotes samples from other sources may have different adhesives present that would vary the effectiveness of the solvents to separate the layers. Other solvents would therefore need to be considered in these instances. However, for the samples used here the xylene and 1,2-indandione solutions were successful in the aim to separate the adhesive layers of the counterfeit banknote samples.

2.4.3 Ethanol Adhesive Separation

In comparison to the xylene based adhesive removal, the ethanol results were almost identical in terms of the procedural methodology but allowed for an easier separation of the adhesive layers. Thus, successfully achieving the aim of separating the adhesive layers of counterfeit banknotes. The one variation in its use was the speed at which the ethanol evaporated was faster, leading to more being applied periodically. Care had to be taken to ensure that a sufficient volume was added when separating the adhesive paper layers to avoid over saturating the paper, to help avoid the tearing of the paper and risking contamination. To avoid tearing the paper layers from within the adhesive layer, the non-serrated edge of the scalpel was used to part the two paper layers. The separation of the paper and adhesive along the edge of the counterfeit banknotes allowed for sterilised tweezers to pull apart the two paper layers along the edges with the further addition of 100% ethanol. In the case of the dot matrix holograms, ethanol was allowed to permeate through the reverse side of the paper to the underside of hologram in a similar manner to the use of xylene (Section 2.2.2). The dot matrix was then lifted using sterilised tweezers, using one of the corners to avoid introducing contamination with repeated handling. This allowed for the dot matrix hologram to be more easily removed from the paper substrate than was found with the use of xylene. The use of 100% ethanol was considered due to a study published by Ruprecht et al. (2021). In the research, a removal solution consisting of a mixture of cyclohexane and propanol was used to separate adhesive stamps from envelopes, followed by swabbing of the adhesive side of the stamps with 100% ethanol. Although their removal solution was not used in this research, in art restoration ethanol is also a commonly used solvent for the removal of adhesive tapes (Mirabile et al. 2020, Smith et al. 1984). Ethanol is also widely used in the preparation of DNA samples for DNA extraction and precipitation so is unlikely to cause any unforeseen downstream negative effects for DNA profiling (Lei et al. 2022). As ethanol has been frequently used as a swabbing agent and in DNA extraction, it was hypothesised that it could be used to separate the paper layers of counterfeit banknotes whilst limiting any damage to any present trace DNA evidence present (Chapter 4).

As with the discussion for the xylene and 1,2-indandione separation techniques, only a small number of samples were initially analysed using this method. Although this would make this limited, further work in Chapter 3 and Chapter 4 highlight the

potential of the use of ethanol to separate the adhesive layers in counterfeit banknotes consistently.

2.4.4 Evaluation of DNA Sampling in Counterfeit Banknotes

The results show that more DNA was detected in samples while using a PCR reaction volume of 12.5 μ L. With the RPPH1 locus there was no detected amplification of the target DNA in any of the unknown samples. The ct values for the IPC indicated that there was no inhibition in the reactions with ct values remaining consistent with the negative controls (Barbisin et al. 2009). All standard curves were also above a R^2 value of 0.95 indicating there was no issues with the use of the standard curves for any of the loci. This was investigated further with positive controls that ruled out any issues with the PCR machinery used or the quantifier kit itself. The lack of the RPPH1 locus appearing in the samples could be due to the level of degradation or inhibition for potential DNA present (Funes-Huacca et al. 2011). Due to the swabbing of the dot matrix holograms removing some of the holographic material, there may have been an inhibitory effect on the VIC dye marker being detected. However, this was not investigated further as an alternative process of removing the whole dot matrix hologram was being considered as more effective from the previous work with the solvent xylene (Sections 2.2.2, 2.3.2 and 2.4.2). Although none of the samples had the human DNA marker (RPPH1) detected, the male chromosomal marker (SRY) was detected in many of the samples. The half volume reactions had the most successful set of results with only 7 of the reactions having no detected sample DNA (Figure 18). Whereas the 25 μ L reactions had 23 of the 36 sample reactions with unsuccessfully detected DNA readings (Figure 17). A Mann Whitney U test was used to establish if there was a difference between the use of the two volumes. From the results of the test, it can be said that there was no statistically significant difference between the two volumes with a p-value of 0.114 ($p > 0.05$, $n = 24$, $r = 0.331$). This suggests that the use of a half volume reactions for the qPCR is not statistically different in the detection of sample DNA, allowing for smaller volumes of the reagents to be used for the same resulting quantification result. The effect size was indicated as being medium by the reported value ($r > 0.3$) indicating the volume differences explained moderate variation in the data. The overall concentrations of Y chromosomal DNA detected were too low to gain potential complete DNA profiles, with highly variable standard errors for the samples due to the small sample size. The consensus in the literature is that the threshold for successful DNA profiling is above

100 pg/ μ L. However, this is not to say that at least partial DNA profiles would be obtainable at amounts lower than 100 pg (Gill et al, 2000 and 2001). Aditya et al. (2011) suggest that quantification data does not directly link to the successful profiling of an evidential sample. In some cases, profiles are still obtainable when no DNA has been detected during the quantification process. The same was suggested by Schniffer et al. (2005) where they obtained partial profiles from as low as 12.5 pg/ μ L concentration samples that had been extracted using Chelex resin. DNA profiling of the swabbed counterfeit samples would need to be carried out to establish the potential contamination from the examiner. There are also other qPCR systems other than the Quantifiler™ Duo kit available that provide higher sensitivities, down to 1 pg/ μ L for low copy number DNA as the Investigator Quantiplex HYres kit (Qiagen, 2021). However, these are not compatible with the available Applied Biosystems Step One Plus system at the university (Thermo Fisher Scientific, 2022a).

Due to this stage of the research occurring after the first loosening of covid-19 restrictions in the UK, the experimental design could not yet rely on volunteers due to the safety concerns at the time. Instead, the samples analysed were of seized counterfeit samples to expand on the preliminary work looking at deposited DNA on dot matrix holograms (Sections 2.2.1, 2.3.1 and 2.4.1). At this stage of the research, xylene had not been used to separate the adhesive layers of the dot matrix hologram. Thus, why the polymer carrier foil was removed off the surface of the dot matrix hologram rather than removing the hologram completely from the paper substrate. This could have affected the qPCR results as the swabbing had to remove as much of the adhesive as possible, to reach the layer at which the paper and adhesive met. Although this removed the need to separate the dot matrix hologram from the paper substrate, this did introduce a lot of the holographic and adhesive material to the extraction process. This could have inhibited the downstream qPCR analysis by introducing too much of the adhesive (Barbaro et al. 2011, Zech et al. 2012). This may have further encapsulated the DNA which has been speculated in research by Ng et al. (2007) in envelope sourced DNA samples. Due to the samples consisting of counterfeit banknotes, there was no way in which to verify if DNA was already present and at what concentration. This would have helped to verify and control the resulting concentration results post extraction. To further investigate this, a simulated procedural study was carried out (Chapter 3).

2.5 Conclusions

The preliminary study sought to establish the possibility of acquiring DNA from the adhesive present on dot matrix holograms. From the data it was not possible to discern whether phenol chloroform or chelex resin extraction was the more optimal methodology to extract the samples. This was not able to meet the objective of establishing an optimum extraction process for the adhesive samples but established if trace levels of DNA could be acquired from one of the adhesive layers of a composite counterfeit banknote. More research was needed to further evaluate this. The use of two primer sets, TH01 and SE33 also proved complicated in the data interpretation. Although the use of two probes was not as successful as hoped, the use of multiplex qPCR systems was considered for further research.

Instead of using a SYBR Green based qPCR, the research moved towards using a multiplex system, the Quantifiler Duo DNA quantification kit, followed by the implementation of other extraction methodologies. To swab the samples the solvent, xylene was used to allow for the removal of the adhesive dot matrix hologram, after the carrier foil had been removed. Although there were similar issues in establishing the optimum extraction methodology

Following from this there was research highlighting the use of solvents as a potential swabbing solution to help remove and release encapsulated DNA present in the adhesives present in the counterfeit banknotes. For the comparison of xylene, 1,2-indandione and ethanol, all three solvent approaches proved successful in the separation of the adhesive layers of the counterfeit banknotes analysed. Successfully achieving the aim of separating the adhesive layers of counterfeit banknotes using these solvents. For the xylene samples it was shown to be successful in the separation of both the double paper layers and the dot matrix holograms. However, there was a concern that there may be DNA degradation due to the hazardous properties of xylene (Chen et al. 2008, Liu et al. 2010).

This led to the investigation of alternative solvents that may be less detrimental to trace DNA samples. Ethanol is often used in the extraction stages of DNA sample processing as well as being used as a swabbing agent for tapelifts (Ruprecht et al. 2021). It was hypothesised that it would be successful in the separation of adhesive layers within counterfeit banknotes. From the samples it was clear that ethanol was an appropriate solvent for the separation of the adhesive layers as it successfully

dissolved the adhesive bonds present in the counterfeits. The solvent also evaporated faster when compared to the application of xylene, preventing any risks of contamination through the handling of the counterfeit. The next steps were to implement the findings from these smaller studies into a larger simulated procedural study to establish how these techniques could be applied together to meet the aim of establishing if a STR profile could be acquired from counterfeit banknotes.

Chapter 3 Simulated Procedural Study to Evaluate the Presence of DNA in Composite Counterfeit Banknotes

3.1 Introduction

The next stage of the research looked to meet the objective of having volunteers make composite counterfeits that are then given to a secondary volunteer for handling thereby simulating the circulation of a counterfeit banknote. The aim of this was to establish what is the optimal extraction process to extract the DNA whilst establishing if there was any risk of DNA transfer for the external surface of a counterfeit banknote into the adhesive layers. This would be evaluated through analysing the quantity of DNA present and the condition of the STR profiles. The idea was to improve on the studies carried out in Chapter 2 and instead have individuals place their fingermarks on the adhesive side of the dot matrix holograms to introduce trace levels of DNA. This was briefly touched upon in Chapter 2 but a large sample size involving volunteers was needed to expand on the aim of developing a methodology of acquiring DNA from a counterfeit banknote.

3.2 Methodology

Ethics Declaration

All experimental designs and involvement of volunteers were approved under Proportional Ethical Approval provided by the Staffordshire University ethics Committee, with written consent given from all volunteers for their involvement in the research herein detailed.

3.2.1 Sample Preparation and Extraction

Three volunteers, two female (volunteers A and B) and one male (volunteer C), were asked to not wash their hands for 1 hour and 30 minutes before placing their individual fingermarks on the adhesive side of dot matrix holograms (provided by the ECB). In this time, they were told to carry out their day as normal, refraining from washing their hands and wearing gloves during this time. This was to allow for natural fingermarks to be placed onto the adhesive (Templeton and Linacre 2014). No analysis was done prior involved of the volunteers of either their shedder status or potential shared alleles. Thirty samples were taken from each volunteer (ten for

each of the extraction techniques applied) producing a total sample set of 90. These were then placed on banknote paper provided by the ECB that had been cut into 2.5cm² squares and stored for 1 week in sterile petri dishes (Tan et al. 2020). This prevented any risk of contamination while the samples were stored and was also beneficial in allowing for easier handling of the samples during processing. All dot matrix holograms and banknote paper used was sterilised first with 70% methylated spirit (Parsons et al. 2016) before placing them in UV light for 15 minutes before use in the research (Templeton and Linacre 2014). Tweezers used were sterilised by soaking them in 70% methylated spirit (Parsons et al. 2016) for 1 hour followed by exposure to UV light for 15 minutes for each use. Two days into the storage period the newly formed composite counterfeit banknotes were handled by the male volunteer (volunteer C) after rubbing their hands behind their ears and neck. The composite counterfeit banknote segments were gently rubbed between the hands of the volunteer for 10 seconds each (Schelte et al. 2021). This was to introduce sebaceous material (McLaughlin et al. 2021) to the external aspects of the composite counterfeit banknote, imitating a circulation event. On removal from storage, the composite counterfeit banknotes were double swabbed (Hedman et al. 2020) with 60 µL of DNA free water using cotton swabs (Deltalab, 2016). Water was used as it is a common swabbing agent (Phetpeng et al. 2015) and there was no adhesive present on the surfaces of the exposed paper or plastic carrier foil of the dot matrix holograms. The dot matrix hologram was then removed manually using sterilised tweezers and the adhesive side was double swabbed by first placing 30 µL of xylene onto the adhesive before using a swab with 30 µ of xylene to swab the surface using cotton swabs (Deltalab, 2016). For the phenol chloroform and the chelex resin extractions the swabs were then added to investigator lyse and spin baskets (Qiagen, 2020) with 300 µL of DNA free water and 2 µL of proteinase K present. These were left for 1 hour in a 56°C heated shaker at 900 rpm. The baskets were then centrifuged according to the specifications provided by Qiagen (2020). The resulting lysis solution was then extracted using phenol chloroform and Chelex resin according to the methodology in Section 2.2.1 and a magnetic bead extraction kit, BTA Prepfil kit, according to the manufacturer's guidelines (Thermo Fisher Scientific, 2022b) detailed in Section 3.2.1.1. The Chelex resin extraction had an additional step of condensing the product from an estimated 300 µL to 30-40 µL using the Microcon[®] DNA Fast Flow Filters (MERCK, 2021) by adding the extract supernatant to the filter tubes and centrifuging at 500 g for 23 minutes. The tube filters were then inverted and centrifuged to remove the sample at 1000 g for 3 minutes (MERCK, 2021).

3.2.1.1 BTA Prepfiler Magnetic Bead Extraction

In preparation before the extraction steps the Eppendorf of magnetic particles was incubated at 37°C for 10 minutes and vortexed till the particles were completely resuspended. The lysis buffer was also incubated at 37°C for 15 minutes. Primary and secondary swabs were snapped into investigator lyse and spin baskets (Qiagen, 2020) with 220 µL of BTA PrepFiler Lysis Buffer and 3 µL of DTT. Tubes were then vortexed and added to a shaker at 900 rpm, for 40 minutes at 70°C. They were then centrifuged for 2 minutes at 12,000 rpm. Samples were then left to reach room temperature before adding 15 µL of the magnetic bead suspension. To ensure the magnetic particles were suspended the Eppendorf was vortexed briefly and inverted every 5 minutes. To each sample, 300 µL of isopropanol was added before vortexing them briefly before pulse spinning them in a centrifuge. The samples were then placed on a shaker at 1000 rpm for 10 minutes. These were then vortexed before a pulse spin and placed onto a magnetic stand until the particles adhered to the side of the Eppendorf. Waste supernatant was then pipetted out, taking care not to disturb the magnetic beads. For the following wash step, the process was repeated three times. First, 600 µL of wash buffer A was added to the sample before vortexing and pulse spinning. The Eppendorf was then placed on the magnetic stand, allowing for the particles to adhere to the side of the tube. Waste liquid was then removed and 300 µL of wash buffer A was added before vortexing and pulse spinning the tube. After placing the samples back onto the stand and the particles had adhered to the side, the waste liquid was again removed. The final wash step had 300 µL of wash buffer B added to the samples with them being vortexed and pulse spun. The samples were then left on the magnetic stand for the particles to adhere on to the side of the tube before removing the waste supernatant. Samples were then left with the tubes open to allow them to dry for no more than 10 minutes. To each sample, 30 µL of elution buffer was added and the sample was vortexed and pulse spun to resuspend the particles. The samples were then placed in a shaker at 70°C and 900rpm for 5 minutes. These were then centrifuged for 7 minutes at max speed (10,000rpm) and the supernatant was transferred to a fresh tube.

3.2.2 DNA Quantification

The resulting extracted samples were then quantified using the Quantifiler™ Duo DNA quantification kit from Applied Biosystems™ (Thermo Fisher Scientific, 2020)

according to the manufacturer's guidelines in half volumes at 12.5 μL and analysed using a StepOnePlus™ real-time PCR system (Thermo Fisher Scientific, 2022a).

3.2.3 DNA Profiling

DNA profiles were produced using the AmpFLSTR™ NGM SElect™ PCR amplification kit at half reaction volumes with 5 μL of Master mix and 2.5 μL of NGM Select primer set alongside 5 μL of DNA sample (Thermo Fisher Scientific, 2021). All reactions were carried out at 29x cycles with positives and negatives present for each plate. The PCR consisted of one step at 95°C for 11 minutes, a second step at 94°C for 20 seconds followed by 59°C for 3 minutes for 29 cycles and a final step of 60°C for 10 minutes (Thermo Fisher Scientific, 2021). The DNA profile PCR products were then loaded onto an Applied Biosystems™ 3500 Genetic Analyser plate with 8.5 μL of Hidi formamide and 0.5 μL of LIZ™ size standard for each 1 μL of DNA template (ThermoFisher Scientific, 2022c). All samples were prepared on ice when loading the plate and a final heating step at 95°C for 3 minutes before moving the plate to an ice box was carried out to ensure any DNA present was single stranded before placing the plate onto the Genetic Analyzer (ThermoFisher Scientific, 2022c). The Genetic Analyzer was run with an injection voltage of 1.2 kV for 15 seconds using POP-4™ separation matrix polymer (ThermoFisher Scientific, 2022c). All sample data sets were loaded onto GeneMapper™ ID – X Software v1.6 alongside an allelic ladder provided with the NGM kit (ThermoFisher Scientific, 2022c). Outputs were analysed using an analytical threshold for the RFU values set to 50 RFU to exclude any detector background noise (Heathfield et al. 2022, Martín et al. 2014). Profiles were then exported to Microsoft Excel (Microsoft Corporation, 2022) for allele composition and RFU analysis. Statistical analysis was carried out using SPSS (IBM Corp., 2022). Heterozygote imbalances were calculated by taking the RFU values for heterozygote locus sets in an STR locus and dividing the RFU value of the smaller height by the larger RFU value (Kelly et al. 2012).

3.3 Results

3.3.1 DNA Quantification

The data from the RPPH1 locus in the external samples did not vary between the three extraction techniques, with the means remaining below 3 $\text{pg}/\mu\text{L}$ (Table 4). In comparison the internal samples had the chelex resin and phenol chloroform at a mean of 1.85 and 0.26 $\text{pg}/\mu\text{L}$ respectively but the BTA prepfilter samples had a higher mean of 13.08 $\text{pg}/\mu\text{L}$ (Table 4). From the SRY locus the data suggested a different

trend for the external samples, with the Chelex resin and phenol chloroform samples having higher means of 5.74 pg/μL for the chelex resin samples and 14.68 pg/μL for the phenol chloroform. The BTA Prepfil kit samples had the highest mean of recovered DNA at 17.68 pg/μL. The mean DNA extracted for the internal samples for the SRY locus indicated similar mean values to the RPPH1 locus for internal samples except from the BTA Prepfil kit which had no detected DNA for any of the samples. The chelex resin extractions had a mean of 2.01 pg/μL and the phenol chloroform samples had a mean of 0.93 pg/μL which closely reflected the RPPH1 locus values for the internal samples (Table 4). Table 4. Descriptive statistics of the DNA concentration (pg/μL) detected by the two markers, SRY and RPPH1 alongside the location of the samples. The only detected SRY locus based samples consisted of the samples produced from volunteer C placing their DNA on the internal adhesive of the dot matrix holograms. There was no SRY locus DNA detected in the samples that had either volunteer A or B's DNA placed on the adhesive dot matrix hologram. This was expected as the volunteer involved with the external deposition of DNA was male, and the volunteers who deposited their DNA in the internal aspect of these samples was female. Although there was a lack of SRY locus compared to the RPPH1 locus for the external samples in comparison. The disparity between the SRY and RPPH1 loci for the external samples was not expected as the male volunteer was the primary source of DNA. This could have been due to the DNA degradation causing the loss of loci (Foran et al. 2006, Swango et al. 2007). Due to the use of the silica system in the BTA Prepfil kit, the DNA could have been lost from the permanent binding of the DNA to the silica matrix (Shaw et al. 2009) or lost from the washing step (Cartozzo et al. 2018).

A normality test was carried out for each location's data set according to the genetic markers RPPH1 and SRY loci. All the groups according to extraction and sample source location were found to not be normally distributed ($p < 0.05$). Kruskal-Wallis tests were therefore carried out comparing the concentrations of the DNA from each extraction method applied to each sample location according to the two genetic markers. For the comparisons of the RPPH1 marker data the external samples had no statistical difference between the concentration of the DNA detected and the extraction method used with a p-value of 0.146 ($p > 0.05$, $\eta^2 = 0.021$, $n = 90$). However, for the samples sourced from the internal adhesive sides of the dot matrix holograms there was a statistical significance with a p-value of 0.001 ($p < 0.05$, $\eta^2 = 0.132$, $n = 90$). A pairwise comparison for the internal extracted samples found that the comparison of the phenol chloroform to both the Chelex resin and BTA Prepfil extractions were statistically significantly different with p-values of 0.018 and < 0.0005

respectively. The mean values for the DNA quantified for the phenol chloroform was 0.26 pg/μL with both the Chelex resin and BTA Prepfiler extraction samples being higher at 1.85 pg/μL and 13.08 pg/μL respectively (Table 4). The comparison of Chelex resin extraction and the BTA Prepfiler kit found a p-value of 1.00 suggesting there was no statistically significant difference ($p > 0.05$).

The Kruskal Wallis tests for the SRY marker had contrasting results for the external and internal comparisons with there being no significant difference in the values for the internal samples ($p = 0.603$, $p > 0.05$, $\eta^2 = -0.011$, $n = 90$) but there was a significant difference in the distribution of the external sourced samples with a p-value of 0.023 ($p < 0.05$, $\eta^2 = 0.064$, $n = 90$). A pairwise comparison was also carried out to establish the differences between the extraction techniques. For the comparison of Chelex resin and phenol chloroform there was a p-value of 1.00 suggesting there was no statistically significant difference in the means of the two groups ($p > 0.05$). The same was true for the BTA comparisons with Chelex resin and phenol chloroform extractions at p-values of 0.084 and 0.131 respectively ($p > 0.05$).

Table 4. Descriptive statistics of the DNA concentration (pg/μL) detected by the two markers, SRY and RPPH1 alongside the location of the samples.

Marker	Location	Extraction	Mean	Std. Deviation	Std. Error	95% Confidence Interval for Mean	
						Lower Bound	Upper Bound
RPPH1	External	Chelex Resin	0.76	0.95	0.17	0.4	1.11
		Phenol Chloroform	1.59	3.15	0.57	0.42	2.77
		BTA Prepfiler	2.72	4.29	0.78	1.12	4.32
	Internal	Chelex Resin	1.85	2.51	0.46	0.92	2.79
		Phenol Chloroform	0.26	0.84	0.15	-0.05	0.58
		BTA Prepfiler	13.08	22.08	4.03	4.83	21.32
SRY	External	Chelex Resin	5.74	11.45	2.09	1.46	10.01
		Phenol Chloroform	14.68	35.76	6.53	1.33	28.03
		BTA Prepfiler	17.68	26.78	4.89	7.68	27.68
	Internal	Chelex Resin	2.01	11	2.01	-2.1	6.12
		Phenol Chloroform	0.93	5.09	0.93	-0.97	2.83
		BTA Prepfiler	0	0	0	0	0

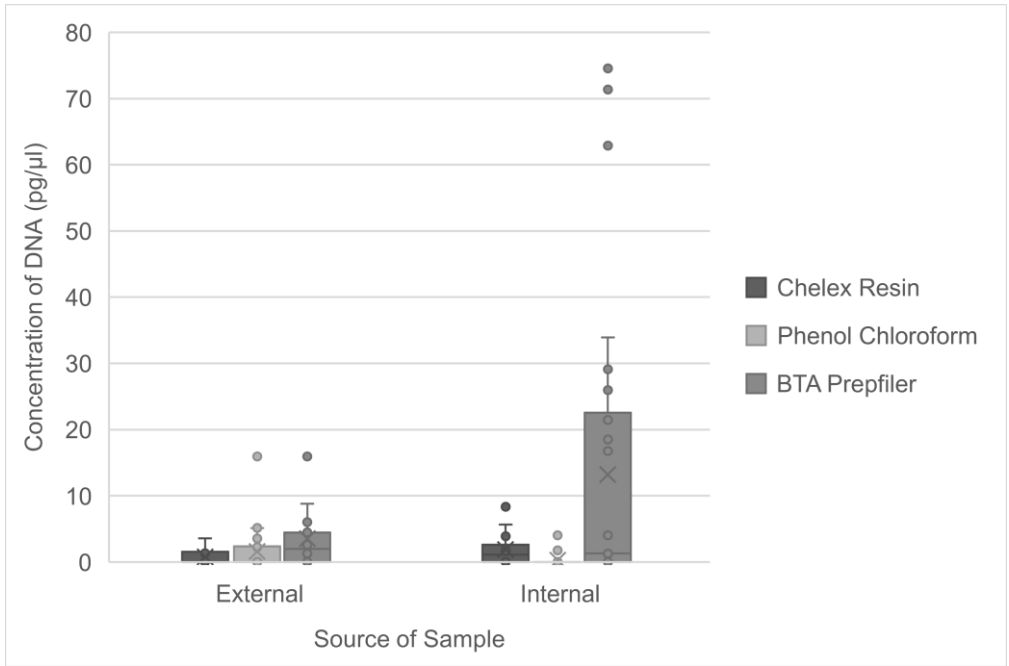


Figure 19. The quantified concentration of DNA for the three extraction techniques using the RPPH1 marker as part of the Quantifiler™ Duo Quantification kit. Error bars indicate the standard error of the data sets.

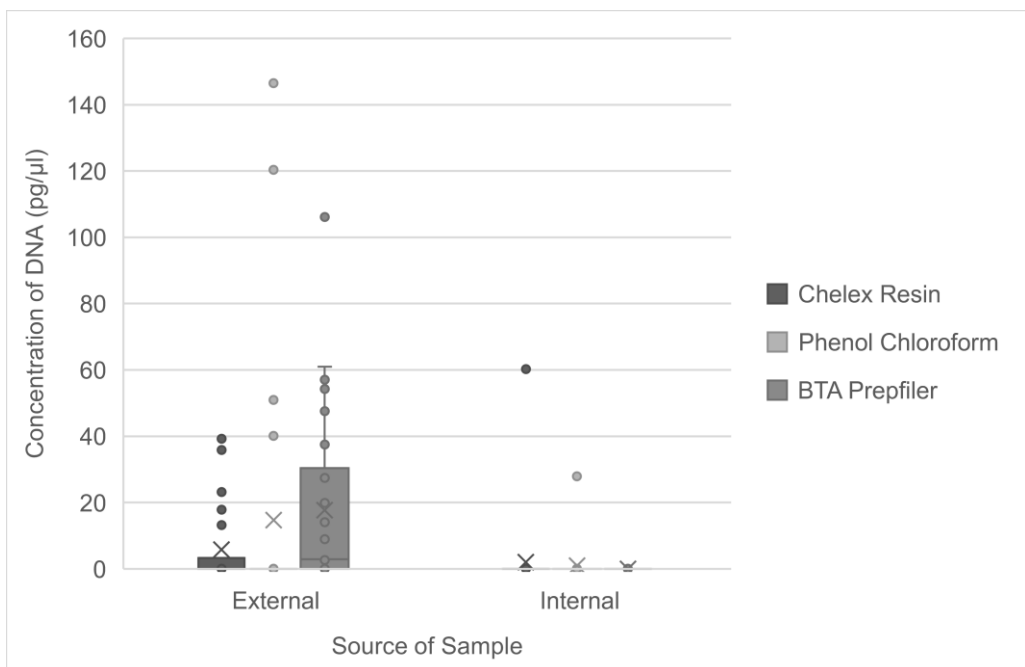


Figure 20. The quantified concentration of DNA for the three extraction techniques using the SRY marker as part of the Quantifiler™ Duo Quantification kit. Error bars indicate the standard error of the data sets.

3.3.2 DNA Profiling

3.3.2.1 Allelic Compositions

In terms of the interpretation of the profiles, all genotypes were considered heterozygote within the samples. Both the Chelex resin and phenol chloroform-based extractions produced partial DNA profiles except for one of the samples for the phenol chloroform extractions. In the case of the BTA Prepfil kit, only 7 of the 40 samples had a partial profile detected (Appendices 10-11).

From the 60 samples taken from the internal adhesive side of the dot matrix holograms, 6 had mixed profiles that contained alleles that were not in the DNA profiles of the volunteer's that placed their fingermarks on the dot matrix hologram adhesive. The alleles detected could be linked uniquely to the male volunteer (volunteer C) within the volunteer group, as the alleles detected were not present in the reference profiles for the 2 female volunteers (A and B) including one detection of the Y Amelogenin marker. Three of the samples were sourced from volunteer A's internal samples. Of the 6 alleles detected of volunteer C in volunteer A's sample set (consisting of 4 alleles in 1 sample and 1 allele present in 2 other samples) 5 of the alleles were unique to the male volunteer (C), the other allele was also present in volunteer B's reference DNA profile. In the case of volunteer B's internal adhesive samples, 2 of the samples (1 from the Chelex extractions and 1 from the phenol chloroform extractions) had 2 alleles that could be contributed to the male volunteer (C), 1 of which was the Y Amelogenin marker.

A normality test for the externally sourced samples was carried out for the three groups of extraction techniques and the total number of alleles detected in each sample taken from the external aspect of the composite banknotes. The data for Chelex resin and phenol chloroform having normally distributed data ($p = 0.288$ and $p = 0.215$ respectively). However, the BTA Prepfil kit data was not normally distributed. A one-way ANOVA was carried out on all three groups as most of the data was normally distributed with only the data points for BTA Prepfil being not normally distributed due to there being no data values. The test showed that there was a statistically significant difference between the extraction groups with a p-value of <0.001 ($p < 0.05$, $\eta^2 = 0.368$). This was followed by a Tukey HSD Post Hoc test to compare the differences between the groups. For the BTA Prepfil kit group there was a statistically significant difference between the Chelex resin and phenol chloroform groups, both of which had a p-value of <0.001 . However, for the

comparison of Chelex resin and phenol chloroform there was no statistical difference between the groups ($p = 0.949$). The same analysis was then repeated for external samples but the values used were only for the number of alleles pertaining to volunteer C who was expected to be the primary contributor. This was to avoid any risk of alleles other than the ones deposited by the volunteer C being accounted for in the analysis as this was individual who came into contact with the outside of the composite counterfeit banknote. Any unique alleles to volunteers A and B alongside unknown alleles that may influence the analysis were therefore removed from the count of alleles. The normality test indicated that the data for the phenol chloroform and Chelex resin samples was normally distributed ($p = 0.493$ and $p = 0.121$ respectively). The normality test for the BTA Prepfil kit indicated that the data was not normally distributed. A one-way ANOVA was selected again as the data points present were again found to be normally distributed. The one-way ANOVA analysis indicated that there was a statistically significant difference between the groups ($p = 0.000$, $\eta^2 = 0.360$). From the Tukey HSD post hoc test the BTA Prepfil kit was statistically significantly different from the Chelex resin and phenol chloroform groups in terms of the number of alleles present for volunteer C. The BTA Prepfil kit samples had the lowest of means at 0.5 alleles with the other extraction techniques performing better at a mean of 3 alleles for Chelex resin and phenol chloroform at 2.6 alleles (Table 5). The comparison of the number of alleles present pertaining to volunteer C for Chelex resin and phenol chloroform extractions was found to be not statistically significant ($p = 0.552$).

For the internal samples a normality test was carried out on the three extractions according to the number of total alleles observed in the three extraction groups. From the normality tests it was found that the Chelex resin extractions had a normal distribution at a p-value of 0.243. However, the BTA Prepfil kit and phenol chloroform extractions had p-values of <0.001 and 0.038 respectively, indicating the data was not normally distributed ($p < 0.05$). A Kruskal-Wallis was therefore used to compare the three groups. The comparison of the three groups established there was a statistically significant difference between them in terms of the average number of alleles observed with a p-value of <0.001 ($\eta^2 = 0.286$). A pairwise comparison was conducted to establish the differences between the groups. For the comparisons, there was no statistical significance found when the phenol chloroform extracted group was compared to the BTA Prepfil kit ($p = 0.055$) and the Chelex resin extractions ($p = 0.608$). However, when comparing the BTA Prepfil kit and the Chelex resin, there was a statistically significant difference ($p = <0.0005$). The Chelex

resin samples had the highest number of alleles at a mean of 13.25 compared to the lower 4.25 mean number of alleles for the BTA Prepfilers samples.

Much like in the external based samples, the internal sample data for the number of alleles was re-analysed but the statistical analysis only considered the number of alleles that were detected for the primary individual who would have come into contact with the sample area. In this case the alleles pertaining to the volunteer A and B reference profiles who placed their fingermarks on the adhesive side of the dot matrix holograms. The normality tests established that the data for the BTA Prepfilers kit ($p = <0.001$) and the phenol chloroform ($p = 0.003$) groups were not normally distributed. The Chelex resin data set was normally distributed ($p = 0.252$). The data was therefore evaluated using a Kruskal-Wallis test that showed there was a statistically significant difference between the groups ($p = <0.001$, $\eta^2 = 0.260$). A pairwise comparison was then conducted to establish the relationship between the three groups. The phenol chloroform when compared to the BTA Prepfilers kit ($p = 0.286$) and the Chelex resin ($p = 0.204$) extractions, were not statistically significant. When comparing the BTA Prepfilers kit and the Chelex resin groups, there was a statistically significant difference between them ($p = 0.000$). This indicates that the higher mean alleles of 12.6 for Chelex is statistically significant to the lower mean of 4.1 alleles for BTA Prepfilers.

Table 5. Descriptive statistics of the number of alleles detected externally from the composite counterfeit banknotes after extraction. These consist of the number of total alleles detected followed by: The number of alleles that can be contributed to the primary individual who handled the composite counterfeit banknote, the alleles that were unique to that individual within the group, the number of alleles that could be contributed to the volunteer who introduced their DNA to the adhesive side of the dot matrix hologram, alleles that were unique to that volunteer and the number of alleles that were shared between the two volunteers.

	Extraction	Mean	Std. Deviation	Std. Error	95% Confidence Interval for Mean	
					Lower Bound	Upper Bound
Number of alleles	Chelex Resin	5.85	2.5	0.56	4.68	7.02
	Phenol Chloroform	5.55	3.97	0.89	3.69	7.41
	BTA Prepfiler	0.85	2.54	0.57	-0.34	2.04
Number of Alleles Contributable to Primary Individual	Chelex Resin	3	1.86	0.42	2.13	3.87
	Phenol Chloroform	2.6	2.09	0.47	1.62	3.58
	BTA Prepfiler	0.5	1.67	0.37	-0.28	1.28
Number of Unique Alleles Contributable to Primary Individual	Chelex Resin	0	0	0	0	0
	Phenol Chloroform	0.05	0.22	0.05	-0.05	0.15
	BTA Prepfiler	0	0	0	0	0
Number of Alleles Contributable to Secondary Individual	Chelex Resin	5.4	2.52	0.56	4.22	6.58
	Phenol Chloroform	4.5	3.15	0.71	3.02	5.98
	BTA Prepfiler	0.8	2.44	0.55	-0.34	1.94
Number of Unique Alleles Contributable to Secondary Individual	Chelex Resin	2.4	1.43	0.32	1.73	3.07
	Phenol Chloroform	2.2	1.61	0.36	1.45	2.95
	BTA Prepfiler	0.3	0.8	0.18	-0.08	0.68
Shared Alleles	Chelex Resin	3	1.86	0.42	2.13	3.87
	Phenol Chloroform	2.35	1.9	0.42	1.46	3.24
	BTA Prepfiler	0.5	1.67	0.37	-0.28	1.28

Table 6. Descriptive statistics of the number of alleles detected internally from the composite counterfeit banknotes after extraction. These consist of the number of total alleles detected followed by: The number of alleles that can be contributed to the primary individual who placed their fingermark onto the adhesive side of the dot matrix hologram banknote, the alleles that were unique to that individual within the group, the number of alleles that could be contributed to the volunteer who introduced their DNA to external aspect of the composite counterfeit banknote, alleles that were unique to that volunteer and the number of alleles that were shared between the two volunteers.

	Extraction	Mean	Std. Deviation	Std. Error	95% Confidence Interval for Mean	
					Lower Bound	Upper Bound
Number of alleles	Chelex Resin	13.25	6.62	1.48	10.15	16.35
	Phenol Chloroform	8.9	8.33	1.86	5	12.8
	BTA Prepfiler	4.25	9.63	2.15	-0.26	8.76
Number of Alleles Contributable to Primary Individual	Chelex Resin	12.6	6.62	1.48	9.5	15.7
	Phenol Chloroform	7.55	8.48	1.9	3.58	11.52
	BTA Prepfiler	4.1	9.41	2.1	-0.3	8.5
Number of Unique Alleles Contributable to Primary Individual	Chelex Resin	4.3	4.62	1.03	2.14	6.46
	Phenol Chloroform	3.25	4.24	0.95	1.27	5.23
	BTA Prepfiler	2.35	5.33	1.19	-0.15	4.85
Number of Alleles Contributable to Secondary Individual	Chelex Resin	6	3.46	0.77	4.38	7.62
	Phenol Chloroform	4.4	4.3	0.96	2.39	6.41
	BTA Prepfiler	1.75	4.09	0.91	-0.16	3.66
Number of Unique Alleles Contributable to Secondary Individual	Chelex Resin	0.1	0.31	0.07	-0.04	0.24
	Phenol Chloroform	0.4	0.99	0.22	-0.07	0.87
	BTA Prepfiler	0	0	0	0	0
Shared Alleles	Chelex Resin	6	3.43	0.77	4.39	7.61
	Phenol Chloroform	4	4.53	1.01	1.88	6.12
	BTA Prepfiler	1.75	4.09	0.91	-0.16	3.66

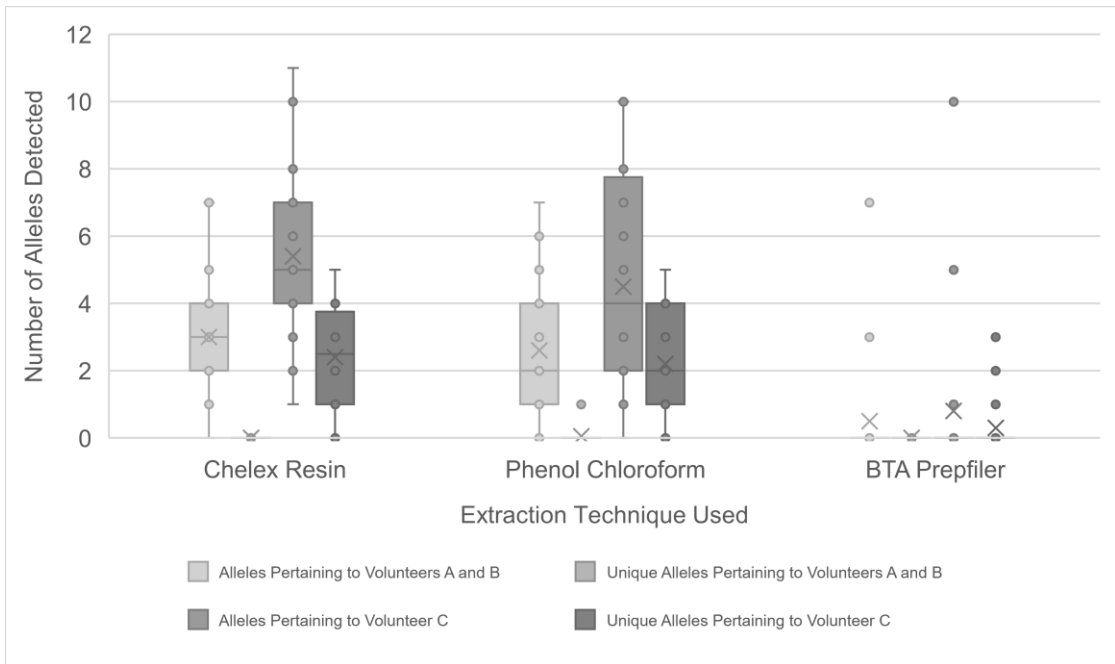


Figure 21. The alleles detected from the external sourced samples from the composite counterfeit banknotes according to the associated volunteer within each extraction group. This comprises of the alleles for volunteer C who handled the external aspects of the composite counterfeit banknote alongside the alleles shared with the other two volunteers that appeared in the DNA profile. Error bars indicate the standard error of the data sets.

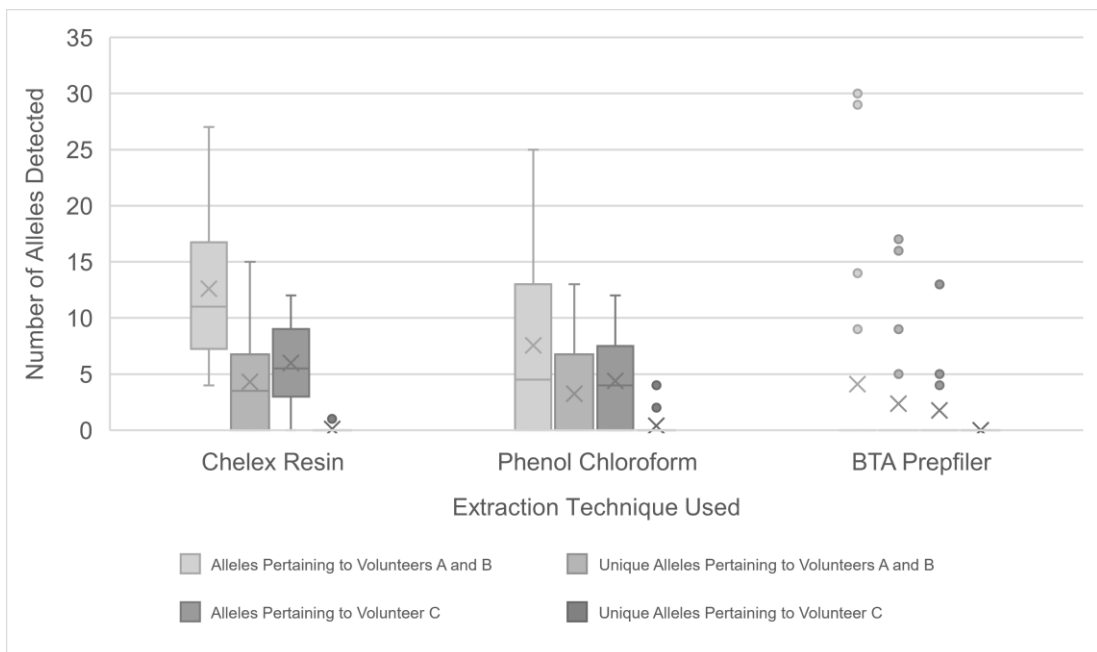


Figure 22. The alleles detected from the internal adhesive layer of the composite counterfeit banknotes according to the associated volunteer within each extraction group. This comprises of the alleles for volunteers A and B who placed their fingermarks on the adhesive side of the dot matrix holograms alongside the alleles shared with the male volunteer (C) that appeared in the DNA profile. Error bars indicate the standard error of the data sets.

3.3.2.2 Allelic Heights and Heterozygote Imbalances

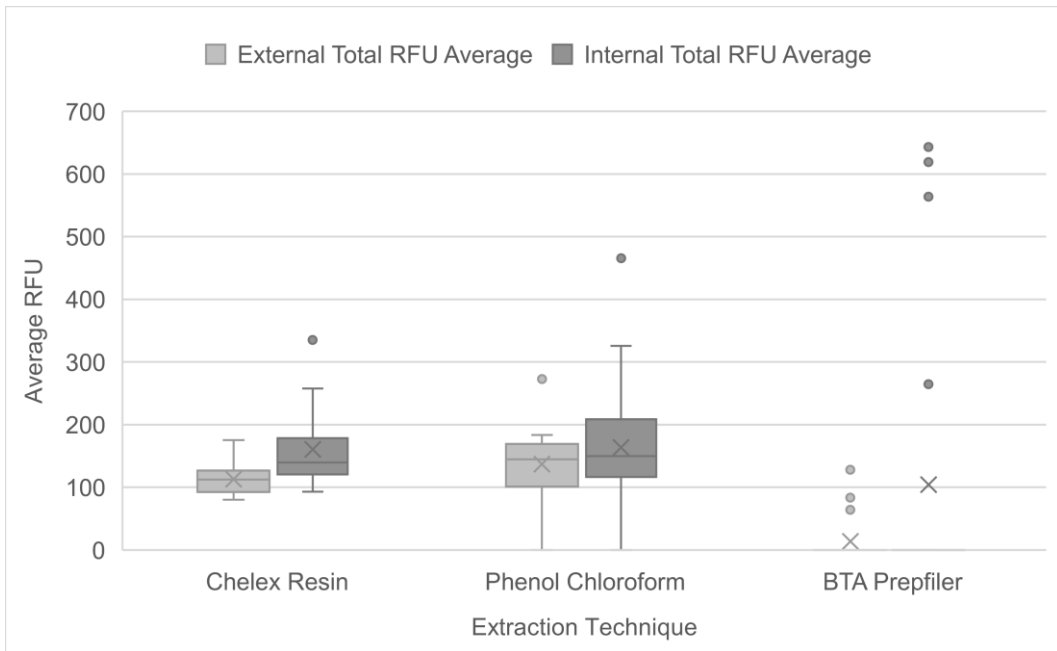


Figure 23. The average RFU for the detected DNA profiles on both the external and internal components of the composite counterfeit banknotes from each extraction methodology. Error bars indicate the standard error of the data sets.

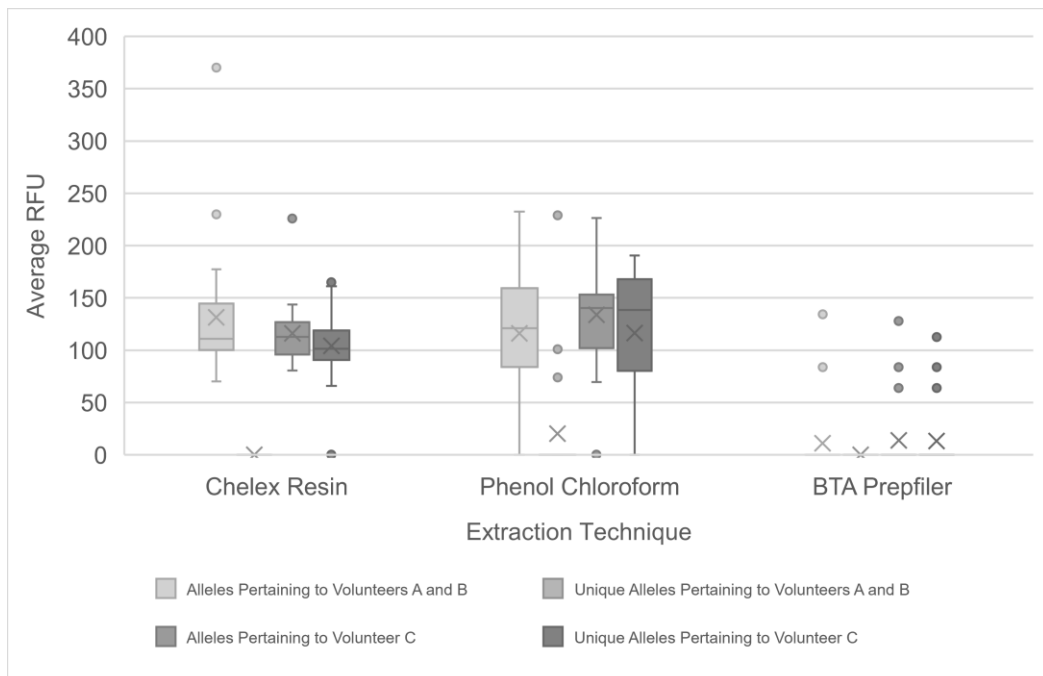


Figure 24. The average RFU for the detected DNA profiles according to the volunteers' profiles on the external surface of the composite counterfeit banknotes from the three extraction methodologies. Error bars indicate the standard error of the data sets.

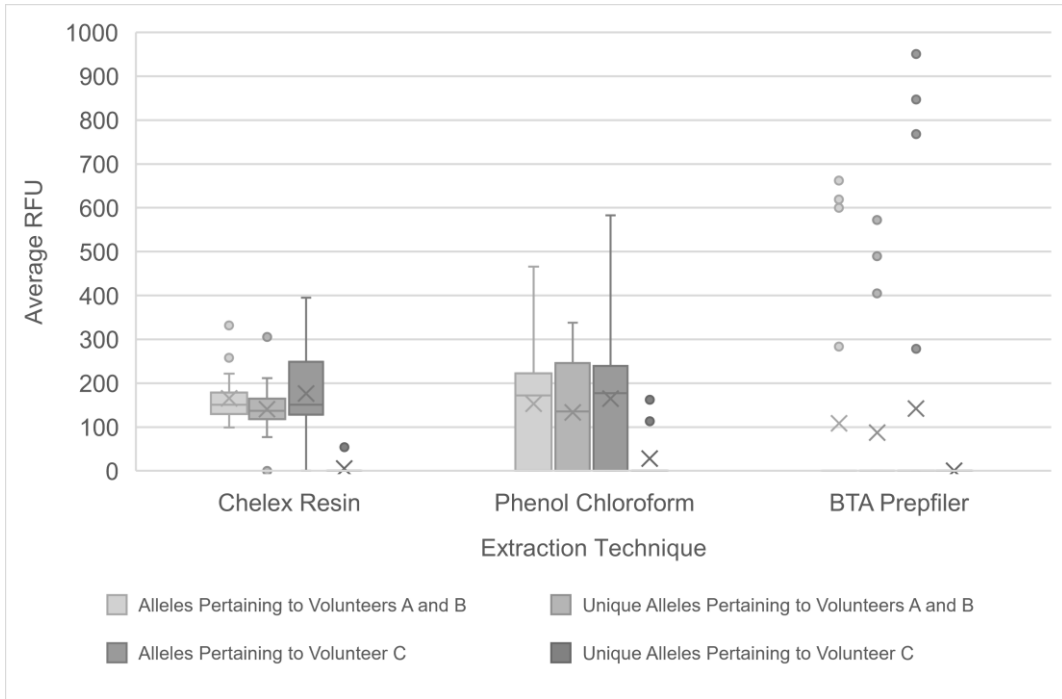


Figure 25. The average RFU for the detected DNA profiles according to the volunteers' profiles on the internal surface of the composite counterfeit banknotes from the three extraction methodologies. Error bars indicate the standard error of the data sets.

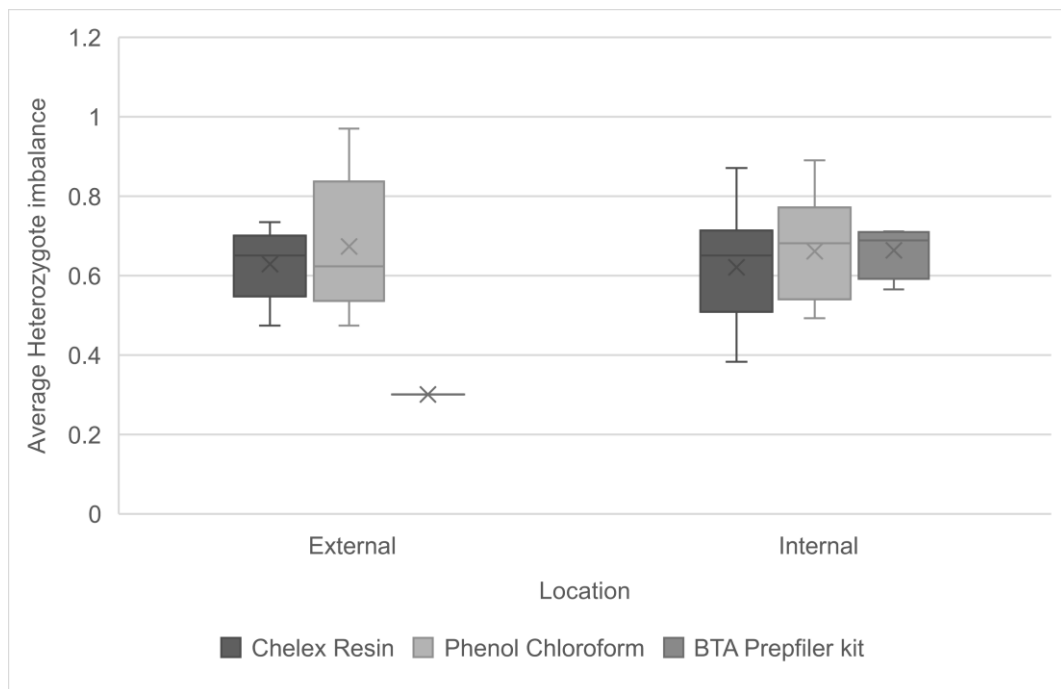


Figure 26. The average heterozygote balance for the DNA profiles taken from the external and internal surfaces of the composite counterfeit banknotes from the three extraction methodologies. Error bars indicate the standard error of the data sets.

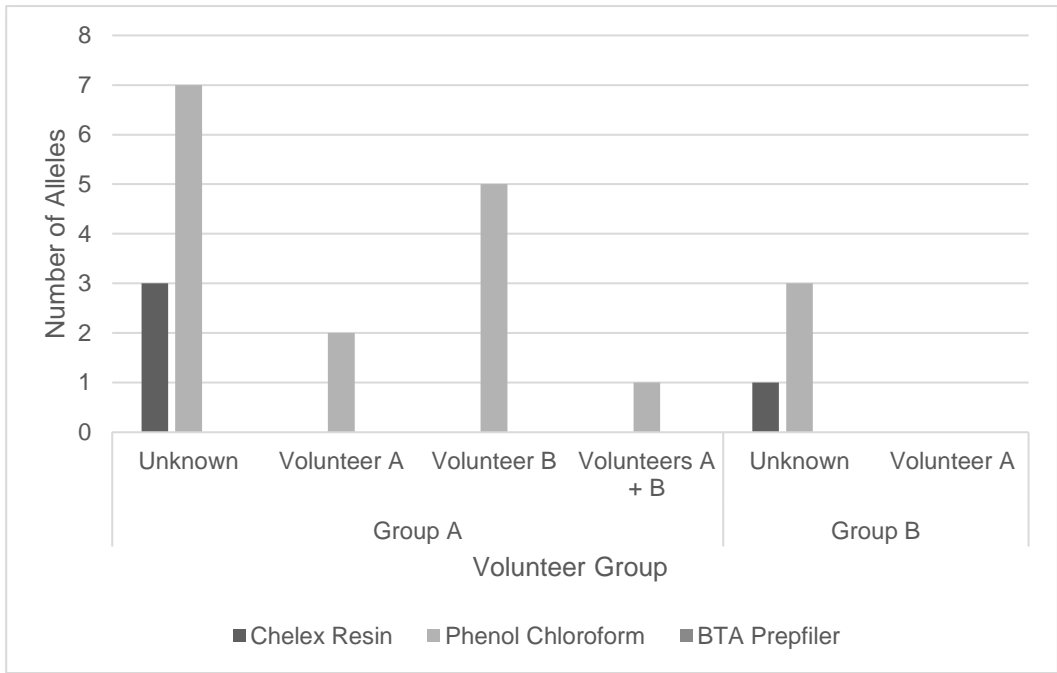


Figure 27. The unique alleles detected that were not directly attributable to volunteer C from the external surface of the composite counterfeit banknotes, split according to the extraction techniques used for the sample.

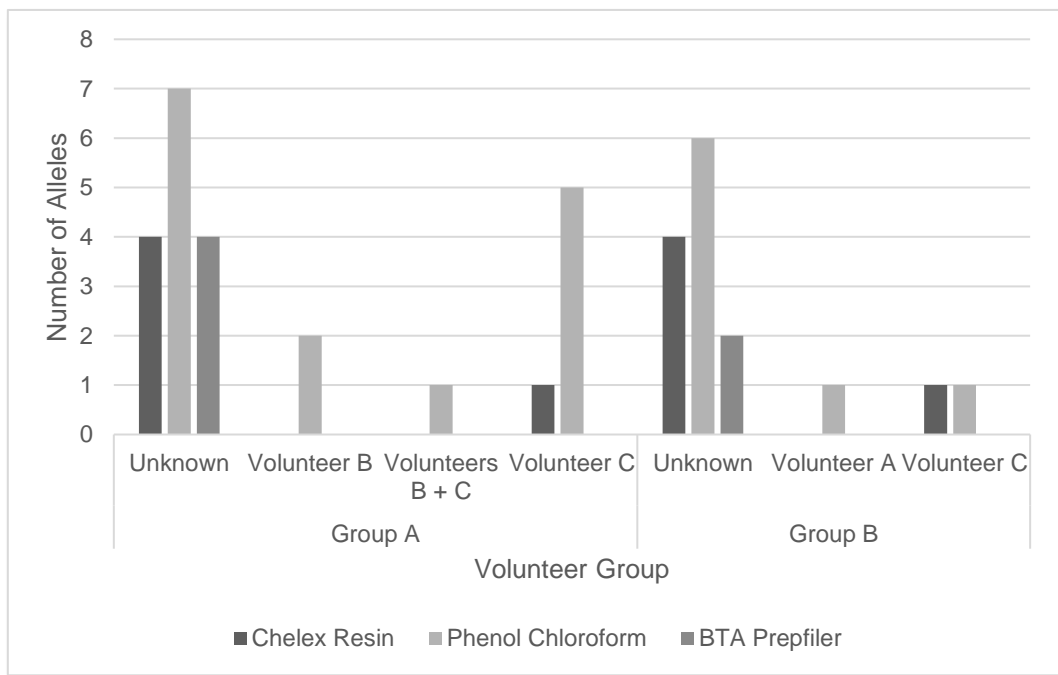


Figure 28. The unique alleles detected that were not directly attributable to volunteers A (group A) or B (group B) from the internal adhesive of the composite counterfeit banknotes, split according to the extraction techniques used for the sample.

Table 7. Descriptive statistics of the RFU values for the external and internal sourced samples alongside the RFU values for the volunteer specific alleles.

	Extraction	Mean	Std. Deviation	Std. Error	95% Confidence Interval for Mean	
					Lower Bound	Upper Bound
Total Average RFU for External Sourced Samples	Chelex Resin	112.86	23.58	5.27	101.83	123.9
	Phenol Chloroform	137.19	53.88	12.05	111.98	162.41
	BTA Prepfilier	13.78	35.29	7.89	-2.74	30.29
Average RFU for External Source Alleles Pertaining to Volunteers A and B	Chelex Resin	131.5	67	14.98	100.14	162.85
	Phenol Chloroform	115.94	73	16.32	81.78	150.1
	BTA Prepfilier	10.9	34.56	7.73	-5.27	27.08
Average RFU for External Source Alleles Pertaining to Volunteer C	Chelex Resin	116.23	31.25	6.99	101.6	130.86
	Phenol Chloroform	133.88	50.99	11.4	110.02	157.75
	BTA Prepfilier	13.78	35.29	7.89	-2.74	30.29
Total Average RFU for Internal Sourced Samples	Chelex Resin	160.41	57.97	12.96	133.28	187.54
	Phenol Chloroform	163.51	111.49	24.93	111.33	215.69
	BTA Prepfilier	104.51	225.45	50.41	-1	210.02
Average RFU for Internal Source Alleles Pertaining to Volunteers A and B	Chelex Resin	165.65	55.38	12.38	139.73	191.57
	Phenol Chloroform	152.92	127.91	28.6	93.05	212.78
	BTA Prepfilier	108.19	232.48	51.98	-0.62	216.99
Average RFU for Internal Source Alleles Pertaining to Volunteer C	Chelex Resin	5.75	17.73	3.97	-2.55	14.05
	Phenol Chloroform	28.38	59.3	13.26	0.62	56.13
	BTA Prepfilier	0	0	0	0	0

The average of the external and internal average RFU values varied between the different extraction processes. From Figure 23, the overall RFU value for the Chelex and phenol chloroform samples can be seen as being relatively similar with most

samples being no higher than 200 RFU. Neither the external nor internal groups for the Chelex resin sample group have an RFU lower than 100 with the same being true for the phenol chloroform samples. The BTA Prepfiler had similar values for the external samples to the other extractions but some of the highest RFU values at above 600 RFU for the internal samples. However, only 7 of the 40 samples had alleles present.

Figure 24 shows that Chelex had no unique alleles for volunteers A and B indicated by the lack of average RFU values. However, alleles present that could be linked the volunteer C had an average of above 100 RFU. The phenol chloroform group had the widest range of RFU values for all categories of alleles compared to the other extraction techniques. However, there were unique alleles to the volunteers' A and B present with average RFU values of 229, 101 and 74.

The average overall RFU values for the externally sourced samples were tested for normality. The test indicated that the BTA Prepfiler data was not normally distributed ($p = 0.000$) while the Chelex resin and phenol chloroform were both normally distributed ($p = 0.154$ and $p = 0.222$) indicating that the data was normally distributed. As most of the data was normally distributed with only the BTA Prepfiler not being normally distributed due to the lack of values, the choice was made to carry out a parametric based test. A one-way ANOVA was carried out between the three groups which found that there was a statistically significant difference ($p = 0.000$, $\eta^2 = 0.657$). The Tukey HSD post hoc test comparison of the three groups found that there was statistically significant difference between the BTA Prepfiler kit when compared to the Chelex resin and phenol chloroform overall RFU values ($p = 0.000$). The sample profiles acquired from the BTA Prepfiler extractions had the lowest overall mean RFU at 13.78 with the Chelex resin and phenol chloroform both being higher than the BTA Prepfiler mean RFU at 112.86 and 137.19 respectively (Table 7). However, the comparison of Chelex resin to the phenol chloroform average RFU values was found to be not statistically significantly different ($p = 0.136$).

To establish the comparison between the three extraction techniques more precisely, the RFU of alleles pertaining to volunteer C were considered as they were the primary individual who handled the external aspect of the composite banknote. The normality test for the three groups established that the BTA Prepfiler kit and Chelex resin data sets were not normally distributed ($p = 0.000$ in both cases) but the phenol chloroform data was normally distributed ($p = 0.445$). Comparisons made using the Kruskal-

Wallis test found there was a statistically significant difference in the average RFU values ($p = 0.000$, $\eta^2 = 0.587$, $n = 60$). A pairwise comparison found that the BTA Prepfiler kit samples were statistically significantly different from the Chelex resin and phenol chloroform groups (both $p = 0.000$). The BTA Prepfiler was again the lowest mean RFU value at 13.78 with both Chelex resin and phenol chloroform being higher at mean RFUs of 116.23 and 133.88 respectively (Table 7). There was no statistical significance between the phenol chloroform and Chelex resin groups ($p = 1.000$).

The normality test for the overall RFU values for the internally sourced alleles from the composite counterfeit banknotes indicated that the phenol chloroform data set was normally distributed ($p = 0.135$) but not the Chelex resin ($p = 0.004$) or BTA Prepfiler kit groups ($p = 0.000$). A Kruskal-Wallis test established that there was a statistically significant difference between the groups ($p = 0.002$, $\eta^2 = 0.181$) for the total average RFU. The pairwise comparison found that there was no statistically significant difference between the phenol chloroform and Chelex resin extraction groups ($p = 1.000$). There was a statistically significant difference when comparing the BTA Prepfiler kit group to both phenol chloroform ($p = 0.016$) and Chelex extraction ($p = 0.013$) RFU values. The BTA Prepfiler mean RFU values were higher in the internal samples at 104.51 than the external RFU values. However, the Chelex resin and phenol chloroform in the internal samples were still higher than the BTA Prepfiler samples at mean RFUs of 160.41 and 163.51 respectively (Table 7).

To evaluate the RFU values in detail the RFUs for alleles pertaining to volunteers A and B were compared for each extraction technique in terms of the internal sourced samples. A normality test indicated that the BTA Prepfiler kit ($p = 0.000$), Chelex resin ($p = 0.004$) and phenol chloroform ($p = 0.047$) groups were not normally distributed ($p < 0.05$). A Kruskal-Wallis test was therefore carried out. The test established that there was a statistically significant difference between the groups with a p-value of 0.007 ($p < 0.05$, $\eta^2 = 0.141$, $n = 60$). The pairwise comparison established that there was a statistically significant difference in the comparison of the BTA Prepfiler kit group to the phenol chloroform ($p = 0.040$) and Chelex resin ($p = 0.009$) extraction groups. The exclusion of volunteer C's alleles for the RFU value evaluation did not vary the mean RFU values for each extraction when compared to the total average RFU of all alleles detected. However, the difference between extraction groups remained the same with the BTA Prepfiler mean RFU values at 108.19 for the lowest RFU mean. The Chelex resin average RFU values for the present alleles for volunteers A and B was the highest at 165.65 and 152.92 for the phenol chloroform

group (Table 7). There was no statistical significance between the phenol chloroform and Chelex resin groups ($p = 1.000$).

From Figure 26 the overall heterozygote imbalances for paired alleles can be seen. Similar means were seen for both the Chelex resin and phenol chloroform extractions for average heterozygote imbalances across the external and internal samples. All imbalances present for the Chelex resin and phenol chloroform were between 1 and 0.4 ratios. Only 5 samples contained alleles from the BTA Prepfiler extractions, 4 of which were taken from the internal adhesive of the composite counterfeit banknotes.

Figure 27 and Figure 28 show the number of alleles present with the samples that were foreign in origin, These were either found to be possible contribution from the other volunteers in the study or unknown alleles that did not appear in any of the reference DNA profiles for the three participants. Group A and group B refers the volunteer's involved in the deposition of the cellular material onto the adhesive side of the imitation holograms used.

3.4 Discussion

3.4.1 DNA Quantification

From the statistical comparison of the RPPH1 based marker it was found statistically that there was no difference between the extraction methods for the external sourced samples but there was a difference in the values for the internal samples ($p = 0.001$). The effect sizes for these groups was found to be small for the external samples ($\eta^2 = 0.021$, $n = 90$) indicating only a small level of the variance was explained by the different extraction techniques ($\eta^2 > 0.01$). The internal samples had a medium effect size ($\eta^2 > 0.06$) indicating the extraction methods explains a moderate level of the variance within the data ($\eta^2 = 0.132$, $n = 90$). From the pairwise comparison of the three extraction techniques of the internal samples, it was shown that the values of the Chelex resin extraction ($p = 0.018$) and BTA Prepfiler kit ($p = 0.00$) compared to the phenol chloroform were statistically significantly different. This can be seen in the means of the BTA Prepfiler and Chelex resin extraction at 13.06 pg/ μ L and 1.85 pg/ μ L respectively compared to the 0.26 pg/ μ L for the phenol chloroform (Table 4). The comparison of the Chelex resin and the BTA Prepfiler means indicated no statistical difference between the extraction techniques ($p = 1.00$). This would suggest that from the three extraction techniques, Chelex resin BTA Prepfiler were the most suitable technique in extracting DNA from the adhesive side of dot matrix holograms, with BTA

Prepfilers potentially obtaining more DNA overall with a mean of 13.06 pg/ μ L. However, these values lie below the 100 picograms threshold for low copy DNA (Gill et al. 2001), the condition of the sample profiles cannot be guaranteed in terms of number of present alleles.

For the SRY marker data the samples taken from the internal adhesive dot matrix hologram layer had no statistical difference indicated by the Kruskal Wallis test ($p = 0.603$). However, the external samples had a p -value of 0.023 suggesting there was a statistically significant difference within the groups. The internal samples had a negative value, a less than small effect size indicating the extraction methods explains a minute level of the variance within the data ($\eta^2 = -0.011$), likely due to the large number of zero values for the SRY locus. The effect size for the external samples was medium at $\eta^2 = 0.064$ ($\eta^2 > 0.06$, $n = 90$) indicating a moderate proportion of the variance is explained by extraction methods used. For the results of the pairwise comparison there was no observed significant difference between each of the three groups when considering the adjusted Bonferroni correction p -values. The p -value is adjusted according to the number of comparative groups being used to avoid obtaining false positives when using multiple test comparisons (Dinno, 2015). This would suggest that although there is an overall significant difference for each of the groups, when considering them individually the statistical difference is not present. It should be noted that the data for the internal samples for the SRY marker only represent the sample set where the volunteer placing their fingermark on the adhesive of the dot matrix hologram was male. No male specific SRY DNA was quantified within any of the female samples in relation to the internal adhesive sourced samples. This could therefore explain the lack of statistical difference between the extraction techniques when considering the internal samples and the male specific SRY marker. All quantification data was verified through observing an exponential amplification for all samples as well as ensuring the presence of the IPC being amplified in all samples including negative wells suggesting there was no PCR inhibition (Barbisin et al. 2009).

Most of the samples with detectable levels of DNA could potentially contain partial profiles with the qPCR data suggesting that for the BTA Prepfilers kit extracted samples, there are higher concentrations of DNA to provide partial DNA profiles (see 3.3.2 and 3.4.2). All samples indicated cycle threshold values of 28 - 29 for the IPC marker suggesting the reactions were successful and indicated no variation between the extraction methods (data not shown).

3.4.2 DNA Profiles

3.4.2.1 Allelic Compositions

In order to evaluate the condition of the samples after three extraction processes, the samples produced using volunteers A and B were DNA profiled. Samples produced using volunteer C's DNA for the internal adhesive samples was not carried forward onto DNA profiling as the expected profiles would be the same for the external and internal samples. Samples were also not run in triplicate or duplicate (Caragine et al. (2009), instead opting for single PCR runs of samples as this was simulated procedural run. The intent was therefore to ensure that samples could be re-examined if any parameters for the PCR were further investigated. The analysis of the profiles consisted of statistically analysing the whole data set of alleles detected and separating the alleles according to the individuals that potentially contributed to the profiles. This was carried out to avoid miss interpreting alleles that could potentially be introduced from secondary contact, presenting as non-self DNA (Szkuta et al. 2018) as well as to establish if there were any foreign alleles that were not expected to be present. In terms of the overall profiles produced, the BTA Prepfil kit was the least successful with the majority of samples not producing any DNA profiles whether externally or internally as can be seen in Figure 21 and Figure 22. Of the 40 extracted samples using the BTA Prepfil kit, only 7 produced any DNA profiles. In comparison the Chelex resin and phenol chloroform extractions were far more successful with all Chelex samples having partial profiles present and phenol chloroform having all except 4 samples with a detected DNA profile. Any stutter present was found to be below the RFU threshold of 50 but evidence of allele drop-out was evident from the partial profiles produced.

From the overall samples taken from the external composite banknotes the majority of the external profile alleles were assignable to volunteer C who was involved in simulating the circulation process (Figure 21). From the analysis of the alleles detected on average as a whole ($p = < 0.001$) and with the inclusion of only volunteer C's present alleles ($p = 0.00$), there was a statistically significant difference found between the three extraction techniques. Both of which had large effect sizes at for the overall allele count data ($\eta^2 = 0.368$, $n = 60$) and for the volunteer C specific alleles ($\eta^2 = 0.360$, $n = 60$), indicating the extraction methods explained substantial and meaningful variation in the data. The statistical comparison through the Tukey HSD Post Hoc tests established that there was only a statistically significant difference between the BTA Prepfil kit samples and the two other extraction processes: phenol

chloroform and Chelex resin extractions. As the mean for the number of alleles detected for the BTA Prefiler kit was 0.80, considerably lower than the 5.4 and 4.5 for the Chelex resin and phenol chloroform extractions respectively.

The number of alleles detected in the internal sample swabs from the adhesive dot matrix holograms were compared using a Kruskal-Wallis test in Section 3.3.2.1. This established that there was a significant difference in the means for the three extractions ($p = <0.001$). The η^2 value ($\eta^2 = 0.286$, $n = 60$) indicating the magnitude of effect sizes were large ($\eta^2 > 0.14$), indicating the extraction methods explained substantial and meaningful variation in the data. The pairwise comparisons showing that the Chelex resin and phenol chloroform had statistically significant greater number of alleles detected compared to the BTA Prefiler. The same was shown for when considering the detected alleles that could be linked to volunteers A and B. This would suggest that in terms of the extractions, the BTA Prefiler kit was the least efficient at extracting DNA from the adhesive side of the dot matrix holograms, with a mean number of alleles detected equal to 4.25, compared to Chelex resin which performed marginally better than phenol chloroform, with a mean of 8.90 alleles detected compared to a mean of 13.25 alleles detected using Chelex. Previous research has found similar results when comparing Chelex resin extraction and phenol chloroform extraction (van Oorschot et al. 2003). However, due to the appearance of shared alleles between all the profiles it is difficult to distinguish one profile volunteer from another when trying to include the maximum number of alleles. There were alleles that only appeared in each individual and could be considered unique in the volunteer group. Of the ones pertaining to volunteers A and B, the unique alleles only appeared within the adhesive sourced samples except for one of the phenol chloroform samples. In the case of internal samples where volunteers A and B's DNA was to be expected, the profiles detected could be contributed to them as a primary contributor in the majority of cases. However, in 6 of the samples there was the presence of alleles not present in volunteers' A and B DNA profiles but were present in volunteer C's the risk of contamination from the simulated circulation process cannot be ruled out. However, as there are also alleles present that are of an unknown origin there is a likely possibility that these have been introduced through secondary transfer from contact from common items. The effect sizes for the statistical comparisons of the allelic profiles for the external and internal samples gave η^2 values greater than 0.14 ($\eta^2 = 0.260$ for the internal), indicating the magnitude of effect sizes were large, indicating the extraction methods explained substantial and meaningful variation in the data.

Foreign alleles were detected with only 2 alleles present that can be established uniquely to volunteer A and 5 from volunteer B (Figure 27). There were also alleles that had an unknown origin that were not present in any of the 3 reference profiles for the volunteers. Figure 28 showed that there were a large number of foreign alleles present in the internal adhesive layer. The samples from volunteer A (Group A) had the highest number in the phenol chloroform extraction samples. Overall, the majority of foreign alleles detected were of an unknown source, with volunteer A's internal samples being the exception with alleles present that could be attributed to volunteer C. This could likely be from secondary transfer from volunteers A and B or an unknown individual to volunteer C's hands from a commonly held object such as a door handle (Jansson et al. 2022). Some alleles may possibly be a result of drop in alleles that was not excluded from the analysis (Petricevic et al. 2010).

There is the possibility that during the volunteers' time period before placing their fingermarks, they could have come into contact with a surface volunteer C had recently or frequently come into contact with such as a door handle on the day of the preparation of extracted samples. What the volunteers did before depositing their fingermarks was not controlled other than the period of time abstaining from hand washing and wearing gloves. While depositing the fingermarks the amount of pressure was not controlled with contact time being no more than 10 seconds. This could have allowed for the variation in the amount of DNA deposited (Hefetz et al. 2019). This was also true for the sebaceous deposits on the external surface of the composite banknotes (Schulte et al. 2021). The research varies for the accumulation period of cellular material to produce natural fingermark deposition (Templeton and Linacre 2014, Burrill et al. 2021c, Lam et al. 2022). The 1 hour and 30 minutes was chosen to ensure DNA had accumulated to natural level whilst remaining close to the literature which can vary between 1 hour and 2 hours (Burrill et al. 2020 and 2021b, Sessa et al. 2019). This may have allowed for the potential risk of secondary DNA transfer to either volunteer A or B as has been shown in research by Meakin et al. (2017) and Fantinato et al. (2022). Both papers have discussed and investigated the transfer of non-self DNA that could potentially lead to complications in the interpretation of criminal evidence. Both volunteers A and B cohabited which would play a factor in the deposition of other alleles that would likely affect the allelic composition of the DNA profiles through secondary transfer (Fantinato et al. 2022). To compensate for this future research should consider the use of volunteers that do not cohabit to limit the potential secondary transfer of DNA. Research by Kita et al. (2008) carried out their volunteer preparation by having the individuals sit in a room

for a set time, refraining from touching their necks which would mitigate the risk of secondary transfer of surface DNA (Kita et al. 2008). This was not done as the volunteers were only selected due to them being in a social bubble at the time of the carrying out of the research over the course of the COVID pandemic when the use of indoor spaces was still regulated. This also prevented any pre-screening of the profiles for shared alleles to make the interpretation of profiles easier as the selection of other volunteers was not possible at the time. Future work could include these methodologies as well as asking volunteers to refrain from touching potentially shared objects and avoid other volunteers to prevent secondary transfer of DNA (Meakin et al. 2017). Secondary transfer could explain the presence of foreign alleles present in the samples as well (Jansson et al. 2022). Foreign alleles that could not be affiliated to any of the volunteers did appear in some of the samples. These largely consisted of one or two alleles rather than whole profiles of alleles that could not be linked to the volunteers. These likely transferred in the form of secondary transfer from a surface or item the volunteer handled in the time leading to the sampling. As these were not present in the volunteer DNA profiles, they were able to be eliminated from the statistical comparisons. Foreign alleles are unlikely to affect the overall interpretation of results as research by Jansson et al. (2022) established that foreign alleles were common in their shedder analysis, with only a small fraction of samples containing foreign DNA than constituted more than 20% of the DNA profile. Factors effecting deposition surface area, surface contact time for both external and internal such as shedder status may have likely had a factor but this was compensated for by including the volunteers in all three extractions processes whilst also collecting deposited samples at the same time of day to avoid any intra-variation in deposited DNA (Kaesler et al. 2022).

The swabbing of the composite counterfeit banknote would likely also reduce the risk of contamination from volunteer C's DNA profile when simulating a circulation event. Similar research by Ruprecht et al. (2021) found the swabbing of stamps before removing them for DNA profiling reduced the risk of external contamination. It should also be noted that instead of DNA extraction, the stamps were segmented before being introducing them directly to the DNA profiling PCR master mix. Highlighting that the effective swabbing of the surface of the stamps allowed for the DNA profiling of the sample to occur without any risk of contamination.

Comparing DNA profiles to the qPCR data (Sections 3.3.1 and 3.4.1) the BTA Prefiler kit samples had the highest average concentrations of DNA. This would have

suggested that there was a greater likelihood of gaining partial DNA profiles compared to the other extraction methods which did not acquire the same concentrations of DNA. However, the inverse was found to be the case for the produced DNA profiles. Although the qPCR data from Sections 3.3.1 and 3.4.1 would have suggested that the BTA Prepfilier kit had substantially more success in the extraction of DNA present on the internal adhesive of the dot matrix holograms, quantified DNA would not necessarily indicate the condition of the DNA profile that could be present in the case of trace DNA (Lin et al. 2018). The data did show that there were several samples that had more alleles present than the means of the other two extraction processes. This may explain the higher concentrations of DNA detected in the BTA Prepfilier samples. As the samples likely contain degraded DNA, the loss of loci is likely (Foran et al. 2006, Swango et al. 2007). Although the RPPH1 locus is detectable in the qPCR data for the BTA Prepfilier extracted samples, this would not indicate the condition of the rest of the potential DNA (Lin et al. 2018). Positives and negatives analysed alongside the samples in the Genetic Analyzer indicated no issues with the set-up of the capillary electrophoresis process as well as re-runs of some of the samples indicated no change in the results. More recent developed qPCR kits such as the Quantifiler™ Trio could compensate for this disparity when considering low template DNA (Lin et al. 2018). The variations in DNA concentration and the number of alleles detected could be due to do with the biochemistry of the extraction processes. The BTA Prepfilier kit is specifically designed and advertised as being useful for the application on tapelifts in forensic case work (ThermoFisher Scientific, 2022b). However, research by Forsberg et al. (2016) has shown that Chelex provided better results than the BTA Prepfilier Express protocol when used directly with SceneSafe FAST tape. This was also true for research by Stoop et al. (2017) that found the use of phenol-chloroform extraction outperformed the BTA Prepfilier kit. Chelex resin and phenol chloroform both use the chemistry of the DNA to allow for sample separation to remove any inhibitors rather than relying on the binding of DNA (Forsberg et al. 2016, Dairawan and Shetty 2020). This could potentially explain the variation between the three extraction processes, affecting how further down inhibition or loss of DNA. There is the potential that the PCR reaction may have been inhibited as the RFU values for the majority of samples did vary between low and high molecular weight STRs (Appendices 10 - 11).

As both the Chelex resin and phenol chloroform produced similar results, the Chelex resin extraction method was selected to be applied to counterfeit banknotes provided by the European Central Bank. Both extractions are relatively cheap in terms of

purchasing the Chelex resin and phenol chloroform reagent but the Chelex resin extraction method requires fewer plastic ware changes and is less hazardous than phenol chloroform. This allows for a wider application of the methodology as there are fewer risks to the practitioner and less training is required. Added to which there are the lower overall costs if this were to be applied at a practitioner level.

3.4.2.2 Allelic Heights and Heterozygote Imbalances

The comparisons of the average RFU values for the external samples found that the average RFU values overall RFU there was a statistically significant difference ($p = 0.000$). The effect sizes for the statistical comparisons gave an effect value of $\eta^2 = 0.657$ ($\eta^2 > 0.14$, $n = 60$), indicating the magnitude of effect sizes were large, indicating the extraction methods explained substantial and meaningful variation in the data. For the comparisons of the Chelex resin and phenol chloroform extractions there was no difference statistically ($p = 0.136$). However, as with the allele totals, there was a statistical difference with the BTA Prepfilers samples compared to the other extraction techniques ($p = 0.000$). The BTA Prepfilers samples had the lowest mean RFU value at 13.78 with the Chelex resin and phenol chloroform being significantly higher at 112.86 and 137.19 respectively. This was also the case for the average RFU values when considering the alleles specific to volunteer C who came into contact with the surface to simulate the circulation of the composite counterfeit banknote ($p = 0.000$). The effect size was again large with $\eta^2 = 0.587$ ($\eta^2 > 0.14$, $n = 60$), showing the extraction methods explained substantial and meaningful variation in the data. A pairwise comparison found that the BTA Prepfilers kit samples were statistically significantly different from the Chelex resin and phenol chloroform groups (both $p = 0.000$). The BTA Prepfilers samples had the lowest mean RFU value at 13.78 with the Chelex resin and phenol chloroform being significantly higher at 116.23 and 133.88 respectively. There was no statistical significance between the phenol chloroform and Chelex resin groups ($p = 1.000$). Dividing the data according to the reference profiles for the volunteers gives a clearer depiction of the RFU as there were alleles of unknown origin or other volunteer's present that will affect the overall RFU (Figure 24). The 95% confidence interval for the average RFU values ranged from 101.83 – 123.90 and 111.98 – 162.41 respectively for the Chelex resin and phenol chloroform extraction groups (Table 7). This was expected due to the low levels of DNA normally associated with trace DNA evidence were deposited (Budowle et al. 2009B).

Overall RFU values for all the present alleles for the internal composite samples A Kruskal-Wallis test established that there was a statistically significant difference

between the groups ($p = 0.002$, $\eta^2 = 0.181$, $n = 60$) for the total average RFU. For the internal sourced samples there were higher RFU values detected when considering all the alleles present compared to the external samples. The BTA Prepfil kit had the lowest average RFU value at 104.51 (Table 7), likely due to the lack of alleles in the majority of samples. However, in the samples that were successfully profiled, some of the highest average RFU values were present at over 600 RFU (Figure 23). Statistically there was an overall significance statistically when considering the RFUs ($p = 0.002$). The effect size of was considered large with a value of $\eta^2 = 0.181$ being greater than 0.14 ($n = 60$), showing the variation in the data was explained substantially by the extraction methods used. The Chelex resin and phenol chloroform extractions had no difference for the overall average RFU values ($p = 1.000$). Significant statistical differences were only found in the comparison of the two solution extraction techniques and the BTA Prepfil kit samples ($p = 0.016$ for phenol chloroform and $p = 0.013$ for Chelex resin). This indicated that of the three extraction techniques, phenol chloroform and Chelex resin extraction provided samples with the highest mean RFU values for the external sourced samples at 160.41 for the Chelex resin and 163.51 for phenol chloroform extracted samples. Similar to the allele number data, the average RFU values for the Chelex and phenol chloroform extraction groups were found not to be statistically significantly different ($p = 1.000$).

To further understand the sample contributions, the RFU values were considered according to the reference profiles in a similar manner to the external samples previously (Figure 25). There was a statistically significant difference between the extraction groups p -value of 0.007 ($p < 0.05$, $\eta^2 = 0.141$, $n = 60$). The effect size was indicated as being large suggesting the variation could be largely explained by the different extraction techniques used. In the pairwise comparison it was found that there was a statistically significant difference for the Chelex resin ($p = 0.009$) and phenol chloroform ($p = 0.040$) compared to the BTA Prepfil kit samples. However, this was not the case when comparing phenol chloroform and Chelex resin extraction RFUs ($p = 1.000$). This would suggest that although the average Chelex resin extraction and phenol chloroform RFU values were statistically different from the BTA Prepfil kit, the phenol chloroform and Chelex resin extraction values did not differ significantly. The BTA Prepfil samples had the lowest mean RFU value at 108.19 with the Chelex resin and phenol chloroform being significantly higher at mean RFUs of 165.65 and 152.92 respectively. The samples for the BTA Prepfil were again lacking in alleles which would have made the comparison of the RFUs in favour of

the other two extraction techniques. This would also contribute to heterozygote imbalances within the RFU values between the samples.

Most of the heterozygote peak imbalances observed had a mean of 1 to 0.4 except for the external BTA Prepfil kit external samples (Figure 26). However, this group had only one sample average present for the data set due to the lack of heterozygote pairings. To establish the heterozygote imbalance between the alleles, only alleles known to be heterozygote within the volunteers were considered heterozygote within the experimental samples. The majority of alleles present were also solitary peaks within the specific STR locus, with two peaks only appearing in a few of the samples. The relatively high imbalances are likely due to the degradation of the samples as the low copy number of DNA present in the sample alongside the efficiency preparation techniques will cause an increase of variance in the peak ratios (Hansson et al. 2017, Chong and Wallin 2022). Kelly et al. (2012) modelled the variability in heterozygote balance and established that in the cases of low template DNA, the imbalance between allelic heights is highly variable. The heterozygote imbalance between alleles could be due to potential inhibition in the case of the internal samples as any adhesive present in the sample from the swabbing process may still be present in the lower down PCR stages of the analysis (Griffin et al. 2022). Although this would be unlikely the case for the external samples as there were no substances that could have potentially inhibited the extraction and PCR processes.

3.5 Conclusion

The simulated procedural study was carried out with the objective of producing and simulating the circulation of composite counterfeits with the intention of evaluating the potential encapsulated DNA. The aim of this was to establish a procedural methodology that could successfully acquire trace levels of DNA if present underneath the dot matrix holograms of counterfeit banknotes. From the findings it was clear that if contact has been made with a counterfeiter and the adhesive side of the dot matrix hologram, there is the potential to get a partial DNA profile. This was successful where samples were extracted using phenol chloroform and chelex resin extractions. The next objective was to apply the chelex resin extraction methodology on counterfeit banknotes with the intent of acquiring a potential DNA profile.

Chapter 4 Genetic Evaluation of Counterfeit Banknotes

4.1 Introduction

The objective of this chapter was to apply the knowledge acquired from the studies detailed in the previous chapters on counterfeit banknotes, with the aim to acquire a DNA profile. This consisted of removing the dot matrix holograms and imitation metallic threads through the application of ethanol before either swabbing the sampling area or introducing a counterfeit banknote component directly into the DNA profiling PCR. In the case of the dot matrix holograms, these were removed using ethanol from the surfaces of counterfeit €50 banknotes and swabbed. For the €500, the paper layers were separated using ethanol and the area around the imitation metallic thread was swabbed. The swabs were then extracted using chelex resin extraction and the resulting extracts were DNA profiled. For the direct PCR, the imitation metallic thread of the counterfeit banknotes was exposed again using ethanol to separate the adhesive paper layers, except instead of swabbing the area the thread was removed. The thread could then be introduced directly to the PCR for the DNA profiling reaction after being segmented to fit the tubes. In both these approaches of extraction and direct PCR, the aim was to successfully establish if DNA could be acquired from the adhesive layers of a counterfeit banknote and establish how much of a DNA profile could be obtained.

The final section of this chapter set to establish if the use of Diamond™ nucleic acid dye, could be used to help target areas of forensic interest in the adhesive layers of counterfeit banknotes. If successful, it could potentially increase the success and efficiency in the processing time to evaluate if components of counterfeit banknotes were to be taken forward for DNA analysis. The methodology applied adapted the use of previous research to establish if a fingerprint is present on the adhesive side of a dot matrix hologram, could it be visualised with the dye. This could then be DNA profiled while avoiding the unnecessary processing of samples with a higher likelihood of having DNA deposits from the counterfeiter.

4.2 Applied Procedural Study

4.2.1 Methodology

Ethics Declaration

All experimental designs were approved under Proportional Ethical Approval provided by the Staffordshire University ethics Committee.

4.2.1.1 Samples

All samples were provided by the ECB having been sourced from National Central Banks from their respective evidence storage. No details were available as to what conditions these were stored in. These consisted of 18 counterfeit €50 banknotes (Table 8), all of which had dot matrix holograms present and 12 counterfeit €500 banknotes (Table 9) with an embedded security thread imitation and dot matrix hologram (heat foil stamp variation). Each counterfeit banknote was seized from a county within the Republic of Ireland (Table 8) or a province within the Netherlands (Table 9) Within the two numerations, the notes had the same indicative characteristics that made them difficult to identify from the same source.

Table 8. Lists the €50 counterfeit banknotes provided by the Central Bank of Ireland with the dot matrix holograms present. The indicative aspect refers to the categorization of the counterfeit banknote by the ECB according to the general area it was from (EU), the series of banknote it is a counterfeit of (A being the first series of euros), the denomination being counterfeited (50 euros), the process applied (P = traditional offset printing or C colour copying using equipment such as inkjet printers) and a final numerical value for the sequential order in which it was found.

Date Received	Indicative	Serial Number	Date Taken Out of Circulation	County
2020	EUA0050C00114a	Y83811672252 Y33811679592 Y43811672505 Y43811672500 Y43811672500 Y33811679592 Y43811672555 Y43811672505 Y33811677792 Y85811672257 Y83811672257 Y43811672500 Y43811672505 Y13811670500 Y43811672500 Y83811672257 Y13811670500 Y83811672252	Unknown	Republic of Ireland

Table 9. Lists the €500 counterfeit banknotes provided by De Nederlandsche Bank alongside the county they were taken out of circulation from. The indicative aspect refers to the categorization of the counterfeit banknote by the ECB according to the general area it was from (EU), the series of banknote it is a counterfeit of (A being the first series of euros), the denomination being counterfeited (500 euros), the process applied (P = traditional offset printing or C colour copying using equipment such as inkjet printers) and a final numerical value for the sequential order in which it was found.

Date Received	Indicative	Serial Number	Date Taken Out of Circulation	County
2019	EUA0500P00011	X02906092514 X02906096285 X01004213369 N35013454996 Y02906033951 Y02906034059 X00943013396 P25001170435 X00942973265 X03603262052 N35013455419 Y00006194134	2017	Groningen Friesland Drenthe Limburg Zeeland Noord-Brabant Gelderland Overijssel Flevoland Noord-Holland Zuid-Holland Utrecht

4.2.1.2 DNA Sampling and Profiling

The dot matrix holograms for the €50 counterfeit banknotes and the embedded security thread imitations in the €50 counterfeit banknotes were processed using the ethanol separation methodology detailed in Section 2.4.2 and according to the Chelex resin extraction methodology (Section 4.2.1.2.2). Samples were not quantified prior to DNA profiling as the aim was to evaluate the potential DNA profiles. DNA profiling was carried out on all samples using the methodology outlined in Section 4.2.1.2.3.

4.2.1.2.1 Ethanol Dot Matrix Removal and Paper Layer Separation

The removal of the dot matrix holograms was achieved through the addition of 200 µL ethanol was allowed to permeate through the reverse side of the paper to the underside of hologram. If more was needed, more ethanol was added till it was able to permeate to the opposing side of the paper. The dot matrix was then lifted using sterilised tweezers, using one of the corners to avoid introducing contamination with repeated handling. Tweezers used were sterilised by soaking them in 70% methylated spirit (Parsons et al. 2016) for 1 hour followed by exposure to UV light for 15 minutes for each use. The adhesive side of the dot matrix hologram was then

double swabbed using 60 μL of 100% ethanol on each cotton swab (DeltaLab, 2016).

For the paper layer separation, ethanol was deposited using a pipette at 1000 μL , ensuring the edges around the banknote were saturated. If more ethanol was needed, a further 1000 μL was added. A sterilised scalpel was used to slide between the top of the region where the imitation metallic thread was exposed. Care was taken to ensure the tip of the blade was manoeuvred between one side of the paper layer and the imitation metallic thread to avoid tearing through the paper layer. With the application of further ethanol, the scalpel blade was able to be manoeuvred around the edges of the counterfeit banknote, ensuring the non-serrated edge of the blade was used to help pry apart the two paper layers. To completely expose the imitation metallic thread, sterilised tweezers were used to pull apart the two layers, taking care to use the tweezers in such a way to avoid cross contaminating the external surface of the banknote with the internal. Tweezers used were sterilised by soaking them in 70% methylated spirit (Parsons et al. 2016) for 1 hour followed by exposure to UV light for 15 minutes for each use. New sterile scalpel blades were used for every counterfeit banknote. The area around the imitation metallic thread was then swabbed twice using cotton swabs (Deltalab, 2016) soaked in 60 μL 100 ethanol.

4.2.1.2.2 Chelex Resin Extraction

Each swab head was snapped into an Eppendorf before adding 300 μL of DNA free water and 2 μL of proteinase K into each of the samples. This was different to the previous methodology in order to reduce the dilution of the sample. The tubes were then vortexed briefly and then incubated in a shaker (1000 rpm) for 30 minutes at 56°C. These were then spun in a microcentrifuge for 3 mins at 13,000 rpm. The swab was then removed and 175 μL of a 5% chelex working solution was added using a 1000ul pipette. The Chelex solution was on a magnetic stirrer for the duration of the time of pipetting to ensure adequate suspension of the resin. The samples were then incubated at 56°C for 30 minutes. Afterwards they were vortexed at high speed for 5 to 10 seconds and incubated at 100°C for 8 minutes using a screw-down rack. The final step had the samples vortexed again at high speed for 5-10 seconds and spun in a microcentrifuge for 2-3 mins at 13,000 rpm before pipetting aliquots of the extract into microcentrifuge tubes (ensuring not to uptake any of the resin). Chelex resin extraction product was condensed from an estimated 300 μL to 30-40 μL using the Microcon[®] DNA Fast Flow Filters (MERCK, 2021) by adding the extract supernatant

to the filter tubes and centrifuging at 500 g for 23 minutes. The tube filters were then inverted and centrifuged to remove the sample at 1000 g for 3 minutes (MERCK, 2021).

4.2.1.2.3 DNA Profiling

DNA profiles were produced using the AmpFLSTR™ NGM SElect™ PCR amplification kit at half reaction volumes with 5 µL of Master mix and 2.5 µL of NGM Select primer set alongside 5 µL of DNA sample (Thermo Fisher Scientific, 2021). All reactions were carried out at 29x cycles with positives and negatives present for each plate. The PCR consisted of one step at 95°C for 11 minutes, a second step at 94°C for 20 seconds followed by 59°C for 3 minutes for 29 cycles and a final step of 60°C for 10 minutes (Thermo Fisher Scientific, 2021). The DNA profile PCR products were then loaded onto an Applied Biosystems™ 3500 Genetic Analyser plate with 8.5 µL of Hidi formamide and 0.5 µL of LIZ™ size standard for each 1 µL of DNA template (ThermoFisher Scientific, 2022c). All samples were prepared on ice when loading the plate and a final heating step at 95°C for 3 minutes before moving the plate to an ice box was carried out to ensure any DNA present was single stranded before placing the plate onto the Genetic Analyzer (ThermoFisher Scientific, 2022c). The Genetic Analyzer was run with an injection voltage of 1.2 kV for 15 seconds using POP-4™ separation matrix polymer (ThermoFisher Scientific, 2022c). All sample data sets were loaded onto GeneMapper™ ID – X Software v1.6 alongside an allelic ladder provided with the NGM kit (ThermoFisher Scientific, 2022c). Outputs were analysed using an analytical threshold for the RFU values set to 50 RFU to exclude any detector background noise (Heathfield et al. 2022, Martín et al. 2014). Profiles were then exported to Microsoft Excel (Microsoft Corporation, 2022) for allele composition and RFU analysis.

4.2.2 Results

Of the 18 €50 counterfeit banknotes (Table 8), one gave a partial DNA profile. However, this particular counterfeit banknote had a damaged dot matrix hologram that was only partially attached to the paper substrate. Of the 12 €500 counterfeit banknotes detailed in Table 9, none of the samples gave a DNA profile from the embedded security thread imitations.

4.2.3 Discussion

As stated in the results, none of the samples were able to give a DNA profile. This was not expected as previous research in Chapter 3 found that a partial DNA profile could be acquired in most of the Chelex resin extracted samples. The lack of DNA could be due to several factors. Firstly, the samples produced in Chapter 3 were aged for one week in total before processing. The counterfeit banknote samples processed in Table 9 were taken out of circulation in 2017, making the minimum age of the sample being 5 years. This would likely reduce the possibility of acquiring a DNA profile through swabbing alone, if there is any DNA from a counterfeiter present (Dissing et al. 2010, Raymond et al. 2009). The way in which the counterfeit banknotes were stored may also have been a factor. However, due to the counterfeit banknotes being seized and placed into secure storage by the central banks. It is therefore unlikely that the conditions they were kept would be detrimental to present DNA as any steps to preserve the condition of the counterfeit banknotes would protect the integrity of the counterfeit banknote itself and any present DNA. This would include conditions such as humidity or direct sunlight that is known to be detrimental to DNA persistence as any moisture or UV damage would also be detrimental to the counterfeit banknote itself (Hall et al. 2014). The act of the counterfeit banknotes being in circulation may be a more important factor in the degradation of any potential present DNA in the adhesive layers as they may have been under different environmental conditions, affecting the fragmentation of present DNA (Alaeddini et al. 2012).

As swabbing and DNA extraction were both being used, there was the potential that DNA was being lost in the steps from between the swabbing of the sample and final Microcon[®] concentration step. Loss of evidential DNA is well documented, with DNA loss occurring at both the swabbing stages and the extraction process. More specifically in Chelex resin and phenol chloroform extractions (van Oorschot et al. 2003). Vandewoestyne et al. (2013) established the potential loss of cell free DNA in DNA extraction especially in trace DNA from contact samples. Although there is research showing that use of DNA purification devices such as the Microcon[®] apparatus does improve the resulting DNA profile (Norén et al. 2013). Romano et al. (2019) successfully acquired DNA profiles from 14-year-old case work fingerprint samples. They applied an automated magnetic bead system (BioRobot EZ1 and EZ1 DNA investigator kit) that may have improved their success rate of DNA profiles acquired through automation. However, their process of directly adding crimescene

tape samples to the extraction process would also reduce the loss of any DNA that is associated with swabbing. This could explain the results moving from the simulated procedural study (Chapter 3) to the applied study (Section 4.2) where the samples are likely from partial fingermarks. As the areas of highlighted fingermark presence that could be introduced to the extraction process avoids the loss of any DNA present when considering partial fingermarks. This was not of concern in the simulated procedural study as the fingermarks present covered the entirety of the dot matrix holograms, removing the possibility that the areas of evidential value could be missed. Ruprecht et al. (2021) found that the use of non-targeted swabbing reduced the possibility of gaining a DNA profile in a similar example. Non-targeting swabbing may be losing the DNA by not allowing for the removal of the DNA from the adhesive matrix or through the further merging of present DNA into the adhesive matrix. Ruprecht et al. (2021) applied the 1,2-indandione working solution to highlight areas of fingermark contact on the adhesive side of stamps. This allowed for the targeting of present fingermarks for swabbing, increasing the recovery of DNA of 83.3% in samples and providing a technique for the dual recovery of evidence from adhesive surfaces. Similar research by Bathrick et al. (2021) an optimised technique in enhancing fingermarks with 1,2-indandione on copy paper with the intention of preventing downstream negative impacts on DNA processing the samples. The identification of DNA containing fingermarks could also be attempted using Diamond™ nucleic acid dye Kanokwongkuwut et al. (2020). Research had suggested the successful use of the dye on adhesive tapelifts for identifying DNA containing fingermarks (Kanokwongkuwut et al. 2020). Through the application of fingermark enhancement techniques, there could be an increased success in the acquiring of DNA from targeted swabbing approaches (Ruprecht et al. 2021).

4.3 Direct PCR

4.3.1 Methodology

Ethics Declaration

All experimental designs were approved under Proportional Ethical Approval provided by the Staffordshire University ethics Committee.

4.3.1.1 Samples

All samples were provided by the ECB having been sourced from National Central Banks. The counterfeits from Table 10 consisted of 24 counterfeit €500 banknotes, all of which had an embedded metallic thread simulated and dot matrix holograms (heat foil stamp variation). Each counterfeit banknote was seized from a province within the Netherlands and had the same indicative characteristics that made them difficult to discern from different sources.

Table 10. Lists the €500 counterfeit banknotes sourced from the Netherlands provided by De Nederlandsche Bank and the respective counties they were found. The indicative aspect refers to the categorization of the counterfeit banknote by the ECB according to the general area it was from (EU), the series of banknote it is a counterfeit of (A being the first series of euros), the denomination being counterfeited (500 euros), the process applied (P = traditional offset printing or C colour copying using equipment such as inkjet printers) and a final numerical value for the sequential order in which it was found.

Date Received	Indicative	Serial Number	Date Taken Out of Circulation	County
2019	EUA0500P00011	X00942973526	2015	Drenthe
		X00943015034	2016	Drenthe
		X01004212235	2015	Zeeland
		N35013451989	2016	Zeeland
		X00943017185	2015	Overijssel
		Y02906031647	2015	Flevoland
		X00943114248	2016	Flevoland
		Y02906034743	2015	North Holland
		X02906040341	2016	North Holland
		X00942973436	2015	South Holland
		P25001135011	2016	South Holland
		Y02906034689	2016	Utrecht
		X05627699929	2015	Groningen
		X00942971771	2016	Groningen
		X03603263195	2015	Limburg
		Y00006193666	2016	Limburg
		P25001179561	2015	North Brabant
		X04524884642	2016	North Brabant
		Y02906031899	2015	Gelderland
		Y00006152653	2016	Gelderland
X00942973625	2015	Friesland		
X02906092541	2016	Friesland		
X01004152061	2016	Overijssel		
X00942954869	2015	Utrecht		

4.3.1.2 DNA Sampling and Profiling

All counterfeit banknotes were processed using the methodology detailed in Section 2.2.3. The imitation metallic thread was removed using sterilised tweezers and placed in a petri dish. A sterile scalpel blade was then used to segment the thread into 5 mm strips before placing them in a PCR tube. The ends of the thread (5 mm) were not

included in the tube and were discarded. DNA profiling was carried out on all samples using the methodology outlined in Section 4.3.1.2.1.

4.3.1.2.1 Direct PCR for DNA Profiling

DNA profiles were produced using the AmpFLSTR™ NGM SElect™ PCR amplification kit at full reaction volumes with 10 µL of Master mix and 5 µL of NGM Select primer set alongside 10 µL of DNA free water (Thermo Fisher Scientific, 2021). This was to make up the reaction volume to 25 µL and helped introduce the imitation metallic thread segments by using the water to adhere the segments to move them to the PCR tube. All reactions were carried out at 30x cycles with positives and negative present for each plate. The PCR consisted of one step at 95°C for 11 minutes, a second step at 94°C for 20 seconds followed by 59°C for 3 minutes for 30 cycles and a final step of 60°C for 10 minutes (Thermo Fisher Scientific, 2021). The DNA profile PCR products were then loaded onto an Applied Biosystems™ 3500 Genetic Analyser plate with 8.5 µL of Hidi formamide and 0.5 µL of LIZ™ size standard for each 1 µL of DNA template (ThermoFisher Scientific, 2022c). All samples were prepared on ice when loading the plate and a final heating step at 95°C for 3 minutes before moving the plate to an ice box was carried out to ensure any DNA present was single stranded before placing the plate onto the Genetic Analyzer (ThermoFisher Scientific, 2022c). The Genetic Analyzer was run with an injection voltage of 1.2 kV for 15 seconds using POP-4™ separation matrix polymer (ThermoFisher Scientific, 2022c). All sample data sets were loaded onto GeneMapper™ ID – X Software v1.6 alongside an allelic ladder provided with the NGM kit (ThermoFisher Scientific, 2022c). Outputs were analysed using an analytical threshold for the RFU values set to 50 RFU to exclude any detector background noise (Heathfield et al. 2022, Martín et al. 2014). Profiles were then exported to Microsoft Excel (Microsoft Corporation, 2022) for allele composition and RFU analysis.

4.3.1.3 Random Match Probability

Random match probabilities were carried out in Microsoft Excel using the calculation described by Balding and Nichols (1994) with a Balding-Nichols correction (or theta) value of 0.01 (Ng et al. 2018). All allele frequencies were taken from the whole European population found in the STRidER database (Bodner et al. 2016). All loci were treated as heterozygous if only one allele was present, with the value 1 being used for the resulting frequency for any missing alleles.

4.3.2 Results

4.3.2.1 DNA Profiles

Of the 24 counterfeit banknotes processed, 3 gave partial DNA profiles. The resulting profiles can be seen in Figure 29, Figure 30 and Figure 31. The three counterfeits were sourced from three Provinces within the Netherlands: South Holland in 2015 (Figure 29), North Holland in 2016 (Figure 30) and North Brabant in 2016 (Figure 31). The South Holland had 16 alleles present in the profile. The North Holland sample had 2 potential alleles with stutter present for both. The North Brabant 14 alleles, with three peaks with RFU values that may suggest they are homozygote alleles.

Table 11. The detected alleles for the two interpretable partial DNA profiles acquired from the imitation metallic threads of two counterfeit banknotes. The * icon indicates alleles that may be homozygous due to the RFU values.

STR Loci	South Holland	North Brabant
D10S1248	14, 16	12, 15
vWA	18	19
D16S539	13	11
D2S1338	23	NR
Amel	X	Y
D8S1179	14	14*
D21S11	NR	33.2
D18S51	17	NR
D22S1045	NR	15*
D19S433	15, 15.2	NR
TH01	21, 22	6
FGA	NR	NR
D2S441	10, 11, 14	11, 14
D3S1358	NR	17*
D1S1656	15.3	15
D12S391	NR	19
SE33	NR	NR

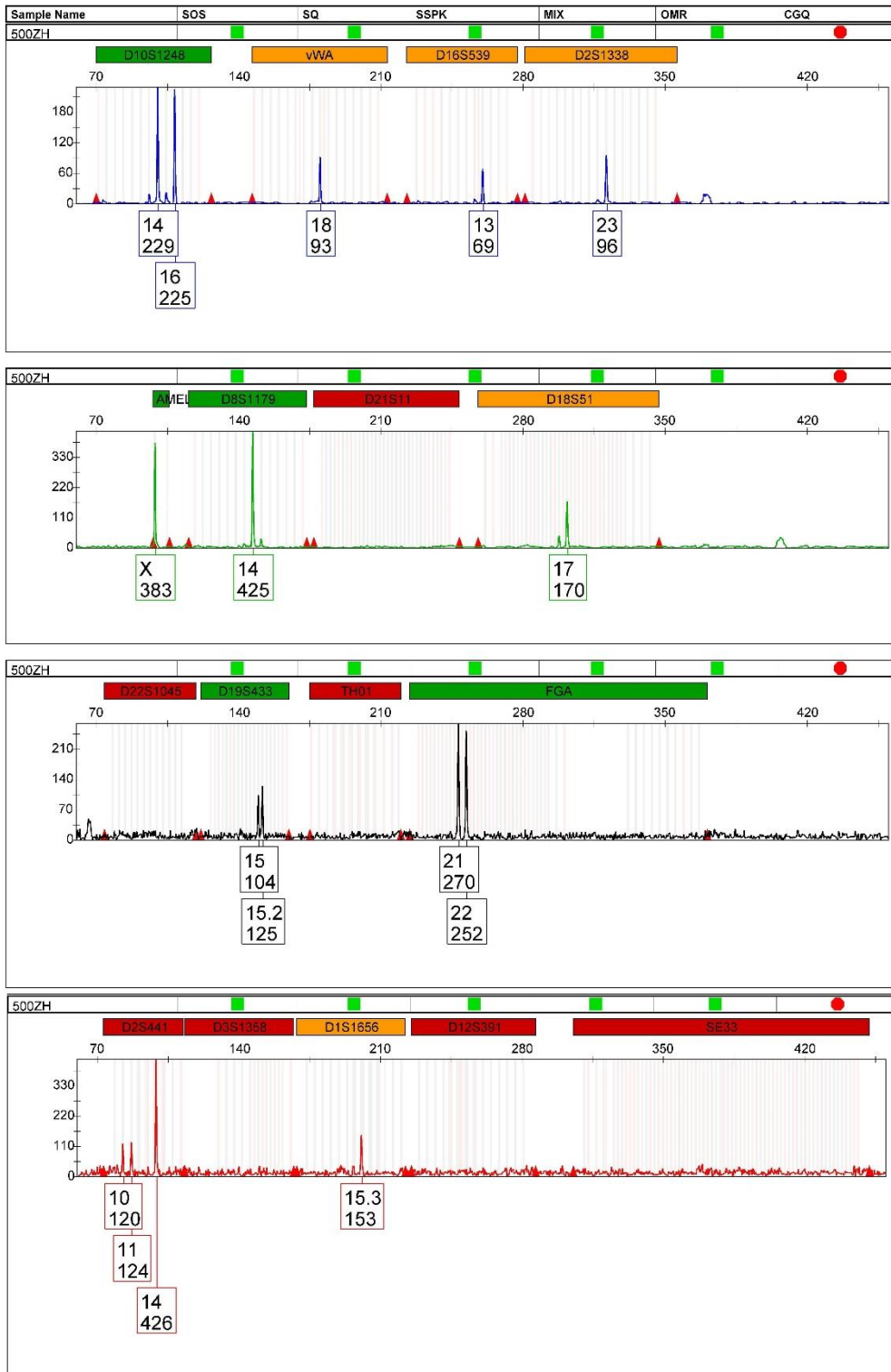


Figure 29. The electropherogram of the partial DNA profile acquired from the 2015 counterfeit banknote removed from circulation in South Holland. Labels highlight the GeneMapper™ ID – X Software identification of alleles (top of the label) and the measured RFU value (bottom of the label).

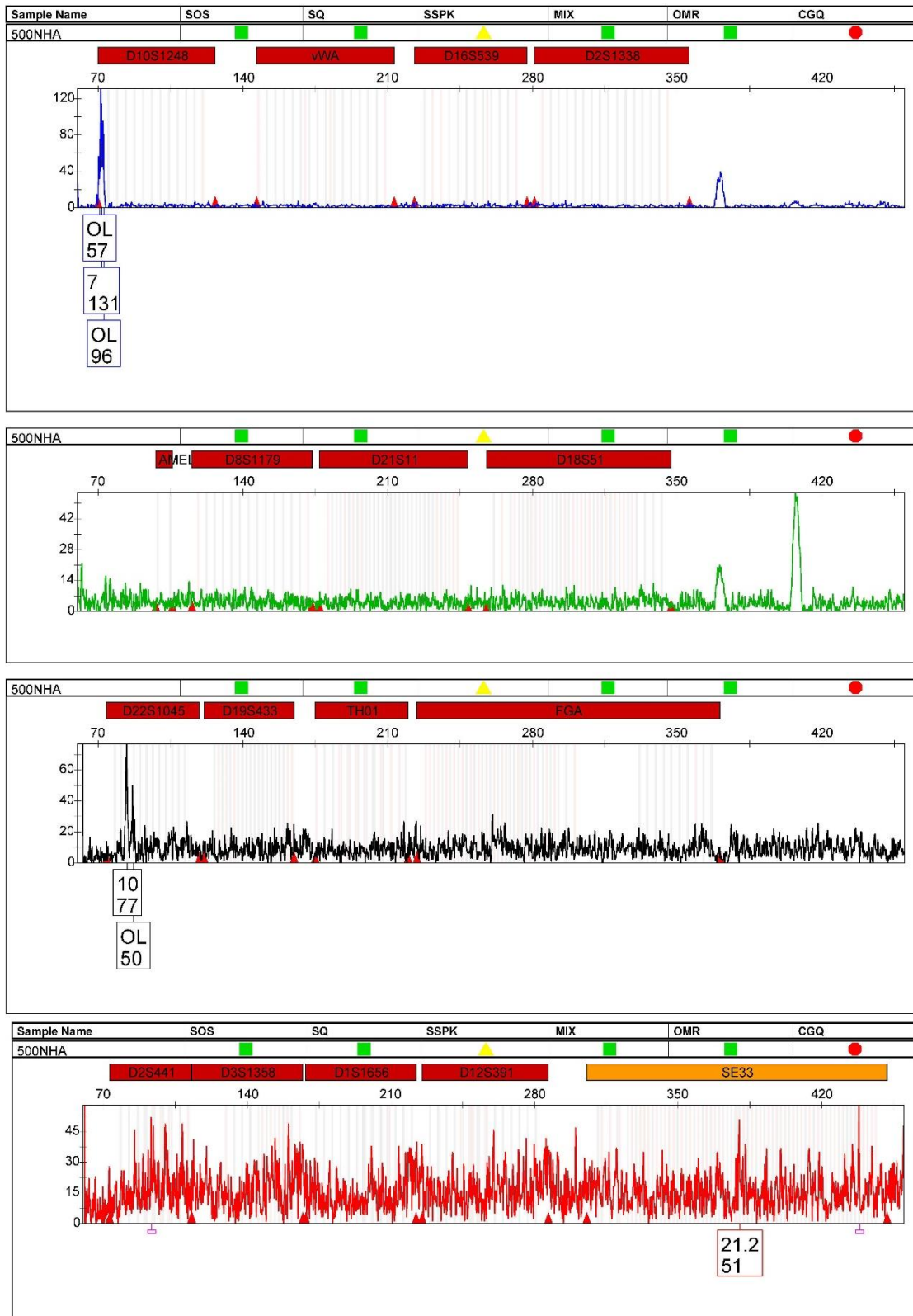


Figure 30. The electropherogram of the partial DNA profile acquired from the 2016 counterfeit banknote removed from circulation in North Holland. Labels highlight the GeneMapper™ ID – X Software identification of alleles (top of the label) and the measured RFU value (bottom of the label).

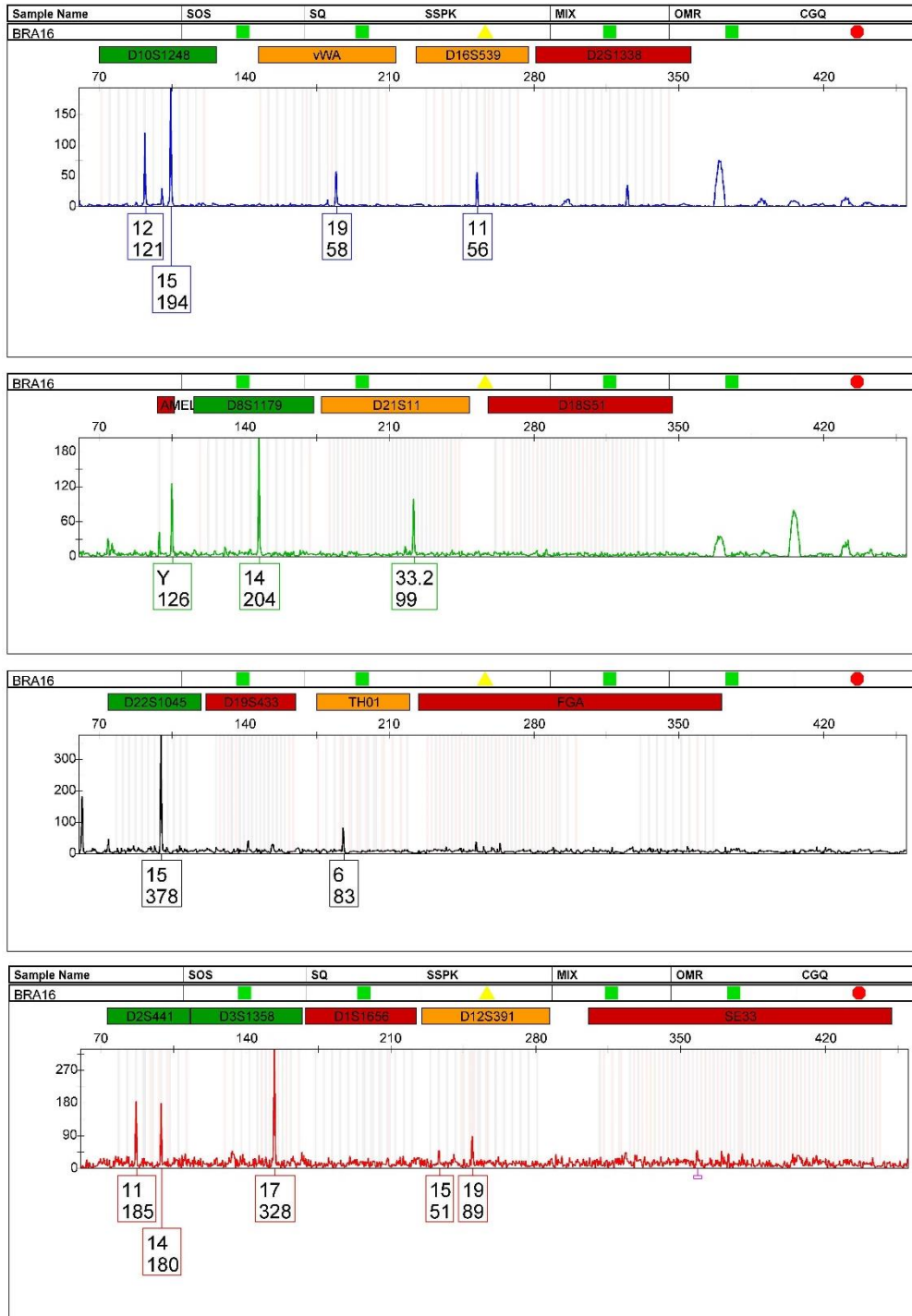


Figure 31. The electropherogram of the partial DNA profile acquired from the 2016 counterfeit banknote removed from circulation in North Brabant. Labels highlight the GeneMapper™ ID – X Software identification of alleles (top of the label) and the measured RFU value (bottom of the label).

4.3.2.2 Random Match Probabilities

The RMP for the partial profiles from the South Holland (2015) and the North Brabant (2016) were calculated using the allele frequencies for Europe taken from STRidER (Bodner et al. 2016). Both calculations used the RMP calculation from Balding and Nichols (1994) with the Balding-Nichols Correction included in the calculation at a value of 0.01.

The RMP for the South Holland sample gave a 1 in 114,061,000 chance that the profile could have come from a random individual in the population. For the calculation, allele 14 (RFU 426) on the D2S441 locus was excluded from the calculation. The North Brabant partial profile gave a 1 in 281,230,693 chance that the profile could have come from a random individual in the population.

4.3.3 Discussion

To overcome the potential loss of DNA during swabbing and extraction without the application of fingerprint enhancement techniques discussed in Section 4.2.3, direct PCR was considered for the imitation metallic threads of double layered counterfeit banknotes. Compared the Chelex resin extraction methodology established in Section 4.2.1, the direct PCR approach proved more successful. Two of the three samples with present alleles within their profile were interpretable to the degree that allowed for RMPs to be calculated. Both the South Holland and North Brabant samples had low levels of allelic stutter present. As the profiles did not contain the full number of expected alleles for every locus, it can be said that they were only partial, likely due to allelic drop out due to DNA degradation (Petricevic et al. 2010, Westen et al. 2009). There was a general decrease in the RFU values from the lower molecular weight STR loci to the higher molecular weight STRs such as the SE33 locus. With most of the allelic drop out occurring at the higher molecular weight STRs (Figure 29 and Figure 31) which was to be expected due to the trace levels of DNA present (Romano et al. 2019). DNA profile degradation can particularly be seen in the North Brabant (Figure 31), where there is a clear sloping effect in the RFU values from low to high molecular weight STRs (Bright et al. 2013). The initial RFU values for the smaller STRs are above 100 RFU, with the larger STRs dropping down to above 50 RFU (Figure 31.). There was evidence of stutter peaks occurring at STR D10S1248 for allele 15 with stutter -1 to the peak. The overall profile could potentially have homozygous alleles present at D8S1179, D22S1045 and D3S1358. In all three STRs the present alleles are double the RFU value

compared with other alleles from other sections of the profile. For this reason, the RMP was calculated with these STRs being considered homozygous for the potential contributor as a homozygote genotype presents as double the heights of heterozygote sets of alleles (Benschop et al. 2011). All these loci were above a RFU value of 200 which has been a suggested threshold of determining true homozygote loci by Roeder et al. (2009).

The South Holland sample profile had varying RFU values across both the small and large loci which is expected in low template DNA samples (Benschop et al. 2013). The D2S441 locus had three alleles potentially present (Figure 29). The alleles consist of allele 10 (RFU of 120), 11 (RFU of 124), and 14 (RFU of 426). Alleles 14 could potentially be a sign of a mixed profile due to its RFU value, but it may also be a result of allele drop-in (Gill et al. 2000B). For this reason, it was excluded from the RMP calculation. The FGA STR locus, a high molecular weight STR locus did have higher RFU values than some of the lower molecular weight STRs. The two alleles present 21 (RFU 270) and 22 (RFU 252), had double the RFU of the alleles found at the D19S433 STR locus of a lower molecular weight. This may suggest a mixture of donors maybe present such as the third allele at D2S441 but due to the low template that is likely present suggested by the high allele drop out, the variability of RFU values between the different molecular weight STRs may also be due to stochastic effects (Benschop et al. 2013). Heterozygote peak balances for the South Holland (Figure 29) and North Brabant (Figure 31) profiles were all largely similar except for the STR D10S1245 in the North Brabant sample. The allele peaks here had RFU values of 121 and 194 indicating a ratio of 0.62.

The North Holland sample did have potential alleles present in the produced profile. However, the three potential peaks all had evidence of potential incomplete adenylation in electropherograms (Figure 30.). STR D10S1248 has allele 7 present with an RFU of 131 with two peaks on either side at 57 and 96 RFU. D22S1045 has a similar case with allele 10 being present at an RFU of 77 and a secondary peak at 50. The presence of the stutter peaks makes the interpretation of the partial profile challenging. The presence of only two potential alleles makes further comparisons from other samples less powerful and less evidentially valuable. However, this does show that potential acquirable DNA profiles vary in condition when using the direct PCR method. In comparison, the South Holland and North Brabant partial profiles were able to produce RMPs of 1 in 114,061,000 and 1 in 281,230,693 respectively (Section 4.3.2.2). Although these RMPs do not meet the 1 in 1 billion probability

normally associated with a full profile (Ng et al. 2018, Semikhodskii et al. 2021), the small probabilities with a partial DNA profile shows the intelligence gathering potential of trace DNA evidence within counterfeit banknotes. The two partial profiles do not share any similar alleles which does not allow for the linking of the two counterfeit banknotes from a similar source. However, it does give the basis of further investigation as it can be assumed that OCGs use several individuals in the manufacturing of counterfeit banknotes.

The emulation of an embedded counterfeit security thread lends itself to direct PCR as it is easy to manipulate and place into PCR tubes. Full reaction volumes were also used as half volumes would not completely submerge the sections of thread in the PCR tube. Research has also shown that full volumes for DNA profiling when considering direct PCR are advisable (Dargay and Roy 2016). The primary drawback of direct PCR is the lack of repeatability (Martin et al. 2022). The majority of the thread was used in this research for each sample PCR mixture, there for removing the possibility of repeating the examination. Direct PCR could potentially provide DNA profiles from counterfeit holograms removed from counterfeit banknotes. However, there is an increased risk of contamination when dealing with external components of a counterfeit banknote as well as contamination for reagents (Ruprecht et al. 2022). Martin et al. (2022) suggested a method of direct PCR that allows for the reproducibility of samples by introducing split tapelift samples to produce replicates. However, the samples were tapelifts where DNA was lifted from evidence multiple times allowing for the accumulation of DNA on known areas on the tapelifts. This may pose practical issues in the case of the embedded security thread imitation as the location of potential DNA is not known. Therefore, by splitting the embedded security thread imitation across profiling reactions to establish a consensus DNA profile may be less successful in establishing a profile in this example. A blended approach of direct PCR and extraction could allow for reproducibility as with Forsberg et al. (2016).

The use of a blended direct PCR and DNA extraction methodology may cause for the same problems when acquiring a DNA profile as was found in Section 4.2.2. However, this would need to be further researched in the context of its application to counterfeit banknote DNA analysis. The successful production of the DNA profiles using direct PCR over the application of Chelex resin extraction (Section 4.2.3) could be due to the inclusion of cell free DNA. Vandewoestyne et al. (2013) established that cell free DNA may be lost in DNA extraction techniques which would account for the improvement of acquiring DNA profiles from the imitation metallic thread. More recent

research has supported the evidential value of cell free DNA when it comes to trace DNA evidence (Burrill et al 2021c). The exclusion of a swabbing and extraction step prior to sample processing proved successful when using direct PCR in research by Cavanaugh and Bathrick (2018), highlighting the need for the inclusion of cell free DNA when considering trace DNA samples (Quinones and Daniel 2012). Other methods are available such as mtDNA sequencing that could provide a higher success rate of acquiring DNA profiles where the concentration has been insufficient for standard profiling (Zapico et al. 2021). Next Generation Sequencing could also provide a more sensitive analysis (Xu et al. 2022) but it currently too costly to be applied in every day forensic examination. Especially when considering multiple counterfeit banknotes that would be processed to establish if a link between the present DNA profiles can be made.

The successful acquiring of partial DNA profiles in the adhesive layers of counterfeit banknotes highlights the potential intelligence value of trace DNA evidence in the context of counterfeiting. The partial profiles that could be potentially acquired could be a major significant asset to anticounterfeiting agencies the fight against counterfeiting. The costs of sampling, extraction and quantification are also reduced considerably, although forensic laboratories may have regulatory requirements that prevent them from circumventing these steps (Cavanaugh and Bathrick 2018). The use of direct PCR in this application shows the capability of its use outside of gaining reference profiles (Martin et al. 2022).

4.4 Diamond Dye Targeting of Fingermarks

Ethics Declaration

All experimental designs were approved under Proportional Ethical Approval provided by the Staffordshire University ethics Committee.

4.4.1 Methodology

A volunteer was asked to rub their hand around their neck and behind their ears to build up sebaceous material on their hands. They were then asked to peel away a dot matrix hologram from the carrying sheet before placing their fingermarks onto the adhesive side of three dot matrix holograms. Two dot matrix holograms simulating the holograms found on the first series of euro banknotes and one dot matrix hologram strip that simulated the holographic DOVID found on the more recent

Europa series of euro banknotes (European Central Bank, 2014). The hologram was preplaced onto a mounting slide using a set of tweezers sterilised with 70% methylated spirit (Parsons et al. 2016). A pre-prepared solution of a 1:20 dilution of the diamond dye and 75% ethanol (Kanokwongnuwut et al. 2018a) was then placed onto the dot matrix hologram adhesive at a volume of 10 μ L. A slide cover was then placed over the hologram to help spread the dye. Images were then taken using the DCS[®] 5 system from Foster and Freeman (Kwok et al. 2023). This consisted of a 36.3 MP camera set up for fluorescent fingermark imaging using a UV imaging module with an illumination bandwidth of 445-510nm and filtered at 549 nm (Kwok et al. 2023). Glass slides were used for negative and positives with the expected fluorescence for a present fingermark and clean slide observed with the addition of the dye.

4.4.2 Results

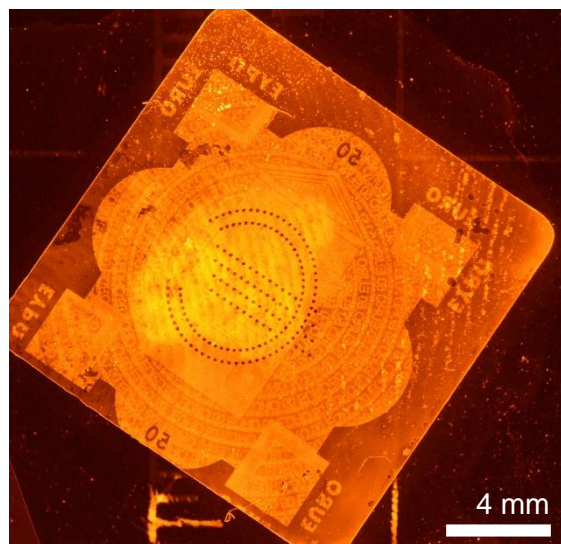


Figure 32. Dot matrix hologram with a sebaceous fingermark material present with ridge detail visible with the addition of diamond dye.

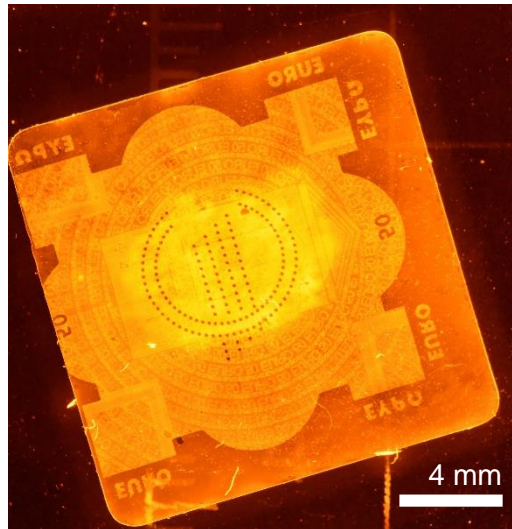


Figure 33. Dot matrix hologram with a sebaceous fingerprint material present but not as visible with the addition of diamond dye.

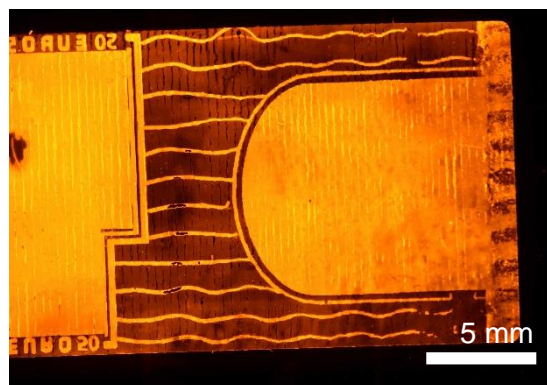


Figure 34. Dot matrix hologram strip with a sebaceous material present but not as visible with the addition of diamond dye. The contrast for the capture of the image has been increased to highlight the lack of fluorescence from cellular material.

The results from the three holograms varied significantly between each dot matrix hologram. The volunteer was asked to repeatedly place their finger onto the adhesive by first removing the dot matrix hologram from the carrying sheet and then directly placing their fingerprint onto the adhesive. From the visualisation of the dot matrix hologram samples, the sample from Figure 32 indicated clear ridge detail. Ridge detail can be seen around the right corner of the hologram from the initial manipulation of the dot matrix with further details faintly visible at the centre of the hologram from the secondary deposition. However, from Figure 33 has no clear ridge detail visible across the hologram with any fluorescence being due to the hologram itself and background fluorescence from the surface of the imaging platform. Figure 34 had a similar issue where there was no ridge detail visible with all the fluorescence observed

being due to the dot matrix hologram itself rather than the dye highlighting cellular material. The holograms themselves in negative controls also exhibited the orange fluorescence present for the holographic sections of the holograms as seen in the Figure 32, Figure 33 and Figure 34.

4.4.3 Discussion

The applications of the diamond dye had a mixed set of outcomes from the three samples tested. The aim for this methodology was to establish if there was any potential to use diamond dye to target areas of forensic interest through the highlighting of genetic material. Although this was successful in one sample, the others were not successful in identifying any cellular material. The variation between the three samples using sebaceous material could be due to several factors. Due to the fluorescence of the components of the dot matrix hologram, there may have been interference with the dye, this can be shown in Figure 34 where the dot matrix hologram strip was composed of a larger area of dot matrix hologram. The adhesive nature may have also been a factor as the application of the dye has shown to work where tapelifts have been used to lift fingerprints off handled items (Haines and Linacre 2018). However, there may be variability in this when the fingerprints have been placed directly onto the adhesive rather than lifted. This would not discredit the use of diamond dye as a potential dual recovery and target swabbing agent as there are several studies showing its functionality in different mock case work samples such as gun casings to the surface of polymer banknotes (Haase et al. 2019, Kanokwongnuwut et al. 2019b).

As the work was only carried out on a small number of dot matrix holograms there would need to be a larger data set to establish the use of diamond dye for the targeted swabbing of adhesive components of counterfeit banknotes. Although it was not able to highlight cellular material in two of the three samples, the successful sample had clear ridge detail that could be used for targeted swabbing. To improve on the effectiveness, more controls could be in place for the use of volunteers by using natural fingerprint deposits on the dot matrix holograms with various individuals with varying shedder status (Kanokwongnuwut et al. 2019b). Studies have shown alternative techniques in applying the dye such as using a spray that may prove more effective in highlighting areas of forensic genetic interest (Hughes et al. 2022).

4.5 Conclusion

In the first section of Chapter 4 the objective was to apply the established methods from the previous chapters with the aim to acquire a DNA profile. Although it was successful in consistently separating the adhesive layers with a potential application in procedural work, none of the samples gave a successful DNA profile. It was therefore hypothesised that the extraction steps were decreasing the amount of DNA present. This could have been through loss between each tube exchange from the lysis step to the final concentration step of the methodology or over dilution of the sample to the point where DNA would not be detected. Instead, a direct PCR approach was adopted and tested in Section 4.3 that was successful in acquiring a set of partial DNA profiles from the direct PCR of the imitation metallic thread taken from counterfeit €500 banknotes. Although the profiles acquired had no matching alleles a random match probability could be produced from them highlighting that there was evidential value to the profiles acquired.

Diamond™ nucleic acid dye has shown to have uses in forensic trace analysis and was therefore considered for its use in targeted swabbing to help improve the success of acquiring a DNA profile from counterfeit banknotes. By applying it onto the adhesive of handled dot matrix holograms it was hypothesised that any highlighted ridge detail could be then targeted for further DNA analysis. However, from the images of the samples there was only one working sample. Although it was not consistently successful in its implementation in the designed methodology, there were likely factors that inhibited the successful application of the dye for trace DNA evaluation. Future work could improve on the methodology applied with a greater variety of volunteers and conditions to evaluate the use of the dye in counterfeit banknotes. Further developments in the technique of using diamond dye for the screening and targeting of evidentially valuable counterfeit banknote adhesive layers could allow for the increased success of acquiring DNA profiles from counterfeit banknotes.

Chapter 5 Conclusions and Future Considerations

5.1 Conclusions

The findings of the work successfully tested the aim of separating the adhesive layers of counterfeit banknotes using solvents such as xylene and ethanol in a novel procedure. This allowed for the access to the adhesive layers of counterfeit banknotes for further DNA analysis.

From the simulated procedural study, it was shown that if trace DNA is present, it can be extracted and profiled from the adhesive of dot matrix holograms. The comparisons of the extraction techniques used indicated that Chelex resin and phenol chloroform were the optimum techniques to apply within the tested parameters. This was shown in both the allelic compositions of the profiles and the resulting RFU values. Thus, achieving the aim of establishing an optimised methodology for the extraction of DNA from composite counterfeit banknotes. From the allelic composition, it was found that the individuals who placed their fingermarks were present on the dot matrix holograms as the primary profiles. Although there were some foreign alleles present this could be from the secondary transfer of DNA to the volunteer's hands.

As Chelex resin extraction is both safer and easier to use than phenol chloroform extraction, the methodology was applied to counterfeit euro banknotes to address the aim of acquiring DNA profiles from the notes. However, none of the extractions of swabs taken from the dot matrix holograms and embedded security thread imitations of counterfeit euro banknotes were successful in acquiring a DNA profile. The concentrations at which DNA is deposited are likely highly variable, which was evident from the application of the method on seized counterfeit banknotes. To further address the aim of evaluating the presence of DNA profile on counterfeit banknotes, direct PCR was investigated. In the case of the counterfeit euro banknotes with double paper layers, it was shown that there is a potential for DNA to be encapsulated on the embedded security thread imitation. Thus, allowing for the move towards a method without sample preparation to acquire a DNA profile. To improve the success of acquiring a DNA profile from counterfeit banknote adhesive layers, Diamond™ nucleic acid dye was applied to handled dot matrix holograms. This was with the intention of highlighting any present deposited DNA that could then be swabbed for

further DNA analysis. However, from the images of the samples there was only one working sample. As the samples were not consistently successful there were likely factors that inhibited the successful application of the dye for trace DNA evaluation as previous research has shown it has a wide range of applications (Haase et al. 2019, Kanokwongnuwut et al. 2019b).

The aim of acquiring DNA profiles from counterfeit banknotes was successfully achieved. However, with there being only two partial profiles with non-matching alleles, a potential link could not be established between the two separately sourced counterfeit euro banknotes. The findings of the study do highlight the potential of acquiring partial DNA profiles present in counterfeit banknotes. The findings have shown that there is evidential potential for acquiring a suspect's DNA profile from a counterfeit banknote. With the application of a direct PCR approach and the use of ethanol to separate the adhesive layers of the counterfeit banknotes it is possible to gain a partial DNA profile of a potential counterfeiting suspect. Although it was not possible to acquire a full DNA profile future work could improve the success rate of acquiring a DNA profile. With further work it could be possible to acquire a greater number of DNA profiles from counterfeit banknotes, providing an increased evidential value to the seizure and forensic investigation of counterfeit banknotes. The research findings indicate the capability of acquiring DNA from counterfeit banknotes for forensic investigations, which with further research could be part of a standard procedure for counterfeit banknote processing to gain intel on OCGs. Through the identification of matching DNA profiles between different geographically sourced counterfeit banknotes, the movement and potential source of counterfeit banknotes could be identified. Not only would this help to investigate and apprehend the networks of OCGs that fund their activities through counterfeiting banknotes but it also maintains the trust that the general public holds in physical currency.

5.2 Future Considerations and Recommendations

Future considerations should focus on the use of ethanol specifically as this would be more beneficial for DNA evidence gathering and easier to implement in a procedural setting when separating the adhesive components of counterfeit euro banknotes. The optimisation of the swabbing methodology for dot matrix holograms could move towards the use of targeted swabbing using fingerprint enhancement techniques. This would allow for the dual recovery of evidence and the potential increase in the success of acquiring DNA profiles from counterfeit samples. Although this has proved

useful with other sample types such as glass (Hughes et al. 2022), tapelifts (Kanokwongnuwut et al. 2020) or swabs (Kanokwongnuwut et al. 2018b), this was not successful when applied to the adhesive sides of the dot matrix holograms. Through the use of Diamond™ nucleic acid dye the success rate of acquiring a DNA profile from a counterfeit banknote's adhesive layers could be increased. Although not reliably successful in its evaluation in Chapter 4, there is the potential to have future work expand on this area further. With further sample collection and evaluation, the use of diamond dye could increase the success of acquiring a DNA sample from the adhesive layers by targeting the highlighted contact points, in a similar manner to the methodology implemented in tape lift samples (Haines and Linacre, 2018). The issues may be due to the chemistry of the counterfeit components such as the adhesive and metallic hologram present in the dot matrix hologram that may have inhibited the fluorescence of the dye. More research would need to be carried out to establish if this is the case. However, the optimization of the carrying reagents and alternative application techniques such as spraying the surface may allow for the locating of fingerprints present in the adhesive counterfeit banknote layers and better surface coverage (Hughes et al. 2022). This would be beneficial in allowing for the prioritising of samples that have known fingerprints present for DNA analysis and ensure the appropriate areas are analysed further for swabbing or direct PCR to optimise the acquisition of DNA profiles (Cook et al. 2021).

To further develop the methodology of acquiring DNA from counterfeit banknotes the processing of dot matrix holograms could be further altered. In Chapter 4 the use of ethanol double swabbing and chelex extraction was unsuccessful in acquiring DNA profiles. However, the use of direct PCR was successful with the use of ethanol to separate the adhesive layers. Although the direct PCR profiling of the samples did give a set of partial DNA profiles, there were only in two of the samples which could be clearly interpreted. A growing area of research has been in the application of NGS or next generation sequencing on low levels of DNA (Xavier and Parson, 2017 and Fordyce et al. 2015). Recent research has also used the method of whole genome amplification (WGA) alongside NGS (Xu et al. 2022) to improve the success of acquiring STR genotypes from trace levels of DNA. This is where the entire genome is replicated to produce a larger amount of DNA, unlike a standard PCR whereby specific sequences are targeted (Xu et al. 2022). The application of both WGA and NGS in future work could therefore increase the amount of a profile acquired and the number of successfully acquired DNA profiles when applied to counterfeit banknote samples. Through the use of NGS, larger sections of sequence can be analysed such

as SNPs and Y-STRs that can be used to further an investigation of potential suspects outside the standard use of STR profiling (Thanakiatkrai et al. 2017). NGS has also been applied in mitochondrial DNA sequencing, a process already used in forensic genetics through the application CE (Templeton et al. 2013). The use of mitochondrial analysis could prove useful if investigated in counterfeit banknotes as mitochondrial DNA has a higher copy number present than autosomal DNA. However, mitochondrial sequencing is less informative compared to STR profiling as the sequence is inherited maternally (Butler and Levin, 1998). The use of next generation sequencing is still a growing area in forensic science however, with costs being the main factor preventing its wide-spread use (Foley and Oldoni, 2023). As the technology develops further with reduced costs and a wider this could a technique that could improve the evidential value of counterfeit banknote from a genetic perspective.

Further work could investigate the success rate of acquiring DNA using direct PCR on the embedded security thread imitation as well as from the dot matrix holograms found on counterfeit banknotes. Such work could also establish the likelihood of acquiring a DNA profile from components of a counterfeit banknote. This could be done through a similar volunteer study as was done in Chapter 3 but instead look to quantify the DNA with a more sensitive qPCR system such as the Quantifiler Trio Quantification kit (Liu et al. 2014b) and vary the surface area contact of the volunteer's fingers to establish how much of a fingerprint would be required to deposit enough trace DNA to acquire a DNA profile. Although the study in Chapter 3 investigated dot matrix holograms specifically, another approach could have volunteers handle metallic thread to establish the potential DNA profile that could be acquired. These studies could asl compare the use of the Chelex resin extraction methodology and the direct PCR approach in terms of the success in acquiring a DNA profile and how much of a profile can be obtained. In these future studies, more prior selection and preparation of the volunteers could also be established to avoid the risk of secondary transfer to the volunteers (Butcher et al. 2019) and establish individuals with as few shared alleles as possible to make any potential mixtures easier to interpret (van den Berge et al. 2016). Thus, further informing forensic examiners of the most evidentially valuable sections of a counterfeit banknote for DNA profiling, helping to streamline and reduce the cost of processing. Similarly in the simulated procedural study, likelihood ratios or Bayesian frameworks (Gill et al. 2022) could have established the activity level probability of acquiring a DNA profile if an individual

had made a counterfeit banknote. This was not carried out as it was not the main aim of the research here.

Due to the regulations surrounding the acquisition of DNA profiles, according to United Kingdom Accreditation Services and the uploading of DNA profiles to the NDNAD, the partial profiles acquired could not be used for a database search. However, further work from forensic practitioners with appropriate accreditation and links could repeat the methodology for the direct PCR of DNA profiles from imitation metallic thread taken from counterfeit banknotes. This could also include evidential interpretation of the profiles in the context of a potential suspect's DNA profile using likelihood ratios. The application of these methodologies detailed in this research are not restricted to counterfeit euro banknotes. Counterfeits of other currencies are likely to possess imitation security threads and dot matrix holograms that have been applied manually especially in case where paper currency is still used, such as in the USA (The Bureau of Engraving and Printing, 2023). Although polymer banknotes are less susceptible to counterfeiting, over time counterfeiting does occur with the advancement of technology available to the public (Mann and Roche, 2022). These counterfeits could include the adhesive dot matrix holograms seen in euro counterfeit banknotes examined in Chapters Chapter 2Chapter 3Chapter 4, instead having them placed on a polymer substrate. Any counterfeit items that possess the adhesive layers to imitate or replicate characteristics of a genuine document, may potentially have the DNA of the counterfeiter present in the adhesive layers present. The acquisition of DNA profiles from counterfeit banknotes, allows for the further gathering of intelligence on OCG activities and ensures that public trust in banknotes is retained.

Chapter 6 References

- Aditya, S., Sharma, A.K., Bhattacharyya, C.N. and Chaudhuri, K. (2011). Generating STR profile from "touch DNA". *Journal of Forensics and Legal Medicine*, [online] 18, pp. 295-298.
- Adler, C.J., Hakk, W., Donlon, D., Cooper, A. and The Genographic Consortium. Survival and recovery of DNA from ancient teeth and bones. *Journal of Archeological Science*, [online] 38, pp. 956-964.
- Alaeddini, R. (2012). Forensic implications of PCR inhibition- A review. *Forensic Science International: Genetics*, [online] 6, pp. 297-305.
- Alaeddini, R., Walsh, S. and Abbas, A. (2012). Forensic implications of genetic analyses form degraded DNA- A review. *Forensic Science International: Genetics*, [online] 4(3), pp. 148-157.
- Alketbi, S. and Saif, A. (2022). Dual recovery of DNA and fingerprints using minitapes. *Journal of Forensic Sciences and Criminal Investigation*, [online] 16(1).
- Alonso, A. and Garcia, O. (2007). Ch. 4. Real-time quantitative PCR in forensic science. *Molecular Forensics*, 1st ed. John Wiley and Sons Ltd., [online], pp. 59-69.
- Alonso, A., Müller, P., Roewer, L. Willuweit, S., Budowle, B. and Parson, W. (2017) European survey on forensic applications of massively parallel sequencing. *Forensic Science International: Genetics*, [online] 9, pp. 23-25.
- Alonso, A., Barrio, P., Müller, P., Köcher, S., Berger, B., Martin, P., Bodner, M., Willuweit, S., Parson, W., Roewer, L. and Budowle, B. (2018). Current state-of-art of STR sequencing in forensic genetics. *Electrophoresis*, [online] 39, pp. 2655-2668.
- Amankwaa, A. and McCartney, C. (2019). The effectiveness of the UK national DNA database. *Forensic Science International: Synergy*, [online] 1, pp. 45-55.
- Amigo, J., Phillips, C., Salas, T., Formoso, L., Carracedo, A. and Lareu, M. (2009). Pop.STR- An online population frequency browser for established and new forensic

STRs. *Forensic Science International: Genetics Supplement Series*, [online] 2, pp. 361-362.

Andres, J., Hersch, R., Moser, J. and Chauvin, A. (2014). A new anti-counterfeiting feature relying on invisible luminescent full color images printed with Lanthanide-based inks. *Advanced Functional Materials*, [online] 24, pp. 5029-5036.

Applied Biosystems (2015). AmpFLSTR® NGM Select™ PCR amplification. *Thermo Fisher Scientific Inc.*, [pdf], Available at: https://assets.thermofisher.com/TFS-Assets/LSG/manuals/cms_089008.pdf [Accessed 16 May 2019]

Applied Biosystem (2022). GeneScan™ 500 LIZ™ dye Size Standard. *Thermo Fisher Scientific Inc.*, [online], Available at: <https://www.thermofisher.com/order/catalog/product/4322682#:~:text=GeneScan%E2%84%A2%20500%20LIZ%E2%84%A2%20Size%20Standard%20is%20designed%20for,450%2C%20490%20and%20500%20nucleotides> [Accessed 14 November 2022]

Assis, A., Costa, C., Alves, M., Melo, J., Oliveira, V., Tonholo, J., Hillman, R. and Ribeiro, A. (2022). From nanomaterials to macromolecules: Innovative technologies for latent fingerprint development. *WIREs Forensic Science*, [online] e1475, pp. 1-34.

Balding, D. and Buckleton, J. (2009). Interpreting low template DNA profiles. *Forensic Science International: Genetics*, [online] 4, pp. 1-10.

Balding, D. and Nichols, R. (1994). DNA profile match probability calculation: how to allow for population stratification, relatedness, database selection and single bands. *Forensic Science International*, [online] 64, pp. 125-140.

Balogh, M., Burger, J., Bender, K., Schneider, P. and Alt, K. (2003). STR genotyping and mtDNA sequencing of latent fingerprint on paper. *Forensic Science International*, [online] 137, pp. 188-195.

Bank of England (2022). Banknote Statistics. [online] Bank of England. Available at: <https://www.bankofengland.co.uk/statistics/banknote> [Accessed 10 May 2022]

Bank of Japan (2022). How many banknotes are being circulated in Japan?

Available at:

<https://www.boj.or.jp/en/announcements/education/oshiete/money/c06.htm/>

[Accessed 3 October 2022]

Bano, H., Mohammed, O., Bensaheb, F., Behl, S. and Nazir, M. (2015). Evaluating emerging technologies applied in forensic analysis. *International Journal of Engineering Research and Science and Technology*, [online] 4(3), pp. 146-171.

Barash, M., Reshef, A. and Brauner, P. (2010). The use of adhesive tape for recovery of DNA from crime scene items. *Journal of Forensic Sciences*, [online] 55(4), pp. 1058-1064.

Barbaro, A., Cormaci, P. and Falcone, G. (2011). Validation of BTA™ lysis buffer for DNA extraction from challenged forensic samples. *Forensic Science International: Genetics Supplement Series*, [online], 3(1), pp. e61-62.

Barbisin, M., Fang, R., O'Shea, C., Calandro, L., Furtado, M. and Shewale, J. (2009). Developmental validation of the Quantifiler® Duo DNA Quantification kit for simultaneous quantification of total human and human male DNA detection of PCR inhibitors in biological samples. *Journal of Forensic Science*, [online] 54(2), pp. 305-319.

Barbisin, M. and Shewale, J. (2010). Assessment of DNA extracted from forensic samples prior to genotyping. *Forensic Science Review*, [online] 22(2), pp. 199-214.

Barbisin, M., Fang, R., Furtado, M. R. and Shewale, J. G. (2011) Quantifiler® Duo DNA Quantification kit: A guiding tool for short tandem repeat genotyping of forensic samples. *Journal of Forensic Research*, 2 (2), pp. 1-11.

Bathrick, A., Norsworthy, S., Plaza, D., McCormick, M., Slack, D. and Ramotowski, R. (2021) DNA recovery after sequential processing of latent fingerprints on copy paper. *Journal of Forensic Sciences*, 67, pp. 149-160.

Behlke, M.A., Huang, L., Bogh, L., Rose, S. and Devor, E.J. (2005). Fluorescence and Fluorescence Applications. *Integrated DNA Technologies*, [online], pp. 1-13.

- Benjamin, D and Berger, J. (2019). Three recommendations for improving the use of p-values. *The American Statistician*, [online] 73(S1), pp. 186-191.
- Benschop, C., van der Beek, C., Meiland, H., van Gorp, A., Westen, A. and Sijen, T. (2011). Low template STR typing: Effect of replicate number and consensus method on genotyping reliability and DNA database search results. *Forensic Science International: Genetics*, [online] 5(4), pp. 316-328.
- Benschop, C., Haned, H. and Sijen, T. (2013). Consensus and pool profiles to assist in the analysis and interpretation of complex low template DNA mixtures. *International Journal of Legal Medicine*, [online] 127, pp. 11-23.
- Berenguel, A., Terrades, O., Lladós, J. and Cañero, C. (2016). Banknote counterfeit detection through background texture printing analysis. *IEEE Xplore*, [online], pp. 66-71.
- Bicknell, D. and Laporte, G. (2009) Forged and counterfeit documents. *Wiley Encyclopedia of Forensic Science*, [online], pp. 1-21.
- Bio-Rad Laboratories (2000a). InstaGene™ Matrix. *Bio-Rad Laboratories* [pdf]. Available at: <https://www.bio-rad.com/sites/default/files/webroot/web/pdf/lsr/literature/LIT544.pdf> [Accessed 12 May 2019]
- Bio-Rad Laboratories (2000b). Ssoadvanced™ universal SYBR® green supermix, Bio-Rad Laboratories *Bio-Rad Laboratories* [online]. Available at: <https://www.bio-rad.com/en-uk/product/ssoadvanced-universal-sybr-green-supermix?ID=MH5H1EE8Z> [Accessed 12 May 2019]
- Bio-Rad Laboratories (2019). Chelex® 100 molecular biology grade resin. Available at: <https://www.bio-rad.com/en-uk/product/Chelex-100-molecular-biology-grade-resin?ID=bd6fd35e-c8ff-4515-9499-8af8ccbb3ca5> (Accessed 1 July 2020)
- Blackie, R., Taylor, D. and Linacre, A. (2018). DNA profiles from clothing fibers using direct PCR. *Forensic Science, Medicine, and Pathology*, [online], pp. 331-335.

- Bodner, M., Bastisch, I., Butler, J., Fimmers, R., Gill, P., Gusmão, L., Morling, N., Phillips, C., Prinz, M., Schneider, P. and Parson, W. (2016). Recommendations of the DNA Commission of the International Society for Forensic Genetics (ISFG) on quality control of autosomal Short Tandem Repeat allele frequency databasing (STRidER). *Forensic Science International: Genetics*, [online] 24, pp. 97-102.
- Boom, R., Sol, C., Salimans, M., Jansen, C., Dillen, W. and van der Noordaa, J. (1990). Rapid and simple method for purification of nucleic acids. *Journal of Clinical Microbiology*, [online], pp. 495-503.
- Bornman, D., Hester, M., Schuetter, J., Kasoji, M., Minard-Smith, A., Barden C., Nelson S., Godbold, G., Baker, C., Yang, B., Walther, J., Tornes, I., Yan, P., Rodriguez, B., Bundschuh, R., Dickens, M., Young, B. and Faith, S. (2012). Short-read, high-throughput sequencing technology for STR genotyping. *Biotech Rapid Dispatches*, [online], pp. 1-6.
- Bowyer, V. (2007). Real-time PCR. *Forensic Science, Medicine and Pathology*, [online] 3(1), pp. 61-63.
- Boyle, E. (2002). Foiling counterfeiters. *Paper, Film and Foil Converter*, [online] 76(8), pp. 38-39.
- Božičević, M., Gajović, A. and Zjakić, I. (2012). Identifying a common origin of toner printed counterfeit banknotes by micro-Raman spectroscopy. *Forensic Science International*, [online] 223 (1-3), pp. 314-320.
- Bragulla, H. and Homberger, D. (2009). Structure and functions of keratin proteins in simple, stratified, keratinized and cornified epithelia. *Journal of Anatomy*, [online] 214, pp. 516-559.
- Breathnach, M. and Moore, E. (2013). Oral intercourse or secondary transfer? A Bayesian approach of salivary amylase and foreign DNA findings. *Forensic Science International*, [online] 229, pp. 52-59.
- Bright, J. and Petricevic, S. (2004). Recovery of trace DNA and its application to DNA profiling of shoe insoles. *Forensic Science International*, [online] 145, pp. 7-12.

- Bright, J., Taylor, D., Curran, J.M. and Buckleton, J.S. (2013). Degradation of forensic DNA profiles. *Australian Journal of Forensic Sciences* [online], 45 (4), pp. 445-449.
- Brown, S. (2004). Latest developments in on- and off-line inspection of bank notes during production. *Proceedings of SPIE*, [online] 5310, pp. 46-51.
- Brown, A., Collard, S. and Spearritt, M. (2017). Recent trends in banknote counterfeiting. *Reserve Bank of Australia: Bullitin March 2017* [online], pp. 67-74.
- Bruijns, B.B., Tiggelaar, R.M. and Gardeniers, H. (2018). The extraction and recovery efficiency of pure DNA for different types of swabs. *Journal of Forensic Science*, [online], 63(5), pp. 1492-1499.
- Bruna, A., Farinella, G., Guarnera, G. and Battiato, S. (2013). Forgery detection and value identification of euro banknotes. *Sensors*, [online] 13, pp. 2515-2529.
- Buckleton, J., Curran, J., Groudet, J., Taylor, D., Thiery, A. and Weir, B. (2016). Population-specific Fst values for forensic STR markers: A worldwide survey. *Forensic Science International: Genetics*, [online] 23, pp. 91-100.
- Budowle, B., Eisenburg, A. and van Daal, A. (2009A). Validity of low copy number typing and applications to forensic science. *Croatia Medical Journal*, [online] 50(3), pp. 207-217.
- Budowle, B., Onorato, A., Callaghan, T., Manna, A., Gross, A., Guerrieri, R., Luttman, J. and McClure, D. (2009B). Mixture interpretation: defining the relevant features for guidelines for the assessment of mixed DNA profiles in forensic casework. *Journal of Forensic Sciences*, [online] 54(4), pp. 810-821.
- Bünzli, J. (2010) Europium in the limelight. *Nature Chemistry*, [online] 2, pp. 696.
- Bünzli, J. (2017) Rising stars in science and technology: luminescent lanthanide materials. *European Journal of Inorganic Chemistry*, [online] 2017(44), pp. 5058-5063.

- Burrill, J., rammenou, E., Alawar, F., Daniel, B. and Frascione, N. (2021a). Corneocyte lysis and fragmented DNA considerations for the cellular component of forensic touch DNA. *Forensic Science International: Genetics*, 51, 102428.
- Burrill, J., Daniel, B. and Frascione, N. (2021b). Accumulation of endogenous and exogenous nucleic acids in “Touch DNA” components on hands. *Electrophoresis*, [online] 00, pp. 1-11.
- Burrill, J., Kombara, A., Daniel, B. and Frascione, N. (2021c). Exploration of cell-free DNA (cfDNA) recovery for touch deposits. *Forensic Science International: Genetics*, [online] 51, 102431.
- Butcher, E., van Oorschot, R., Morgan, R. and Meakin, G. (2019). Opportunistic crimes: Evaluation of DNA from regularly-used knives after a brief use by a different person. *Forensic Science International: Genetics*, [online] 42, pp. 135-140.
- Butler, J. and Levin, B. (1998). Forensic applications of mitochondrial DNA. *Trends in Biotechnology*, [online] 16(4), pp. 158-162.
- Butler, J. (2006) Genetics and genomics of core short tandem repeat loci used in human identity testing. *Journal of Forensic Sciences*, [online] 51(2), pp. 253-265.
- Butler, J. (2007) Short tandem repeat typing technologies used in human identity testing. *Biotechniques*, [online] 43(4), pp. 2-5.
- Butler, J., Buel, E., Crivellente, F. and McCord, B. (2004) Forensic DNA typing by capillary electrophoresis using the ABI prism 310 and 3100 genetic analyzers for STR analysis. *Electrophoresis*, [online] 25, pp. 1397-1412.
- Butler, J., Chalmers, J., McVean, G. and Tully, G. (2017). *Forensic DNA analysis: A primer for courts*. [pdf] London: Royal Society, pp. 1-60.
- Campos, P. and Gilbert, M. (2019). DNA extraction form keratin and chitin. In: Shapiro, D., Barlow, A., Heintzman, P., Hofreiter, M., Pajmans, J. and Soares, A. ed., *Ancient DNA*, 2nd ed. Springer Protocols, [online], pp. 57-63.

Caputo, M., Bobillo, M., Sala, A. and Corach, D. (2016). Optimizing direct amplification of forensic commercial kits for STR determination. *Journal of Forensic and Legal Medicine*, [online] 47, pp. 17-23.

Carter, M. and Milton, I. (1993). An inexpensive and simple method for DNA purifications on silica particles. *Nucleic Acids Research*, [online] 21(4), 1044.

Cartozzo, C., Singh, B., Boone, E. and Simmons, T. (2018). Evaluation of DNA extraction methods from waterlogged bones: A pilot study. *Journal of Forensic Sciences*, [online] 63(6), pp. 1830-1835.

Cavanaugh, S. and Bathrick, A. (2018). Direct PCR amplification of forensic touch and other challenging DNA samples: A review. *Forensic Science International: Genetics*, [online] 32, pp. 40-49.

Chambers, J., Yan, W., Garhwal, A. and Kankanhalli, M. (2015). Currency security and forensics: A survey. *Multimedia Tools and Applications*, [online] 74(11), pp. 4013-4043.

Chacon-Cortes, D. and Griffiths, L. (2014). Methods for extracting genomic DNA from whole blood samples: current perspectives. *Journal of Biorepository Science for Applied Medicine*, [online] 2, pp. 1-9.

Chen, C., Hseu, Y., Liang, S., Kuo, J. and Chen, S. (2008). Assessment of genotoxicity of methyl-tert-butyl ether, benzene, toluene, ethylbenzene, and xylene to human lymphocytes using comet assay. *Journal of Hazardous Materials*, [online] 153(1-2), pp. 351-356.

Cho, Y., Kim, H.S., Kim, M., Park, M., Kwon, H., Lee, Y.H. and Lee, D.S. (2017). Validation of reduced reagent volumes in the implementation of the quantifiler® trio quantification kit. *Journal of Forensic Science*, 63 (2), pp. 1-9.

Ciancaglini, V., Balduzzi, M., Goncharov, M. and McArdie, R. (2013). Deepweb and cybercrime: It's not all about TOR. *Trend Micro*, [online], pp. 1-22.

Cohen, J. (1988). *Statistical power analysis for the behavioural sciences*. 2nd Edition, Lawrence Erlbaum Associates Publishers, New York.

Comte, J., Baechler, S., Gervaix, J., Lock, E., Milon, M., Delémont, O. and Castela, V. (2019). Touch DNA collection- Performance of four difference swabs. *Forensic Science international: Genetics*, 43, 102113.

Cook, R., Mitchell, N. and Henry, J. (2021). Assessment of Diamond™ Nucleic Acid Dye for the identification and targeted sampling of latent DNA in operational casework. *Forensics Science International: Genetics*, 55, 102579.

Correa, H.S.D., Brescia, G., Cortellini, V., Cerri, N. and Verseletti, A. (2020). DNA quantitation and degradation assessment: a quantitative PCR protocol designed for small forensic genetics laboratories. *Electrophoresis*, [online] 41 (9), pp. 714-719.

Corzo, R., Subedi, K., Trejos, T. and Almirall, J. (2016). Evaluation of forensic utility of scanning electron microscopy-energy dispersive spectroscopy and laser ablation-inductively coupled plasma-mass spectrometry for printing ink examinations. *Journal of Forensic Sciences*, [online] 61(3), pp. 725-734.

Cowell, R., Grversen, T., Lauritzen, S. and Mortera, J. (2015) Analysis of forensic DNA mixtures with artefacts. *Applied Statistics*, [online] 64(1), pp. 1-48.

Cropper, E., Coble, M. and Kavlick, M. (2022). Assessment of human nuclear and mitochondrial DNA qPCR assays for quantification accuracy utilizing NIST SRM 2372a. *Forensic Genetics International: Genetics*, 59, 102711.

Dairawan, M. and Shetty, P. (2020). The evolution of DNA extraction methods. *American Journal of Biomedical Science and Research*, [online] 8(1), pp. 39-45.

Daly, D., Murphy, C. and McDermott, S. (2012). The transfer of touch DNA from hands to glass, fabric and wood. *Forensic Science International: Genetics*, [online] 6(1), pp. 41-46.

Dargay, A. and Roy, R. (2016). Direct Y-STR amplification of body fluids deposited on commonly found crime scene substrates. *Journal of Forensic and Legal Medicine*, [online] 39, pp. 50-60.

de Heij, H. (2009). Banknote design for the visually impaired. *DNB Occasional Studies*, [online] 7(2), pp. 1-68.

de Heij, H. (2010a). Banknote design for retailers and public. *DNA Occasional Studies* [pdf] Amsterdam: De Nederlandsche Bank NV, 8 (4), 1-246.

de Heij, H. (2010b). Innovative approaches to the selection of banknote security features. [pdf] Amsterdam: De Nederlandsche Bank NV, pp. 1-84.

Defence Science and Technology Laboratory (2019). Fingermark Visualization Newsletter, November 2019. *DSTL*, [pdf] United Kingdom: UK DSTL.

Deltalab (2016). Sterile swab in round tube. *Deltalab*. [online]. Available at: <https://www.deltalab.es/en/producto/sterile-swab-in-round-tube/> (Accessed 28 February 2023)

Dhanasekaran, S., Doherty, T., Kenneth, J. and TB Trials Study Group (2010). Comparison of different standards for real-time PCR-based absolute quantification. *Journal of Immunological Methods*, [online] 354(1-2), pp. 34-39.

Dinno, A., (2015). Nonparametric pairwise multiple comparisons in independent groups using Dunn's test. *The State Journal*, [online] 15(1), pp. 292-300.

Dissing, J., Søndervang, A. and Lund, S. (2010). Exploring the limits for the survival of DNA in blood stains. *Journal of Forensic and Legal Medicine*, [online] 17, pp. 393-396.

Donadio, R. (2012) In Southern Italy, fake euros that even the police admire. *The New York Times*, [online]. Available at: <https://www.nytimes.com/2012/05/01/world/europe/in-italy-counterfeiting-with-artisanal-care.html> [Accessed 11 May 2019]

Dørum, G. and Bouzga, M. (2015) Urns and forensics. *CHANCE*, [online] 28(1), pp. 4-11.

Dragan, A. Pavlovic, R., McGivney, J., Casas-Finet, J., Bisop, E., Strouse, R., Schernerman, M. and Geddes, C. (2012). SYBR green I: fluorescence properties and interaction with DNA. *Journal of Fluorescence*, [online] 22 (4), pp. 1189-1199.

Durney, B., Crieffield, C. and Holland, L. (2015). Capillary electrophoresis applied to DNA: determining and harnessing sequence and structure to advance bioanalyses (2009-2014). *Analytical and Bioanalytical Chemistry*, [online] 407(23), pp. 6923-6938.

Edwards, A. Civitello, A., Hammond, H. Caskey, C. (1991). DNA typing and genetic mapping with trimeric and tetrameric tandem repeats. *The American Journal of Human Genetics*, [online] 49(4), pp. 746-756.

ENFSI, (2017). DNA database management review and recommendations: ENFSI DNA working group April 2017. *ENFSI* [online] Available at: <https://enfsi.eu/wp-content/uploads/2017/09/DNA-databasemanagement-review-and-recommendatations-april-2017.pdf> [Accessed 10 October 2022]

European Central Bank (2005). The euro banknotes: Developments and future challenges. *ECB Monthly Bulletin* [online] Available at: https://www.ecb.europa.eu/pub/pdf/other/p041-048_mb200508en.pdf?926a06d4b574de7eb339a3cb7dff0326 [Accessed 21 July 2019]

European Central Bank (2014). The €10 banknote of the Europa series. *European Central Bank*, [online]. Available at: https://www.ecb.europa.eu/euro/cashprof/trainingmat/shared/pdf/2014-03-18_The_10_note_of_the_Europa_series.pdf [Accessed 16 May 2019]

European Central Bank (2018). Euro banknote counterfeiting remained low in the first half of 2018. *European Central Bank Press Release*, [online]. Available at: <https://www.ecb.europa.eu/press/pr/date/2018/html/ecb.pr180727.en.html> [Accessed 16 May 2019]

European Central Bank (2019). Euro banknote counterfeiting decreased further and remained low in the second half of 2018. *European Central Bank Press Release*, [online]. Available at: <https://www.ecb.europa.eu/press/pr/date/2019/html/ecb.pr190125~c64c7e8683.en.html> [Accessed 16 May 2019]

European Union (1998). *Council regulation (EC) No 974/98 of 3 May 1998 on the introduction of the euro*. Official Journal of the European Communities, [online] 139, pp. 1-5. Available at: <https://publications.europa.eu/en/publication-detail/-/publication/3937aa6f-3cba-4fea-aaa0-6fce2c99bb60> [Accessed 16 May 2019]

European Union (2000). *Council framework decision of 29 May 2000 on increasing protection by criminal penalties and other sanctions against counterfeiting in connection with the introduction of the euro*. Official Journal of the European Communities, [online] 140, pp. 1-3. Available at: <https://eur-lex.europa.eu/legal-content/EN/TXT/PDF/?uri=CELEX:32000F0383&from=EN> [Accessed 16 May 2019]

European Union (2001). *Council regulation (EC) No 1339/2001 of 28 June 2001 extending the effects of Regulation (EC) No 1338/2001 laying down measures necessary for the protection of the euro against counterfeiting to those Member States which have not adopted the euro as their sing currency*. Official Journal of the European Communities, [online] 181, pp. 1. Available at: <https://eur-lex.europa.eu/legal-content/EN/TXT/PDF/?uri=CELEX:32001R1339&from=EN> [Accessed 16 May 2019]

European Union (2009). *Council resolution of 30 November 2009 on the exchange of DNA analysis results (2009/C 296/01)*. Official Journal of the European Union, [online] 296, pp. 1-3. Available at: <https://eur-lex.europa.eu/LexUriServ/LexUriServ.do?uri=OJ:C:2009:296:0001:0003:EN:PDF> [Accessed 16 May 2019]

European Union (2014). *Directive 2014/62/EU of the European Parliament and the council of 15 May 2014 on the protection of the euro and other currencies against counterfeiting by criminal law, and replacing Council Framework Decision 2000/383/JHA*. Official Journal of the European Union, [online] 151, pp. 1-8. Available at: <https://eur-lex.europa.eu/legal-content/EN/TXT/?uri=CELEX%3A32014L0062> [Accessed 16 May 2019]

Europol, (2016a). *Successful hit against Bulgarian and Slovenian euro counterfeiters*. [online] Available at: <https://www.europol.europa.eu/newsroom/news/successful-hit-against-bulgarian-and-slovenian-euro-counterfeiters> [Accessed 13 May 2019]

Europol, (2016b). *Europol and Lithuania prevent production of millions of counterfeit euro*. [online] Available at: <https://www.europol.europa.eu/newsroom/news/europol-and-lithuania-prevent-production-of-millions-of-counterfeit-euro> [Accessed 13 May 2019]

Europol, (2018). *Two euro counterfeit rings in France and Italy cause millions in damage circulating fake banknotes across Europe*. [online] Available at: <https://www.europol.europa.eu/newsroom/news/two-euro-counterfeit-rings-in-france-and-italy-cause-millions-in-damage-circulating-fake-banknotes-across-europe> [Accessed 13 May 2019]

Europol, (2019). *Europe's second-largest counterfeit currency network on the dark web taken down in Portugal*. [online] Available at: <https://www.europol.europa.eu/media-press/newsroom/news/europe%E2%80%99s-second-largest-counterfeit-currency-network-dark-web-taken-down-in-portugal> [Accessed 3 October 2022]

Europol, (2022). *14 arrests for euro counterfeiting in Spain*. [online] Available at: <https://www.europol.europa.eu/media-press/newsroom/news/14-arrests-for-euro-counterfeiting-in-spain> [Accessed 4 October 2022]

FBI, (2019). CODIS- NDIS statistics. FBI [online] Available at: <https://www.fbi.gov/services/laboratory/biometric-analysis/codis/ndis-statistics> [Accessed 13 May 2019]

FBI, (2022). Frequently asked questions on CODIS and NDIS. FBI [online] Available at: <https://www.fbi.gov/how-we-can-help-you/dna-fingerprint-act-of-2005-expungement-policy/codis-and-ndis-fact-sheet> [Accessed 10 October 2022]

Feine, I., Shpitzen, M., Geller, B., Salmon, E., Peleg, T., Roth, J. and Gafny, R. (2017). Acetone facilitated DNA sampling from electrical tapes improves DNA recovery and enables latent fingerprints development. *Forensic Science International*, [online] 276, pp. 107-110.

Fenton, N., Neil, M. and Berger, D. (2016). Bayes and the law. *Annual Review of Statistics and Its Application*, [online] 3, pp. 51-77.

- Findley, I., Taylor, A., Quirke, P., Frazier, R. and Urquhart, A. (1997). DNA fingerprinting from single cells. *Nature*, [online] 389, pp. 555-556.
- Flegar, I. and Radovanovic, R. (2013). Forensic aspects of the protections of euro. *Academy of Criminalistic and Police Studies* [online] pp. 67-82.
- Foley, M. and Oldoni, F. (2023). A global snapshot of current opinions of next-generation sequencing technologies usage in forensics. *Forensic Science International: Genetics*, [online] 63, 102819.
- Foran, D. (2006). Relative degradation of nuclear and mitochondrial DNA: An experimental approach. *Journal of Forensic Science*, [online] 51(4), pp. 766-770.
- Fordyce, S., Mogensen, H., Børsting, C., Lagacé, R., Chang, C., Rajagopalan, N. and Morling, N. (2015). Second-generation sequencing of forensic STRs using the Ion Torrent™ HID STR 10-plex and the Ion PGM™. *Forensic Science International: Genetics*, [online] 14, pp. 132-140.
- Forgery and Counterfeiting Act 1981*. Available at:
<https://www.legislation.gov.uk/ukpga/1981/45> [Accessed 16 May 2019]
- Forsberg, C., Jansson, L., Ansell, R. and Hedman, J. (2016). High-throughput DNA extraction of forensic adhesives tapes. *Forensic Science International: Genetics*, [online] 24, pp. 158-163.
- Fregeau, C.J. and Laurin, N. (2015) The Qiagen investigator® quantiplex HYres as an alternative kit for DNA qquantification. *Forensic Science International: genetics*, 16, pp. 148-162.
- Fridez, F. and Coquoz, R. (1996). PCR DNA typing of stamps: evaluations of the DNA extraction. *Forensic Science International*, [online] 78, pp. 103-110.
- Fujii, K., Fukagawa, T., Watahiki, H., Mita, Y., Kitayama, T. and Mizuno, N. (2018). Ratios and distances of pull-up peaks observed in GlobalFiler kit data. *Legal Medicine*, [online] 34, pp. 58-63.

Funes-Huacca, M., Opel, K., Thompson, R. and McCord, B. (2011). A comparison of the effects of PCR inhibition in quantitative PCR and forensic STR analysis. *Electrophoresis*, [online] 32, pp. 1084-1089.

Funk, M., Gillich, E., Dörksen, H., Lohweg, V., Hofmann, J., Türke, T., Chassot, D. and Schaede, J. (2016). Intaglio quality measurement. *Optical Document Security*, [online] 5, pp. 1-17.

Geneva Convention, (1929). International convention for the suppression of counterfeiting currency and protocol. Signed at Geneva, April 20, 1929. *League of Nations Treaty Series*, [online] 45(112), pp. 372-393. Available at: <http://www.worldlii.org/int/other/LNTSer/1931/45.html> [Accessed 16 May 2019]

Genesig, 2020. Genesig easy DNA/RNA extraction. Genesig [online]. Available at: <https://www.genesig.com/products/9660-genesig-easy-dna-rna-extraction-kit> [Accessed: 25/10/2020]

Geusebroek, J., Markus, P. and Balke, P. (2011). Learning banknote fitness for sorting. *2011 International Conference on Pattern Analysis and Intelligence Robotics*, [online], pp. 41-46.

Giesse, H., Lam, R., Selden, R. and Tan, E. (2009). Fast multiplexed polymerase chain reaction for conventional and microfluidic short tandem repeat analysis. *Journal of Forensic Sciences*, [online] 54(6), pp. 1287-1296.

Gill, P., Sparkes, R. and Kimpton, C. (1997). Development of guidelines to designate alleles using an STR multiplex system. *Forensic Science International*, [online] 89, pp. 185-197.

Gill, P., Sparkes, R., Fereday, L. and Werrett, D. (2000A). Report of the European Network of Forensic Science Institutes (ENSFI): formulation and testing of principles to evaluate STR multiplexes. *Forensic Science International*, [online] 108, pp. 1-29.

Gill, P., Whitaker, J., Flaxman, C., Brown, N. and Buckleton, J. (2000B). An investigation of the rigor of interpretation rules for STRs derived from less than 100pg of DNA. *Forensic Science International*, [online] 112, pp. 17-40.

Gill, P. (2001). Application of low copy number DNA profiling. *Croatian Medical Journal*, [online] 42(3), pp. 229-232.

Gill, P. Haned, H., Bleka, O., Hansson O., Dørum, G. and Egeland, T. (2015). Genotyping and interpretation of STR-DNA: Low template, mixtures and database matches- twenty years of research and development. *Forensic Science International: Genetics*, [online] 18, pp. 100-117.

Gill, P., Bleka, Ø. And Fonneløp, E. (2022) RFU derived LR's for activity level assignments using Bayesian Networks. *Forensic Science International: Genetics*, 56, 102608.

Gillich, E., Hoffman, J., Dörksen, H., Lohweg, V. and Schaede, J. (2016). Data collection unit- A platform for printing process authentication. *Conference: Optical Document Security- The Conference on Optical Security and Counterfeit Detection*, [online] 5, pp. 1-11.

Giovanelli, G., Natali, S. and Bozzini, B. (2006). Silver coated lead coins: An appraisal of ancient technology. *Journal of Applied Electrochemistry*, [online] 36, pp. 951-956.

Goldberg, L. (2010). Is the international role of the dollar changing? *Federal Reserve Bank of New York: Current Issues in Economics and Finance*, [online] 16(1), pp. 1-7.

Goldstein, M.C., Cox, J.O., Seman, L.B. and Cruz, T.D. (2020). Improved resolution of mixed STR profiles using a fully automated differential cell lysis/DNA extraction method. *Forensic Sciences Research*, [online] 6(2), pp. 106-112.

Goray, M. van Oorschot, R. and Mitchell, J. (2012). DNA transfer within forensic exhibit packaging: Potential for DNA loss and relocation. *Forensic Science International: Genetics*, [online] 6, pp. 158-166.

Green, M. and Sambrook, J. (2018). Isolation and quantification of DNA. *Cold Spring Harbor Laboratory Press*, [online], pp. 403-414.

Green, M. and Sambrook, J. (2019). Polymerase chain reaction. *Cold Spring Harbor Laboratory Press*, [online], pp. 436-456.

Green, R., Lagacé, R., Oldroyd, N., Hennessy, L. and Mulero, J. (2013). Developmental validation of the AmpFLSTR® NGM Select™ PCR amplification kit: A next-generation STR multiplex with the SE33 locus. *Forensic Science International: Genetics*, [online] 7, pp. 41-51.

Griffin, A., Henry, J., Kirkbride, K., painter, B. and Linacre, A. (2022). A survey of the effects of common illicit drugs on forensic DNA analysis. *Forensic Science International*, [online] 336, 111314.

Guo, F., Yu, J., Zhang, L. and Li, J. (2017). Massively parallel sequencing of forensic STRs and SNPs using the Illumina® ForenSeq™ DNA signature prep kit on the MiSeq FGx™ forensic genomics system. *Forensic Science International: Genetics*, [online] 31, pp. 135-148.

Haase, H., Mogensen, H., Petersen, C., Petersen, J. Holmer, A., Børsting, C. and Pereira, V. (2019). Optimization of the collection and analysis of touch DNA traces. *Forensic Science International: genetics Supplement Series*, [online] 7(1), pp. 98-99.

Haines, A., Tobe, S., Kobus, H. and Linacre, A. (2013). Detection of DNA within fingermarks. *Forensic Science International: Genetics Supplement Series*, [online] 4, pp. e290-291.

Haines, A., Tobe, S., Kobus, H., Linacre, A. (2015). Properties of nucleic acid staining dyes used in gel electrophoresis. *Electrophoresis*, 36(6), pp. 941-944.

Haines, A. and Linacre, A. (2018). Detection of latent DNA on tape-lifts using fluorescent in situ detection. *Australian Journal of Forensic Sciences*, [online], pp. 455-465.

Ham S., Kim, S., Seo, B. Y., Woo, K., Lee, S. and Choi, C. Y. (2016). Differential pre-amplification of STR loci for fragmented forensic DNA profiling, *Electrophoresis* [online], 37, pp. 3002-3009.

- Hanegraaf, R., Jonker, N., Mandley, S. and Miedema, J. (2016). Life cycle assessment of cash payments. *DNB Working Paper*, [online] 610, pp. 1-27.
- Hall, A., Sims, L. and Ballantyne, J. (2014). Assessment of DNA damage induced by terrestrial UV irradiation of dried bloodstains: Forensic Implication. *Forensic Science International: Genetics*, [online] 8(1), pp. 24-32.
- Harrel, M., Mayes, C., Gangitano, D. and Hughes-Stamm, S. (2018). Evaluation of a powder-free DNA extraction method for skeletal remains. *Journal of Forensic Science*, [online] 63(6), pp. 1819-1823.
- Hares, D. (2015). Selection and implementation of expanded CODIS core loci in the United States. *Forensic Science International: Genetics*, [online] 17, pp. 33-34.
- Hartl, A., Grubert, J., Schmalstieg, D. and Reitmayr, G. (2013). Mobile interactive hologram verification. *2013 IEEE International Symposium on Mixed and Augmented Reality (ISMAR)*, [online], pp. 75-82.
- Heathfield, L.J., Hitewa, A.N., Gibbon, A., Mole, C.G. (2022). The effect of NucleoSpin® Forensic Filters on DNA recovery from trace DNA swabs. *Science and Justice*, [online], pp 284-287.
- Hedman, J., Nordgaard, A., Rasmusson, B., Ansell, R. and Rådström, P. (2009). Improved forensic DNA analysis through the use of alternative DNA polymerases and statistical modelling of DNA profiles. *BioTechniques*, [online] 47, pp. 951-958.
- Hedman, J., Jansson, L., Akel, Y., Wallmark, N., Liljestränd, R., Forsberg, C. and Ansell, R. (2020). The double-swab technique versus single swabs for human DNA recovery from various surfaces. *Forensic Science International: Genetics*, [online] 46, 102253.
- Hefetz, I., Einot, N., Faerman, M., Horowitz, M. and Almog, J. (2019). Touch DNA: The effect of the deposition pressure on the quality of latent fingerprints and STR profiles. *Forensic Science International: Genetics*, [online] 38, pp. 105-112.

Heinonen, A. (2015). The first euros: The creation and issue of the first euro banknotes and the road to the Europa series. *European Central Bank*, [online], pp. 1-276.

Higushi, R., Fockler, C., Dollinger, G. and Watson, R. (1993). Kinetic PCR analysis: Real-time monitoring of DNA amplification reactions. *Bio/Technology*, [online] 11, pp. 1026-1030.

Hill, C., Butler, J. and Vallone, P. (2009). A 26plex autosomal STR assay to aid human identity testing. *Journal of Forensic Sciences*, [online] 54(5), pp. 1008-1015.

Hofman, J., Gillich, E., Dörksen, H., Chassot, D., Türke, T. and Lohweg, V. (2014). New strategies in image processing for standardized intaglio quality analysis in the printing process. *Conference: Optical Document Security- The Conference on Optical Security and Counterfeit Detection*, [online] 4, pp. 1-15.

Hohoff, C., Schnöink, K., Brinkmann, B. and Schneider, P. (2013). The GEDNAP (German DNA profiling group) proficiency testing system. *GEDNAP*, [online].

Holland, P.M., Abramson, R.D., Watson, R. and Gelfand, D.H. (1991) Detection of specific polymerase chain reaction product by utilizing the 5' to 3' exonuclease activity of *Thermus aquaticus* DNA polymerase. *Proceedings of the National Academy of Sciences of the United States of America*, [online] 88, pp. 7276-7280.

Home Office, (2020). National DNA database strategy board biennial report 2018-2020. Home Office [online] Available at: https://assets.publishing.service.gov.uk/government/uploads/system/uploads/attachment_data/file/913011/NDNAD_Strategy_Board_AR_2018-2020_Web_Accessible.pdf [Accessed 10 October 2022]

Horjan, I., Barbaric, L. and Mrsic, G. (2016). Applicability of three commercially available kits for forensic identification of blood stains. *Journal of Forensic and Legal Medicine*, [online] 38, pp. 101-105.

Hu, Q., Liu, Y., Yi, S. and Huang D. (2014). A comparison of four methods for PCR inhibitor removal. *Forensic Science International: Genetics*, [online] 16, pp. 94-97.

Hughes, D., Szkuta, B., van Oorschot, R. and Conlan, X. (2022). "Technical note:" optimisation of Diamond™ Nucleic Acid Dye preparation, application, and visualisation, for latent DNA detection. *Forensic Science International*, [online] 330, 111096.

IBM Corp. (2022). IBM SPSS Statistics for Windows, Available at: <https://www.ibm.com/uk-en/products/spss-statistics>

Itrić, K. and Modrić, D. (2017). Banknote characterization using the FTIR spectroscopy. *Technical Journal*, [online] 11(3), pp. 83-88.

Iyavoo, S., Hadi, S. and Goodwin, W. (2013). Evaluation of five DNA extraction systems for recovery of DNA from bone. *Forensic Science International: Genetics Supplement Series*, [online] 4, pp. e174-e175.

Jackson, G., Kaye, D., Neumann, C., Ranadive, A. and Reyna, V. (2015). Communicating the results of forensic science examinations. *Penn State Law Research Paper*, [online] 22, pp. 1-86.

Jiang, X., He, J., Jia, F., Shen, H., Zhao, J., Chen, C., Bai, L., Liu, F., Hou, G. and Guo, F. (2012). An integrated system of ABO typing and multiplex STR testing for forensic DNA analysis. *Forensic Science International: Genetics*, [online] 6, pp. 785-797.

Joel, J., Glanzmann, B., Germann, U. and Cossu, C. (2015). DNA extraction of forensic adhesive tapes- A comparison of two different methods. *Forensic Science International: Genetics Supplement Series*, [online] 5, pp. e579-581.

Kaesler, T., Kirkbride, K. and Linacre, A. (2022). DNA deposited in whole thumbprints: A reproducibility study. *Forensic Science International: Genetics*, [online] 8, 102683.

Kanokwongnuwut, P., Kirkbride, P. and Linacre, A. (2018a). Speed of accumulation of DNA in a fingermark. *Australian Journal of Forensics Sciences*, [online] 52(3), pp. 293-302.

Kanokwongnuwut, P., Kirkbride, P. and Linacre, A. (2018b). Visualising latent DNA on swabs. *Forensic Science International*, [online] 291, pp. 115-123.

Kanokwongnuwut, P., Kirkbride, P. and Linacre, A. (2019a). Detection of cellular material in lip-prints. *Forensics Science, Medicine and Pathology*, [online] 15(3), pp. 363-368.

Kanokwongnuwut, P., Kirkbride, P. and Linacre, A. (2019b). Enhancement of fingermarks and visualizing DNA. *Forensic Science International*, [online] 300, pp. 99-105.

Kanokwongnuwut, P., Kirkbride, P. and Linacre, A. (2020). An assessment of tape-lifts. *Forensic Science International: Genetics*, [online] 47, 102292.

Karkar, S., Alfonse, L., Grgicak, C. and Lun, D. (2018). Statistical modelling of short-tandem repeat capillary electrophoresis profiles. *2018 IEEE International Conference on Bioinformatics and Biomedicine (BIBM)*, [online], pp. 869-876.

Kaur, S. and Kumar, R. (2015). Comparative analysis of parametric and non-parametric tests. *Journal of Computer and Mathematical Sciences*, [online] 6(6), pp. 336-342.

Kayser, M. and de Knijff, P. (2011). Improving human forensics through advances in genetics, genomics and molecular biology. *Nature Reviews Genetics*, [online] 12, pp. 179-192.

Kimpton, C., Gill, P., Walton, A., Urquhart, A., Millican, E. and Adams, M. (1993). Automated DNA profiling employing multiplex amplification of short tandem repeat loci. *Cold Spring Harbor Laboratory Press*, [online] 3, pp. 13-22.

Kinegram® (2019) Selected banknote references with Kinegram®. [online] Kinegram® Available at: <https://www.kinegram.com/en/banknotes/references/> [Accessed 16 May 2019]

Klimek, L. (2012). Counterfeiting and protection of the euro: from early beginnings to the current legislative development. *Issues of Business and Law*, [online] 4, pp. 12-24.

Kopka, J., Leder, M., Jaureguiberry, S., Brem, G. and Boselli, G. (2011). New optimized DNA extraction protocol for fingerprints deposited on a special self-adhesive security seal and other latent samples used for human identification. *Journal of Forensic Sciences*, [online] 56(5), pp. 1235-1240.

Kramvis, A., Bukofzer, S. and Kew, M. (1996). Comparison of hepatitis B virus DNA extractions from serum by the QIAamp blood kit, genereleaser, and the direct-chloroform method. *Journal of Clinical Microbiology*, [online] 34(11), pp. 2731-2733.

Kruse, C., (2013). The Bayesian approach to forensic evidence: Evaluating, communicating, and distributing responsibility. *Social Studies of Science*, [online] 43, pp. 657-680.

Kruskal, W. and Wallis, A. (1952). Use of ranks in one-criterion variance analysis. *Journal of the American Statistical Association*, [online] 47(260), pp. 583-621.

Kumar, M., (2011). Verification of documents with social values using watermark exclusion. *International Journal of Scientific and Engineering Research*, [online] 2(9), pp. 1-3.

Kumar, S. and Aswath, N. (2016) DNA isolation from teeth by organic extraction and identification of sex of the individual by analysing the AMEL gene marker using PCR. *Journal of Forensic Dental Sciences*, [online] 8(1), pp. 18-21.

Kuś, M., Ossowski, A. and Zielińska, G. (2016). Comparison of three different DNA extraction methods from a highly degraded biological material. *Journal of Forensic and Legal Medicine*, [online] 40, pp. 47-53.

Kwok, R., Kenny, D. and Williams, G. (2019). Evaluating the viability of obtaining DNA profiles from DNA encapsulated between the layers of composite counterfeit banknotes. *Forensics Science International: Genetics Supplement Series*, [online] 7, pp. 438-440.

Kwok, R., Parsons, R., Fieldhouse, S. and Walton-Williams, L. (2023). An evaluation of two adhesive media for the recovery of DNA from latent fingermarks: A preliminary study. *Forensic Science International*, [online] 344(4), 111574.

Kyrychok, T., Kyrychok, P., Havenko, S., Kibirštis, E. Milliūnas, V. (2014). The influence of pressure during intaglio printing on banknotes durability. *Mechanika*, [online] 20(3), pp. 327-331.

Lam, R., Hockey, D., Williamson, J. and Hearn, N. (2022). Latent fingermark development on fired and unfired brass ammunition under controlled and blind conditions. *Forensic Science International*, [online] 337, 111369.

Lancaster, I. (2004). Holograms an authentication: Meeting future demands. *Proceedings SPIE*, [online] 5290, pp. 318-324.

Lazaruk, K., Walsh, P., Oaks, F., Gilbert, D., Rosenblem, B., Menchen, S., Scheibler, D., Wenz, H., Holt, C. and Wallia, J. (1998). Genotyping of forensic short tandem repeat (STR) systems based on sizing precision in a capillary electrophoresis instrument. *Electrophoresis*, [online] 19, pp. 86-93.]

Lee, H., Park, M., Kim, N., Sim, J., Yang, W. and Shin, K. (2010). Simple and highly effective DNA extraction methods from old skeletal remains using silica columns. *Forensic Science International: Genetics*, [online] 4, pp. 275-280.

Lee, H., Yim, J. and Eom, Y. (2019). Effects of fingerprint development reagents on subsequent DNA analysis. *Electrophoresis*, [online] 40, pp. 1824-1829.

Lei, Y., Mei, Z., Chen, Y, Deng, N. and Li, Y. (2022). Facile purification and concentration of DNA origami structures by ethanol precipitation. *ChemNanoMat*, [online], e202200161.

Li, C., Zhao, S., Zhang, N., Zhang, S. and Hou, Y. (2013). Differences of DNA methylation profiles between monozygotic twins' blood samples. *Molecular Biology Reports*, [online] 40(9), pp. 5275-5280.

Lin, S., Li, C. and Ip, S., (2018). A performance study on three qPCR quantification kits and their compatibilities with the 6-dye DNA profiling systems. *Forensic Science International: Genetics*, [online] 33, pp. 72-83.

Liu, Y., Zhou, Q., Xie, X., Lin, D. and Dong, L. (2010). Oxidative stress and DNA damage in the earthworm *Eisenia fetida* induced by toluene, ethylbenzene and xylene. *Ecotoxicology*, [online] 19, pp. 1551-1559.

Liu, J.Y. (2014a). Direct qPCR quantification of unprocessed forensic casework samples. *Forensic Science International: Genetics*, [online] 11, pp. 96-104.

Liu, J.Y. (2014b). Direct qPCR quantification using the quantifiler® trio DNA quantification kit. *Forensic Science International: Genetics*, [online] 13, pp.10-19.

Lounsbury, J., Coult, N., Miranian, D., Cronk, S., Haverstick, D., Kinnon, P., Saul, D. and Landers, J. (2012). An enzyme-based DNA preparation method for application to forensic biological samples and degraded stains. *Forensic Science International: Genetics*, [online] 6, pp. 607-615.

Lowe, A., Murray, C., Richardson, P., Wivell, R., Gill, P., Tully, G. and Whitaker, J. (2003). Use of low copy number DNA in forensic inference. *International Congress Series*, [online] 1239, pp. 799-801.

Lui, J. Y. (2014). Direct qPCR quantification using the quantifiler® trio DNA quantification kit. *Forensic Science International: Genetics*, 13, pp. 10-19.

Mann, M., Shukla, S. and Gupta, S. (2015). A comparative study on security features of banknotes of various countries. *International Journal of Multidisciplinary Research and Development*, [online] 2(6), pp. 83-91.

Marabello, D., Benzi, P., Lombardozzi, A. and Strano, M. (2017). X-ray powder diffraction or characterization of raw materials in banknotes. *Journal of Forensic Sciences*, [online] 62(4), pp. 962-970.

Marchand, A. and Palazzeschi, E. (2014). Innovation at work: introducing the first banknote in the Europa series. *Banque de France: Quarterly Selection of Articles*, [online] 32, pp. 113-135.

Martín, P., Fernández de Simón, L., Luque, G., Farfán, M., and Alonso, A. (2014). Improving DNA data exchange: Validation studies on a single 6 dye STR kit with 24 loci. *Forensic Science International: Genetics*, [online] 13, pp. 68-78.

Martin, B., Taylor, D. and Linacre, A. (2022). Exploring tapelifts as a method for dual workflow STR amplification. *Forensic Science International: Genetics*, [online] 57, 102653.

Martire, K., (2018). Clear communication through clear purpose: understanding statistical statements made by forensic scientists. *Australian Journal of Forensic Sciences*, [online] 50(6), 619-627.

May, R. and Thompson, J. (2009). Optimisation of cellular DNA recovery from tape-lifts. *Forensic Science International: Genetics Supplement Series*, [online] 2, pp. 191-192.

McLaughlin, P., Hopkins, C., Springer, E. and Prinz, M. (2021). Non-destructive DNA recovery from handwritten documents using a dry vacuum technique. *Journal of Forensic Sciences*, [online] 66, pp. 1443-1451.

Meakin, G., Butcher, E., van Oorchot, R. and Morgan, R. (2017). Trace DNA evidence dynamics: An investigation into the deposition and persistence of directly- and indirectly-transferred DNA on regularly-used knives. *Forensic Science International: Genetics*, [online] 29, pp. 38-47.

Menchhoff, S.I., Solomon, A.D., Cox, J.O., Hytinen, M.E., Miller, M.T. and Cruz, T.D. (2020). Effects of storage time on DNA profiling success from archived latent fingerprint samples using an optimising workflow. *Forensics Sciences Research*, [online], pp. 1-8.

Merck (2019). Phenol:chloroform:isoamyl alcohol 25:24:1, saturated with 10mM Tris, pH 8.0, 1mM EDTA. [online] Available at: https://www.sigmaaldrich.com/catalog/product/sigma/p3803?lang=en®ion=GB&clid=EAlalQobChMI6PKt9ISs6gIVhe3tCh2b9gXCEAAYASAAEglyJ_D_BwE (Accessed 1 July 2020).

Microsoft Corporation (2022), Microsoft Excel, Available at: <https://www.microsoft.com/en-us/microsoft-365/excel>

Mi, Y. and Vanderpuye, O. (2013). Comparison of different DNA extraction methods for forensic samples. *Journal of Natural Sciences Research*, [online] 3(11), pp. 32-39.

Moore, D. and Rid, T. (2016). Cryptopolitik and the darknet. *Survival*, [online] 58(1), pp. 7-38.

Moretti, T., Moreno, L., Smerick, J., Pignone, M., Hizon, R., Buckleton, J., Bright, J. and Onorato, A. (2016). Population data on the expanded CODIS core STR loci or eleven populations of significance for forensic DNA analyses in the United States. *Forensic Science International: Genetics*, [online] 25, pp. 175-181.

Mutanen, J., Jaaskelainen, T. and Parkkinen, J. (2003). Luminescent security properties of banknotes. *The PICS Conference*, [online], pp. 421-424.

Nagy, A., Vitásková, E., Černíková, L. et al. (2017). Evaluation of TaqMan qPCR system integrating two identically labelled hydrolysis probes in single assay. *Nature: Scientific Reports*, [online] 7 (41392), pp. 1-10.

Negru, I., Vasilache, V., Sandu, I., Olariu, R., Tanasa, P., Potolinca, D. and Sandu, I. (2017). Depth profiling of diffraction-based security features in authentic and counterfeit banknotes. *Materiale Plastice*, [online] 54(2), pp. 321-325.

Ng, L., Ng, A., Cholette, F. and Davis, C. (2007). Optimization of recovery of human DNA from envelope flaps using DNA IQ™ system for STR genotyping. *Forensic Science International: Genetics*, [online] 1(1-3), pp. 283-286.

Ng, J., Oldt, R. and Kanthaswamy, S. (2018). Assessing the FBI's Native American STR database for random match probability calculations. *Legal Medicine*, [online] 30, pp. 52-55.

Nicklas, J. and Buel, E. (2003). Quantification of DNA in forensic samples. *Analytical and Bioanalytical Chemistry*, [online] 376(8), pp. 1160-1167.

Nicolasora, N., Downham, R., Hussey, L., Luscombe, A., Mayse, K. and Sears, V. (2018). A validation study of the 1,2-indandione reagent for operational use in the

UK: Part 1 – formulation optimization. *Forensic Science International*, [online] 292, pp. 242-253.

Nimbkar, P. and Bhatt, V. (2022). A review on touch DNA collection, extraction, amplification, analysis and determination of phenotype. *Forensic Science International*, [online] 336, 111352.

Norén, L., Hedell, R., Ansell, R. and Hedman, J. (2013). Purification of crime scene DNA extracts using centrifugal filter devices. *Investigative Genetics*, [online] 4(8), pp. 1-8.

Opel, K., Chung, D. and McCord, B. (2010). A study of PCR inhibition mechanisms using real time PCR. *Journal of Forensic Science*, [online] 55(1), pp. 25-33.

Papadimitriou, P. (2013). SPARK[®] Innovative optical technology for document sophistication and identity protection. *Keesing Journal of Documents and Identity*, [online], pp. 1-3.

Parsons, R., bates, L., Walton-Williams, D., Fieldhouse, S. and Qwinnett, C. (2013). DNA from fingerprints: Attempting dual recovery. *CSEye*, [online] 6, pp. 8-17.

Peterson, D. and Kaplan, M. (2011). The use of Hemastix[®] severely reduces DNA recovery using the BioRobot[®] EZ1. *Journal of Forensic Sciences*, [online] 56(3), pp. 733-735.

Petricevic, S., Whitaker, J., Buckleton, J., Vintiner, S., Patel, J., Simon, P., Ferraby, H., Hermiz, W. and Russel, A. (2010). Validation and development of interpretation guidelines for low copy number (LCN) DNA profiling in New Zealand using the AmpFLSTR[®] SGM Plus[™] multiplex. *Forensic Science International: Genetics*, [online] 4, pp. 305-310.

Pfeifer, A., Gillich, E., Lohweg, V. and Schaede, J. (2016). Detection of commercial offset printing in counterfeited banknotes. *Conference: Optical Document Security- The Conference on Optical Security and Counterfeit Detection*, [online] 5, pp. 1-13.

Phetpeng, S., Kitpipit, T., Asavutmangkul, V., Duangshatome, W., Pongsuwan, T. and Thanakiatkrai, P. (2013). Touch DNA collection from improvised explosive

devices: A comprehensive study of swabs and moistening agents. *Forensic Science International: Genetics Supplement Series*, [online] 4, pp. e29-30.

Phetpeng, S., Kitpipit, T., and Thanakiatkrai, P. (2015). Systematic study for DNA recovery and profiling from common IED substrates: From laboratory to casework. *Forensic Science International: Genetics*, [online] 17, pp. 53-60.

Phillips, K., McCallum, N. and Welch, L. (2012). A comparison of methods for forensic DNA extraction: Chelex-100® and the QIAGEN DNA investigation kit (manual and automated). *Forensic Science International: Genetics*, [online] 6, pp. 282-285.

Phillips, C., Gelabert-Besada, M., Fernandez-Formoso, L., Garcia-Magariños, M., Santos, C., Fondevila, M., Ballard, D., Court, D., Carracedo, Á. And Lareu, M. (2014). "New turns from old STaRs": enhancing the capabilities of forensic short tandem repeat analysis. *Electrophoresis*, [online] 35, pp. 3173-3187.

Pîrlea, S., Puiu, M., Răducan, A. and Oancea, D. (2016). Permanganate-assisted removal of PCR inhibitors during the DNA Chelex extraction from stained denim samples. *International Journal of Legal Medicine*, [online] 131(2), pp. 323-331.

Poon, H., Elliott, J., Modler, J. and Frégeau, C. (2009). The use of Hemastix® and the subsequent lack of DNA recovery using the Promega DNA IQ™ system. *Journal of Forensic Sciences*, [online] 54(6), pp. 1278-1286.

Pope, S. and Puch-Solis, R. (2021). Interpretation of DNA data within the context of UK forensic science – investigation. *Emerging Topics in Life Sciences*, [online] 5, pp. 395-404.

Prime, E. and Solomon, D. (2010). Australia's plastic banknotes: fighting counterfeit currency. *Angewandte Chemie International Edition*, [online] 49(22), pp. 3726-3736.

Promega (2020). Human - specific DNA quantification. Promega [online]. Available at: <https://www.promega.co.uk/products/forensic-dna-analysis-ce/human-specific-dna-quantitation/> [Accessed 25 September 2020]

Qiagen (2020). Investigator lyse and spin basket kit. Qiagen [online]. Available at: <https://www.qiagen.com/gb/products/human-id-and-forensics/investigator-solutions/investigator-lyseandspin-basket-kit/#orderinginformation> [Accessed 25 September 2020]

Quinones, I., and Daniel, B. (2012). Cell free DNA as a component of forensic evidence recovered from touched surfaces. *Forensic Science International: Genetics*, [online] 6, pp. 26-30.

R v Hartley (John Gerrard) (2011). Court of Appeal, Criminal Division, EWCA Crim 1957. *Westlaw* [online]. Available at: <https://login.westlaw.co.uk/maf/wluk/app/document?&srguid=i0ad8289e0000016abfe6eb9265cdd1b9&docguid=I657B7CF0C20D11E0B896F4A2589092D8&hitguid=I657B7CF0C20D11E0B896F4A2589092D8&rank=8&spos=8&epos=8&td=1580&crumb-action=append&context=17&resolvein=true> [Accessed 16 May 2019]

R. v Edirin-Etareri (Jamil) (2014). Court of Appeal, Criminal Division, EWCA Crim 1536. *Westlaw* [online]. Available at: <https://login.westlaw.co.uk/maf/wluk/app/document?&srguid=i0ad832f20000016abfe7e30075b740ed&docguid=I75F4BB20134D11E4BC73DA64EEA0AA54&hitguid=I75F4BB20134D11E4BC73DA64EEA0AA54&rank=1&spos=1&epos=1&td=7&crumb-action=append&context=21&resolvein=true> [Accessed 16 May 2019]

R. v T (2010). Court of Appeal, Criminal Division, EWCA Crim 2439. *Westlaw* [online]. Available at: <https://login.westlaw.co.uk/maf/wluk/app/document?&srguid=i0ad832f10000016abfeb4727d074e4e8&docguid=IA60AF29033D911E08E6E960452C500D3&hitguid=IA60AF29033D911E08E6E960452C500D3&rank=18&spos=18&epos=18&td=51&crumb-action=append&context=33&resolvein=true> [Accessed 16 May 2019]

Raymond, J., van Oorschot, R., Gunn, P., Walsh, S. and Roux, C. (2009). Trace evidence characteristics of DNA: A preliminary investigation of the persistence of DNA at crime scenes. *Forensic Science International: Genetics*, [online] 4, pp. 26-33.

Revolugen, 2020. Fire monkey high molecular weight DNA (HMW-DNA) extraction kit. Revolugen [online]. Available at: <https://revolugen.co.uk/fire-monkey/> [Accessed 25/10/2020]

Roeder, A., Elsmore, P., Greenhalgh, M. and McDonald, A. (2009). Maximizing DNA profiling success from sub-optimal quantities of DNA: A staged approach. *Forensic Science International*, [online] 3(2), pp. 128-137.

Roewer, L. (2013). DNA fingerprinting in forensics: past, present future. *Investigative Genetics*, [online] 4(22), pp. 1-10.

Rohland, N. and Hofreiter, M. (2007). Ancient DNA extraction from bones and teeth. *Nature Protocols*, [online] 2(7), pp. 1756-1762.

Rohland, N., Glocke, I., Aximu-petri, A. and Meyer, M. (2007). Extraction of highly degraded DNA from ancient bones, teeth and sediments for high-throughput sequencing. *Nature Protocols*, [online] 2, pp. 1756-1762.

Romano, C., Mangiaracina, R., Donato, L., D'Angelo, R., Scimone, C. and Sidoti, A. (2019). Aged fingerprints for DNA profile: First report of successful typing. *Forensic Science International*, [online] 302, 109905.

Roy, A., Halder, B. and Garain, U. (2010). Authentication of currency notes through printing technique verification. *Proceedings of the Seventh Indian Conference on Computer Vision, Graphics and Image Processing*, [online], pp. 383-390.

Ruan, T., Barash, M., Gunn, P. and Bruce, D. (2017). Investigation of DNA transfer onto clothing during regular daily activities. *International Journal of Legal Medicine*, [online] 132, pp. 1035-1042.

Ruprecht, R., Suter, R., Manganelli, M., Wehrli, A., Ender, M. and Jung, B. (2021). Collection of evidence from the reverse side of self-adhesive stamps: A combined approach to obtain dactyloscopic and DNA evidence. *Forensic Science International*, [online] 330, pp. 1-9.

Samsuwan, J., Somboonchokepisal, T., Akaraputtiporn, T., Srimuang, T., Phuengsukdaeng, P., Suwannarat, A., Mutirangura, A. and Kitkumthorn, N. (2018).

A method for extracting DNA from hard tissues for use in forensic identification. *Biomedical Reports*, [online] 9, pp. 433-438.

Schelte, K., Hewitt, C., Manley, T., Reed, A., Baniasad, M., Albright, N., Powals, M., LeSassier, D., Smith, A., Zhang, L., Allen, L., Ludolph, B., Weber, K., Woerner, A., Freitas, M. and Gardner, M. (2021). Fractionation of DNA and protein from individual latent fingerprints for forensic analysis. *Forensic Science International: Genetics*, [online] 50, 102405.

Scherer, S. (2016). (2012) Italian police seize millions in fake euros, including new 20-euro bills. *Reuters*, [online]. Available at: <https://uk.reuters.com/article/uk-italy-crime-counterfeit-euros/italian-police-seize-millions-in-fake-euros-including-new-20-euro-bills-idUKKCN1001GB> [Accessed 15 May 2019]

Schiebelhut, L., Abboud, S., Daglio, L., Swift, H. and Dawson, M. (2017). A comparison of DNA extraction methods for high-throughput DNA analyses. *Molecular Ecology Resources*, 17, pp. 721-729.

Schiffner, L.A., Bajda, E.J., Prinz, M., Sebestyén, J., Shaler, R. and Caragine, T.A. Optimization of a simple, automatable extraction method to recover sufficient DNA from low copy number DNA samples for generation of short tandem repeat profiles. *Croatian Medical journal*, [online] 46(4), pp. 578-586.

Semikhodskii, A. (2021). Logical errors and fallacies in DNA evidence interpretation. In: Dash, H., Shrivastava, P. Lorente, J. (eds) *Handbook of DNA Profiling*. Springer, Singapore.

Sessa, F., Salerno, M., Bertozzi, G., Messina, G., Ricci, P., Ledda, C., Rapisarda, V., Cantatore, S., Turillazzi, E. and Pomara, C. (2019). Touch DNA: Impact of handling time on touch deposit and evaluation of different recovery techniques: An experimental study. *Scientific Reports*, 9 (9542), pp. 1-9.

Sethi, V., Panacek, E.A., Green, W.M., Ng, J. and Kanthaswamy, S. (2013). Yield of male touch DNA from fabrics in an assault model. *Journal of Forensic Research*, pp. 1-4.

Shaw, K.J., Thain, L., Docker, P.T., Dyer, C.E., Greenman, J., Greenway, G.M. and Haswell, S.J. (2009). The use of carrier RNA to enhance DNA extraction from microfluidic-based silica monoliths. *Analytica Chimica Acta*, 652, pp. 231-233.

Shewale, J., Schneida, E., Wilson, J., Walker, J., Batzer, M. Sinha, S. (2007). Human genomic DNA quantitation system, h-quant: development and validation for use in forensic casework. *Journal of Forensics Sciences*, [online] 52(2), pp. 364-370.

Sidstedt, M., Jansson, L., Nilsson, E., Noppa, L., Forsman, M., Rådström, P. and Hedman, J. (2015). Humic substances cause fluorescence inhibition in real-time polymerase chain reaction. *Analytical Biochemistry*, 487, 30-37.

Sigma Aldrich (2019). Phenol:Chloroform:Isoamyl Alcohol 25:24:1 Saturated with 10 mM Tris, pH 8.0, 1 mM EDTA. [online] Merck. Available at: https://www.sigmaaldrich.com/GB/en/product/sigma/p2069?gclid=CjwKCAjwh-CVBhB8EiwAjFEPGY_4N40M6i3kcxtxuE2seX8IZdYscFOXiWoVht2OdJOhyrD5ZzZ4HBoCvcAQAvD_BwE [Accessed 15 May 2019]

Singh, U., Kumari, M. and Iyengar, S. (2018). Method for improving the quality of genomic DNA obtained from minute quantities of tissue and blood samples using Chelex 100 resin. *Biological Procedures Online*, [online] 20(12), pp. 1-8.

Siriboonpiputtana, T., Rinthachai, T., Shotivaranon, J., Peonim, V. and Rekamnuaychoke, B. (2018). Forensic genetic analysis of bone remain samples. *Forensic Science International*, [online] 284, pp. 167-175.

Sobiah, R., Syeda, R., Zunaira, E., Nageen, Z., Maria, K., Syeda, A., Shahana, S., Akifa, M., Abdul J. and Muhammad, R. (2018). Implications of targeted next generation sequencing in forensic science. *Journal of Forensic Research*, [online] 9(1), pp. 1-8.

Soukup, D., Bodenhofer, U., Mittendorfer-Holzer, M. and Mayer, K., (2009). Semi-automatic identification of print layers from a sequence of sample images: A case study from banknote print inspection. *Image and Vision Computing*, [online] 27, pp. 989-998.

- Staub, R. and Tompkin, W. (2000). Self-refencing diffractive features of OVDs. *Proceedings of SPIE*, [online] 3973, pp. 216-223.
- Steadman, S., Hofer, S., Geering, S., King, S. and Bennett, M. (2015). Recovery of DNA from latent fingerprint tape lifts archived against matte acetate. *Journal of Forensic Sciences*, [online] 60(3), pp. 777-782.
- Stern, H. (2017). Statistical issues in forensic science. *Reviews in Advance*, [online] 4(11), pp. 1-11.
- Studel, F., Johnson, J., Johnson, C. and Schweizer, S. (2018). Characterization of luminescent materials with ¹⁵¹Eu Mössbauer spectroscopy. *Materials*, [online] 11(828), pp. 1-27.
- Stoop, B., Defaux, P., Utz, S. and Zieger, M. (2017). Touch DNA sampling with SceneSafe Fast™ minitapes. *Legal Medicine*, [online] 29, pp. 89-71.
- Subhani, Z., Daniel, B. and Frascione, N. (2019). DNA profiles from fingerprint lifts-enhancing the evidential value of fingermarks through successful DNA typing. *Journal of Forensic Sciences*, [online] 64(1), pp. 201-206.
- Sullivan, G. and Feinn, R. (2012). Using effect size or why the P value is not enough. *Journal of Graduate Medical Education*, [online] 4(3), pp. 279-282.
- Sun, G., McGarvey, S., Bayoumi, R., Mulligan, C., Barrantes, R., Raskin, S., Zhong, Y., Akey, J., Chakraborty, R. and Deka, R. (2003). Global genetic variation at nine short tandem repeat loci and implications on forensic genetics. *Journal of Human Genetics*, [online] 11, pp. 39-49.
- Suyver, J. and Meijerink, A. (2002). Europium safeguards the euro. *Chemisch2Weekblad*, [online] 98(4), pp. 12-13.
- Swango, K., Hudlow, W., Timken, M. and Buoncristiani, M. (2007). Developmental validation of a multiplex qPCR assay for assessing the quantity and quality of nuclear DNA in forensic samples. *Forensic Science International*, [online] 170, pp. 35-45.

Szkuta, B., Ballantyne, K., Kokshoorn, B. and van Oorschot, R. (2018). Transfer and persistence of non-self DNA on hands over time: Using empirical data to evaluate DNA evidence given activity level propositions. *Forensic Science International: Genetics*, [online] 33, pp. 84-97.

Tajadini, M., Panjehpour, M. and Javanmard, S.H. (2014). Comparison of SYBR Green and Taqman methods in quantitative real-time polymerase chain reaction analysis of four adenosine receptor subtypes. *Advanced Biomedical Research*, [online] 3, 85, pp. 1-12.

Takola, J., Timonen, J., Sampo, J., Rantala, M., Siltanen, S. and Lassas, M. (2015). Using properties of underlying paper structure for distinguishing counterfeits from genuine banknotes. *Research Gate*, [online], pp. 1-13.

Tamulevičius, T., Tamulevičius, S., Andrulevičius, M., Guobiene, A., Puodžiukynas, L., Janušas, G. and Griškoniš, E. (2007). Formation of OVD using laser interference lithography. *Materials Science*, [online] 13(3), pp. 183-187.

Tamulevičius, T., Juodėnas, M., Klinavičius, T., Paulauskas, A., Jankauskas, K., Ostreika, A., Žutautas, A. and Tamulevičius, S. (2018). Dot-matrix hologram rendering algorithm and its validation through direct laser interference patterning. *Scientific Reports*, [online] 8(14245), pp. 1-11.

Tam, S.C. and Yiap, B.C. (2009). DNA, RNA, and protein extraction: The past and the present. *Journal of Biomedicine and Biotechnology*, [online] 2009, 1-10.

Templeton, J., Brotherton, P., Llamas, B., Soubrier, J., Haak, W., Cooper, A. and Austin, J. (2013). DNA capture and next-generation sequencing can recover whole mitochondrial genomes from highly degraded samples for human identification. *Investigative Genetics*, [online] 4(26), pp. 1-13.

Templeton, J., Ottens, R., Paradiso, V., Handt, O., Taylor, D. and Linacre, A. (2013). Genetic profiling from challenging samples: Direct PCR of touch DNA. *Forensic Science International: Genetics Supplement Series*, [online] 4, pp. e224-e225.

Templeton, J. and Linacre, A. (2014). DNA profiles from fingerprints. *BioTechniques*, [online] 57, pp. 259-266.

Templeton, J., Taylor, D., Handt, O., Skuza, P. and Linacre, A. (2015). Direct PCR improves the recovery of DNA from various. *Journal of Forensic Sciences*, [online] 60(6), pp. 1558-1562.

Templeton, J., Taylor, D., Handt, O. and Linacre, A. (2016). Typing DNA profiles from previously enhanced fingerprints using direct PCR. *Forensic Science International: Genetics*, [online] 29, pp. 276-282.

Thanakiatkrai, P., Phetpeng, S., Sothibandhu, S., Asawutmangkul, W., Piwpankaew, Y., Foong, J., Koo, J. and Kitpipit, T. (2017). Performance comparison of MiSeq forensic genomics system and STR-CE using control and mock IED samples. *Forensic Science International: Genetics Supplement Series*, [online] 6, pp. e320-e321.

The Bureau of Engraving and Printing (2023). The buck starts here: How money is made. *The Bureau of Engraving and Printing* [online]. Available at: <https://www.bep.gov/currency/how-money-is-made> [Accessed 6 February 2023]

Thelwell, N., Millington, S., Solinas, A., Booth, J. and Brown, T. (2000). Mode of action and application of scorpion primers to mutation detection. *Nucleic Acid Research*, [online] 28(19), pp. 3752-3761.

Thermo Fisher Scientific (2020). DNA Quantification Kits. *Thermo Fisher Scientific* [online]. Available at: <https://www.thermofisher.com/uk/en/home/industrial/forensics/human-identification/forensic-dna-analysis/dna-quantification-solutions/dna-quantification-kits.html> [Accessed 25 September 2020]

Thermo Fisher Scientific (2021). AmpFLSTR™ NGM SElect™ PCR Amplification Kit. *Thermo Fisher Scientific* [online]. Available at: <https://www.thermofisher.com/order/catalog/product/4457889>

Thermo Fisher Scientific (2022a). StepOnePlus™ Real-Time PCR System. *Thermo Fisher Scientific* [online]. Available at:

<https://www.thermofisher.com/order/catalog/product/4376600> [Accessed 23 March 2022]

Thermo Fisher Scientific (2022b). PrepFiler™ BTA Forensic DNA Extraction Kit. *Thermo Fisher Scientific* [online]. Available at: <https://www.thermofisher.com/order/catalog/product/4463352> [Accessed 23 March 2022]

Thermo Fisher Scientific (2022c). 3500 Genetic Analyzer for Fragment Analysis. *Thermo Fisher Scientific* [online]. Available at: <https://www.thermofisher.com/order/catalog/product/A30468>

Thomas, J., Berlin, R., Barker, J. and Cruz, T. (2013). Qiagen's investigator™ quantiplex kit as a predictor of STR amplification success from low-yield DNA samples. *Journal of Forensic Sciences*, [online] 58(5), pp. 1306-1309.

Thomasma, S. and Foran, D. (2012). The influence of swabbing solutions on DNA recovery from touch samples. *Journal of Forensic Sciences*, [online] 58(2), pp. 465-469.

Thomson, W., Taroni, F. and Aitken, C. (2003). How the probability of a false positive affects the value of DNA evidence. *Journal of Forensic Science*, [online] 48(1), pp. 1-19.

Thompson, W., Grady, R., Lai, E. and Stern, H. (2018). Perceived strength of forensic scientists' reporting statements about source conclusions. *Law, Probability and Risk*, [online] 17(2), pp. 133-155.

Tobe, S., Watson, N. and Daéid, N. (2007). Evaluation of six presumptive tests for blood, their specificity, sensitivity, and effect on high molecular-weight DNA. *Journal of Forensic Science*, [online] 52(1), pp. 102-109.

Toom, V. (2018) Cross-border exchange and comparison of forensic DNA data in the context of the Prüm Decision. *Policy Department of Citizens' Rights and Constitutional Affairs*, [online], pp. 1-62.

- Valasek, M. and Repa, J. (2005). The power of real-time PCR. *Advances in Physiology Education*, [online] 29, pp. 151-159.
- Vandewoestyne, M., Hoofstat, D., Fransson, A., Nieuwerburgh, F. and Deforce, D., *Forensic Science International: Genetics*, [online] 7, pp. 316-320.
- van den Berge, M., Ozcanhan, G., Zijlstra, S., Lindenbergh, A. and Sijen, T. (2016). Prevalence of human cell material: DNA and RNA profiling of public and private objects and after activity scenarios. *Forensic Science International: Genetics*, [online] 21, pp. 81-89.
- van der Gaag, K. and de Knijff, P. (2015). Forensic nomenclature for short tandem repeats updated for sequencing. *Forensic Science International: Genetics Supplement Series*, [online] 5, pp. e542-544.
- van der Horst, F., Eschelbach, M., Sieber, S., Miederna, S. (2016). Does banknote quality affect counterfeit detection? Experimental evidence from Germany and the Netherlands. *DNB Working Papers*, [online] 499, pp. 1-53.
- Van Nieuwerburgh, F., Goetghebeur, E., Vandewoestyne, M. and Deforce, D. (2009). *Bioinformatics* [online], 25 (2), pp. 225-229.
- van Oorschot, R. and Jones, M. (1997). DNA fingerprints from fingerprints. *Nature*, [online] 387(767), pp. 767.
- van Oorschot, R., Phelan, D., Furlong, S., Scarfo, G., Holding, N. and Cummins, M. (2003). *International Congress Series*, [online] 1239, pp. 803-807.
- van Oorschot, R., Ballantyne, K. and Mitchell, R. (2010). Forensic trace DNA: a review. *Investigative Genetics*, [online] 1(14), pp. 1-17.
- van Renesse, R. (1998). Verifying versus falsifying banknotes. *Proceedings of SPIE*, [online] 3314, pp. 71-85.
- Verikas, A., Lundström, J., Bacauskiene, M. and Gelzinis, A. (2011). Advances in computational intelligence-based print quality assessment and control in offset colour printing. *Expert Systems with Applications*, [online] 38, pp. 13441-13447.

- Vernarecci, S., Ottaviani, E., Agostino, A., Mei, E., Calandro, L. and Montagna, P. (2015). Quantifiler® Trio kit and forensic samples management: A matter of degradation. *Forensic Science International: Genetics*, [online] 16, pp. 77-85.
- Voinea, D., Lăpăduși, V. and Dobreanu, R. (2015). Some methods of falsification and counterfeiting of banknotes. *Forensic Science*, [online] 4(100), pp. 1996-1998.
- Vraneš, M., Scherer, M. and Elliott, K. (2017). Development and validation of the investigator® quantiplex pro kit for qPCR-based examination of the quantity and quality of human DNA in forensic samples. *Forensic Science International: Genetics Supplement Series*, [online] 6, pp. e516-e519.
- Walsh, P., Metzger, D. and Higuchi, R. (1991). Chelex 100 as a medium for simple extraction of DNA for PCR-based typing from forensic material. *Biotechniques*, [online] 10(4), pp. 506-513.
- Wang, Z., Zhou, D., Wang, H., Jia, Z., Liu, J., Qian, X., Li, C. and Hou, Y. (2017). Massively parallel sequencing of 32 forensic markers using the precision ID globalfiler™ NGS STR panel and the ion PGM™ system. *Forensic Science International: Genetics*, [online] 31, pp. 126-134.
- Westen, A., Nagel, J., Benschop, C., Weiler, N., Jong, B. and Sijen, T. (2009). Higher capillary electrophoresis injection settings as an efficient approach to increase the sensitivity of STR typing. *Journal of Forensic Sciences*, 54(3), pp. 591-598.
- Whitcombe, D., Theaker, J., Guy, S., Brown, T. and Little, S. (1999). Detection of PCR products using self-probing amplicons and fluorescence. *Nature Biotechnology*, 17, pp. 804-807.
- Xavier, C. and Parson, W. (2017). Evaluation of the Illumina ForenSeq™ DNA signature Prep kit- MPS forensic application for the MiSeq FGx™ benchtop sequencer. *Forensic Science International: Genetics*, [online] 28, pp. 188-194.
- Xavier, C., Eduardoff, M., Strobl, C. and Parson, W. (2019). SD quants- Sensitive detection tetraplex-system for nuclear and mitochondrial DNA quantification and degradation inference. *Forensic Science International: Genetics*, 42, pp. 39-44.

Xu, Q., Wang, Z., Kong, Q., Wang, X., Huang, A., Li, C. and Liu, X. (2022). Evaluating the effects of whole genome amplification strategies for amplifying trace DNA using capillary electrophoresis and massive parallel sequencing. *Forensic Science International Genetics*, [online] 56, 102599.

Yu, Y., Lee, C., Kim, J. and Hwang, S. (2005). Group-specific primer and probe sets to detect methanogenic communities using quantitative real-time polymerase chain reaction. *Biotechnology and Bioengineering*, 89(6), pp. 670-679.

Zapico, S., Crucet, K., Antevska, A., Fernandez-Paradas, R., Burns, C., DeGaglia, C. and Ubelaker, D. (2021). From your eyes only: Efficiency of nuclear and mitochondrial DNA isolation from contact lenses at crime scenes. *Electrophoresis*, [online] 42, 122-125.

Zech, W., Malik, N. and Thali, M. (2012). Applicability of DNA analysis on adhesive tape in forensic casework. *Journal of Forensic Sciences*, [online] 57(4), pp. 1036-1041.

Zoppis, S., Muciaccia, B., D'Alessio, A., Ziparo, E., Vecchiotti, C. and Filippini, A. (2014). DNA fingerprinting secondary transfer from different skin areas: Morphological and genetic studies. *Forensic Science International: Genetics*, 11, pp. 137-143.

Appendix

Appendix 1. shows the data for the DNA concentration of the counterfeit hologram samples extracted using Chelex and phenol chloroform extractions and quantified using the loci TH01 and SE33.

Planted DNA (pg/ μ L)	Chelex Extraction: TH01 (pg/ μ L)	Chelex Extraction: SE33 (pg/ μ L)	Phenol Chloroform Extraction: TH01 (pg/ μ L)	Phenol Chloroform Extraction: SE33 (pg/ μ L)
0.074	1.262	5.383	1.139	8.844
0.074	0.081	51.822	0.000	3.014
0.074	0.275	5.016	0.205	16.477
0.148	9.356	2.914	0.036	1.328
0.148	6.253	3.689	0.480	1.340
0.148	4.430	3.742	0.850	1.356
0.295	0.019	1.497	0.059	0.724
0.295	0.273	1.327	0.019	0.611
0.295	19.805	1.457	0.082	0.633
0.590	0.074	0.919	0.033	0.582
0.590	0.005	0.715	0.078	0.327
0.590	0.054	0.766	0.027	0.351
1.180	0.003	0.462	0.066	0.203
1.180	2.193	0.387	0.033	0.152
1.180	0.001	0.439	0.019	0.198

Appendix 2. shows the raw quantification data for the swabs from a counterfeit hologram taken from a counterfeit hologram that have been extracted using Chelex resin. A1-A3 in the sample name presents the triplicate set for each sample of the primary swab. B1-B3 in the sample name represents the triplicate set for each sample of the secondary swab. All samples were quantified using the Quantifiler Duo Quantification kit at half the recommended reaction volume (12.5 µL). IPC corresponds to the internal positive control, SRY is the male chromosomal marker and RPP (RPPH1) is the human autosomal marker.

Extraction	Sample/Marker	Ct	Ct mean	Ct SD	Quantity
Chelex Extraction	41A1 IPC	30.24	30.02662	0.193086	0.333109
	41A1 RPP	Undetermined		NaN	
	41A1 SRY	Undetermined	31.02344	0.319762	
	41A2 IPC	29.977	30.02662	0.193086	1.384477
	41A2 RPP	Undetermined		NaN	
	41A2 SRY	31.25	31.02344	0.319762	0.009125
	41A3 IPC	29.863	30.02662	0.193086	2.580989
	41A3 RPP	Undetermined		NaN	
	41A3 SRY	30.797	31.02344	0.319762	0.01322
	41B1 IPC	29.713	29.68099	0.077156	5.825882
	41B1 RPP	Undetermined		NaN	
	41B1 SRY	30.325	30.19045	0.43107	0.019472
	41B2 IPC	29.737	29.68099	0.077156	5.118053
	41B2 RPP	Undetermined		NaN	
	41B2 SRY	30.538	30.19045	0.43107	0.016348
	41B3 IPC	29.593	29.68099	0.077156	11.19255
	41B3 RPP	Undetermined		NaN	
	41B3 SRY	29.708	30.19045	0.43107	0.032286
	44A1 IPC	29.574	29.62265	0.056562	12.39829
	44A1 RPP	Undetermined		NaN	
	44A1 SRY	Undetermined	29.47261	0.266492	
	44A2 IPC	29.685	29.62265	0.056562	6.795093
	44A2 RPP	Undetermined		NaN	
	44A2 SRY	29.661	29.47261	0.266492	0.033558
	44A3 IPC	29.609	29.62265	0.056562	10.25818
	44A3 RPP	Undetermined		NaN	
	44A3 SRY	29.284	29.47261	0.266492	0.045707
	44B1 IPC	29.561	29.80254	0.21563	13.32478
	44B1 RPP	Undetermined		NaN	
	44B1 SRY	29.34	30.48994	1.017329	0.043664
	44B2 IPC	29.871	29.80254	0.21563	2.464104
	44B2 RPP	Undetermined		NaN	
	44B2 SRY	31.273	30.48994	1.017329	0.008954
	44B3 IPC	29.975	29.80254	0.21563	1.400473
	44B3 RPP	Undetermined		NaN	
	44B3 SRY	30.857	30.48994	1.017329	0.012585

Appendix 3. shows the raw data for the swabs from a counterfeit hologram taken from a counterfeit hologram that have been extracted using silica spin columns. A1-A3 in the sample name presents the triplicate set for each sample of the primary swab. B1-B3 in the sample name represents the triplicate set for each sample of the secondary swab. All samples were quantified using the Quantifiler Duo Quantification kit at half the recommended reaction volume (12.5 µL). IPC corresponds to the internal positive control, SRY is the male chromosomal marker and RPP (RPPH1) is the human autosomal marker.

Extraction	Sample/Marker	Ct	Ct mean	Ct SD	Quantity
Silica Spin Column	070A1 IPC	29.745	29.79224	0.045618	4.892102
	070A1 RPP	Undetermined		NaN	
	070A1 SRY	30.689	30.57464	0.149601	0.01445
	070A2 IPC	29.795	29.79224	0.045618	3.72919
	070A2 RPP	Undetermined		NaN	
	070A2 SRY	30.63	30.57464	0.149601	0.015165
	070A3 IPC	29.836	29.79224	0.045618	2.981576
	070A3 RPP	Undetermined		NaN	
	070A3 SRY	30.405	30.57464	0.149601	0.018231
	070B1 IPC	29.74	29.76405	0.082849	5.033174
	070B1 RPP	Undetermined		NaN	
	070B1 SRY	30.615	30.33816	0.408278	0.015347
	070B2 IPC	29.696	29.76405	0.082849	6.39693
	070B2 RPP	Undetermined		NaN	
	070B2 SRY	30.53	30.33816	0.408278	0.016461
	070B3 IPC	29.856	29.76405	0.082849	2.675285
	070B3 RPP	Undetermined		NaN	
	070B3 SRY	29.869	30.33816	0.408278	0.028291
	640A1 IPC	29.744	29.65075	0.081487	4.91177
	640A1 RPP	Undetermined		NaN	
	640A1 SRY	33.372	31.32764	1.850955	0.001601
	640A2 IPC	29.597	29.65075	0.081487	10.95762
	640A2 RPP	Undetermined		NaN	
	640A2 SRY	29.766	31.32764	1.850955	0.030785
	640A3 IPC	29.611	29.65075	0.081487	10.15511
	640A3 RPP	Undetermined		NaN	
	640A3 SRY	30.844	31.32764	1.850955	0.012719
	640B1 IPC	29.589	29.6945	0.092947	11.41758
	640B1 RPP	Undetermined		NaN	
	640B1 SRY	29.757	29.73641	0.02951	0.031012
	640B2 IPC	29.729	29.6945	0.092947	5.354219
	640B2 RPP	Undetermined		NaN	
	640B2 SRY	Undetermined	29.73641	0.02951	
	640B3 IPC	29.766	29.6945	0.092947	4.380317
	640B3 RPP	Undetermined		NaN	
	640B3 SRY	29.716	29.73641	0.02951	0.032092

Appendix 4. shows the raw data for the swabs from a counterfeit hologram taken from a counterfeit hologram that have been extracted using magnetic bead extraction. A1-A3 in the sample name presents the triplicate set for each sample of the primary swab. B1-B3 in the sample name represents the triplicate set for each sample of the secondary swab. All samples were quantified using the Quantifiler Duo Quantification kit at half the recommended reaction volume (12.5 µL). IPC corresponds to the internal positive control, SRY is the male chromosomal marker and RPP (RPPH1) is the human autosomal marker.

Extraction	Sample/Marker	Marker	Ct	Ct mean	Ct SD	Quantity
Magnetic Bead Extraction	555A1 IPC	IPC	29.787	29.75986	0.084382	3.89351
	555A1 RPP	RPP	Undetermined		NaN	
	555A1 SRY	SRY	30.981	30.56892	0.582437	0.011374
	555A2 IPC	IPC	29.665	29.75986	0.084382	7.558781
	555A2 RPP	RPP	Undetermined		NaN	
	555A2 SRY	SRY	Undetermined	30.56892	0.582437	
	555A3 IPC	IPC	29.827	29.75986	0.084382	3.133971
	555A3 RPP	RPP	Undetermined		NaN	
	555A3 SRY	SRY	30.157	30.56892	0.582437	0.022345
	555B1 IPC	IPC	29.502	29.62308	0.108441	18.31712
	555B1 RPP	RPP	Undetermined		NaN	
	555B1 SRY	SRY	30.822	30.12668	0.983223	0.012956
	555B2 IPC	IPC	29.712	29.62308	0.108441	5.853429
	555B2 RPP	RPP	Undetermined		NaN	
	555B2 SRY	SRY	Undetermined	30.12668	0.983223	
	555B3 IPC	IPC	29.655	29.62308	0.108441	8.004076
	555B3 RPP	RPP	Undetermined		NaN	
	555B3 SRY	SRY	29.431	30.12668	0.983223	0.040509
	951A1 IPC	IPC	29.7	29.70025	0.034105	6.254617
	951A1 RPP	RPP	Undetermined		NaN	
	951A1 SRY	SRY	Undetermined	29.11102	NaN	
	951A2 IPC	IPC	29.734	29.70025	0.034105	5.186696
	951A2 RPP	RPP	Undetermined		NaN	
	951A2 SRY	SRY	29.111	29.11102	NaN	0.052678
	951A3 IPC	IPC	29.666	29.70025	0.034105	7.51471
	951A3 RPP	RPP	Undetermined		NaN	
	951A3 SRY	SRY	Undetermined	29.11102	NaN	
	951B1 IPC	IPC	29.581	29.50894	0.095998	11.94121
	951B1 RPP	RPP	Undetermined		NaN	
	951B1 SRY	SRY	29.703	29.743	0.361498	0.032427
	951B2 IPC	IPC	29.4	29.50894	0.095998	31.95478
	951B2 RPP	RPP	Undetermined		NaN	
	951B2 SRY	SRY	29.403	29.743	0.361498	0.041456
951B3 IPC	IPC	29.546	29.50894	0.095998	14.466	
951B3 RPP	RPP	Undetermined		NaN		
951B3 SRY	SRY	30.123	29.743	0.361498	0.02298	

Appendix 5. shows the raw data for the swabs from a counterfeit hologram taken from a counterfeit hologram that have been extracted using Chelex extraction. A1-A3 in the sample name presents the triplicate set for each sample of the primary swab. B1-B3 in the sample name represents the triplicate set for each sample of the secondary swab. All samples were quantified using the Quantifiler Duo Quantification kit at the recommended reaction volume (25 µL). IPC corresponds to the internal positive control, SRY is the male chromosomal marker and RPP (RPPH1) is the human autosomal marker.

Extraction	Sample/Marker	Ct	Ct mean	Ct SD	Quantity
Chelex Extraction	41A1 IPC	29.881	29.90075	0.02618525	
	41A1 RRP	Undetermined			
	41A1 SRY	Undetermined			
	41A2 IPC	29.93	29.90075	0.02618525	1.96E+36
	41A2 RRP	Undetermined			
	41A2 SRY	Undetermined			
	41A3 IPC	29.891	29.90075	0.02618525	
	41A3 RRP	Undetermined			
	41A3 SRY	Undetermined			
	41B1 IPC	29.771	29.788458	0.10288848	
	41B1 RRP	Undetermined			
	41B1 SRY	Undetermined			
	41B2 IPC	29.695	29.788458	0.10288848	
	41B2 RRP	Undetermined			
	41B2 SRY	Undetermined			
	41B3 IPC	29.899	29.788458	0.10288848	
	41B3 RRP	Undetermined			
	41B3 SRY	Undetermined			
	44A1 IPC	29.802	29.786125	0.10783566	
	44A1 RRP	Undetermined			
	44A1 SRY	33.11	31.588673	2.1517093	0.0040488
	44A2 IPC	29.885	29.786125	0.10783566	
	44A2 RRP	Undetermined			
	44A2 SRY	Undetermined	31.588673	2.1517093	
	44A3 IPC	29.671	29.786125	0.10783566	
	44A3 RRP	Undetermined			
	44A3 SRY	30.067	31.588673	2.1517093	0.0447653
	44B1 IPC	29.775	29.879374	0.09079018	
	44B1 RRP	Undetermined			
	44B1 SRY	30.323	30.907238	0.82694006	0.0365913
	44B2 IPC	29.927	29.879374	0.09079018	4.01E+36
	44B2 RRP	Undetermined			
44B2 SRY	Undetermined	30.907238	0.82694006		
44B3 IPC	29.937	29.879374	0.09079018	5.60E+35	
44B3 RRP	Undetermined				
44B3 SRY	31.492	30.907238	0.82694006	0.0145311	

Appendix 6. shows the raw data for the swabs from a counterfeit hologram taken from a counterfeit hologram that have been extracted using silica spin columns. A1-A3 in the sample name presents the triplicate set for each sample of the primary swab. B1-B3 in the sample name represents the triplicate set for each sample of the secondary swab. All samples were quantified using the Quantifiler Duo Quantification kit at the recommended reaction volume (25 µL). IPC corresponds to the internal positive control, SRY is the male chromosomal marker and RPP (RPPH1) is the human autosomal marker.

Extraction	Sample/Marker	Ct	Ct mean	Ct SD	Quantity
Silica Spin Column	070A1 IPC	29.873	29.897654	0.03074235	
	070A1 RRP	Undetermined			
	070A1 SRY	Undetermined			
	070A2 IPC	29.932	29.897654	0.03074235	1.35E+36
	070A2 RRP	Undetermined			
	070A2 SRY	Undetermined			
	070A3 IPC	29.887	29.897654	0.03074235	
	070A3 RRP	Undetermined			
	070A3 SRY	Undetermined			
	070B1 IPC	29.79	29.794167	0.00843498	
	070B1 RRP	Undetermined			
	070B1 SRY	Undetermined	32.201286		
	070B2 IPC	29.788	29.794167	0.00843498	
	070B2 RRP	Undetermined			
	070B2 SRY	32.201	32.201286		0.0082991
	070B3 IPC	29.804	29.794167	0.00843498	
	070B3 RRP	Undetermined			
	070B3 SRY	Undetermined	32.201286		
	640A1 IPC	29.994	29.88182	0.09711216	8.82E+30
	640A1 RRP	Undetermined			
	640A1 SRY	Undetermined	30.436556	0.25999683	
	640A2 IPC	29.825	29.88182	0.09711216	
	640A2 RRP	Undetermined			
	640A2 SRY	30.253	30.436556	0.25999683	0.0386646
	640A3 IPC	29.827	29.88182	0.09711216	
	640A3 RRP	Undetermined			
	640A3 SRY	30.62	30.436556	0.25999683	0.0289208
	640B1 IPC	29.743	29.817465	0.07934871	
	640B1 RRP	Undetermined			
	640B1 SRY	30.169	30.393597	0.31832403	0.041323
	640B2 IPC	29.808	29.817465	0.07934871	
	640B2 RRP	Undetermined			
	640B2 SRY	Undetermined	30.393597	0.31832403	
	640B3 IPC	29.901	29.817465	0.07934871	
	640B3 RRP	Undetermined			
	640B3 SRY	30.619	30.393597	0.31832403	0.0289601

Appendix 7. shows the raw data for the swabs from a counterfeit hologram taken from a counterfeit hologram that have been extracted using magnetic bead extraction. A1-A3 in the sample name presents the triplicate set for each sample of the primary swab. B1-B3 in the sample name represents the triplicate set for each sample of the secondary swab. All samples were quantified using the Quantifiler Duo Quantification kit at the recommended reaction volume (25 µL). IPC corresponds to the internal positive control, SRY is the male chromosomal marker and RPP (RPPH1) is the human autosomal marker.

Extraction	Sample/Marker	Ct	Ct mean	Ct SD	Quantity
Magnetic Bead Extraction	555A1 IPC	29.851	29.831017	0.04394183	
	555A1 RRP	Undetermined			
	555A1 SRY	Undetermined			
	555A2 IPC	29.862	29.831017	0.04394183	
	555A2 RRP	Undetermined			
	555A2 SRY	Undetermined			
	555A3 IPC	29.781	29.831017	0.04394183	
	555A3 RRP	Undetermined			
	555A3 SRY	Undetermined			
	555B1 IPC	29.924	29.807808	0.10388439	6.40E+36
	555B1 RRP	Undetermined			
	555B1 SRY	Undetermined			
	555B2 IPC	29.724	29.807808	0.10388439	
	555B2 RRP	Undetermined			
	555B2 SRY	Undetermined			
	555B3 IPC	29.775	29.807808	0.10388439	
	555B3 RRP	Undetermined			
	555B3 SRY	Undetermined			
	951A1 IPC	29.972	29.76564	0.18023679	6.75E+32
	951A1 RRP	Undetermined			
	951A1 SRY	Undetermined	30.127563	0.0864678	
	951A2 IPC	29.689	29.76564	0.18023679	
	951A2 RRP	Undetermined			
	951A2 SRY	30.189	30.127563	0.0864678	0.0406691
	951A3 IPC	29.636	29.76564	0.18023679	
	951A3 RRP	Undetermined			
	951A3 SRY	30.066	30.127563	0.0864678	0.0447923
	951B1 IPC	29.689	29.642378	0.05630757	
	951B1 RRP	Undetermined			
	951B1 SRY	30.163	30.741497	0.8175369	0.0414896
	951B2 IPC	29.58	29.642378	0.05630757	
	951B2 RRP	Undetermined			
951B2 SRY	Undetermined	30.741497	0.8175369		
951B3 IPC	29.658	29.642378	0.05630757		
951B3 RRP	Undetermined				
951B3 SRY	31.32	30.741497	0.8175369	0.0166502	

Appendix 8. The mean DNA concentration data (using the RPPH1 human autosomal marker) of swabs taken from counterfeit holograms prepared by volunteers to produce composite banknotes and extracted according to the three extraction techniques: Chelex resin extraction, phenol chloroform extraction and BTA Prepfiler kit.

Volunteer	Sample no.	Location	Phenol	BTA	Chelex
A	1	External	0.00	1.99	0.12
A	1	Internal	0.00	1.32	0.00
A	2	External	0.00	1.32	1.60
A	2	Internal	0.00	0.00	1.06
A	3	External	2.28	0.00	0.89
A	3	Internal	0.00	0.00	2.68
A	4	External	5.13	0.00	1.84
A	4	Internal	0.00	2.38	1.13
A	5	External	0.00	8.77	0.00
A	5	Internal	0.00	1.34	0.00
A	6	External	0.00	1.34	1.91
A	6	Internal	0.00	0.00	0.00
A	7	External	2.24	1.26	2.27
A	7	Internal	0.00	1.26	1.79
A	8	External	0.00	0.00	1.88
A	8	Internal	1.77	0.00	0.00
A	9	External	0.28	0.00	1.49
A	9	Internal	0.00	1.48	1.73
A	10	External	0.00	0.00	1.89
A	10	Internal	0.00	0.00	5.65
B	1	External	0.00	4.44	0.00
B	1	Internal	0.00	21.44	1.87
B	2	External	0.00	4.51	0.92
B	2	Internal	0.00	30.04	2.60
B	3	External	2.28	3.62	3.56
B	3	Internal	0.00	18.51	4.51
B	4	External	5.13	6.01	0.00
B	4	Internal	0.00	62.87	2.41
B	5	External	0.00	16.07	0.00
B	5	Internal	0.00	74.54	8.34
B	6	External	0.00	16.36	0.00
B	6	Internal	0.00	25.95	9.37
B	7	External	2.24	3.31	0.00
B	7	Internal	0.00	71.38	4.57
B	8	External	0.00	5.61	0.00
B	8	Internal	1.77	33.94	3.87
B	9	External	0.28	1.79	0.00
B	9	Internal	0.00	16.77	0.00
B	10	External	0.00	1.93	1.34
B	10	Internal	0.00	29.10	1.64

C	1	External	0.00	0.00	0.84
C	2	External	0.00	0.00	1.19
C	3	External	15.92	15.92	0.00
C	4	External	2.59	2.59	0.94
C	5	External	0.00	0.00	0.00
C	6	External	3.14	3.14	0.00
C	7	External	2.68	2.68	0.00
C	8	External	0.00	0.00	0.00
C	9	External	0.00	0.00	0.00
C	10	External	3.56	3.56	0.00
C	1	Internal	0.00	0.00	2.39
C	2	Internal	0.00	0.00	0.00
C	3	Internal	0.00	0.00	0.00
C	4	Internal	0.32	0.32	0.00
C	5	Internal	0.00	0.00	0.00
C	6	Internal	4.01	4.01	0.00
C	7	Internal	0.00	0.00	0.00
C	8	Internal	0.00	0.00	0.00
C	9	Internal	0.00	0.00	0.00
C	10	Internal	0.00	0.00	0.00

Appendix 9. The mean DNA concentration data (using the SRY male human autosomal marker) of swabs taken from counterfeit holograms prepared by volunteers to produce composite banknotes and extracted according to the three extraction techniques: Chelex resin extraction, phenol chloroform extraction and BTA Prepfil kit.

Volunteer	Sample no.	Location	Phenol	BTA	Chelex
A	1	External	0.00	0.00	13.14
A	1	Internal	0.00	0.00	0.00
A	2	External	146.48	0.00	0.00
A	2	Internal	0.00	0.00	0.00
A	3	External	0.00	2.64	39.22
A	3	Internal	0.00	0.00	0.00
A	4	External	0.00	3.99	0.00
A	4	Internal	0.00	0.00	0.00
A	5	External	0.00	3.14	0.00
A	5	Internal	0.00	0.00	0.00
A	6	External	0.00	0.00	0.00
A	6	Internal	0.00	0.00	0.00
A	7	External	0.00	0.00	18.80
A	7	Internal	0.00	0.00	0.00
A	8	External	0.00	3.37	0.00
A	8	Internal	0.00	0.00	0.00
A	9	External	40.06	0.00	0.00
A	9	Internal	0.00	0.00	0.00
A	10	External	0.00	0.00	0.00
A	10	Internal	0.00	0.00	0.00
B	1	External	0.00	14.02	24.10
B	1	Internal	0.00	0.00	0.00
B	2	External	120.32	0.00	0.00
B	2	Internal	0.00	0.00	0.00
B	3	External	0.00	27.99	0.00
B	3	Internal	0.00	0.00	0.00
B	4	External	0.00	19.85	0.00
B	4	Internal	0.00	0.00	0.00
B	5	External	0.00	47.57	0.00
B	5	Internal	0.00	0.00	0.00
B	6	External	0.00	37.46	35.86
B	6	Internal	0.00	0.00	0.00
B	7	External	0.00	27.41	0.00
B	7	Internal	0.00	0.00	0.00
B	8	External	0.00	106.10	0.00
B	8	Internal	0.00	0.00	0.00
B	9	External	0.00	8.92	17.83
B	9	Internal	0.00	0.00	0.00
B	10	External	40.75	57.04	0.00
B	10	Internal	0.00	0.00	0.00

C	1	External	0.00	0.00	0.00
C	2	External	0.00	54.23	23.20
C	3	External	0.00	0.00	0.00
C	4	External	0.00	0.00	0.00
C	5	External	0.00	0.00	0.00
C	6	External	0.00	55.60	0.00
C	7	External	0.00	0.00	0.00
C	8	External	50.90	60.95	0.00
C	9	External	41.90	0.00	0.00
C	10	External	0.00	0.00	0.00
C	1	Internal	0.00	0.00	60.25
C	2	Internal	0.00	0.00	0.00
C	3	Internal	0.00	0.00	0.00
C	4	Internal	27.86	0.00	0.00
C	5	Internal	0.00	0.00	0.00
C	6	Internal	0.00	0.00	0.00
C	7	Internal	0.00	0.00	0.00
C	8	Internal	0.00	0.00	0.00
C	9	Internal	0.00	0.00	0.00
C	10	Internal	0.00	0.00	0.00

Appendix 10. The corresponding alleles and RFU values for the allelic peaks detected for swabs taken from counterfeit holograms prepared by volunteer A to produce composite banknotes and extracted using Chelex resin and phenol chloroform extractions (BTA Prepfilers were left out as there were no alleles detected in the samples). The columns consist of where the sample was taken, how it was extracted and the corresponding STR loci. Colours indicate the potential source of the alleles according to the reference profiles of each volunteer (profiles on request). Green indicates the allele can be associated with volunteer A, orange indicates that it is a shared allele present in volunteer A's and volunteer C's profile, light blue indicates an allele that is present in volunteer C's profile, dark blue indicates an allele pertaining to volunteer C when analysing the internal samples, light green indicates an allele that is associated with volunteer A and B's reference profiles, purple indicates a unique allele that is not found in volunteer A's profile but is present in volunteer B's profile who was not involved with these samples and yellow indicates an allele not found within any of the volunteer's reference profiles.

Location	Extraction	AMEL	D10S1248	vWA	D16S539	D2S1338	D8S1179	D21S11	D18S51
External	Chelex			17 75					
Internal			13 68		12 60		10 64		
External			13 81						
Internal		X 404							10 165
External						24 66			
Internal		X 137	13 335		12 81		14 172		10, 127
External								32.2 86	16 99
Internal		X 61	13 81		12 117		14 114	30.2 59	10 128
External			13 70						
Internal									10 258
External						9 83			

Location	Extraction	D22S1045	D19S433	TH01	FGA	D2S441	D3S1358	D1S1656	D12S391	SE33		
External	Chelex						16 120		22 62			
Internal			14 104			11 90	16 172					
External						24 85	11 83	14 113	16 97			
Internal			14 173	15.2 90	7 63	19 84		15 225	16 207	23 131	30.2 86	
External		16, 102										
Internal		15 210	16 87	14 116		24 94		16 105	16 104	24 51		
External		16 93			9 104				17.3 61			
Internal		15 118	16 113		7 118	8 90	24 84		15 145	16 235	12 80	16 211
External							14 161					
Internal		15 112			7 81				12 78	16 151		
External		16 120		14 111		24 97			14 151			

Location	Extraction	AMEL	D10S1248	vWA	D16S539	D2S1338	D8S1179	D21S11	D18S51			
Internal	Chelex		13 172									
External		Y 63	13 71		12 96			32.2 100				
Internal												
External		X 138				24 59						
Internal		X 278	13 117	15 77	11 70		15 143	33.2 250				
External				18 69					14 113			
Internal			13 259		11 157	12 220	14 114	15 197	16 68			
External			16 103			24 76						
Internal		X 691	13 521	14 271	15 73	11 243	12 140	14 197	15 112	30.2 113	10 358	16 103
External		Phenol		13 81				10 202				
Internal			16 195				12 82	13 73				
External							13 93		16 124			

Location	Extraction	D22S1045	D19S433	TH01	FGA	D2S441	D3S1358	D1S1656	D12S391	SE33		
Internal	Chelex			8 86		11 120		18.3 82	21 111			
External						11 72						
Internal			14 113	15.2 245	7 93	8 81	10 79		12 84		13 65	30.2 108
External		16 96	14 104				14 150					
Internal			14 218				10 153			23 263		
External		14 65	16 71	13 97		22 86	24 129					
Internal		15 113	16 64	14 117	7 123		11 255	16 104	12 89	16 58	13 93	30.2 5
External		16 254		14 206	9 115				14 97	15 88		
Internal		15 103		14 401	15.2 27	8 121	24 186	10 170	11 205	15 108	16 199	14 61
External	Phenol		13 58									
Internal		11 124				14 104						
External			13 170	14 203		24 108			14 163			

Location	Extraction	AMEL	D10S1248	vWA	D16S539	D2S1338	D8S1179	D21S11	D18S51
Internal	Phenol	X 178	13 195	14 56					
External			14 233						
Internal									
External		X 408				9 97	12 136		
Internal									
External		Y 246						14 229	
Internal			14 131					32.2 122	33.2 179
External						9 72			
Internal									
External		X 88	13 116	14 178	17 75			13 111	
Internal		Y 170						15 104	
External		X 185	14 105		15 93	16 93			
Internal									
External		X 142			17 146				

Location	Extraction	D22S1045	D19S433	TH01	FGA	D2S441	D3S1358	D1S1656	D12S391	SE33			
Internal	Phenol	16 118	14 245	15.2 75		11.3 89	15 287						
External						14 132							
Internal									22 127				
External		16 137		13 247	14 132				14 92	23 218			
Internal						13.3 66							
External		16 53			9.3 124			14 179	15 134	28.2 104			
Internal													
External						14 273							
Internal													
External		16 134				24 219	11 101	14 98					
Internal				12.2 157	7 128			15 126	17.3 88				
External		11 146	15 159	16 366	13 145	14 290	9.3 135	21 116	11 195	14 289	16.3 82	19 114	30.0 51
Internal								14 114		19 130	30.2 113		
External				13 235		24 78	13.3 762						

Appendix 11. The corresponding alleles and RFU values for the allelic peaks detected for swabs taken from counterfeit holograms prepared by volunteer B to produce composite banknotes and extracted using Chelex resin, phenol chloroform and BTA Prepfilr extractions. The columns consist of where the sample was taken, how it was extracted and the corresponding STR loci. Colours indicate the potential source of the alleles according to the reference profiles of each volunteer (profiles on request). Green indicates the allele can be associated with volunteer B, orange indicates that it is a shared allele present in volunteer B's and volunteer C's profile, light blue indicates an allele that is present in volunteer C's profile, dark blue indicates an allele pertaining to volunteer C when analysing the internal sample, purple indicates a unique allele that is not found in volunteer B's profile but is present in volunteer A's profile who was not involved with these samples and yellow indicates an allele not found within any of the volunteer's reference profiles.

Location	Extraction	AMEL	D10S1248	vWA	D16S539	D2S1338	D8S1179	D21S11	D18S51						
External	Chelex	X 366						32.2 127							
Internal		X 114	14 98	17 126			14 153								
External								32.2 139	14 107						
Internal		X 242	Y 54			12 175		13 69	14 281	16 89					
External			Y 142		17 60										
Internal		X 130			17 66			29 87							
External			16 117		18 77										
Internal		X 495	13 401	14 175	17 72			13 120		16 149					
External		X 88			17 71										
Internal		X 1167	13 422	14 570	17 89	19 178	12 51	17 92	13 164	14 153	29 100	31 152	16 220		
External		X 115	13 61	16 121					12 59						
Internal		X 1286		13 515	14 274	17 221	19 131	12 200	16 239	17 76	13 349	14 462	29 394	31 158	16 451

Location	Extraction	D22S1045			D19S433		TH01		FGA		D2S441		D3S1358		D1S1656		D12S391		SE33	
External		16					9							17.3				19	28.2	
		37					75							88				99	98	
		4																		
Internal		15		16	15		6			11		15	16				21			
		20		197	126		120			325		106	67				189			
		4																		
External		16			14				24			16		17.3				19		
		31			149				130			113		85				110		
		7																		
Internal		15		16	14	15	9.3			11				12		17		26		
		11		104	70	156	160			196				215		150		77		
		2																		
External		16			13		9.3					16				15				
		93			153		57					225				63				
Internal		16								11		15				17	21			
		11								225		122				196	136			
		8																		
External		16					9													
		15					100													
		8																		
Internal		14	15	16	14		6	9.3		11		15	16	12		21				
		72	316	237	127		286	159		310		147	315	74		160				
External										11		16		15						
										118		125		72						
Internal		15		16	14	15	6	9.3	20		11	15	16	12		17				
		30		287	80	119	172	186	234		449	236	316	160		277				
		9																		
External		16			13	14				11		16		14						
		81			91	114				167		103		173						
Internal		15	16	17	14	15	6	9.3	20	24	11	15	16			17	21	26		
		74	447	69	171	543	262	197	119	222	393	519	286			310	234	108		
		9																		

Location	Extraction	AMEL	D10S1248	vWA	D16S539	D2S1338	D8S1179	D21S11	D18S51		
External	Chelex		13 98								
Internal		X 120	13 108	14 73	17 159	19 79	16 83	13 84	14 373	29 287	31 118
External					18 63						
Internal		X 220	13 271	14 98		12 135		14 181		29 94	16 157
External			13 84		18 77			12 253	13 120		
Internal								14 74			
External			13 153	16 69				13 106			
Internal			14 97		17 63			13 131	14 189	29 124	
External											
Internal	Phenol	X 259								16 130	
External		X 358	Y 135								
Internal		X 1889	13 279	14 543	17 96	19 217		13 274	14 316	29 438	31 244

Location	Extraction	D22S1045	D19S433	TH01	FGA	D2S441	D3S1358	D1S1656	D12S391	SE33		
External	Chelex	16 105				11 99				28.2 157		
Internal		15 143	16 218	14 212	9.3 278	24 122	11 219	16 81	17 119			
External		16 118		13 95		24 133			17.3 178			
Internal		15 155	16 247	14 494	15 214	6 101		11 422	15 101	14 75	17 21 72 222	26 27.2 88 69
External		16 81		14 138				16 156				
Internal				14 261		20 86	24 58	11 101		18 83		
External		16 229		14 87	9 240	9.3 108	22 87	11 173	14 180	16 201		28.2 82
Internal				14 109	15 128	6 146	24 104	11 234				
External		Phenol						16 117		21 74		
Internal												
External				14 103				13 111				
Internal	15 428		16 477	14 610	6 282	9.3 883	20 90	24 688	11 826	15 16 528 182	12 14 407 261	17 223

Location	Extraction	AMEL	D10S1248	vWA	D16S539	D2S1338	D8S1179	D21S11	D18S51				
External		Y 79											
Internal		X 550	13 231	14 321	19 86	12 316	14 332						
External		X 219	16 263		12 62	19 111	13 114						
Internal		X 226	13 172				14 445	29 181					
External			16 79					30.2 109					
Internal		X 59	13 326	15 215	12 160		13 110						
External		Y 228	13 165	16 218	17 53	9 63	12 136						
Internal		X 792	13 494	19 130	12 234	16 57	17 74	13 391	14 154	31 147	16 566		
External		X 115											
Internal		X 901	13 106	14 540	17 165	19 115	17 69	13 298	14* 77				
External		X 72			17 113								
Internal		X 258	13 530	14 356	17 65	19 84	12 108	17 157	13 53	14 213	31 128	15 51	16 223
External											16 99		
Internal		X 121	14 85		17 85	19 62	12 136		14 85		29 201	31 146	

Phenol

Location	Extraction	D22S1045	D19S433	TH01	FGA	D2S441	D3S1358	D1S1656	D12S391	SE33							
External	Phenol																
Internal		15 275	14 123		24 218	11 105	15 444	12 207									
External				9 119		11 254		17.3 75									
Internal		15 124	14 208			12 94	14 162										
External					22 147	11 182	14 75	16 283									
Internal		16 397	14 407	15 229	6 220	24 134	11 366	15 81		17 150	21 80						
External		16 355	14 124				11 89	16 101		18 79							
Internal		16 176	15 819	14 417	15 588	6 405	9.3 182	19 77	20 269	24 75	11 672	15 507	16 636	12 94	14 163	17 91	21 257
External							11 110	13.3 64			18 186						
Internal		15 176	16 109	14 106	15 74	6 136	9.3 190	24 67			10 112	11 479	16 300	12 52	14 76	17 179	
External																	
Internal		15 232	16 94	15 235			20 471				11 190		16 549		14 224		
External				14 127							11 193		16 99		17.3 154		
Internal		11 179		14 108	6 121		24 179				11 325	11.3 122	15 120				

Location	Extraction	AMEL	D10S1248		vWA		D16S539		D2S1338		D8S1179		D21S11		D18S51
External	Phenol		13	16				19	24	13					
			98	76				83	83	136					
Internal	Phenol	X	13	14									29		
			140	108	82								156		
External	BTA														
Internal		X	13	14	17	19	12	16	17	13	14	29	31	16	
			1367	597	856	547	340	1318	485	433	812	486	366	838	262
External		Y		16											
			84												
Internal		X	13	14	17	19	12	16		13	14	29	31	16	
			1681	616	852	613	331	594	528	1363	842	323	536	834	
External								9	12		12	13			
								60	62		91	77			
Internal															
External															
Internal					17	19	12	16	17	13	14	29	31		
				392	362	1706	405	873	552	458	76	99			
External							19								
							64								
Internal				17	19	12	16	17	13	14					
				134	70	343	634	479	207	177					

Location	Extraction	D22S1045		D19S433		TH01		FGA		D2S441		D3S1358		D1S1656		D12S391		SE33	
External	Phenol							24		11		16		17.3		18			
Internal		16		14	15	9.3								12					
External	BTA																		
Internal		15	16	14	15	6	9.3	20	24	11	15	16	12	14	17	21	26		27.
External		1234	826	415	391	143	180	252	665	1835	545	579	388	579	435	252	552		584
Internal		16		14		9	9.3	24		11	16		14						
External		437		84		173	52	71		121	91		85						
Internal		15	16	14	15	6	9.3	20	24	11	15	16	12	14	17	21	26	26.	27.
External		875	1114	1044	301	145	337	384	237	1779	915	670	441	640	224	411	100	91	467
Internal		16																	28.
External		112																	100
Internal																			
External																			
Internal		15	16							11								26	26.
External	253	162							1941								793	60	
Internal																			
External																			
Internal									11	11							26		
External									430	98							75		